

**THE UNIVERSITY OF HULL**

**Development of a Novel Designs Assessment and Selection System  
for Green Office Buildings in China**

Thesis submitted to the University of Hull for the Degree of  
Doctor of Philosophy

By

**Zishang Zhu**

MSc University of Nottingham, UK  
BArch Shandong Jianzhu University, China

May 2017

## **Abstract**

China is facing-severe problems in fossil fuel consumption and pollutant emission largely owing to the construction of buildings. Office buildings, as a major building type in China, contribute around 22% of the national fossil fuel energy use and 14% of carbon emissions. The identification of the most appropriate solution to energy saving and pollutant emissions reducing at the earlier design stage of office buildings is significantly important to China's sustainability development and environmental protection.

This PhD research aims to establish a simple and straight-forward assessment method that can predict fossil fuel energy use and the associated pollutant emissions of the Chinese office buildings at their early conceptual design stage (when the detailed material and constructional information is unavailable), and further, develop a computer-aided assessment and selection process that can identify the best design solution to the office buildings of China. This work is carried out through a standard research process including literature review, methodology development, computer model establishment, case study and results analysis with comparisons, followed by recommendations. As a result, the research provides a variety of important outputs, i.e., the life-cycle energy and air-pollutants estimation method, the generalized environmental impact metric system, and the green office building design solution assessment and selection system (GBAS). It has been demonstrated that the simplified energy and pollutants estimation method can predict the energy consumption and associated pollutant emissions at each office building life-cycle phase, based on the refined mathematical correlations and associated computerized toolkits. By using the generalized environmental impact metric system, the pollutant equivalent (PE), which reflects the combined environmental impact of the emission of four common pollutants, is derived and its values are discussed in detail. Based on the estimation of life-cycle energy and PE, the GBAS system is developed to identify the "best" design solution on both the quantitative survey and qualitative analyses.

A combination of all the above outcomes leads to the development of a comprehensive computerized tool that can conduct faster assessment, optimization and selection of the

“best” design solutions for Chinese office buildings at their very earlier stage of design. The prediction results have been proven to be rational, realistic and applicable to practical engineering projects.

The outcomes of the research can help in the design of energy efficient and “green” office buildings in China, thus contributing to China’s sustainable development and environmental protection.

## **Acknowledgement**

I would like to express my sincere and heartfelt gratitude to my supervisor Professor Xudong Zhao for his continuous support and guiding, for his patience, motivation, enthusiasm, immense knowledge and dedicated involvement throughout the whole process of my PhD research. From the beginning to the final level, his encouragement, guidance and assistance help me to develop a better understanding of this PhD subject. I would also like to thank my other supervisors and teachers of the University of Hull for their support and suggestions.

I wish to thank University of Hull and China Academy of Building Research for their financial support on this project. Also, I appreciate the European Commission Marie Curie action for the academic exchange opportunities it provided.

I am indebted to many of my supportive colleagues in our research team. They are Prof Zhongzhu Qiu, Prof. Wei He, Prof. Kaijin Zhu, Prof. Peng Xu, Dr. Xiaoli Ma, Dr. Xingxing Zhang, Dr. Yin Bi, Mr.Jinzhi Zhou, Mr.Yi Fan and Ms. Min Yu.

Finally, but by no means least, I would like to thank my family and friends. I cannot say enough about my father Wei Zhu and my mother Wei Shang for making me who I am today. And no words can express my gratitude to my wife, Yanyi Sun for being supportive all the time in all that I have done and I ever wanted to do. My most heartfelt thanks to my son, Bailin, who was born during my PhD study. I could never have accomplished so much without them.

# Table of Contents

<b>Chapter 1. Introduction</b> . . . . .	1
1.1 Research background . . . . .	2
1.2 The current research gap . . . . .	4
1.3 Research aim and objectives . . . . .	5
1.4 Research novelty and timeliness . . . . .	6
1.5 The methodologies applied in this research . . . . .	7
1.6 Thesis structure and general description of the research concept . . . . .	9
<b>Chapter 2. Literature Review</b> . . . . .	12
2.1 Introduction . . . . .	13
2.2 Review of the building's environmental impact . . . . .	15
2.2.1 Energy consumption of office building . . . . .	15
2.2.2 Pollutant emissions from office building sector . . . . .	16
2.3 Review of active green building technologies and design strategies . . . . .	18
2.3.1 Building integrated solar thermal collectors . . . . .	18
2.3.2 Building integrated PV system (BIPV) . . . . .	19
2.4 Review of passive green building design strategies . . . . .	20
2.4.1 Building geometry design . . . . .	20
2.4.2. High performance insulated envelope . . . . .	22
2.4.3 Green roof . . . . .	24
2.5 Review of green building simulation and optimization tools . . . . .	27
2.5.1 Simplified manual calculation method (stead-state) . . . . .	27
2.5.2 The quasi-steady-state calculation tools . . . . .	29
2.5.3 The dynamic calculation tools . . . . .	30
2.6 Review of green building codes and evaluation systems . . . . .	33

2.6.1 Building energy saving codes .....	34
2.6.2 Green building evaluation tools .....	35
2.7 Summary of literature review .....	38
<b>Chapter 3. Development of the operational energy estimation model applicable to the earlier stage conceptual design for Chinese office buildings .....</b>	<b>41</b>
3.1 Introduction.....	42
3.2 The Methodology applied in this chapte .....	43
3.3. The principles of the original EN ISO13790 estimation method .....	46
3.3.1 The basic heat balance framework of the EN ISO13790 hourly method.....	46
3.3.2 The mathematic correlation between the variables of the 5R1C model.....	48
3.3.3 The calculation procedure for indoor temperature and heating/cooling energy demand.....	52
3.4 Generating the HVAC module for the operational energy estimation of Chinese office buildings by refining of EN ISO13790 .....	55
3.4.1 The Simplified approach for building zone definition.....	55
3.4.2 A Simplified approach for building thermal mass related variables .....	57
3.4.3 The refined and China-focused model for transparent windows and glazing curtain walls.....	60
3.4.4 The refinement and China-focused model for the opaque walls and roofs. ....	63
3.4.5 The refined and localised model for underground space. ....	66
3.4.6 The simplified and localised model to generate the HVAC electricity demand.....	70
3.5 The Validation of the CN 13790 HAVC module for the Chinese office building. ....	71
3.5.1 The accuracy assessment of CN13790 HAVC module.....	72
3.5.2 The verification of climate adaptability for different climate regions in China .....	79
3.5.3 The assessment of computing time for the CN13790 method.....	82
3.6 Adding the additional energy consumption module and renewable energy generation module to the CN13790. ....	83
3.6.1 The Development of the additional energy consumption module for the other regular energy consumption .....	84

3.6.2 The Development of the renewable energy generation module for additional energy saving from renewable energy systems.....	85
3.7 Chapter Conclusion .....	87
<b>Chapter 4. Development of the simplified life-cycle energy and pollutants assessment method applicable to conceptual design of the buildings . . . . .</b>	<b>89</b>
4.1 Introduction.....	90
4.2 Methodology .....	91
4.2.1 Research scope for different phases and time scopes for the LCE & LCP .....	91
4.2.2 Research scope for energy sources and pollutant emissions .....	92
4.2.3 Research scope relating to the building materials, components and systems .....	93
4.2.4 The principles of the assessment method for a building`s LCE and LCP.....	94
4.2.5 The approaches for the simplified LCE and LCP assessment methods .....	96
4.3 The development of the simplified assessment method for the building material phase`s embodied energy and pollutant emissions .....	97
4.3.1 The general description of the simplified assessment method for EM and PM,j.....	97
4.3.2 Generating the regression models for EM and PM,j from the fixed main structure section.....	98
4.3.3 Generation of the simplified assessment method for EM and PM,j from the variable components section.....	114
4.4 The development of the simplified assessment method for the on-site construction phase`s embodied energy and pollutant emissions .....	126
4.4.1 Development of the simplified assessment method for the energy consumption and pollutant emissions from the material transportation between factory and building site .....	127
4.4.2 Generating the simplified assessment method for the energy consumption and pollutant emissions from the on-site construction work .....	128
4.4.3 Generating the simplified assessment method for the energy consumption and pollutant emissions from change of land use.....	130
4.5 The development of the simplified assessment method for the building operation phase`s embodied energy and pollutant emissions .....	131
4.5.1 Generating the simplified assessment method for the energy consumption and pollutant	

emissions caused by the operation of building service system .....	131
4.5.2 Generating the simplified assessment method for the energy consumption and CO <sub>2</sub> e emission from the fugitive emissions .....	132
4.6 The development of the simplified assessment method for the building demolition phase`s embodied energy and pollutant emissions .....	133
4.6.1 Generating the simplified assessment method for the energy consumption and pollutant emissions from the on-site demolition work.....	133
4.6.2 Generating the simplified assessment method for the energy consumption and pollutant emissions from transportation of building demolition waste .....	134
4.6.3 Generating the simplified assessment method for the embodied energy consumption and pollutant emissions from final treatment of building demolition waste .....	135
4.7 Conclusions .....	136
<b>Chapter 5. Development of a general environmental impact assessment system associated with the office buildings` pollutant emissions. ....</b>	<b>138</b>
5.1 Introduction.....	139
5.2 Definition of the general environmental impact metric .....	140
5.3 Methodology .....	141
5.3.1 The overall methodology .....	141
5.3.2 The Principle of the AHP method - the mathematical foundation for the weights of the PE. ....	143
5.4 Recognizing the environmental impact from pollutants and collecting related data. ....	146
5.5 Generating the conversion factor (weight) for the PE by an AHP based method .....	150
5.6 The case study and results discussion: using PE in the office building designs comparison...153	
5.6.1 A description of an example building (original and improved design). ....	153
5.6.2 Calculating the life-cycle PE for the original and improved design of example building	155
5.6.3 Analyzing the environmental impact reflected by the PE in example building design. ...156	
5.7 The chapter conclusion .....	158
<b>Chapter 6. ..Establishment of the multiple criteria based green design assessment and selection system. ....</b>	<b>160</b>



6.1 Chapter Introduction.....	161
6.2 Criteria and decision-making scenarios involved in the GBAS .....	162
6.2.1 Criteria involved in the GBAS .....	162
6.2.2 The decision-making scenarios in the GBAS. ....	163
6.3 The methodology of green building design assessment and selection.....	166
6.3.1 The overall methodology for green building design assessment and selection. ....	166
6.3.2 The principle of the TOPSIS based method in the GBAS.....	167
6.3.3 The weight assignment method for “subjective” preference scenarios by an expert survey and AHP method.....	170
6.4 Weight assignment for the energy consumption saving oriented preference scenarios (Group 1). .....	172
6.4.1 The reliability testing to the survey results.....	173
6.4.2 Weight assignment for “subjective” scenarios: 1.1-MWEC and 1.2-MOEC.....	173
6.4.3 Weight assignment for the “objective” scenarios: 1.3-WECS and 1.4-OECS .....	173
6.4.4 Weight assignment for the 1.5 WEC-OC scenario:.....	177
6.5 Weight assignment for environmental impact reducing oriented scenarios (Group 2).....	182
6.5.1 Weight assignment for 2.1-MWEI, 2.2-MOEI, 2.3-WEIR and 2.4-OEIR scenarios:.....	182
6.5.2 Weight assignment for the 2.5 WEI-OC scenario:.....	185
6.6 Weight assignment for the comprehensive preference scenarios group (Group 3). ....	189
6.6.1 Weight assignment for the 3.1 WB-BTL scenario:.....	189
6.6.2 Weight assignment for 3.2 - WB-SU scenario: .....	190
6.7 Conclusion .....	191
<b>Chapter 7: Development of an integrated computer aided tool to enable fast and convenient green design optimization and selection . . . . .</b>	<b>193</b>
7.1 Introduction.....	194
7.2 Development of the computer aided tool .....	194
7.3 The Validation of the computer aided tool by case study.....	198

7.3.2 Possible design solutions and their key “green performance” as generated by the computer aided tool.....	200
7.3.3 The optimized office building design solution selected by the computer aided tool.....	203
7.4 Conclusion:.....	209
<b>Chapter 8: Conclusion</b> .....	<b>211</b>
8.1 Thesis conclusion.....	212
8.2 Recommendations for further work.....	216
<b>Appendix I: Datasets for building material</b> .....	<b>218</b>
<b>Appendix II: Questionnaire</b> .....	<b>220</b>
<b>Appendix III: The simplified life-cycle office building cost estimation method</b> .....	<b>227</b>
<b>Appendix IV: Calculation data for validation of CN13790</b> .....	<b>234</b>
<b>References</b> .....	<b>235</b>

## List of Figures

Figure 1.1 The proportion of energy usage for China office buildings and specific users.....	3
Figure 1.2: The importance of early design stage for decision making.....	4
Figure 1.3: The structure for the implementation of research objectives .....	8
Figure 1.4: Thesis structure flow chart.....	10
Figure 2.1: The number and distribution of research papers regarding to related fields and the top countries with most certificated green buildings .....	14
Figure 2.2: The average energy distribution for office building in US, UK, and China.....	16
Figure 2.3: The flat plate collector panel and evacuated tube collector array on roof.....	19
Figure 2.4: The possible positions to integrate PV into building .....	20
Figure 2.5: The typical intensive and extensive green roof.....	25
Figure 2.6: The structure and working flow of the DOE-2.1 engine.....	31
Figure 2.7: Working flowchart of EnergyPlus .....	32
Figure 2.8: Energy performance certificates and Environmental impact certificates .....	34
Figure 2.9: BREEAM outstanding certificate for a building in University of Nottingham.....	36
Figure 2.10: The “Three Star” label for a building in Shanghai .....	38
Figure 3.1: The research method applied in the module development.....	44
Figure 3.2: The schematic of 5R1C model .....	47
Figure 3.3: The flow chart for 4-setp calculation procedure .....	53
Figure 3.4: The diagrams of the zone definition approach .....	56
Figure 3.5: Am per m <sup>2</sup> conditioned floor area of example buildings from each structure type: .....	59
Figure 3.6: Cm per m <sup>2</sup> conditioned floor area of example buildings from each structure type .....	60
Figure 3.7: Schematic drawing of the glazing layers .....	62
Figure 3.8: Schematic drawing of the 4-layer external wall structure.....	63
Figure 3.9: The schematic structure drawing for the 4-layer-model of roof.....	64
Figure 3.10: The heat transfer approach and parameter definition for basement .....	66
Figure 3.11: Flow chart for the principal of accuracy assessment. ....	73

Figure 3.12: the appearance of the 9 building cases (EnergPlus OpenStudio model) ..... 76

Figure 3.13: The annual heating demand from each calculation method ..... 77

Figure 3.14: The difference between the heating demand from the CN13790, from a degree-day method and the benchmark value..... 78

Figure 3.15: The annual cooling demand from each calculation method..... 78

Figure 3.16: The difference between the cooling demand from the CN13790, from degree-day method and the benchmark value..... 79

Figure 3.17: The selected cities` location and monthly average temperature distribution. .... 80

Figure 3.18: The heating and cooling demand from each calculation method for the 5 cities.. 81

Figure 3.19: The difference between the results from the CN13790, from the degree-day method and the benchmark value..... 82

Figure 3.20: the definition of the simplified BIPV model ..... 86

Figure 4.1: Four-phase cycle and their sources for building LCE&LCP ..... 91

Figure 4.2: Direct and indirect emission sources for LCP ..... 93

Figure 4.3: Schematic diagram of two sections and their components ..... 94

Figure 4.4: Building samples distribution and appearance of the selected samples. .... 103

Figure 4.5: The group`s contribution to EM and PM,j for MS-RCF & HR-RCF structure buildings ..... 105

Figure 4.6: The group`s contribution to EM and PM,j for the HR-RCF-SW/T structure buildings ..... 106

Figure 4.7: The group`s contribution to EM and PM,j for the HR-SF-SW/T structure buildings ..... 106

Figure 4.8: Scatter plot and the regression line of EM and PM,j and building stories numbers for the FMS of MS-RCF and HR-RCF office building ..... 109

Figure 4.9: Scatter plot and the regression line of EM and PM,j and building stories numbers for FMS of HR-RCF-SW/T office building. .... 111

Figure 4.10: Scatter plot and the regression line of EM and PM,j and building stories numbers for FMS of HR-SF-SW/T office building. .... 113

Figure 5.1: Approach to recognizing the environmental impact from pollutants ..... 141

Figure 5.2: The research processes of Chapter 5 ..... 142

Figure 5.3: An architectural rendering of the large-scale data centre .....	153
Figure 5.4: The layout for the ground floor of the example office building .....	154
Figure 5.5: The emission and PE figures for each pollutant .....	156
Figure 5.6: The PE distribution among building life stages and source specification.....	157
Figure 5.7: The changing in PE and its sources specification .....	158
Figure 6.1: Criteria in GBAS .....	162
Figure 6.2: The scenarios group and scenarios in GBAS.....	164
Figure 6.3: The overall method for design solution assessment and selection in GBAS.....	167
Figure 6.4: 3-dimension coordination systems of the GBAS for the two designers' preferences. .....	169
Figure 6.5: The example pages of the questionnaire .....	171
Figure 6.6: Variable weight for severe cold & cold climate zones .....	180
Figure 6.7: Variable weight for hot summer cold winter climate zone .....	181
Figure 6.8: Variable weight for hot summer warm winter climate zone.....	181
Figure 6.9: Variable weight for severe cold & cold climate zones. ....	188
Figure 6.10: Variable weight for hot summer cold winter climate zone .....	188
Figure 6.11: Variable weight for hot summer warm winter climate zone.....	188
Figure 7.1: The tool interface 1 .....	196
Figure 7.2: The tool interface 2 .....	196
Figure 7.3: The tool interface 3 .....	197
Figure 7.4: The example dataset CSV file for wall infill block (screenshot in Excel) .....	197
Figure 7.5: The example output CSV file (screenshot in Excel) .....	197
Figure 7.6: Schematic site and example building .....	199
Figure 7.7: Radar chart for CDBP and CDBR of design solution no. 95 .....	204
Figure 7.8: Radar chart for CDBP and CDBR of design solution no. 75 .....	205
Figure 7.9: The Radar chart for CDBP and CDBR of design solution no. 31 .....	206
Figure 7.10: Radar chart for CDBP and CDBR of design solution 47 .....	206
Figure 7.11: Radar chart for CDBP and CDBR of design solution 46 .....	208
Figure 7.12: Radar chart for CDBP and CDBR of design solution 43 .....	208
Figure 7.13: Radar chart for CDBP and CDBR of design solution 45 .....	209

## List of Tables

Table 2.1: The typical thermal performance for insulation material in China market .....	23
Table 2.2: The basic thermal performance of XPS and EPS .....	23
Table 2.3: The U-Value reduction caused by green roof on different insulated roofs.....	26
Table 3.1: The key features of the building design examples with higher/lower thermal mass.	58
Table 3.2: Adjustment factor for $A_m$ and $C_m$ .....	60
Table 3.3: The dataset for typical windows/GCW frames in China .....	61
Table 3.4: China-focused typical material dataset for the opaque walls.....	64
Table 3.5: China-focused typical material dataset for the opaque roof. ....	65
Table 3.6: the calculation of $U_{bf}$ and $U_{bw}$ for basement heat transfer .....	67
Table 3.7: the calculation of $\Phi_m$ for basement heat transfer.....	68
Table 3.8: The dataset for typical basement envelope.....	68
Table 3.9: The China-focused input dataset for basement related parameters.....	70
Table 3.10: The typical EER from the Daikin HVAC system .....	70
Table 3.11: The starting and ending hour of each month .....	71
Table 3.12: Specifications for the standard office building case .....	74
Table 3.13: The specification for 8 office cases. ....	75
Table 3.14: The average computing time from the EnergyPlus, ESP-r and the CN13790 method. .....	83
Table 3.15: the typical value for other energy consumers is used in the CN13790 (per $m^2$ ) .....	84
Table 3.16: the typical EER for typical air-source heat pump.....	85
Table 3.17: The typical parameter for BIPV in China .....	86
Table 3.18: The typical parameter for solar thermal collector in China .....	87
Table 4.1: The method used to generated the simplified and localised estimation models.....	97
Table 4.2: Wastage ratio for building materials in this research .....	98
Table 4.3: Designed service lift for building components in this research .....	98
Table 4.4: $EF_M$ and $PF_{M,j}$ for the buildings with fixed structure .....	100
Table 4.5: Data source description for $EF_M$ and $PF_{M,j}$ .....	100
Table 4.6: The weighted average usage proportion ( $R$ ) for each office building type.....	102

Table 4.7: Overall EFM and PFM, j of the ready-mixed concrete for each office building types .....	102
Table 4.8: The information and distribution of samples .....	103
Table 4.9: Calculation table for a six-storage sample office building .....	103
Table 4.10: the specification of 3 major materials groups in FMS .....	105
Table 4.11: RSD checking Table for each material group of typical structures.....	105
Table 4.12: Basic descriptive statistics of EM and PM, j from MS-RCF and HR-RCF samples	108
Table 4.13: Regression functions and key indicators for FMS of MS-RCF and HR-RCF office building.....	108
Table 4.14: Basic descriptive statistics of EM and PM, j from the HR-RCF-SW/T samples...	110
Table 4.15: Regression functions and key indicators for FMS of HR-RCF-SW/T office building	110
Table 4.16: Basic descriptive statistics of EM and PM, j from HR-SF-SW/T samples .....	112
Table 4.17: Regression functions and key indicators for FMS of HR-SF-SW/T office building..	112
Table 4.18: Options of Block/brick and insulation layer for building envelope and their specification .....	115
Table 4.19: Additional material and accessories dataset for building block/brick per m <sup>3</sup> .....	116
Table 4.20: Additional material and accessories dataset for insulation layer per m <sup>2</sup> .....	117
Table 4.21: Dataset for the general EFM and PFM, j of glazed facing tile external decoration .....	118
Table 4.22: Dataset for the general EFM and PFM, j of dry hanging stone external decoration .....	118
Table 4.23: Dataset for the general EFM and PFM, j of lime mortar plaster internal decoration .....	118
Table 4.24: The localized dataset for general EFM, i, gla and PFM, i, j, gla of building glass	119
Table 4.25: The localized dataset for general EFM, i, fra and PFM, i, j, fra of window frame .....	120
Table 4.26: Dataset for typical material usage, EM (MJ) and PM, j (kg) from accessories per 1m <sup>2</sup> glass curtain wall.....	121
Table 4.27: Dataset for EFM, i, fra and PFM, i, j, fra of curtain wall's frame for lower buildings (≤10 storeys).....	121

Table 4.28: The materials usage and $EM \& PM, j$ of frame and accessories for each wind load level.....	122
Table 4.29: linear regression equations for design wind load and $EM, i, fra$ & $PM, j, i, fra$ ...	122
Table 4.30: Height adjust factor for urban area .....	122
Table 4.31: the scatter plots and the regression equations for the relationship of building storeys and the $EFM, i, fra$ & $PFM, j, i, fra$ for 10-25 storey buildings.....	123
Table 4.32: The average material usage proposition in VRV system. ....	124
Table 4.33: The investigated VRV units and their typical weight by cooling capacity .....	124
Table 4.34: the average materials` weight by cooling capacity in VRV system. ....	125
Table 4.35: The materials` average proportion and weight by cooling capacity of ACCW and WCCW HVAC type. ....	125
Table 4.36: The general energy consumption factor and pollutant emission factor for 4 types of HVAC.....	125
Table 4.37: the general $EFM, light, i$ and $PFM, light, j, i$ for typical lighting systems.....	126
Table 4.38: The $EFCon-T$ & $PFCon-T, j$ for China building material transportation .....	127
Table 4.39: The average transportation distance ( $D_i$ ) for typical building materials in China .	128
Table 4.40: The general $EFCon-O, i$ for on-site construction work of typical structure types .....	129
Table 4.41: The emissions data for unit energy consumption (kg/MJ) of 3 energy sources....	129
Table 4.42: The general energy factor (MJ/m <sup>2</sup> ) and emission factor (kg/m <sup>2</sup> ) of each construction type .....	129
Table 4.43: The emission factor of original land use ( $PFBe_f, i, j$ ).....	131
Table 4.44 The local emission factors for energy resources ( $PFr, j$ ) .....	132
Table 4.45: General specification of RAC unit applied in this research .....	133
Table 4.46: The emission factors ( $CF_i$ ) for the general refrigerant used in 3 typical RAC.....	133
Table 4.47: The $EFDe-On$ and $PFDe-On, j$ for on-site demolition work .....	134
Table 4.48: The proportions of material waste in each treatment method .....	135
Table 4.49: The general $EF_i, I$ and $PF_i, I, j$ for typical waste incineration plants in China .	136
Table 5.1: Pairwise relative importance of criteria.....	144
Table 5.2: Random consistency index (RI) .....	145



Table 5.3: Monetization environmental cost statistic dataset by type and region .....	149
Table 5.4: The pairwise comparison result for the monetization environmental cost from 25 data sources .....	150
Table 5.5: The overall average normalized results .....	151
Table 5.6: The ranking of criteria for each data source type .....	152
Table 5.7: Overall weights for 4 criteria.....	153
Table 5.8: Basic information for the original design.....	154
Table 5.9: Specifications for improved design.....	155
Table 5.10: Pollutant and environmental cost for original and improved design.....	155
Table 6.1: The Energy saving oriented preferences scenarios group .....	164
Table 6.2: The Environmental impact oriented preferences scenarios group.....	165
Table 6.3: The comprehensive considered preference scenarios group .....	166
Table 6.4: Weight of criteria and criteria for each solution.....	169
Table 6.5: Fundamental verbal scale for pair-wise importance .....	172
Table 6.6: The selected key criteria in 1.3 - WECS and 1.4 - OECS scenarios .....	174
Table 6.7: The pair-wise comparison among criterion for 1.3 - WECS and 1.4 - OECS preference scenarios .....	174
Table 6.8: Weight assignment for 1.3 WECS and 1.4 OECS scenarios .....	175
Table 6.9: The higher-point and lower-point definition for different regions in China.....	178
Table 6.10: The pair-wise comparison among criteria in the 1.5 WEC-OC scenario .....	179
Table 6.11: Weight assignment for 1.5 WEC-OC scenarios .....	179
Table 6.12: The selected key criteria in 2.3-WEIR and 2.4-OEIR scenarios .....	183
Table 6.13: The pairwise comparison among criteria in 2.3WEIR and 2.4OEIR scenario.....	183
Table 6.14: Weight assignment for 2.3WEIR and 2.4OEIR scenarios .....	184
Table 6.15: Energy consumption and proportion of each energy source .....	186
Table 6.16: Typical emission factors for each energy source .....	186
Table 6.17: Suggested environmental impacts at the operational stage .....	187
Table 7.1: The input for the possible design solutions generating module.....	195
Table 7.2: The specification of possible component design options.....	199
Table 7.3: The key “green performance” value for 96 design solutions.....	200

Table 7.4: Statistical analysis factors for criteria values in 96 results .....	202
Table 7.5: ODSs, RDSs and the specification for energy saving oriented preference scenarios group .....	203
Table 7.6: ODSs, RDSs and the specification for the environmental impact reducing oriented preference scenarios group.....	207
Table 7.7: ODSs, RDSs and the specification for the comprehensive considered scenario preference group.....	209

## Abbreviations

<b>ACCW</b>	Air-cooled chilled water system
<b>AHP</b>	Analytic hierarchy process
<b>BIPV</b>	Building integrated photovoltaics

<b>CR</b>	Consistency ratio
<b>EER</b>	Energy efficiency ratio
<b>GBAS</b>	Green building assessment and selection system
<b>GFA</b>	Gross floor area
<b>HVAC</b>	Heating, ventilation and air conditioning
<b>LCE</b>	Life-cycle energy consumption
<b>LCP</b>	Life-cycle pollutant emissions
<b>MWEC</b>	Minimizing the whole energy consumption preference scenario
<b>MOEC</b>	Minimizing the operational energy consumption preference scenario
<b>MWEI</b>	Minimizing the whole environmental impact preference scenario
<b>MOEI</b>	Minimizing the operational environmental impact preference scenario
<b>NIS</b>	Negative ideal solution
<b>ODS</b>	Optimal design solution
<b>OECS</b>	Operational energy saving dominated preference scenario
<b>OEIR</b>	Operational environmental impact reducing dominated preference scenario
<b>PE</b>	Pollutant equivalent
<b>PIS</b>	Positive ideal solution
<b>RAC</b>	Refrigeration and air-conditioning equipment
<b>RI</b>	Average random consistency index
<b>RDS</b>	Reference design solution
<b>VRV/VRF</b>	Variable refrigerant volume/flow
<b>WEC-OC</b>	Whole environmental impact reducing oriented with overall consideration preference scenario
<b>WB-BTL</b>	Well-balanced consideration for build-to-let offices preference scenario
<b>WB-SU</b>	Well-balanced consideration for self-use office preference scenario
<b>WECS</b>	Whole energy saving dominated preference scenario
<b>WEC-OC</b>	Whole energy saving oriented with overall consideration preference scenario
<b>WEIR</b>	Whole environmental impact reducing dominated preference scenario
<b>WCCW</b>	Water-cooled chilled water system

## Nomenclature

<b>Chapters 2 and Chapters 3</b>	
<b>Symbols</b>	

$A$	area	$m^2$
$A_{tot}$	the total surface area adjacent to the conditioned zone of the building	$m^2$
$A_m$	effective mass area	$m^2$
$A_f$	conditioned floor area	$m^2$
$A_{sol}$	solar effective collecting area	$m^2$
$a_{s,c}$	the absorption coefficient for solar radiation of the opaque part	--
$b_{ve}$	supply air temperature adjustment factor	--
$C_m$	internal thermal mass	J/K
$D$	thickness	m
$F_{sh}$	shading reduction factor	--
$F_F$	the ratio of the projected frame area to the overall projected area of a building part	--
$F_r$	factor between the building element and sky	--
$F_{ac}$	the area ratio of the air-conditioned area to gross floor area	--
$g_{gl}$	total solar energy transmittance of the transparent part	--
$H$	heat transfer rate between temperature nodes	W/K
$h_{ms}$	heat conductance between building mass and surface	W/m <sup>2</sup> K
$h_r$	the external radioactive heat transfer coefficient	W/m <sup>2</sup> K
$I$	solar radiation on a horizontal surface	W
$K$	the internal heat capacity per m <sup>2</sup> of building element	J/K m <sup>2</sup>
$q_{ve,k,mn}$	time average airflow rate	m <sup>3</sup> /s
$R_{se}/R_{Si}$	the external surface heat resistance of the of the opaque part	m <sup>2</sup> .K/W
$R_{So}$	internal heat resistance value	m <sup>2</sup> .K/W
$R_{gap}$	R-value of the air gap	m <sup>2</sup> .K/W
$R_{medium}$	the thermal resistance of medium (earth)	m <sup>2</sup> .K/W
$T_{fo}$	outlet water temperature	K
$T_{fi}$	the inlet water temperature	K
$T_{sa}$	outdoor integrated temperature	K
$T_a$	outdoor air temperature	K
$U_{gre}$	U-value of green roof	W/m <sup>2</sup> K
$U_e$	equivalent U-value	W/m <sup>2</sup> K
$U_g$	U-value of glazing part	W/m <sup>2</sup> K
$U_f$	U-value of the frame part	W/m <sup>2</sup> K
$\alpha_e$	outside surface heat transfer coefficient	W/m <sup>2</sup> K
$\varepsilon$	heat emissivity coefficient	--
$\lambda$	heat conductivity	W/mK
$\rho_s$	solar radiation absorption coefficient	--
$\delta$	periodic penetration depth for specific ground type	m
$\theta$	temperature at different node	K
$\Delta\theta_{er}$	the average difference between the external air temperature and apparent sky temperature	K
$\varphi$	heat flow rate	W
$\Phi_{HC,nd}$	heating / cooling need	W
$\Phi_{HC,nd,un}$	unrestricted heating / cooling need	W

$\Phi_{HC,nd,ac}$	actual heating / cooling need	W
$\Phi_C$	HVAC cooling capacity	W
$\Phi_H$	HVAC heating capacity	W
<b>Subscripts</b>		
<i>air</i>	internal air	
<i>bf</i>	basement`s floor	
<i>bw</i>	basement`s wall	
<i>e</i>	external air	
<i>fl</i>	the floor between first floor and basement	
<i>gl</i>	moveable shading device on glass	
<i>HC,nd</i>	heating/cooling need	
<i>int,H,set</i>	heating set point	
<i>int,C,set</i>	cooling set point	
<i>int</i>	internal gain	
<i>M</i>	building material phase	
<i>m</i>	building mass	
<i>ms</i>	conductance bwtween building mass and surface	
<i>ob</i>	external obstacles	
<i>s</i>	building internal surface	
<i>sup</i>	supplied air	
<i>sol</i>	solar heat gain	
<i>tr,w</i>	very light building elements with “zero” thermal mass (i.e. windows)	
<i>tr,op</i>	opaque and heavy building elements	
<i>tr,em</i>	the connection of external air to building mass	
<i>tr,ms</i>	the connection of internal surface to building mass	
<i>tr,is</i>	coupling conductance	
<i>ve</i>	ventilation	

#### Chapter 4

##### Symbols

<i>A</i>	application area of building element	m <sup>2</sup>
<i>E</i>	Energy consumption	MJ
<i>EF</i>	Energy consumption factor	MJ/kg or MJ/m <sup>2</sup>
<i>F<sub>g</sub></i>	area factor of glass part	--
<i>P</i>	pollutant emission	kg
<i>p</i>	proportion of demolition waste that treated by different method	%
<i>PF</i>	pollutant emission factor	kg/kg or kg/m <sup>2</sup>
<i>R</i>	rate of fugitive emission	%
<i>t<sub>B</sub></i>	service time of building	Year
<i>t<sub>i</sub></i>	service time of building elements	Year
<i>ρ<sub>i</sub></i>	Density of building material	kg/m <sup>3</sup>

**Subscripts**

<i>con</i>	building construction phase
<i>Op</i>	building operational phase
<i>De</i>	building demolition phase
<i>Con-T</i>	material transportation
<i>Con-O</i>	on-site construction
<i>Con-L</i>	change of land use
<i>Op-ser</i>	building service system operation
<i>Op-fug</i>	refrigerants fugitive emission
<i>De-on</i>	on-site demolition work
<i>De-T</i>	building waste transportation
<i>De-Treat</i>	building waste final treatment
<i>mai</i>	main material and accessories
<i>add</i>	additional materials and accessories
<i>gla</i>	glass of window / of curtain wall
<i>ins</i>	installation process of RAC equipment
<i>a</i>	annual leakage during RAC operation
<i>d</i>	demolition process of RAC equipment
<i>fra</i>	frame of window / of curtain wall
<i>LF</i>	land fill waste treatment method
<i>I</i>	incineration waste treatment method
<i>Re</i>	recycle waste treatment method

**Chapters 5 and Chapter 6****Symbols**

<i>F</i>	Convert factor for PE	--
<i>Emi</i>	Emission amount for each pollutant	kg
<i>V</i>	solution matrix	--
<i>W</i>	Weight of criteria	--
$S_i^*$	Separation of design solution from the PIS	--
$S_i^-$	Separation of design solution from the NIS	--
$\lambda_{max}$	the eigenvalue of matrix	--
$\varepsilon$	Differences rate	%

## Chapter 1. Introduction

## 1.1 Research background

Building-related activities make significant contributions to global concerns over energy resources and the environment. It is universally acknowledged that these concerns have been developing in recent decades, owing to rapidly growing industrialization, construction and enhanced living standards. Building-related human activities account for a large proportion of the overall energy usage and have a great impact on global climate and environment deterioration. Statistics show that nearly 40% of primary energy is used in buildings in the US [1], while the figure in Canada is 30% [2]. In Europe, a similar situation prevails and building-related human activities account for more than 40% of the overall energy delivery [3]. Consequently, the pollutant emissions from buildings are dramatically high, with percentages of 38% of CO<sub>2</sub>, 52% of SO<sub>2</sub>, and 20% of NO<sub>x</sub> emission in the US, and 29% and 36% of greenhouse gas emissions in Canada and the EU respectively [4]. The situation is not optimistic in China as well. Although energy saving systems and high energy efficiency building designs have already been implemented into many new / existing buildings [5] [6], the proportion of building energy consumption in the whole country's demand will reach 40% in 2020 [7], following the growth trends from 1978 (10%) to 2007 (8%) [8].

China has become the most critical country in terms of energy and pollution problems related to building-activities. This is because: (1) it develops over 50% of the world's new buildings every year (1 billion m<sup>2</sup>) [9], which consumes over 40% of global concrete and steel production as well as massive amounts of energy; (2) the construction approach in China is changing quickly from the energy efficient "traditional styles" (i.e. low-rise, brick / wooden structured, naturally ventilated) to the energy-greedy "modern style" (i.e. high-rise, concrete / steel structured, central HVAC supplied). Thus the research and practice of green building in China is urgently needed, more than most other countries.

In China's critical building-related energy and environment problems, the "green performance" of office buildings is recognized as a major issue because of its great energy density, significant environmental effect, and complex function with mutative



comfortable requirement and occupant time. In China, office buildings (including other public buildings) only account for around 5% of the total building area, whereas they use over half of the total energy demand from the building sector (22% of the whole society energy needs) by its HVAC, lighting, hot water and other appliances (Figure 1.1). Similar to energy consumption, great environmental impacts will emerge during the whole life-cycle of an office building, which is normally difficult to define and compute. Researches show that the air pollution relating to the operational stage of an office building is 10 to 20 times higher [5] than a residential building in a unit area.

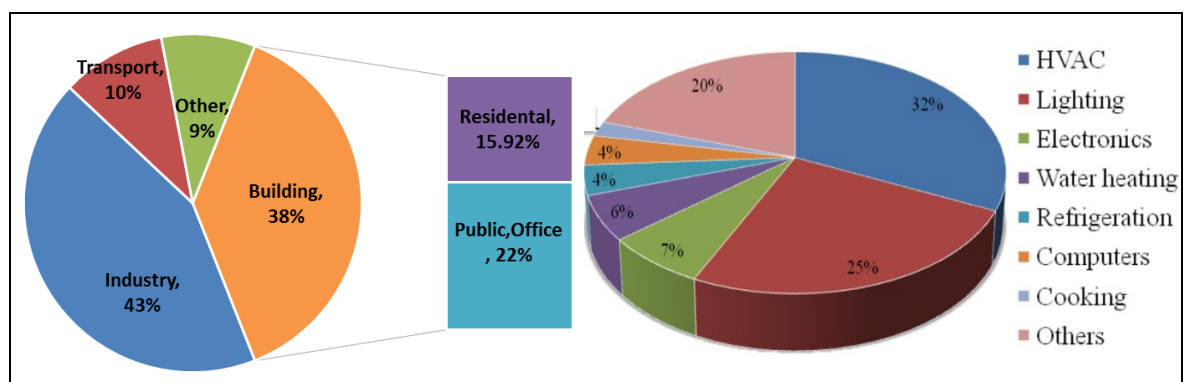


Figure 1.1 The proportion of energy usage for China office buildings and specific users [11]

The “green performance” of an office building is largely dependent upon the quality of its conceptual design at the early design stage. A well-designed green building should minimise its life-cycle energy consumption and environmental impact when bringing the same level of comfort at a minimum cost. To achieve this target, decisions made at the conceptual design stage that is usually delivered by architects can impose a considerable impact to its final performance (Figure 1.2). The minimized mistakes made in the conceptual stage can lead to the maximized “green performance” of the building, compared to those made in the follow-on design stages (e.g. the detail design stage and the construction drawing design stage) [8].

Thus, improving the quality of the concept design for Chinese green office building plays a key role in enhancing its energy efficiency and reducing the environment harming pollution. This has been well reflected in China’s governmental R&D policies / actions.

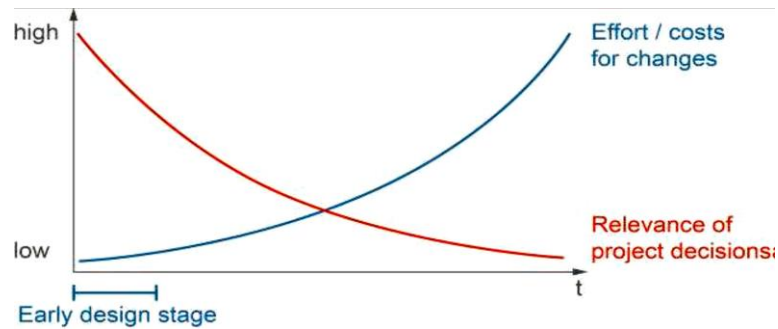


Figure 1.2: The importance of early design stage for decision making [8]

## 1.2 The current research gap

Research into “green office buildings” was mainly focused in high energy efficiency building service systems and green design theories. However, the research activities focusing on the integration of building engineering aspects (e.g. building material, building service system, renewable energy system) and architectural design aspects (e.g. basic shape, layout and other conceptual design definition) are still insignificantly reported. This leads to limited improvement in the overall “green performance” of office buildings. The gaps in the architectural design and engineering solutions are outlined as follows:

- (1) The study on comprehensive environmental impacts from the whole life-cycle of office buildings is not widely reported. As we understand that any design decision is a trade-off process among numerous key factors, (e.g. one pollutant can be reduced while the other is increased). The current research is largely focused on single impact factors, there is no practical solution developed that can reflect the overall building environmental impact from multi-factors (i.e. CO<sub>2</sub>e, SO<sub>2</sub>, NO<sub>x</sub>, PM emission) in combination in a system.
- (2) The interaction of multi green building technologies and geometric design features is incomplete. Although active and passive building energy saving technologies and green architectural design theories have been broadly studied, the interaction among them, particularly the active technology and passive green design, is still an unexplored area. Consequently, the method of selecting and optimizing various applicable technologies and assessing the performance of the building with the

integration of multiple technologies is a topic for particular attention.

- (3) The current building energy computational tool is not applicable to the early stage design of Chinese green office buildings, owing to multiple inputs needed and the complex process features. The existing energy calculation methods are either complicated (e.g. dynamic simulation methods require complex detailed input unavailable in the early design stage) or inaccurate (e.g. manual calculation methods) for this design stage. In this case, the development of a simple and straightforward computational tool with fewer parametrical input requirements is mostly desired for architects and engineers who are engaged at the early conceptual design stage.
- (4) A results-oriented green building performance assessment system applicable for green office buildings in China is still unavailable. The current green building performance assessment systems are all process-oriented and credit-based systems. These systems can only reflect the points collected from green measurements, rather than the final energy and environmental impact. A result-oriented green office building performance assessment system that can rank the building design solutions directly based on their estimated energy and environmental impact has not yet been established.

### 1.3 Research aim and objectives

With regard to the energy saving and environmental protection of Chinese office buildings, the design-decision-making system applicable for the early stage conceptual design has to be established. **This PhD research aims to investigate the characteristics of the life-cycle “green performance” (i.e. energy, pollution and cost) of Chinese office buildings, thus establishing a series of “green performance” estimation methods, as well as an associated design solution assessment and optimization system applicable to earlier stage conceptual design. This research can therefore contribute to the quality of conceptual design for green offices in China.**

To achieve the research aim, the following objectives are specified:

- (I) Understanding the existing green building technologies, building codes, design assessment methods and simulation tools that can be applied to the Chinese office buildings, thus enabling the identification of the existing research gaps in current green design practice. This part of the research work will be addressed in Chapter 2.
- (II) Establishing the life-cycle energy and air pollutants (four types) emission estimation methods for typical Chinese office buildings. These methods and associated datasets are specifically developed for Chinese office buildings, in order to obtain a quick and reliable feedback from results while only simple inputs are available at the conceptual design stage. This part of the research work will be addressed in Chapters 3 and 4.
- (III) Establishing an innovatively generalized environmental impact metric system, namely pollutant equivalent (PE) that can reflect the overall environmental impact from four main pollutants types, thus allowing the measurable, reportable and verifiable environmental performance assessment in the early design stage of China's office building. This work will be addressed in Chapter 5.
- (IV) Developing the green office building design solution assessment and selection system. This system is able to quantify the trade-offs in satisfying different green design objectives. It, meanwhile, can help select the optimised conceptual design solution for particular design tasks. This work will be addressed in Chapter 6.

#### **1.4 Research novelty and timeliness**

In brief, this research has the following identifiable novel aspects with dedicated timeliness:

**For the concept of this research** – This research focuses on the investigation of life-cycle “green performance” specifically for office building in China. This would create a series of unique assessment and optimization methods specifically applicable to the early stage conceptual design of Chinese green office building. These effects will

therefore improve the quality of conceptual design for green office building in China and further help to solve the critical building-related energy and environment problems in China

**For the “green performance” estimation methods** – The life-cycle energy consumption and pollutant emission estimation method is the first theoretical system dedicated for Chinese office building in the early conceptual design stage. With the help of established datasets, this innovated method is more advanced than the existing tools in terms of input efficiency and output reliability. Meanwhile, the new metric PE, as one of the outputs of the estimation method, provides an innovated perspective for the generalized environmental impact of building. These timely innovations would provide a proper tool for conceptual green design in China, meanwhile helping to reduce the comprehensive environmental impact (as China’s environment problem is caused by the interaction of multiple pollutants).

**For the green building design assessment and selection tool (GBAS)** – The GBAS is the first “result-orientated” green design assessment tool, the design solutions are evaluated by the energy and environmental impact results rather than credit collected from green design measurements (e.g. the credit-based system: LEED). The innovated GBAS selected the “optimized” design solution based on both qualitative opinion (through expert surveys) and qualitative analyses (through the TOPSIS method), which will fulfil the urgent requirement of the suitable design aided tool in China.

### **1.5 The methodologies applied in this research**

The overall structure for the implementation of research objectives is outlined in Figure 1.3. In order to facilitate the objectives, several methods are applied, including a literature review, statistical analysis, comparative study, case study, product surveys, expert surveys and interviews, as described below.

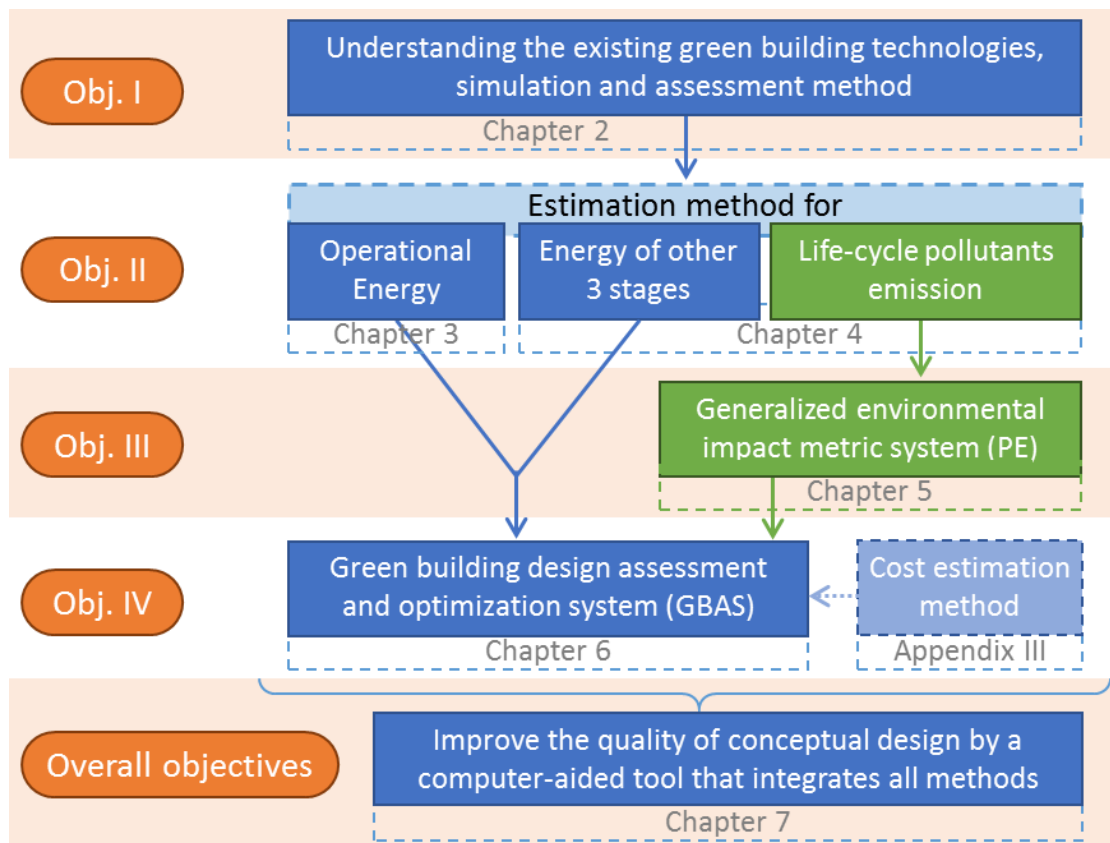


Figure 1.3: The structure for the implementation of research objectives

**The approach to objective I:** The understanding of the current research situation and gap on the related field is gained through a literature review. This involves the quantitative and qualitative reviews for the (1) the building-related environmental impact, (2) green office building technologies and design methods appropriate to Chinese office building, (3) building simulation/estimation tools, and (4) green building performance assessment systems.

**The approach to objective II:** The life-cycle energy and air pollutants (four types) emission estimation methods for Chinese office buildings are formed of two sets of estimation methods. These are the estimation methods for the buildings' operational stage and the estimation methods for the other stages of their life-cycle. The former method is generated based on the literature review of existing methods, as well as their localization and refinement through the market product survey and statistical analyses of data from a case study. The latter method is established by summarizing the energy and pollution characteristics through literature review and deriving the mathematical

relationship through statistical analysis of the case study.

**Approach to objective III:** The establishment of the generalized environmental impact metric (pollutant equivalent - PE) system is achieved by summarizing the existing research results of the pollutants' environmental impact through the literature review, and then identifying the PE metric by comparing relative importance, using the AHP method. The practicability of PE is tested through the comparative study (using PE or the single emission data in a design case).

**Approach to objective IV:** The development of the green office building design solution assessment and selection system is achieved by the following two steps: (1) summarizing the typical design objectives and their comparative importance in green office building design in China through the expert survey results processed using the APH method, and then (2) deriving the mathematical equations based on the TOPSIS method to quantify the design trade-offs in green office design. The practicability of PE is tested by means of a case study (applying GBAS in a design case).

## 1.6 Thesis structure and general description of the research concept

The thesis structure is outlined in Figure 1.4, the research concept of each chapter is described as follows:

Following a brief introduction, Chapter 2 will review the recent research work relating to green building design and engineering practices, with particular focus on the building-related environmental impacts, green office building technologies and design methods, building simulation/estimation tools, as well as the green building performance assessment systems. On this basis, the potential research gaps in existence are identified. This part of the work will formulate the foundation of the PhD research. In brief, a feasible and simplified "green performance" estimation and assessment tool appropriate for the conceptual design of green office buildings in China is the major gap to be filled by this research.

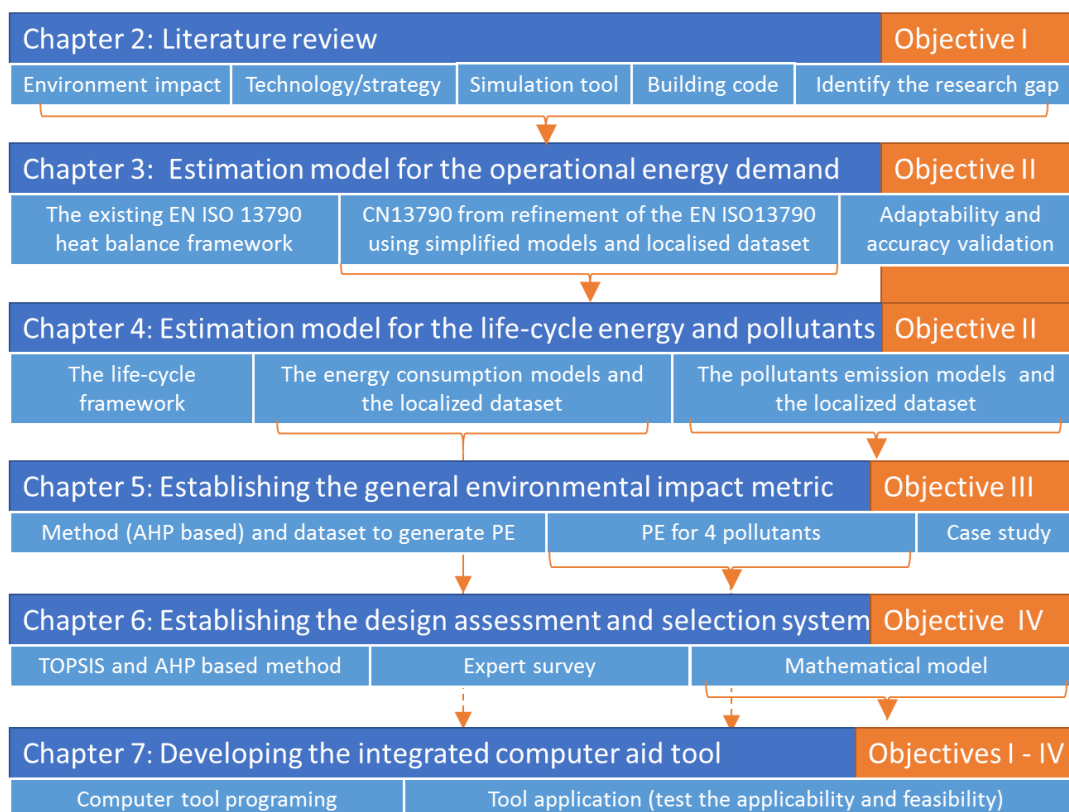


Figure 1.4: Thesis structure flow chart

In Chapter 3, an office building operational energy estimation tool, namely the CN 13790, will be developed. This toolkit is ideally suitable for use in the early conceptual design stage, during which the available inputs are limited and a quick feedback is required. On this basis, the existing EN ISO 13790, which is the foundation of the heat-balance framework of CN 13790, will be simplified and refined. The simplified models and calculation methods for typical components of a Chinese office building are incorporated into the existing framework. Throughout the selected case study, the adaptability and accuracy of this estimation tool will thus be approved.

In chapter 4, an estimation method for the life-cycle energy consumption (LCE) and life-cycle pollutants (i.e. CO<sub>2</sub>e, SO<sub>2</sub>, NO<sub>x</sub>, PM) emissions (LCP) of Chinese office building will be developed. The operational energy consumption of a building is computed on the basis of the computation tool developed in Chapter 3, while the energy consumption for other life-cycle stages and associated pollutant emissions will be computed based on components involved in the building. As a result, the dedicated energy and emission models and the China-focused dataset appropriate to most typical construction types



and materials will be obtained.

In chapter 5, an environmental impact metric, namely the pollutant equivalent (PE), will be defined and the associated computation method will be established. This will enable the reflection of the overall environmental impact from 4 types of pollutants in combination. The environmental impact from each pollutant will be studied and the data will be integrated into a dataset. The data processing will be undertaken through an AHP method, to generate the factors (i.e. the weighting of each pollutant) in the PE metric. A case study will then be carried out to examine the practicality of the PE metric. As a result, the pollutant emissions data generated by the method in Chapter 4 will be converted into the PE that can be applied to the follow-on Chapters.

In chapter 6, a green building design assessment and optimization system (GBAS) will be developed. This system will be functionalized to quantify the trade-offs among different green design objectives and thus select the best design solution. The key criteria (i.e. energy, PE and cost for different building stages) for the assessment of the design plans will be identified and the correlation among them will be developed by using the AHP expert survey method. The TOPSIS method will be applied to sort out the best design solution in a quantitative way, while the qualitative analysis is commonly used in the conventional building design process.

In Chapter 7, a computer-aided tool for Chinese office building design will be established. This tool, by integrating the energy and environmental impact assessment methods (in Chapter 3, 4, 5) and the GBAS, will generate various possible design solutions and on this basis, select the most suitable one. Through a dedicated case study, the performance of the computer-aided tool will be examined and concluded. The results derived from the chapter work are not only applicable to the validation of the newly established computer-aided tool but also appropriate to the examination of the proposed GBAS indicated in Chapter 6.

## Chapter 2. Literature Review

## 2.1 Introduction

Building energy consumption accounts for 40% of the total energy consumption world-wide, meanwhile, the pollution generated during the whole life-cycle of building accounts for the similar Figure of the total pollution [10]. In the whole building stock, take China for example, office building only accounts for 5% in term of area, but over 50% in term of energy demand [11]. This means increase attention to improve the energy and environmental performance of office building can greatly contribute to energy conservation and environment protection. Following by this background, green office buildings have been deeply studied in recent years, as well as the related design methods and assessment tools.

A “well-designed” green building is a building designed with technologies and strategies that can effectively reduce building environmental impact and create healthy environment for people to live and work, whilst minimize the building costs [12]. The environmental impact of a building, which mainly influenced by energy consumption and pollutant missions, is generally the most significant factor in green building design [13]. To allow the reductions of environmental impact, advanced energy saving technologies have been integrated into buildings with innovational design theories. To assess green building performance, the assessment/certificating tools for estimating energy consumption and pollutant emission were established to enable the green technologies and strategies are measurable, reportable and verifiable (MRV) [14].

Figure 2.1 shows the number and distribution of research papers regarding to relative fields in recent 13 years as the data were collected from ScienceDirect, as well as the top 10 countries with most certificated green buildings. The number of paper rise fast after 2003, which match the time when the assessment tools (e.g. LEED) became widely spread [15], meanwhile the distribution of paper and certificated green buildings are also similar.

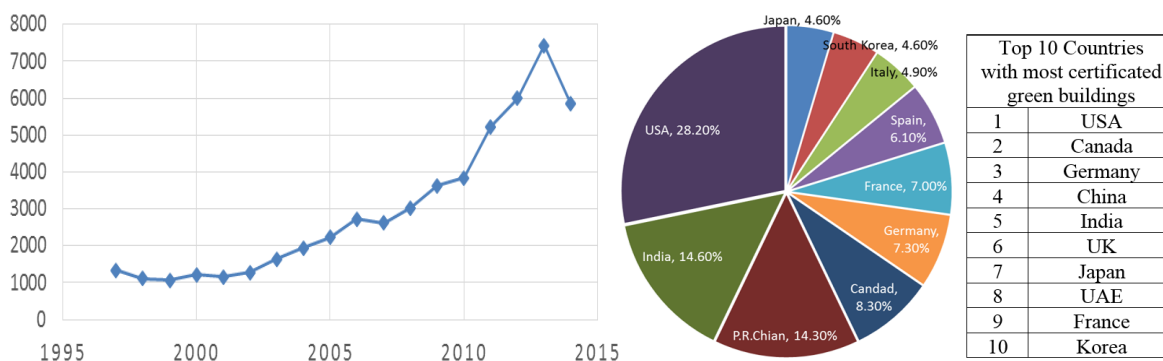


Figure 2.1: The number and distribution of research papers regarding to related fields and the top countries with most certificated green buildings

**The aim of this chapter is to comprehend recent research in the field of green building,** especially the building related environmental impact, green office building technologies and design methods, building simulation/estimation tools and green building assessment systems. Based on the review, research gaps between current research and actual need of the conceptual design stage of green office building will be summarized at the end of chapter.

To achieve this aim, four objectives are put forward as list below.

- (1) The current research on office buildings' energy consumptions and pollutant emissions (mainly air pollution in this research) as well as the pathways that they affect environment need to be reviewed.
- (2) The most appropriate technologies and design strategies for green office building need to be identified and emphatically reviewed. Active technologies that suitable for office building, which mainly include BIPV (building integrated photovoltaics) and solar thermal technologies, will be reviewed; following by passive design strategies, such as proper design of building orientation, shape coefficient and other architecture design features, use of high performance building envelopes and green roofs, etc.
- (3) The current status of building energy/environmental impact estimation tools also needs to be studied, including the simplified manual calculation method, the quasi-steady-state method and dynamic computer simulation tools.
- (4) The current development on green building code and evaluation systems will be

reviewed and summarized. The typical green building evaluation systems in US, EU and China will be selected and studied respectively.

## **2.2 Review of the building's environmental impact**

A critical review of the relative research will be provided to identify the current research progress and avoid the possible repetition in the new research.

### **2.2.1 Energy consumption of office building**

The office building sector consumes 18%, 12% and 22 % of society energy consumption in US [16], UK [17] and China [18] respectively, which is still increasing in China since the urbanization process is speeding up. The energy is provided by electricity and gas in Europe and US, whereas in China, electricity is the only energy resource except for buildings connected with district heating network in northern regions (gas is generally not used as energy source for northern China office buildings that connected to district heating network). In term of office building in China, the average energy consumption is 66.9 kWh/m<sup>2</sup>a in 2011, while the values for large office building (i.e. over 20000 m<sup>2</sup>) and small office building are 70-300 kWh/m<sup>2</sup>a and 50-70 kWh/m<sup>2</sup>a respectively [18]. The significant difference is because the former ones normally have “modern” façade design with high Window to Wall Ratio (WWR) or even with fully glazed curtain wall; meanwhile they highly rely on full mechanical ventilation systems and central air-conditioning systems [18].

The distribution of energy usage for office buildings varies among different regions, climates and indoor comfort requirements. The average energy usage distribution for office buildings in US, UK, and China [16] [17] can be seen in Figure 2.2. For office buildings' energy consumption in China, 59% is used in HVAC, 22% is used in hot water system and the rest is for lighting and office appliance [19]. The number is also different between cities as the location deeply effects the climate and human comfort zone, for instance, the proportion of HVAC energy demand for Beijing (north China) is higher than it is for Guangzhou (south China).

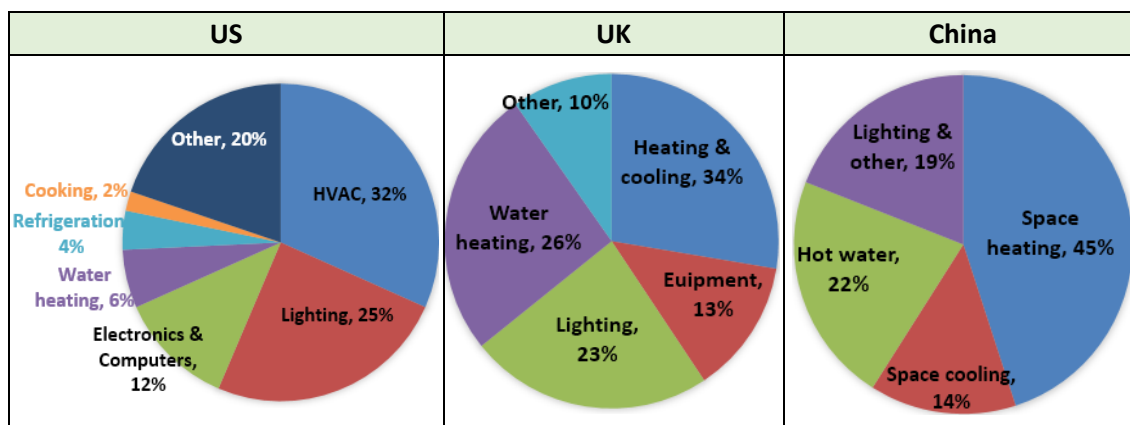


Figure 2.2 : The average energy distribution for office building in US, UK, and China [16] [17]

### 2.2.2 Pollutant emissions from office building sector

Pollutants, which include air pollution, water pollution, solid waste pollution, noise and light pollution, are continuously discharged from the whole life-cycle of office building. This research restricted itself to the air pollution only, because in current stage either the building code or the accurately measured method (e.g. for noise and light pollution) are lacking for other types of building pollutions.

The air pollution is one of the most serious pollution type in terms of the large amount during the whole life-cycle of office building and long duration of their environment harm. It is the fourth most important health-risk factor in less developed countries where 40% of the world's population live, and is estimated to be responsible for 2.7% of the global burden of disease [20]. According to IPCC [21], the most noteworthy and measurable building related air pollutant are CO<sub>2</sub> equivalents, SO<sub>2</sub>, NO<sub>x</sub> and PM. All of these come from both direct emission (on-site construction machinery operation) and indirect emission (energy generation and material producing that consumed by building).

**CO<sub>2</sub> equivalents (CO<sub>2</sub>e)**, which is the key factor of global-warming, represents six different greenhouse gases (GHGs): CO<sub>2</sub>, CH<sub>4</sub>, N<sub>2</sub>O, HFCs, PFCs and SF<sub>6</sub> [22]. The former three are contributed by the fossil fuel combustion in power station and the production process of building material [21]. The latter three are discharged from fugitive emission of refrigeration and air-conditioning (RAC) operation [21]. All GHGs emissions are converted to equivalent CO<sub>2</sub> (CO<sub>2</sub>e) for a comparable result by using specific global

warming potential (GWP) from UNEP-SBCI [21].

**The mono-nitrogen oxides (NO<sub>x</sub>)**, which include NO and NO<sub>2</sub>, is another serious air pollutant type from office building sector. They are produced from the reaction among nitrogen, oxygen and even hydrocarbons (during combustion) [23]. NO<sub>x</sub> is harmful for human health, which mainly impacts on respiratory conditions causing inflammation of the airways at high levels [24]. It also has a negative effect on ecosystems, such as harmful for vegetation including leaf damage and reduced growth [24]. The main discharge source for NO<sub>x</sub> is the coal-fired power station and industry process of producing building material especially cement. The diesel engine of the on-site construction or demolition machineries and of the vehicle for material transporting is another emission source but only take small proportion.

**Sulfur dioxide (SO<sub>2</sub>)** is another main pollutant that harmful for ecosystem and human health by easily react with other substances to form harmful compounds, such as sulfuric acid, sulfurous acid and sulfate particles [25]. It mainly discharged from the coal-fired power station and industry process of steel and plastic producing [26]. Similarly with NO<sub>x</sub>, a small proportion of SO<sub>2</sub> also emitted from the diesel engine of on-site machinery and transportation.

**The Particulate matter (PM)** is microscopic solid or liquid matter suspended in the atmosphere and adversely affects human health. The most harmful PM for human health, PM<sub>2.5</sub> and PM<sub>10</sub>, are mainly emitted from electric generation, followed by the metal production. The on-site construction process also contributes to PM emission, but the amount is much less and lack of measurement method.

The emission amount of pollutant is affected by different key factors. For example, the SO<sub>2</sub> emission can be dramatically reduced by applying advanced desulphurization equipment on coal-fired power station and using vehicles that matching the updated emission regulation to transport building materials. Future more, the overall emission for a specific office building is also highly dependent on building construction type. For instance, according to Canada wood council [27], the steel structure and reinforced-

concrete structure will averagely discharge 1.23 times and 1.5 time CO<sub>2</sub>e emission respectively than wood structure while keep the same building quality in their life-cycle.

### 2.3 Review of active green building technologies and design strategies

Due to the great expectance of improvement on environmental protection, a lot of research has been conducted in the active green building technologies building technologies. In the following section, they are reviewed in details.

#### 2.3.1 Building integrated solar thermal collectors

Solar thermal collectors are wildly integrated into green buildings to provide energy for hot water, space heating and cooling [28]. Rainer Aringhoff [29] mentioned that at least 100 -120 GWh energy are available from 1 km<sup>2</sup> solar thermal collector every year in many position on the earth (i.e. mid-latitudes region), which means a saving of 50MW fossil fuel energy per year. The solar collectors are conventional mounted on the roof of a building [30], however it can also be designed as a part of building facades, constructing as a gazebo or shading device [31].

**The flat plate collector** [32] (Figure 2.3) is the most common type, which consists a flat-plate absorber that contains water or antifreeze fluid, a transparent cover that reduces heat losses and a heat insulating backing and case. The efficiency are normally below 40% and 25% for collector itself and whole system respectively. Benefits from the cost efficiency on its manufacture and maintenance, it is wide used in building integration in Europe countries.

**The evacuated tube collector** [33] (Figure 2.3) is widely used as well. The vacuum tube greatly reduces convection and conduction heat loss, therefore achieving greater efficiency than flat-plate collectors, especially in cold weather. The gathered heat is removed by direct flow through the tube (e.g. most case in China) or by heat pipes (e.g. most case in middle Europe).The evacuated tube collector has higher efficiency than flat-plate collects, especially in cold weather. For example, a typical building integrated flat-plate collectors can reach 38% and 15% efficiency at 10 °C, and at -20 °C, while the



efficiency for evacuated tube collector are 48% and 38% respectively [34].

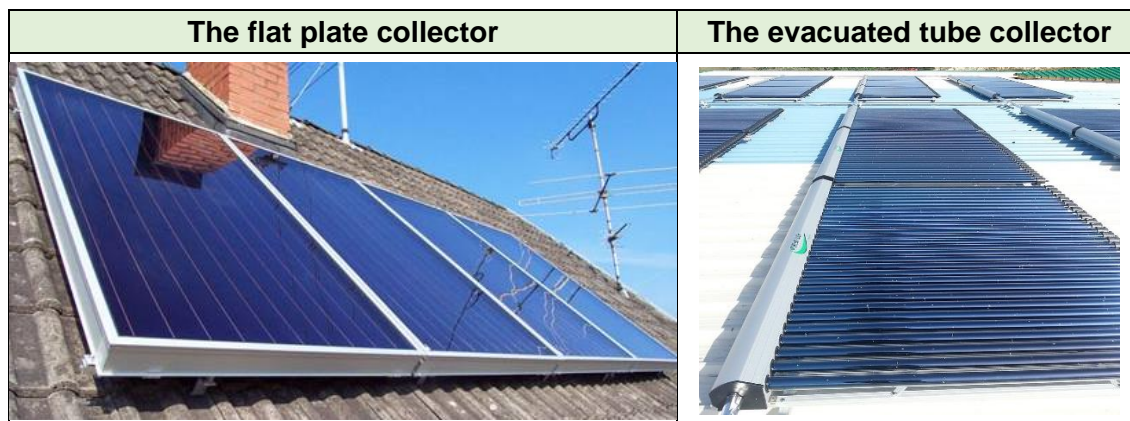


Figure 2.3: The flat plate collector panel and evacuated tube collector array on roof

Traditionally, the heat collected through solar collector is mainly used to pre-heat the medium (i.e. air and water) in the space heating system through heat exchanger, or to raise the temperature of supply water for hot water system [35], an application case in China for district hot water supply involved 40m<sup>2</sup> flat plate collector with heat pump can rise 1000L domestic hot water from 20°C to 50°C [30]. Besides, using solar thermal as additional energy source for space cooling was studied just recently. According to Sumathy K [36], solar cooling system normally uses single stage lithium bromide absorption chiller, which is driven by hot water, to achieve space cooling. High efficient solar collector such as vacuum tube collector can raise the water temperature to 80-90°C to actuate the chiller while keeps the performance efficiency of chiller at around 80% [37]. In Haywood`s research [38], a 10 tons lithium bromide absorption chiller unit driven by 50.2kW 88°C water were able to provide 35.2kW cooling power [39].

### 2.3.2 Building integrated PV system (BIPV)

BIPV generate electricity rather than heat with lower efficiency (around 11%-19% excluding inverter and cabling loss) than solar thermal collector. One of the advantages of PV is flexibility of its installation [40]. Recent research in this field paid more attention to improve the conveniences of integrating and using PV, especially for the small sized PV cell and thin film PV [41].

PV arrays are always installed on roofs or external walls of existing buildings, but they

can also be put separately from the building itself in some new designs [42]. The possible positions to integrate PV with a building can be seen in Figure 2.4. The install positions are distinct in different countries: more than four-fifth of PV arrays are set on the roof in Germany and China in 2010 [43], while in UK, the number is lower especially for large scale application [44]. An additional benefit of PV panel is studied in 2011 [45]. In their research, there is a natural air loop between PV panel and the installed vertical wall, passive cooling can be given at daytime and a proportion of heat can stay in the gap at night.

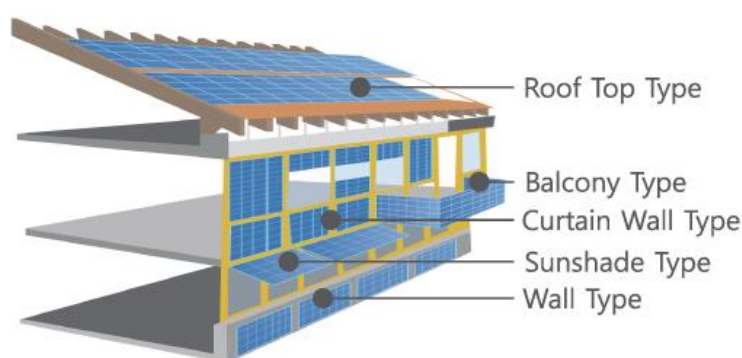


Figure 2.4: The possible positions to integrate PV into building [46]

## 2.4 Review of passive green building design strategies

### 2.4.1 Building geometry design

Geometry design of a building is able to dramatically affect the building's energy demand, and it is an effective method to provide a comfortable indoor environment before active ventilation and air-conditioning was embodied [47]. Due to the significant effect on indoor comfort level, it eventually influences the building energy used for space heating and cooling. There are three key factors in geometry design that have direct influence on building energy performance, including orientation, shape coefficient and window-wall ratio.

**The building orientation** normally refers to the direction that a building's main façade facing to. Since the main façade is generally on the long side of a building and has a largest window area, the building orientation will affect the solar gain of whole building to

a large extent [48]. In the rule-of-thumb of transitional architecture design, the main façade of a building always faces south in cold climate region to encourage maximizing solar gain and thus reduce energy demands for space heating and vice-versa. But the optimized orientation varies in different locations, depending on its local heating and cooling months. For example, the optimized orientation (calculated by Ecotect) for an design case in Hong Kong is 205°, which ensure the solar energy receiving in cold months and the solar gain reducing in hot months is balanced.

**The shape coefficient** (SC) is a key factor to evaluate the building energy efficiency. It is the ratio of the building surface area exposed to air ( $m^2$ ) and the building volume ( $m^3$ ). Since most of the heat is transmitted through building surface, the surface area should be controlled as small as possible while providing same usable volume in cold climate [48]. The SC is strictly limited by building regulation in some countries. For instance, the maximum SC is 0.35 and 0.4 for rectangular shaped building and cube building respectively according to “China building energy saving code for hot summer and cold winter zone” [49]. Meanwhile, for building with larger SC, the heat resistance requirement of building envelope will be higher [49]. The effect of SC varies in different regions and building types, research shows that for a well-insulated building in north China, a 5% energy demand difference exists between a high SC design and a low SC design.

**The window-to-wall ratio** (WWR) is an important variable affecting energy performance of a building, which has impacts on the building's heating, cooling, and lighting. The WWR is the measure of the percentage area determined by dividing the building's total glazed area by its exterior envelope wall area [50]. Since the heat resistance of a glazing part is normally lower than an opaque part, even for newly developed high performance windows, higher WWR design always leads to undesired thermal performance of the whole building envelope. The window-to-wall ratio is limited by building regulation in some countries especially in cold region. For example, details for maximum WWRs of each façade of public buildings in different climate regions are required by China building regulation GB 50189-2015 [51].

Due to the building appearance and function design are highly relied on WWR, and thus the suggested WWR cannot be satisfied in some building cases. According to GB 50189-2015 [51], if the WWR is higher than suggested value, the U-value of windows must be improved to a certain level. For example in “hot summer and cold winter region” of China, the heat resistance should be below 4.7 W/m<sup>2</sup>K for building with WWR lower than 0.2, whereas the resistance must be as high as 2.5 W/m<sup>2</sup>K for building with WWR between 0.5-0.7. In modern design practice, a building with high WWR (i.e. over 0.5 in “hot summer and cold winter region” of China) and high-performance glazing systems that combination with interior and exterior shading or/ and dynamic glazing systems (e.g. thermochromic or smart window) are able to reduce the unwanted solar gain through the large window area, while allowing natural daylight to enter spaces which results in low lighting demand [50].

#### 2.4.2. High performance insulated envelope

A high performance insulated envelope, as a most essential feature in modern green building, is capable to dramatically reduce the heat transfer between internal and external environment. A high performance insulation layer, an infill wall and a well-insulated window are the key components of a high performance insulated envelope.

**The high performance insulation materials** used in recent buildings are normally lightweighted cellular materials or fiber materials. **A typical cellular material is Polystyrene including expanded polystyrene (EPS) and extruded polystyrene (XPS).** EPS performs as well or better than XPS with lower cost. Research shows that the EPS costs 10% to 30% less than XPS per equivalent R-value and compressive strength [52], whereas XPS can provide a higher compressive strength (over 100 psi) which is easier for mounting and transporting. A common fiber material is mineral wool, including rock wool and slag wool. They are worse in thermal resistant than EPS but they are more cheaper and environmental friendly than EPS as 75% of its content comes from post-industrial recycled material and they are naturally fire resistant without any additional chemical treatment [53]. The typical thermal performance for insulation material in China

market are listed in table 2.1.

Table 2.1: The typical thermal performance for insulation material in China market [52]

	Conductivity (W/m•K)	Density (kg/m <sup>3</sup> )
XPS	0.033	30
EPS	0.041	25
Mineral wool	0.046	64
Glass wool	0.035	50

**The modern infill wall** generally uses light-weighted and thermal resistant masonry material to separate the inner and outer space. The masonry enclosure walls are made of aggregate concrete units or autoclaved aerated concrete units, rather than clay units, to reduce the structure weight load while provide high thermal performance. Typical materials for modern infill walls include Autoclaved aerated concrete (AAC), Concrete hollow block (CHB), Ceramsite concrete hollow block (CCHB) and Concrete solid block (CSB), the last one is normally applied to provide certain thermal mass [54] [55]. Their basic thermal performance can be seen in table 2.2 below.

Table 2.2: The basic thermal performance of XPS and EPS [54]

	Conductivity (W/m•K)	Density (kg/m <sup>3</sup> )
AAC	0.12	600
CHB	0.76	800
CCHB	0.27	600
CSB	1.28	1760

**The well-insulated windows** play an important role in building envelope: solar heat gain and light transmittance must be balanced while providing enough thermal resistance. Three indicators are normally used to reflect window's performance, which are (1) solar heat gain coefficient (SHGC), (2) visible light transmittance (VLT) of the glass, (3) thermal conductance (U-value) of the whole window (glass part and frame).

(1) The SHGC is the fraction of solar heat that go through a window, a typical clear glass have SHGC of 0.86. For the same solar irradiation level, windows with high SHGC transmit more solar energy and provide low shading effect [56].

(2) The VLT is a measure of the amount of the visible spectrum (380 to 720 nanometers) light that transmitted through the glazing, a typical value for clear glass is 0.9 [57].

Generally speaking, the windows facing east or west that may have high level of solar gain in morning and afternoon should use glass with lower SHGC but higher VLT; whereas windows for green house or space specially designed for solar heating should use glass with higher SHGC.

(3) The thermal conductance (U-value) of a whole window must be controlled as low as possible in green building. Double or triple glazing layers with air gaps are normally used to reduce the conduction heat loss, in which low-emissivity (Low-E) film can coated to glazing to further suppress radiative heat flow. Besides, the gap between glazing layers can be filled with noble gases, typically with argon or Krypton, to further reduce the heat conduction transfer. The distance of glass layers is controlled at around 10 mm - 30 mm. A wider gap over 30 mm cannot directly bring higher thermal resistance since the convection heat loss rate through the inner air will be increased [58].

The window frame will dramatically affect the thermal performance of the whole window as well. The aluminum frame and PVC frame are usually used with thermal break (e.g. PA66 rubber strap) to offer a low thermal conductance. But the latter cannot be used in high building since the limited wind force resistance, while the former are usable for any building height but the cost is also higher. The typical U value for China market available aluminum frame, Aluminum frame with PA66 insulation thermal break, PVC frame and wood frame are 6.21w/m<sup>2</sup>K, 3.72w/m<sup>2</sup>K, 1.91w/m<sup>2</sup>K and 2.37w/m<sup>2</sup>K respectively.

### **2.4.3 Green roof**

There are two type of green roof in term of landscape garden design, which are simple green roof (intensive) and garden style (extensive) green roof [59]. Different landscape design level brings difference growing medium weight and roof construction requirements, roof's design live load should no less than 2.9 kN/m<sup>2</sup> for simple green roof, however, the minimum value for garden style green roof is 3.0 kN/m<sup>2</sup>, and its suggested value is more than 5.0 kN/m<sup>2</sup>. The research and application of modern intensive green roof system start in Germany in 70`s, which have reliable technology that provided sophisticated irrigation and protection against root ingress for rooftop gardens [60]. The

extensive green roof was developed in 80`s, which provide a lighter, cheaper and easy maintained systems for large flat roofs. The typical intensive and extensive green roof can be seen in Figure 2.5

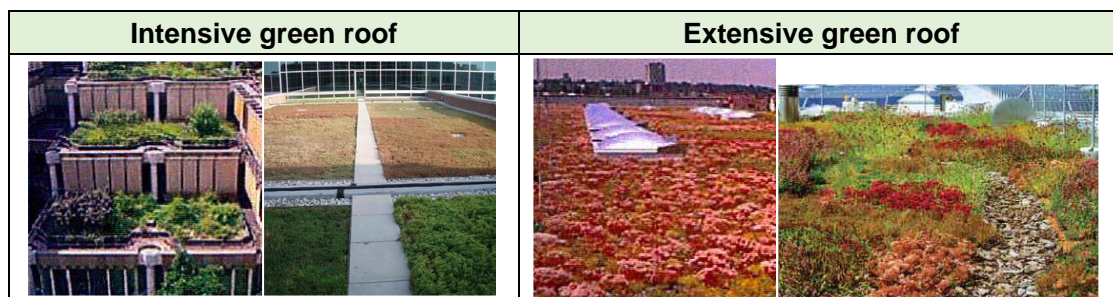


Figure 2.5: The typical intensive and extensive green roof [60]

**For both green roof types, the energy saving effect was brought by three aspects.**

Firstly, it can reduce the amount of energy absorbed by roof from solar radiation; Secondly, it can provide extra thermal insulation, as well as, increasing thermal mass ability by various growing medium, such as soil, and the moisture content and air inside it. Besides, it can reduce heat gain by evaporative cooling from plants and soil system [61]. Whereas, only the first two effects will be considered in the presented research in the following chapters, the last one normally not be accounted as it can be easily influenced by continuously changing variables, such as, ambient temperature, air and soil moisture content.

● **Reducing the solar absorption of a roof**

The ratio of total reflected to incident electromagnetic radiation is defined as albedo. Roof surface temperature can be dramatically decreased by increasing the albedo from green surface. According to FiBRE [62], in summer, the exposed area of a black roof can reach 80 °C when a same area beneath a green roof is only 27°C. This is benefit from the reduced latent heat and improved reflectance of incident solar radiation. Gaffin (2005) [63] mentioned that green roofs cool as effectively as the brightest possible white roofs, with an equivalent albedo of 0.7–0.85, compared with a typical value of 0.1–0.2 of a bitumen/tar/gravel roof [64].

For the convenience of calculation, equivalent albedo of green roof is normally set at 0.8

for all planting species. The outdoor integrated temperature  $t_{sa}$  can be reduced by a decreased equivalent albedo, expressed by Eqs. 2.1 to 2.2.

$$T_{sa} = T_a + \frac{\rho_s I}{\alpha_e} \quad (2.1)$$

$$\Delta T_{sa} = \frac{\Delta \rho_s I}{\alpha_e} \quad (2.2)$$

Where:  $T_{sa}$  is the outdoor integrated temperature, in K;  $\Delta T_{sa}$  is the integrated temperature difference between indoor and outdoor, in K;  $T_a$  is the outdoor air temperature, in K;  $\rho_s$  is solar radiation absorption coefficient,  $\rho_s = 1 - \text{albedo}$ ;  $\Delta \rho_s$  is solar radiation absorption coefficient difference;  $I$  is solar radiation on a horizontal surface, in W;  $\alpha_e$  is the outside surface heat transfer coefficient, taking  $19 \text{ W}/(\text{m}^2\text{K})$ .

- **Increasing extra thermal insulation of a roof**

Although previous researchers [60] indicated that the U-value of green roof cannot be directly included in the roof's U-value, as it is generally considered to be saturated. An equivalent U-value / -value R is introduced by researchers to reflect the additional thermal resistance from green roof.

Nichaou et al. [65] studied the green roof energy saving effect with different roof constructions. They found that, for the non-insulated roofs with or without the green roof, the estimated differences of the heat transfer coefficients varied from  $6\text{-}16 \text{ W}/(\text{m}^2\text{K})$ . Similarly, for the moderate insulated roofs the corresponding reduction were almost steady and equal to  $0.2 \text{ W}/\text{m}^2\text{K}$ . Finally, for the well-insulated roofs the differences of the heat transfer coefficients are much lower ranging from  $0.02$  to  $0.06 \text{ W}/\text{m}^2\text{K}$ . Based on this research, the U-Value reductions, which were caused by green roof (extensive, 100mm depth growing medium) on different insulated roofs are calculated and listed in table 2.3 below.

Table 2.3: The U-Value reduction caused by green roof on different insulated roofs

	Excellent insulated ( $\text{W}/\text{m}^2\text{K}$ )	Well insulated ( $\text{W}/\text{m}^2\text{K}$ )	Moderately insulated ( $\text{W}/\text{m}^2\text{K}$ )	Non insulated ( $\text{W}/\text{m}^2\text{K}$ )
U-value without green roof	$\leq 0.26$	0.26–0.4	0.74–0.80	7.76–18.18
U-value reduction from green roof	none	0.02 - 0.06	0.2	6-16



U-value with green roof	≤ 0.26	0.24–0.34	0.55–0.59	1.73–1.99
Equivalent R-value of green roof	none	0.36	0.46	0.45

In order to recognize the insulation effect from various growing medium depth, the simplified approach is suggested by Wong [66] who using DOE-2 in thermal simulation. The increasing of growing medium will bring certain thermal resistance which is 0.4 m<sup>2</sup>K/W per 100mm dry soil and 0.063 m<sup>2</sup>K/W per 100mm 40% moisture soil. Thus, the green roof equivalent U-value is calculated as Eq. 2.3 below.

$$\frac{1}{U_{gre}} = \frac{1}{U_e} + R_{medium} \times h \quad (2.3)$$

Where:  $U_{gre}$  is the U-value of green roof, in W/m<sup>2</sup>.K;  $U_e$  is the equivalent U-value, in W/m<sup>2</sup>.K, taking from table above;  $R_{medium}$  is the thermal resistance of medium, using 0.063 m<sup>2</sup>K/W per 100mm in this research;  $h$  is the thickness of growing medium, in m.

## 2.5 Review of green building simulation and optimization tools

To minimize the building energy demand and maximize energy performance, the principle and characteristic of building energy calculation tools need to be understood. Generally current energy estimate methods are forward modeling methods that based on a physical description of the building energy systems [67]. They can be used to determine the energy end-use as well as predict the energy saving effect from any energy saving measures. There are two basic types of energy demand calculation methods: steady-state methods and dynamic methods. The characteristic and the most typical example of each type will be described as follow.

### 2.5.1 Simplified manual calculation method (steady-state)

The simplified manual calculation methods for building energy estimation are generally convenient to be used by engineers as the calculations steps can be easily performed by hand or Excel. The energy demand are estimated by steady-state equations without involving the consideration of dynamic heat transfer, instantaneous change of building service system or their interactive effects. Recently, the most widely used steady-state methods recently are degree-day method and bin method.

**The “Degree Day” method proposed by Thom H.C. at 1952** [68] was the pioneer research of building energy mathematical estimation, which estimate the energy consumption within a period of time. The “degree day” method was firstly developed to compare the indoor comfort conditions and outdoor temperatures [68]. The heating degree day (HDD) was introduced with a threshold temperature of 65°F (traditionally used in USA), assumes that as long as the outdoor temperature drops below 65°F, the space heating is required. Originally, the earliest degree day method was only developed for heating period, and the result is roughly accurate only for domestic buildings without large heat gains, especially in cold countries. To improve its accuracy, a fixed correction factor for monthly heat gains is applied to deal with solar gains and internal gains from people and equipment.

To overcome the limitation of Degree Day method and to extend its application scope, following improvement were carried out. The accuracy for energy estimation is studied [69] by comparing the calculation results from degree-day method and the MBLTIIM method for commercial and industrial building examples. Meanwhile, its accuracy is highly depend on the accuracy of degree-day definition for specific region. An advanced degree-day calculation procedures was developed by Kusuda [70], the internal heat gains effects is involved by separating occupancy period into occupied and unoccupied. As almost all air-conditioning systems run at intermittent operations, some so-called “Extent Degree Day” (EDD) methods were developed to raise the prediction accuracy to reflect the effects of the running schedule of air-conditioning systems. The average solar transmission coefficient was defined to estimate the effect of blind, and the time correction coefficient was also involved to consider the unstandardized running time of air-conditioning systems [71]. Through the improvement of degree-day method, it is capable for a rough energy estimation and the accuracy can satisfy the basic engineering need especially for space heating.

**Another wide-recognized steady-state method is the bin method** [72], which is similar with and developed from the variable-base degree day method (an improved degree day method) but relies on bin weather data. In a classical bin method, the outdoor

temperature are grouped into bins of equal size, typically 5 °F (2.8°C) bins. The number of hours of occurrence is determined for each bin. For other weather variables, only average values coincident to each temperature bin are determined. The resulting weather data from classical bin method is often referred as one-dimensional bin weather data. The accuracy of classical bin method is adequate only for building dominated by sensible heat loads and without significant thermal mass effects [73] [74]. To improve its accuracy for buildings with heavy latent loads, ASHRAE introduced the two-dimensional weather data bins which generated based on bins obtained for day-bulb temperature and humidity ratio. Benefit from it improved accuracy that considered more reliable than Degree-day method, bin methods were used not only for hand conceptual calculation, but also involved in some computer building simulation tools [75], especially for residential or small scale public buildings.

### **2.5.2 The quasi-steady-state calculation tools**

The quasi-steady-state methods, which developed in 1980s, improved a lot than steady-state methods in terms of calculation accuracy for buildings with heavy heat gains. The quasi-steady-state methods calculate the heat balance over a sufficiently long time (months or seasons), which estimate the dynamic effects by empirically determined gain and/or loss utilization factor. One of the most typical and widely recognized quasi-steady-state methods is the monthly heat balance method for heating. The representing approach is the CEN standard--EN ISO832, which is able to estimate the monthly or seasonal heating energy needs [76]. It involves a specific calculation process for monthly heat gains (internal, solar, etc.) and relative monthly correction factors, such as gain utilization factor. The correction factor are introduced to deal with the mismatch of hourly patterns for gains and losses. To fulfill the requirement of building cooling need, monthly heat balance methods was developed continually. EN ISO 13790:2008, which is the inheritor of EN ISO 832, includes an updated monthly heat balance method with extended estimating capability of monthly energy need for cooling with heat loss utilization factor [77].

To keep its consistency, accuracy and accessibility, monthly (or seasonal) quasi-steady-state calculation method for heating and cooling requires a large number of pre-defined, general input values for specific region. In the application of quasi-steady-state methods, it is suggested that using a dynamic simulation to improving and tuning the proposed quasi-steady state method, and in particular to refine the correlation used to calculate the utilization factors (i.e. The dynamic parameters that reduce the thermal gains value in heating and the thermal losses value for cooling) for every specific regions. Using similar method, some researchers (e.g. Jokisalo, Corrado, J.A. Orosa and Oliveira Panão) have carried out studies to improve the correlations and specific correction factors [78] [79] [80] [81], in order to adapt different weather conditions (especially for the cooling season) and building stocks' characteristics in respective countries.

Moreover, complicated building service systems can also be added to quasi-steady-state calculation method. For example, researchers added the pre-heating / pre-cooling and heat recovery feature in the calculation by using the hourly data of the typical day each month (to reduce the computation load) [82].

### **2.5.3 The dynamic calculation tools**

The study of dynamic methods starts from 1970`s, which use numerical or analytical methods to determine energy transfer among various building components and systems. These methods calculate the heat balance with short time-steps (typically one hour or quarter) and they are able to determine the energy transfer among various building systems. Since the huge time-consuming for boundary setting and computation load, these methods are always used in computer simulation programs, such as DOE-2, EnergyPlus and TRNSYS. They are able to account for several parameters that are crucial for accurate energy use prediction, especially for buildings with significant thermal mass, thermostat setbacks or setups, explicit energy storage, or climate control systems.

**DOE-2.1, developed by DOE, is one of the famous energy simulation tools, which have been widely used for more than 25 years around the world** [75]. There are five sub-programs in DOE-2.1: the BDL Processor works as translator of input data; LOADS

and SYSTEMS, PLANT, ECON work as simulation cores. The four simulation cores only work in a forward direction, which means no feedback can be sent back to previous step. The first core “LOADS” calculates the heat/cooling loads in a space, the heat transfer is based on the temperature difference between two adjacent spaces with thermal mass that accounted by weight factor method. The loads results are sent to the second core “SYSTEM” as input for the HVAC system calculations. Following by this, core “PLANT” and core “ECONOMICS” generate the energy need of building service system and the economic cost [83]. The Structure and working flow of the DOE-2.1 engine can be seen in Figure 2.6.

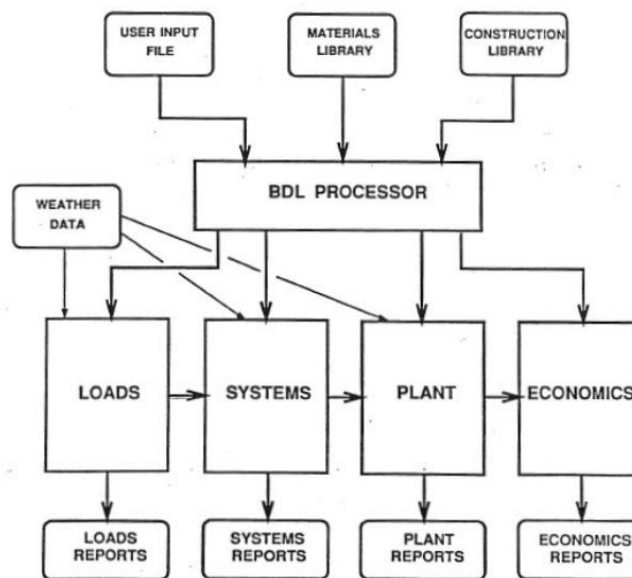


Figure 2.6: The structure and working flow of the DOE-2.1 engine [84]

Mathematically, the simulation cores of DOE correspond to a set of coupled integral-differential equations with complex boundary and initial conditions. DOE-2 program (sub-program) simulate the thermodynamic behavior of the building by approximately solving the mathematical equations. By far, based on the same simulation cores, more than 20 interfaces are developed to improve the usability of DOE.

**EnergyPlus, which based on two existing programs: DOE-2 and BLAST, was developed by US federal agency in 1996 and released in early 2001 [85].** It has a number of innovative simulation features, including variable time steps, user-configurable modular systems that are integrated with a heat and mass balance-based zone simulation, and input / output data structures tailored to facilitate third party module

and interface development. Other advanced simulation capabilities include multi-zone air-flow, solar thermal generation and photovoltaic power generation simulation [86].

The internal heat balance is the core method of energy calculation in EnergyPlus. The heat balance model include 4 coupled heat transfer approach [87], involving: 1) conduction through the building elements, 2) convection to the air, 3) short wave radiation absorption and reflectance and 4) longwave radiant interchange. The incident short wave radiation is from the solar radiation entering the zone through windows and emitted from internal sources such as lights. The longwave radiation interchange includes the absorption and emittance of low temperature radiation sources, such as zone surfaces, equipment, and people [88]. Based on the heat balance model above, the energy demand is calculated by workflow in Figure 2.7 below.

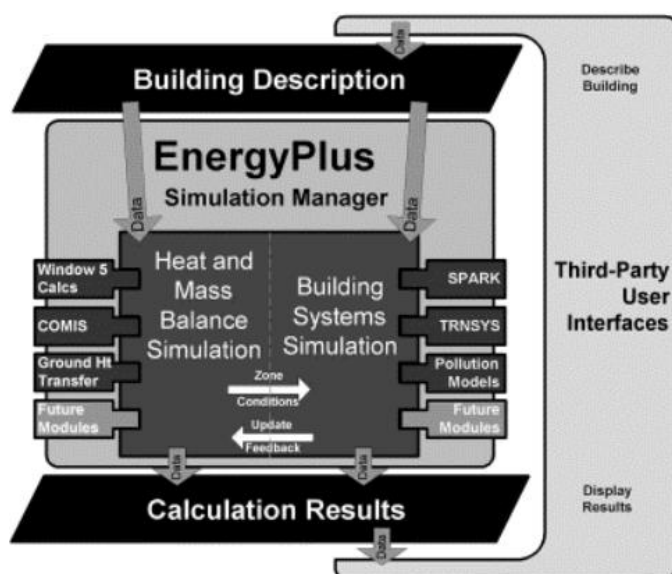


Figure 2.7: Working flowchart of EnergyPlus [85]

EnergyPlus is able to generate building energy profiles on 15 mins basis but requiring a significant amount of time, experience and effort to enter detailed building parameters. By the help of third-party user interface for geometry and system modeling, boundary condition definition and results refinement, the usability is much better but the simulation process is still not transparent to the user.

**ESP-r is a multi-purpose building energy simulation tool that developed since 1974**

[89]. It can simulate a wide range of building performance, including heat transfer through

building fabric (1/2/3D), the air flow (network and/or coupled, transient CFD), electrical power, embedded renewables, plant system components, indoor air quality and lighting assessments via Radiance. Building and flow simulations can be undertaken at frequencies of one minute to one hour and system simulations can be from fractions of a second to an hour [89].

Many building energy performance research has been done by ESP-r, including passive cooling test, active solar space integrate and even PCM performance prediction in buildings. Similar with EnergyPlus, the accuracy of ESP-r is widely recognized and validated [90], but still highly rely on the quality of detailed input of boundary conditions and the experience of user.

**In summary**, the dynamic calculation tools requires highly detailed physical descriptions and boundary conditions of a building to guarantee a relatively accurate energy estimation. Therefore, they are normally used in building performance research, building service analysis, detailed building design, or be a calibration tool in the adjustment of utilization factors of quasi-steady-state methods. However, they are not suitable as a primary guide tool in the early conceptual design stage.

## **2.6 Review of green building codes and evaluation systems**

The building energy codes and evaluation systems, which depend on different climates and energy supply conditions, are diverse in different countries and regions [91]. The Kyoto Protocol, established in 1997 and implemented in 2005 by all of the signed countries, is considered as an inducement and macro-guidance for modern building energy codes [92]. It is issued by the United Nations Framework Convention on Climate Change (UNFCCC) aiming at reducing the greenhouse gas level in the atmosphere which involve significant contribution from building sector. It is The specific building energy regulations and evaluation systems, which are formulated to help achieving Kyoto Protocol`s target, described as follow.

### 2.6.1 Building energy saving codes

**In Europe**, the European Directive 93/76 [93] is the first approach to calculate the building energy demands and establish energy certification system [94]. Then, the EnEv2002 and EnEv2006 regulations in Germany generated to control the primary energy use in building aspect. The Directive 2002/91/EC has been introduced to enhance the building energy efficiency and thermal performance in EU [95] and then became a European Law in January 2003. It became the national building regulation in the next few years, e.g. be reviewed in Scotland in 2006 and became part of it`s building regulation in 2007 [96]. Based on EU Directive 2002/91/EC, very specific energy and emission code is developed in each country. Such as in UK, the Building Regulations Part L2A (Part L2A) [97], which became effective from 2006, mentioned the U-value of roof, wall, floor and window should be limited under 0.25W/m<sup>2</sup>K, 0.350 W/m<sup>2</sup>K, 0.25 W/m<sup>2</sup>K and 2.2 W/m<sup>2</sup>K respectively, which are more strict than developing countries [98].

The directive covers 4 implements in all EU countries [99], including (1) establishing and applying a standard method for calculating building energy performance, (2) applying the minimum standards (improved for every 5 years) on energy performance for new building and renovated existing buildings, (3) establishing the energy performance certificates (EPCs) and environmental impact certificates (see Figure 2.8) for all constructed, sold or rented buildings, and (4) establishing the inspection and advising schemes on the energy efficiency of boiler and air-conditioning system.

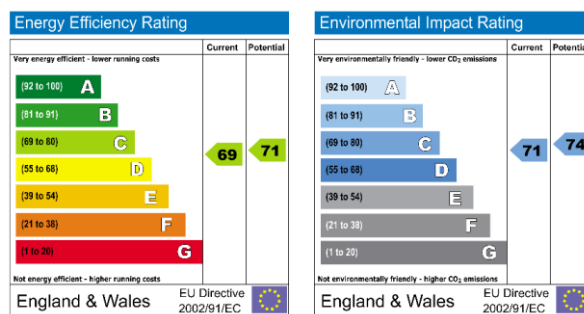


Figure 2.8: Energy performance certificates and Environmental impact certificates [99]

**In US**, the building energy codes for private and federal sector are different. The ANSI/ASHRAE/IESNA Standard 90.1 energy standard for Buildings [100], which



developed by ASHRAE, is the main energy code applied to private buildings, and enforced by state governments. It provides specific requirements for building envelope, HVAC, hot water, power and lighting system. Another main code for private buildings is the International Energy Conservation Code (IECC), which is published by International Code Council (ICC) specific for residential and commercial buildings and references several ASHRAE standards [101]. For Federal sector buildings, a final rule was established in 2007 based on ANSI/ASHRAE/IESNA Standard 90.1-2004. It is applied to new federal commercial and multi-family high-rise residential buildings [101]. For other public housing and FHA-insured housing, the “Energy Codes for HUD-Assisted and FHA-Insured Properties” set by the US Housing and Urban Development (HUD) agency are applied to control the minimum energy performance [102].

**In China**, the building energy code started from the “Design standard for energy efficiency of civil buildings (JGJ26-86)” in 1986 [103]. A 30% energy saving target was set based on a benchmark line from standard building model. Then the energy saving target was raised to 50% in the updated “Design standard for energy efficiency of civil buildings (JGJ26-95)” in 1995 [104]. The similar target can be found in “Design standard for energy efficiency of residential buildings in hot summer and warm winter zone (JG75-2003)” [105], as well as in “Design standard for energy efficiency of residential buildings in hot summer and cold winter zone (JGJ134-2010)” [106]. Specifically for public buildings, the most important code is the “Design standard for energy efficiency of public buildings (GB50189-2015)” [107], a 50% energy saving aim was set for all climate regions of China. For the most updated energy codes, such as “Design standard for energy efficiency of residential buildings in severe cold and cold zones” mandatory applied from 2010, a higher target of 65% energy saving is required in some specific regions.

### **2.6.2 Green building evaluation tools**

The green building evaluation system, unlike the building code, is not mandatory for decision-makers. They are more comprehensive assessment systems, which reflect the whole environmental-friendly level of a building, in terms of concerning over energy, air,

water, material, land use aspects and etc.

**In UK, BREEAM, as a representative Europe green building evaluation tool, was launched in 1990 by BRE.** It is the first green building evaluation tool and the foundation of LEED and many other evaluation tools. Up to now, there are more than 250,000 BREEAM certified buildings in the world and the BREEAM registered building is even 5 times more. BREEAM is highly flexible. It can be applied to virtually any building and location, with specific versions for new buildings, existing buildings, refurbishment projects and large developments.

A BREEAM certified building need to gain points from 49 individual evaluation aspects spanning 9 environmental categories, plus one “innovation” category. The categories include the aspects of management, health and well-being, energy, transport, water, material, waste, land use and ecology and pollution. For every evaluation aspects, as long as the building meets the “best practice” performance level defined by BREEM, the points are given to this building. The building will then be labeled by BREEAM rating based on the sum of gained points with different weight. A building rated with BREEAM outstanding means its performance laid in top 1% of UK buildings, the excellent, very good, good, pass rating means the building is in top 10%, 25%, 50% and 75% respectively. Figure 2.9 shows the BREEAM outstanding certificate for a building in University of Nottingham.

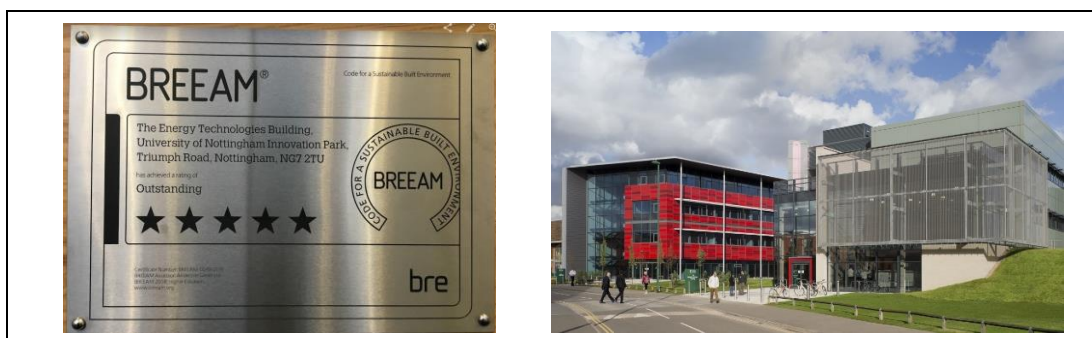


Figure 2.9: BREEAM outstanding certificate for a building in University of Nottingham

**In US, Leadership in Energy & Environmental (LEED) was developed in 1998 by USGBC.** It has iterated 5 versions and the latest one LEED 3.0 was published in 2009[76]. Today, LEED consists of a set of nine rating systems for the design, construction and

operation of buildings, homes and neighborhoods. Five overarching categories correspond to the specialties available under the LEED Accredited Professional program. In the latest version, there are 100 possible base points distributed across five major credit categories: Sustainable Sites, Water Efficiency, Energy and Atmosphere, Materials and Resources, Indoor Environmental Quality, plus an additional 6 points for Innovation in Design and an additional 4 points for Regional Priority. Under LEED evaluation system, buildings can be qualified by four levels of certification [108]. LEED is widely applied in many countries. Since its inception in 1998, the U.S. Green Building Council has grown to encompass more than 7,000 projects in the United States and 30 countries, covering over 1.501 billion square feet (140 km<sup>2</sup>) of development area [109].

**In China, the “Green Building Evaluation Standard (Three Star)” was published by China green building council (CGBC) and took effect in 2006 [110].** This Green Building Evaluation Standard is regarded as a counterpart to LEED in China [111]. The standard cover six sections, which are: (1) land conservation, (2) energy conservation, (3) water conservation, (4) material conservation, (5) indoor environmental quality, and (6) operation and management throughout the life cycle of residential and public buildings [112]. Each section contains control items (requirements), recommended, general items and preferred items with different weighing in rating point system. Since 2006, CGBC has developed a series of regulations and programs to promote green buildings, such as the “Green Building Demonstration Projects” (2007) and “Green Building Evaluation Labeling” (2008) [113], which label the building base on its scores gained from Green Building Evaluation Standard. Similar to LEED system, the China green building evaluation standard labels building in three levels. Moreover, the “three star” evaluation system allows developers to submit the building design and achieve “pre-certification”, which they can then market to prospective tenants before the building is built [113]. Up to now, there are over 3000 building projects labeled with “Green Building Evaluation Labeling” system, in which over 1200 and 600 got the “two star” label and top “three star” label respectively [114].

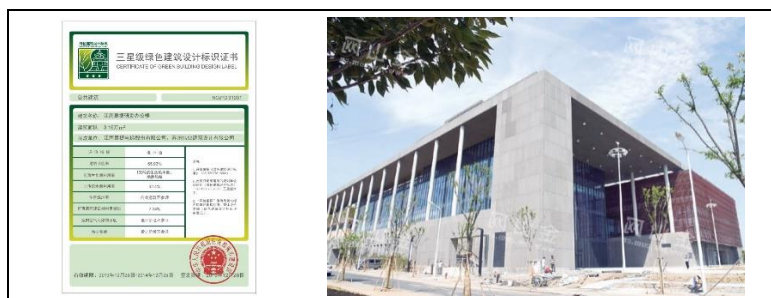


Figure 2.10: The “Three Star” label for a building in Shanghai

## 2.7 Summary of literature review

Through the literature reviewed in this chapter, (1) the current situation of office building energy consumptions and related pollutant emissions are studied; (2) the most appropriate green building technologies and design strategies are identified; (3) the available building energy estimation tools are investigated; and at last (4) the popular building energy codes and green building evaluation systems are summarized.

According to the understanding of related literature in this field, limitations and shortcomings in the previous research are summarized and listed below:

- **There is no mature method to comprehensively reflect the generalized environmental impact from whole life-cycle of office building.** Although the energy consumption and pollutant emissions caused by office building is deeply studied, the previous studies are mostly focus on the environmental haze from a single factor, e.g. energy or CO<sub>2</sub>e itself. Comprehensive environmental impact that involving the effects from both energy consumption and multi pollutant emissions is still missing. Applying a design feature in real practice is a trade-off for the green effect, e.g. one pollutant can be reduced while another one will increase. The investigation of energy and pollutant along is not able to provide the overall understanding for the quality of green design. **Thus**, a comprehensive analysis method and an innovated metric for the building overall environmental impact need to be developed in this research, in order to reflect the overall environmental impacts from all pollutants during whole building life-cycle together. By using this metric and the energy consumption data, the “green performance” for whole buildings (or

specific design features) can be evaluated and compared.

- **The study for the interaction of multi green building technologies is still incomplete.** In the previous research, many novel technologies for building energy saving were deeply developed and their effect were well proved. But unfortunately, the research for the interaction between different technologies, especially between active technologies and passive design strategy is incomplete. The building design is a trade-off of different measures under limited budget. For instance, a small building shape coefficient brings smaller envelop heat transfer area thereby reduce the insulation requirement, whereas it also reduce the available wall/roof area for solar thermal collector installation. The interaction results from the combination of green building technologies and design strategies are not fully investigated. **Therefore**, developing a method to select most suitable technologies and evaluate the proper assortment of technologies integrated in one specific office building is necessary.
- **The current energy estimation tool is either too complicated or too inaccurate for green building design in early conceptual design stage.** The dynamic energy estimation method are accurate enough, but it require too much design details on building geometry and building service system that are not available for the early conceptual design stage. Whereas, the hand calculation method has been proved lack of accuracy especially for office building type (huge internal gain and cooling need). The lack of proper energy estimation tool in the early design stage will lead to the undesired green building design and bring bad consequence for further detailed design stage. **Therefore**, a simplified energy estimation method is need, which requires limited input based on conceptual design (e.g. building floor area, shape, approximate orientation, proposed green building measures, etc.) and provide quick feedback with acceptable accuracy.
- **The current green building evaluation systems are all process-orientated which cannot directly control the final environmental impact.** The current green building evaluation tools are all point-based system, assessing and giving points to each environment related aspects accounted in the evaluation system. The

evaluation result (sum of points) only reflects the application of measures rather than fully represents the environmental impact of building design, since the points for one aspect is not interchangeable. For instance, the point of using localized materials cannot be gained once the material is transported from long distance. Even if the environmental benefit for energy saving and pollutants reducing by using the material (which might be an advance insulation material) is far more than enough to offset the environmental harm during transporting. **Therefore**, a result-orientated green building evaluation system needs to be developed, based on the estimated overall environmental impact from energy and all main pollutants during life-cycle of building. The results from the innovated evaluation system need to be more simple and comparable. They are also required to directly reflect the environmental related design quality.

To overcome the mismatch between current research and actual design needs of green building described above, in the following chapters: **(1)** an simplified operational energy estimation tool specialized for the early conceptual design stage of China office building will be developed in **Chapter 3**; **(2)** a calculation method for the energy consumption and pollutant emissions for whole life-cycle of office building will be established in **Chapter 4**; **(3)** based on the pollutant data, a general environmental impact metric for building relevant pollutants will be established in **Chapter 5**, in order to reflect the building comprehensive environmental impact; and at last; **(4)** a multiple criteria based green design evaluation and selection system will be developed in **Chapter 6**, enabling the result-oriented green building evaluation and selection, based on its energy consumption, environmental impact and cost; and **(5)** in the last, a computer aided tool that integrate all methods together is developed in **Chapter 7**, to enable the fast and convenient green design optimization and selection.

**Chapter 3. Development of the operational energy estimation model applicable to the  
earlier stage conceptual design for Chinese office buildings**

### 3.1 Introduction

Building operational energy consumption is one of the key factors in green building design assessment. For conceptual design in the building's early design stage, the estimated operational energy demand is a significant reference for design selection and modification. Although the detailed energy simulation tools (e.g. ESP-r, EnergyPlus etc.) are able to provide a more accurate result, they need a lot more details in building characterization, detailed parametrical inputs and long computing time, which are not available during the early design stage.

A compared simple building operational heating / cooling demand estimation method, the EN ISO13790 [77] has been established based on the compulsory building energy performance assessment requirements by EPBD (European Directive on the energy performance of buildings). A lot of previous researches have been undertaken to assess the performance of buildings on the basis of EN ISO13790; these include justification of accuracy testing, analysis of discrepancies between different applications in new or existing buildings and the relationship between the estimated energy and internal comfort level. Although this needs less computing time compared to detailed energy simulation tools, it still needs extensive design details that cannot be obtained in the early design stage.

**The aim of this chapter is to develop a building operational energy estimation tool that needs less parametrical inputs, has a quick results feedback, and is therefore applicable to the early design stage of Chinese office buildings.** An hourly energy estimation method refined from EN ISO 13790 for the main energy (i.e. HVAC) consumption of Chinese office buildings is established using labelling through the HVAC module, accompanied by the additional energy (i.e. lighting, office appliance and hot water) consumption module and renewable energy generation module, to form a new tool, which is termed as **CN13790**. In order to enhance its adaptability for the new task in China and to reduce calculation time, during the generation of CN13790, some complicated building component models have been replaced by simplified models with



localized datasets while maintaining the basic heat balance framework. This is achieved in correspondence to typical designs under Chinese building design regulations and weather conditions.

**The advantage of the new energy estimation tool is that** the input is highly simplified, excluding the consideration of indoor space partition and detailed building service systems which cannot be given at the conceptual design stage. Benefits from the prepared dataset, which are particularly localized for the China office buildings, are the limitation in inputs requirement. They are even simpler and faster. Meanwhile, the results can be fed back to the designer in seconds, which is dramatically time saving for the early design stage.

In the following context, **(1)** the **methodology** for the whole chapter is given; **(2)** followed by the **detailed description** for the principle of original EN ISO 13970 heat balance framework for the HVAC calculation. **(3)** Next, the refinement for the EN ISO13790 is carried out with some simplified model and calculation method for typical components of China office building added to the existing framework, by which the HVAC module of CN13790 is generated. **(4)** After that, the adaptability and accuracy validation for the HVAC module of CN13790 is performed as well as the calculation efficiency test, by comparing to estimation results for typical building cases using existing simulation tools. **(5)** At the end of the Chapter, the additional energy consumption module and the renewable energy generation module are added to the CN 13790 to generate the overall building energy demand. Thus, the new operational energy estimation tool for the Chinese office building is complete.

### 3.2 The Methodology applied in this chapter

In order to generate the CN13790 method for the operational energy estimation of China's office buildings, three modules (i.e. the HVAC module, additional energy consumption module and the renewable energy generation module) are established. Each of the modules is comprised of several sub-models derived from the refinement of EN

ISO13790 or existing methods respectively. The research method applied to the module development is described in Figure 3.1 below.

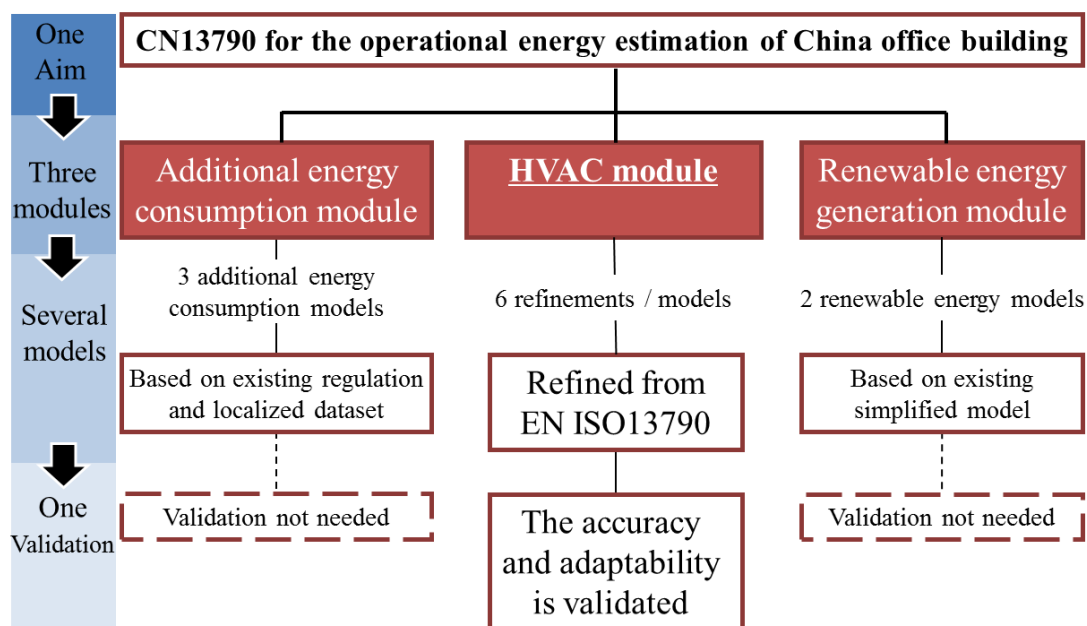


Figure 3.1 : The research method applied in the module development

**The HVAC module consists of** , six models, i.e., five models refined from original EN ISO13790 and one model calculating the electricity demand, all of which make use of the localized datasheets as the source of the parametric input.

The research methods applied to the models refinements and development are outlined as follows:

- The development of a simplified method for classification of the building zone. The building selected in the HVAC module is treated as a single zone that can simplify the parametric inputs of the models at the earlier design stage. A Literature review was conducted to generate the adjustment factor that is used in the correction of the energy demand results.
- The development of a simplified method for determination of the thermal mass of a office building. The thermal mass values for four typical types of office structures were computed and applied to the the established HVAC module, while the calculation of the thermal mass for each single building element is exempted. A case

study was then carried out to gather the highest and lowest thermal mass figures for each office structure type. On this basis, statistical analysis was undertaken to generate the representative thermal mass values and the correlation between the thermal mass value and the building's floor area.

- The development of a simplified and China-focused model for the windows and the glazing wall. This model will be then implemented into the HVAC module. During the model development, heat transfer equations appropriate to the frame, glass, filled gap and low-e coating are identified from the literature reviews. Furthermore, the China-focused datasets for the window/glazing wall components are then established by market products investigation.
- The development of the simplified and localised model for opaque walls and the roof. This refinement is similar to the last section, the structure for both the wall and the roof is summarised into a "4 layer model" by a study of the general wall/roof structure in China, the data set for materials of each layer is gathered from the literature review and the available market products investigation. Meanwhile, the suitable heat transfer model is referenced from the building standards through a literature review as well.
- A simplified and China-adaptive model for underground space is developed and integrated into the HVAC module based on the established national building standards. A China-focused dataset relating to the typical materials applicable to the underground construction was also established based on the literature studies and market products investigation of currently available building elements for underground space construction and associated Chinese building regulations.
- A simplified and China-focused electricity demand model for HVAC systems was developed and integrated into the HVAC module. This, by applying the HVAC EER (energy efficiency ratio) method, enabled the conversion of the heating and cooling loads into the electricity demand. On this basis, a dataset for electricity demand of the currently available HVAC systems is established.

- The whole HVAC module was then tested through a dedicated case study. The module comprises nine models that can represent the key design factors relating to the Chinese office buildings. These models are compared each other through a dedicated case study and as a result, the china-adaptability of the models was consequently assessed.

**In the additional energy estimation module**, the lighting and office appliance energy needs were collected from the regional and national design guides, while the hot water energy need was calculated from the dataset for the currently available building compoments.

**In the renewable energy generation module**, the existing models for solar PV and thermal systems are set to the default ones, while the energy generation estimation methods for both systems are quoted from the literature review. Meanwhile, a dataset for soalr PV and thermal products was established based on the products investgation to the currently available ones of these kinds.

### 3.3. The principles of the original EN ISO13790 estimation method

#### 3.3.1 The basic heat balance framework of the EN ISO13790 hourly method.

The basic heat balance framework of the EN ISO13790 hourly method is described in this section. In the EN ISO13790, a quasi-steady-state dynamic model of building heat transfer is established in the form of the electrical scheme with RC elements, voltage and current source, based on the thermal-electrical analogy. To be more specific, the heat transfer for any given building zone can be described by a thermal resistance-capacitance model with 5 resistances and 1 capacitance (5R1C). The schematic of the 5R1C model is shown in Figure 3.2.

There are 5 nodes that represent the temperatures at different nodes, namely, **(1)** internal air node( $\theta_{air}$ ), **(2)** surface node( $\theta_s$ ), **(3)** builidng mass node( $\theta_m$ ), **(4)** external air node ( $\theta_e$ ), and **(5)** supply air node( $\theta_{sup}$ ). Between the nodes, five resistances representing the thermal conductance characteristics are in place; these are (1) the thermal transmission

coefficients for transparent or very light building elements with “zero” thermal mass ( $H_{tr,w}$ ), such as windows, doors, curtain wall, etc; the thermal transmission through opaque and heavy building elements ( $H_{tr,op}$ ) are split into (2)  $H_{tr,em}$  and (3)  $H_{tr,ms}$  representing the connection of external air to the building mass and internal surface to building mass respectively; (4) the ventilation thermal transfer ( $H_{ve}$ ) and, (5) the coupling conductance ( $H_{tr,is}$ ). Apart from the internal heat capacity ( $C_m$ ) and effective mass area ( $A_m$ ), the key elements of building heat transfer are built by the use of nodes, resistances and capacity in the 5R1C model.

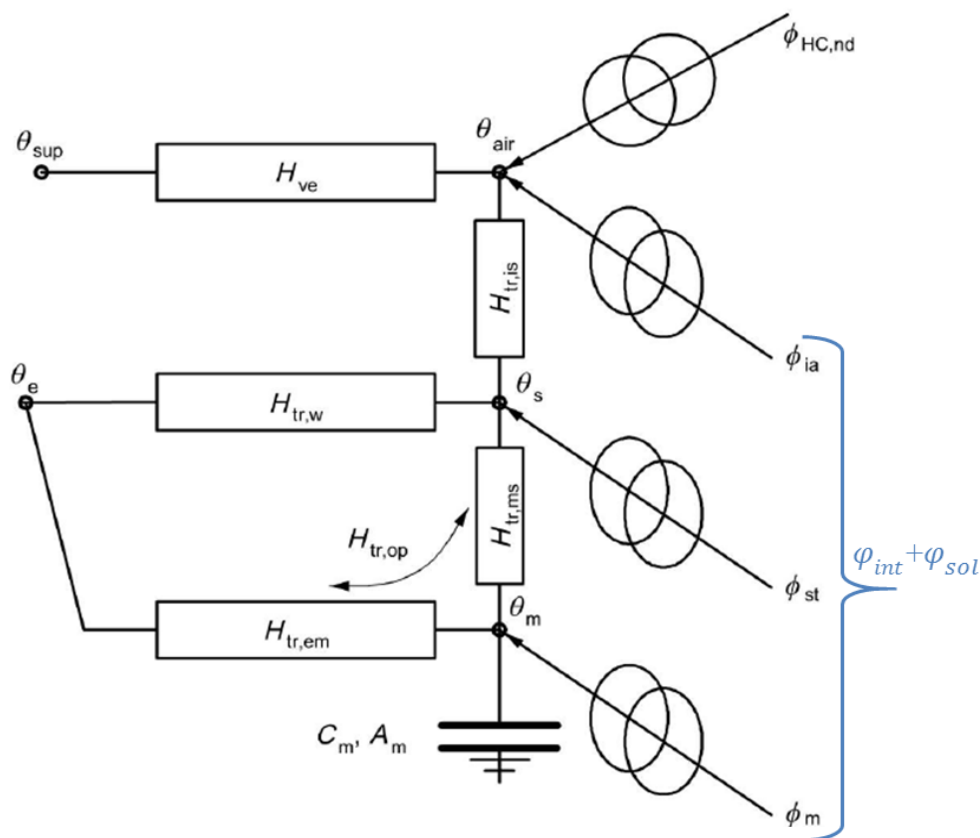


Figure 3.2: The schematic of 5R1C model [77]

**The thermal transfer principle for the 5R1C model are described as follows:**

The heating/cooling needs ( $\phi_{HC,nd}$ ) refer to supply and discharge of heat energy from the indoor air node ( $\theta_{air}$ ), in order to maintain the required indoor air temperature ( $\theta_{int,H,set}$  for heating set point and  $\theta_{int,C,set}$  for cooling set point). The total internal heat gain ( $\phi_{int}$ ) and solar heat gain ( $\phi_{sol}$ ) are distributed into three sections (i.e.,  $\phi_{ia}$ ,  $\phi_{st}$

and  $\varphi_m$ ) that represented by the heat transfer of internal air through the indoor air node ( $\theta_{air}$ ), between the indoor air and the internal façade surface using surface node ( $\theta_s$ ), and within building fabric block via the building mass nodes ( $\theta_m$ ). Apart from the internal gain and solar gain, the indoor air temperature ( $\theta_{air}$ ) will also be affected by the supplied air temperature ( $\theta_{sup}$ ) through ventilation heat transfer ( $H_{ve}$ ) and by the external environment temperature ( $\theta_e$ ) through heat transfer within transparent ( $H_{tr,w}$ ) and opaque ( $H_{tr,op}$ ) building elements. The heat will be transferred and balanced by the comprehensive effect of the potential between the nodes (caused by the temperature difference of the nodes), through thermal resistance and capacity.

### 3.3.2 The mathematical correlation between the variables of the 5R1C model

The state and measurable variables (e.g. temperature, thermal capacity) of the 5R1C model are taken from the physical parameters of the building/environment as the initial input, whereas the immeasurable variables are derived by the following mathematic equations.

- The building thermal mass related variables, the effective mass area ( $A_m$ ) expressed in  $m^2$ , and the internal thermal mass ( $C_m$ ) expressed in J/K, are delivered by the Eqs. 3.1 and 3.2 below.

$$A_m = C_m^2 / (\sum A_j k_j^2) \quad (3.1)$$

$$C_m = \sum k_j A_j \quad (3.2)$$

Where,  $A_j$  is the area of the building element  $j$ , in  $m^2$ ;  $k_j$  is the internal heat capacity per  $m^2$  of building element,  $j$ . In this research, the “effective thickness” of 0.1m (refers to ISO 13786) is applied.  $A_m$  and  $C_m$  are generated by a simplified calculation method, described in section 3.4.2 below.

- The correlations between the thermal transmission coefficients of the opaque building parts,  $H_{tr,em}$ ,  $H_{tr,ms}$ , and  $H_{tr,op}$  are shown in Eqs. 3.3 and 3.4.

$$H_{tr,ms} = h_{ms} A_m \quad (3.3)$$

$$H_{tr,em} = 1 / \left( \frac{1}{H_{tr,op}} - \frac{1}{H_{tr,ms}} \right) \quad (3.4)$$

Where:  $h_{ms}$  is the heat transfer conductance between building mass node( $\theta_m$ ) and surface node( $\theta_s$ ). According to ISO13790, the value of  $h_{ms}$  is 9.1 W/(m<sup>2</sup>K), while  $A_m$  and  $H_{tr,op}$  are previously indicated.

- The coupling conductance,  $H_{tr,is}$ , between  $\theta_{air}$  and  $\theta_s$  is given by Eq. 3.5.

$$H_{tr,is} = h_{is} A_{tot} \quad (3.5)$$

Where,  $h_{is}$  is the heat transfer coefficient between the  $\theta_{air}$  and  $\theta_s$ , with the value of 3.45W/(m<sup>2</sup>K) (refer to ISO 13790);  $A_{tot}$  is the surface area adjacent to the conditioned zone of the building that can be measured from the planning of the building, in m<sup>2</sup>.

- The ventilation heat transfer rate,  $H_{ve}$ , in W/K, is expressed by Eq. 3.6.

$$H_{ve} = \rho_a c_a \left( \sum_k b_{ve,k} q_{ve,k,mn} \right) \quad (3.6)$$

Where,  $\rho_a c_a$  is the thermal capacity of air, taken as 1200 J/(m<sup>3</sup>K);  $q_{ve,k,mn}$  is the time average airflow rate from an air flow source  $k$ , expressed in m<sup>3</sup>/s;  $b_{ve,k}$  which is the supply air temperature adjustment factor, where  $b_{ve,k}$  is not equal to 1 in the case of pre-heating/cooling or the heat recovery system applied.

- The building heat gains from solar and internal heat sources, are reflected by the internal air temperature node( $\theta_{air}$ ), the building mass temperature node( $\theta_m$ ), and the surface node( $\theta_s$ ). The heat gain fluxes distributed across 3 nodes are represented by  $\Phi_{ia}$ ,  $\Phi_m$  and  $\Phi_{st}$  respectively, which are expressed in Eqs 3.7, 3.8 and 3.9.

$$\Phi_{ia} = 0.5\Phi_{int} \quad (3.7)$$

$$\Phi_m = A_m/A_{tot}(0.5\Phi_{int} + \Phi_{sol}) \quad (3.8)$$

$$\Phi_{st} = \left( 1 - \frac{A_m}{A_t} - H_{tr,w}/9.1A_t \right) (0.5\Phi_{int} + \Phi_{sol}) \quad (3.9)$$

Where,  $A_m$  (the effective mass area),  $A_{tot}$  (the surface area adjacent to the conditioned zone) and  $H_{tr,w}$  (the heat transfer within transparent elements) are previously defined;  $\Phi_{int}$  is the heat flow rate from the internal heat sources, obtained from the building's real data or building standard, in W;  $\Phi_{sol}$  is the heat flow rate from the solar heat source, in W, which can be calculated by using Eqs 3.10 to 3.12, as below:

$$\Phi_{sol} = F_{sh,ob,k} A_{sol,k} I_{sol,k} - F_{r,k} \Phi_{r,k} \quad (3.10)$$

Where,  $F_{sh,ob,k}$  is the shading reduction factor for external obstacles influencing the effective solar collection area of elements surface  $k$ ;  $A_{sol,k}$  is the solar effective collecting area of surface  $k$ , equal to the area of a black body having the same solar heat gain as surface  $k$ , in  $m^2$ , given by Eq. 3.11 for transparent elements and Eq. 3.12 for opaque elements;  $I_{sol,k}$  is the solar irradiance on the collecting area of surface  $k$ , with the given orientation and tilt angle over the calculation time step, in  $w/m^2$ ;  $I_{sol,k}$  is the provided anisotropy by considering both circumsolar and isotropic terms including direct, diffuse and reflected radiation, in  $w/m^2$ , corresponding to the common Hay's method [115];  $F_{r,k}$  is a factor between the building element and sky, its value is 1 for horizontal roof and 0.5 for vertical wall;  $\Phi_{r,k}$  is the heat flow by thermal radiation from building surface  $k$  to the sky, in W, as determined in Eq. 3.13.

$$A_{sol,tra} = F_{sh,gl} g_{gl} (1 - F_F) A_{w,p} \quad (3.11)$$

$$A_{sol,opa} = a_{s,c} R_{se} U_c A_c \quad (3.12)$$

Where,  $A_{sol,tra}$  and  $A_{sol,opa}$  are the solar effective collecting area for transparent and opaque elements respectively, in  $m^2$ ;  $F_{sh,gl}$  is the shading reduction factor for the moveable shading device;  $g_{gl}$  is the total solar energy transmittance of the transparent part (e.g. glass);  $F_F$  is the ratio of the projected frame area to the overall projected area of a building part (e.g. a window);  $A_{w,p}$  is the overall projected area of a building part (e.g. window), in  $m^2$ ;  $a_{s,c}$  is the absorption coefficient for solar radiation of the opaque part;  $R_{se}$  the external surface heat resistance of the of the opaque part, in  $m.K/W$ ;  $U_c$  is the thermal transmittance of the opaque part, in



W/m<sup>2</sup>.K;  $A_c$  is the projected area of the opaque element, in m<sup>2</sup>.

$$\Phi_{r,k} = R_{se} U_c A_c h_r \Delta\theta_{er} \quad (3.13)$$

Where,  $R_{se}$ ,  $U_c$  and  $A_c$  are previous defined;  $h_r$  is the external radioactive heat transfer coefficient, in W/(m<sup>2</sup>k), with correspondence to a 10°C average temperature is used in this method;  $\Delta\theta_{er}$  is the average difference between the external air temperature and apparent sky temperature. The suggested value in ISO13790 9K, 11K, and 13K are used for sub-polar, intermediate and tropical regions respectively.

- The indoor air temperature,  $\theta_{air}$ , can be calculated by applying the heating/cooling energy balance approach, expressed by Eq. 3.14:

$$\theta_{air} = (H_{tr,is}\theta_s + H_{ve}\theta_{sup} + \Phi_{ia} + \Phi_{HC,nd}) / (H_{tr,is} + H_{ve}) \quad (3.14)$$

Where,  $\theta_s$  is the temperature of the surface node, in K, and expressed by Eq. 3.15; all other variables are previously defined.

$$\theta_s = \left[ H_{tr,ms}\theta_m + \Phi_{st} + H_{tr,w}\theta_e + H_{tr,1}(\theta_{sup} + \frac{\Phi_{ia} + \Phi_{HC,nd}}{H_{ve}}) \right] / (H_{tr,ms} + H_{tr,w} + H_{tr,1}) \quad (3.15)$$

Where,  $\theta_m$  is the average temperature of the building mass for the temperature of given time step ( $\theta_{m,t}$ ), and the temperature of last time step ( $\theta_{m,t-1}$ ), in K; determined in Eq.3.16:

$$\theta_m = (\theta_{m,t} + \theta_{m,t-1}) / 2 \quad (3.16)$$

Where, the  $\theta_{m,t}$  is the building mass's temperature of given time step;  $\theta_{m,t-1}$  is the building mass's temperature of last time step. The building mass temperature of the given time step,  $\theta_{m,t}$ , can be expressed by Eq.3.17:

$$\theta_{m,t} = \left\{ \theta_{m,t-1} \left[ \left( \frac{C_m}{3600} \right) - 0.5(H_{tr,3} + H_{tr,em}) \right] + \Phi_{mtot} \right\} / \left[ \left( \frac{C_m}{3600} \right) + 0.5(H_{tr,3} + H_{tr,em}) \right] \quad (3.17)$$

Where, all the variables have been previously defined, whereas four intermediate variables,  $\Phi_{mtot}$ ,  $H_{tr,1}$ ,  $H_{tr,2}$  and  $H_{tr,3}$ , (addressed in box below) are applied to increase the readability.

$$\Phi_{mtot} = \Phi_m + H_{tr,em}\theta_e + H_{tr,3} \left[ \Phi_{st} + H_{tr,w}\theta_e + H_{tr,1}(\theta_{sup} + \frac{\Phi_{ia} + \Phi_{HC,nd}}{H_{ve}}) \right] / H_{tr,2} \quad (3.18)$$

$$H_{tr,1} = 1/(1/H_{ve} + 1/H_{tr,is}) \quad (3.19)$$

$$H_{tr,2} = H_{tr,2} + H_{tr,w} \quad (3.20)$$

$$H_{tr,3} = 1/(1/H_{tr,2} + 1/H_{tr,ms}) \quad (3.21)$$

### 3.3.3 The calculation procedure for indoor temperature and heating/cooling energy demand.

Using the key variables generated in the above section, the indoor air temperature,  $\theta_{air}$ , and the corresponding energy needed for heating/cooling,  $\Phi_{HC,nd,ac}$ , can be calculated by a Crank-Nicolson scheme [116] based solution model in the form of a 4-step approach.

**The principle of this 4-step calculation procedure** is to constantly ensure the indoor air temperature,  $\theta_{air}$  to reach the set-point temperature with the assistance of the actual heating/cooling power,  $\Phi_{HC,nd,ac}$ . The indoor air temperature,  $\theta_{air}$ , and the heating/cooling supply,  $\Phi_{HC,nd}$ , are calculated on hour basis by using Eq.3.14. For each single hour in which the normal control strategy to the HVAC system is applied, if the  $\theta_{air}$  is lower than the heating set point temperature,  $\theta_{int,H,set}$ , or higher than the cooling set point temperature,  $\theta_{int,C,set}$ , the heating and cooling energy will be supplied to buildings with the power at  $\Phi_{HC,nd}$  (no excess the maximum HVAC heating capacity  $\Phi_{H,max}$  or the cooling capacity  $\Phi_{C,max}$ ). If  $\Phi_{HC,nd}$  is sufficient, at the beginning of next time-step (next hour),  $\theta_{air}$  is kept at the set-point temperature, no air conditioning is in need, the  $\Phi_{HC,nd}$  will be set as 0, otherwise, a given  $\Phi_{HC,nd}$  will still be supplied to the building. The 4 step calculation procedure can be seen in Figure 3.3.

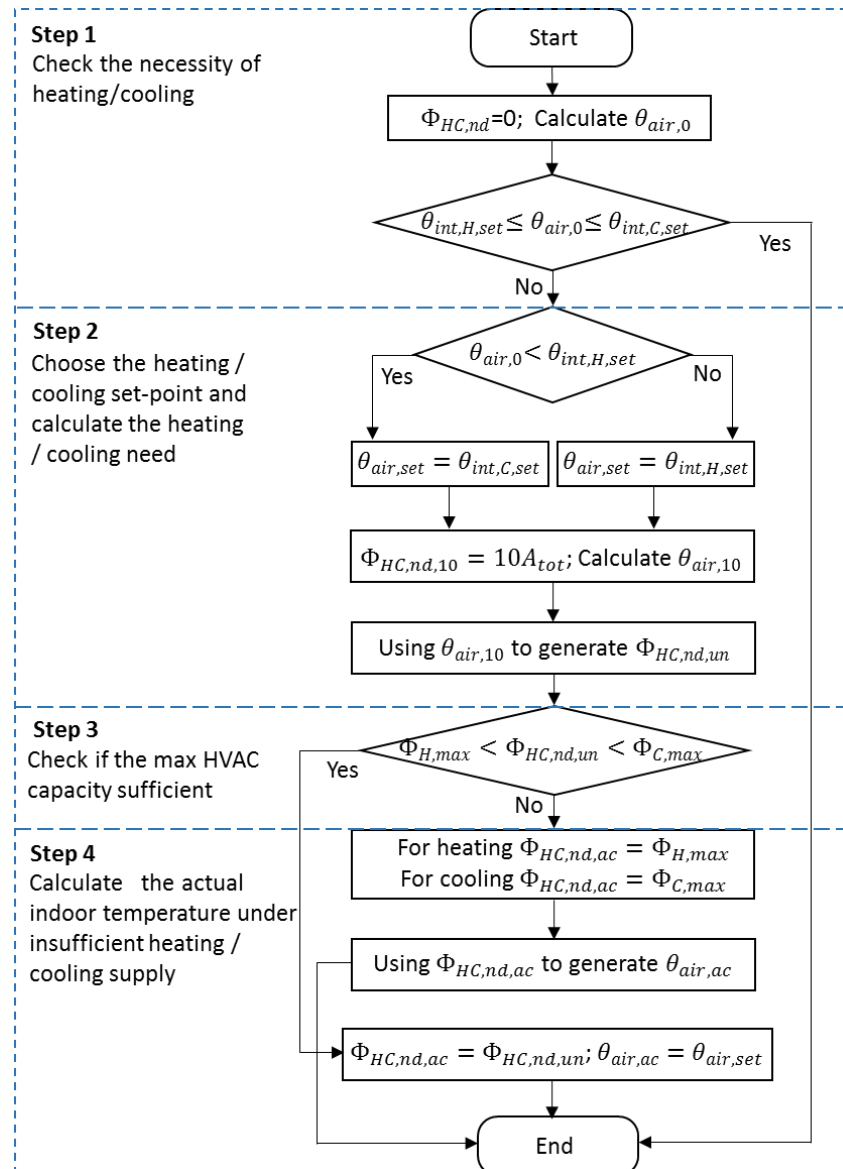


Figure 3.3: The flow chart for 4-setp calculation procedure

**Each calculation step is explained as follows:****Step 1:** Checking the necessity of heating/cooling.

In this step, the heating/cooling necessity will be checked by calculating the indoor temperature under free floating conditions.

Assuming  $\Phi_{HC,nd}=0$ , calculating the indoor air temperature by using Eq. 3.14. By naming the calculated result  $\theta_{air}$  as  $\theta_{air,0}$ , finding out the indoor temperature without HVAC at the initial time step.

If  $\theta_{int,H,set} \leq \theta_{air,0} \leq \theta_{int,C,set}$ , the indoor temperature is right within the comfort zone therefore no heating or cooling is needed. When  $\Phi_{HC,nd,ac} = 0$  and the actual internal temperature  $\theta_{air,ac} = \theta_{air,0}$ , no further step is in needed.

If  $\theta_{air,0}$  is laid beyond the comfort temperature zone, then step 2 should be implemented.

**Step 2 :** Choosing the set-point and calculating the heating/cooling need

If the  $\theta_{air,0}$  is higher than the comfort zone, the actual indoor set point for this case is,  $\theta_{air,set} = \theta_{int,C,set}$ . If the  $\theta_{air,0}$  is lower than the comfort zone, the actual indoor set point for this case is,  $\theta_{air,set} = \theta_{int,H,set}$ . An experimental heating/cooling power,  $\Phi_{HC,nd,10}$  ( $\Phi_{HC,nd,10} = 10W/m^2 \times$  floor area of total conditioned zone), will be given to  $\Phi_{HC,nd}$ . By applying  $\Phi_{HC,nd}$  to Eq.3.14, the by resulting  $\theta_{air}$  will be named as  $\theta_{air,10}$ . Further, the unrestricted heating or cooling power  $\Phi_{HC,nd,un}$ , (regardless of the max HVAC capacity) is calculated using Eq.3.22.

$$\Phi_{HC,nd,un} = \Phi_{HC,nd,10}(\theta_{air,set} - \theta_{air,0})/(\theta_{air,10} - \theta_{air,0}) \quad (3.22)$$

**Step 3:** Comparison between the maximum HVAC capacity and he required heating/cooling power.

If the  $\Phi_{HC,nd,un}$  is less than the maximum HVAC heating capacity  $\Phi_{H,max}$  or the cooling capacity  $\Phi_{C,max}$  ( $\Phi_{H,max} < \Phi_{HC,nd,un} < \Phi_{C,max}$ ), the actual heating/cooling power  $\Phi_{HC,nd,ac}$  is equal to  $\Phi_{HC,nd,un}$ , and the actual indoor temperature  $\theta_{air,ac}$  is equal to  $\theta_{air,set}$ , the calculation can be terminated and the heating or cooling power need and indoor temperature are obtained.

If the required heating or cooling power exceeds the maximum HVAC capacity, the  $\Phi_{HC,nd,ac}$  will be set to  $\Phi_{C,max}$  or  $\Phi_{H,max}$  and step 4 will be implemented.

**Step 4:** Calculating the actual indoor temperature under insufficient heating/cooling supply.

If the required heating or cooling power exceeds the maximum HVAC capacity, for the heating case, the maximum heating power  $\Phi_{H,max}$  will be used as the actual heating or cooling power  $\Phi_{HC,nd,ac}$ , for the cooling case,  $\Phi_{C,max}$  will be used as the actual heating/cooling power  $\Phi_{HC,nd,ac}$ . The  $\Phi_{HC,nd,ac}$  will then be applied into Eq. 3.14 that allows the  $\theta_{air,ac}$  to be generated.

**By using the 4-step approach, the actual indoor temperature for the given hour,  $\theta_{air,ac}$ , and the corresponding heating or cooling energy demand,  $\Phi_{HC,nd,ac}$ , will be generated.**

It is worth noting that the heating/cooling energy demand,  $\Phi_{HC,nd,ac}$ , is only for the heat that needs to be supplied or extracted from the building rather than the actual electricity needed from the HVAC system, as the energy efficiency ratio (EER) of HVAC is not accounted for.

### **3.4 Generating the HVAC module for the operational energy estimation of Chinese office buildings by refining of EN ISO13790**

Based on the heat transfer framework of EN ISO 13790, the HVAC module of CN13790 with the simplified input and quick results feedback ability, that suitable for the early design stage of China office building, is developed. Compared to the EN ISO13790, the input need of the HVAC module is simplified and the computing load (computing time need) is thus further reduced. Meanwhile, the data set of the typical input for a Chinese office building is summarized in this section. There are 6 main refinements and simplifications on the HVAC module of the new CN13790. These are described as follows:

#### **3.4.1 The Simplified approach for building zone definition**

In the original EN ISO13790 method, an office building should be divided into multi-zones with thermal couplings between them. This zone classification strategy is certainly more comprehensive as it involves the thermal transmission and air movement between different building areas, especially between the air-conditioned office space and none air-conditioned equipment rooms and stairs. However, the new CN13790 method is

proposed in this research to enable a quick energy estimation at the conceptual office building design stage, at which the building floor plan and layout are not detailed. In this case, the geometrical model for CN13790 should be a simple single-zone box, based on the basic measurement to a preliminary building design (e.g. height, width, length, orientation, windows-wall ratio, etc.).

The boundary of a single-zone model consists of all building elements that separate the internal space from the external environment, including the **external wall, external window, roof, the floor of ground floor, but excluding the basement space** (the basement is calculated separately in section 3.4.5). The diagrams of the zone definition approach in EN ISO13790 and CN13790 are illustrated in Figure 3.4.

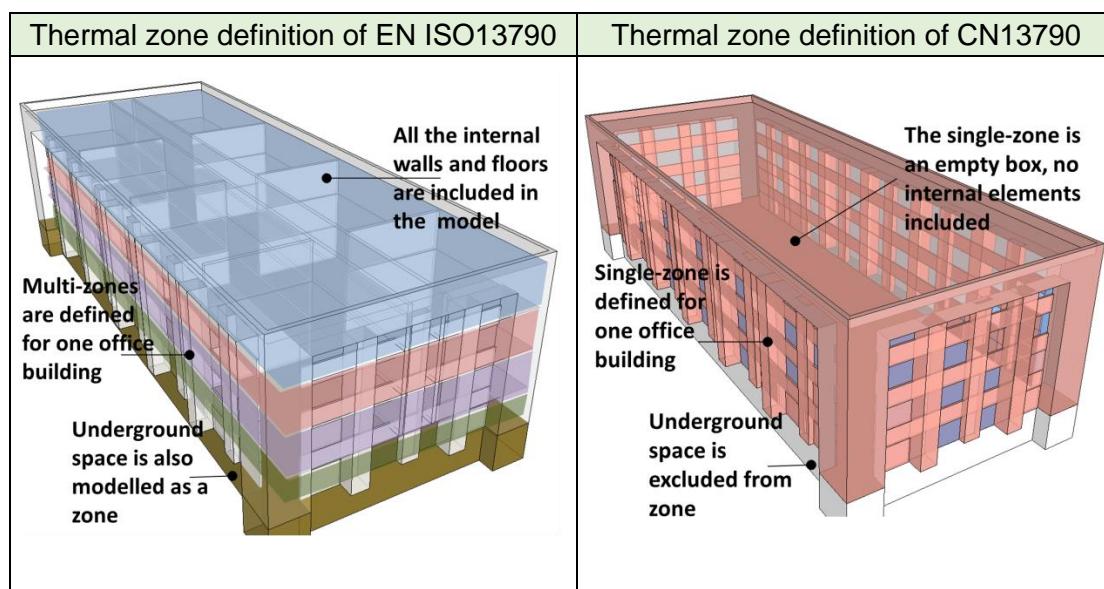


Figure 3.4: The diagrams of the zone definition approach

In order to overcome the disadvantage of single-zone modelling, three methods beyond the original EN ISO13790 are applied in the energy estimation process:

- (1) An adjustment factor ( $F_{ac}$ ) is introduced to reflect the ratio of the air-conditioned area ( $A_{adj}$ ) to gross floor area (GFA), which is simply expressed in Eq. 3.23.  $F_{ac}$  is defined as 0.75 as referring to the office building survey research in Shanghai [117]. Then, the  $A_{adj}$  rather than the GFA are used in the calculation of  $\Phi_{HC,nd,10}$  and the heating/cooling demand calculation in Eq. 3.22.

Also,  $F_{ac}$  is applied to the actual heating/cooling power  $\Phi_{HC,nd,ac}$ , to reduce the actual energy need, as expressed in Eq.3.24. The adjusted heating or cooling power  $\Phi_{HC,nd,ac,adj}$  rather than the original  $\Phi_{HC,nd,ac}$  is used in Eqs. 3.41 and 3.42 to generate the monthly and annual energy demand.

$$A_{ac} = F_{ac}GFA \quad (3.23)$$

$$\Phi_{HC,nd,ac,adj} = F_{ac}\Phi_{HC,nd,ac} \quad (3.24)$$

(2) In the single-zone model, the thermal mass for all building internal components, such as partition walls, staircases and weight-loaded structures, are not counted. Thus, thermal mass from these components will not affect the energy estimation. In order to facilitate the energy estimation with thermal mass effect, a set of typical conditions for the value of thermal mass for each office building types are summarised and added to the energy calculation. The detailed study are addressed in section 3.4.2 below.

(3) The basement space, which is normally none air-conditioned, is excluded in the single-zone model. The heat balance of the basement and ground is considered separately, allowing the heat transmission between basement space and the single-zone model to be counted. The detailed study can be seen in section 3.4.5.

By these measurements, the single-zone modelling method in the CN13790 model is more convenient and flexible for the conceptual office building design stage. Meanwhile, it is capable of providing similar energy estimation as to the multi-zones method in the original EN ISO13790.

### 3.4.2 A Simplified approach for building thermal mass related variables

According to EN ISO13790, the  $A_m$  and  $C_m$  are based on the calculation of summing the thermal capacities of each building's elements that are directly exposed to indoor air in conditioned building spaces. In order to facilitate the energy estimation at the building conceptual design stage, the general value of  $A_m$  and  $C_m$  for each office building types are surmised to allow the quick calculation with a certain degree of high accuracy.

The four typical structure types of the Chinese office buildings, i.e., multi-storey reinforced concrete frame structure (MS-RCF), high-rise reinforced concrete frame structure (HR-RCF), high-rise reinforced concrete frame shearing wall / tube structure (HR-RCF-SW/T) and high-rise steel frame - tube structure (HR-SF-SW/T), are analysed respectively. For each structure type, two building design examples are selected to represent the higher and lower thermal mass values. The example building for higher thermal mass will have small window areas (taking the lower limit value of the window-wall ratio from building regulation) and heavy-weighted structure; while the example building for lower thermal mass is designed conversely. The key features of the design examples with higher or lower thermal mass for each structure type are described in Table 3.1. The MS-RCF and HR-RCF structures are jointly analysed as they have the same basic structural layout.

Table 3.1: The key features of the building design examples with higher/lower thermal mass.

	Higher thermal mass example	Lower thermal mass example
MS-RCF HR-RCF	<p><b>Columns:</b> 500mm×500mm, C25 concrete + 12mm steel bars</p> <p><b>Column spacing:</b> 6.6m×6.6m</p> <p><b>Main beam:</b> RC 550mm×220mm</p> <p><b>External Wall:</b> AAC block</p> <p><b>Floor:</b> 100mm cast-in-place RC</p> <p><b>Roof:</b> 120mm cast-in-place RC</p> <p><b>Area ratio of window to wall (overall):</b> 0.30</p>	<p><b>Columns:</b> 375mm×375mm, C25 concrete + 12mm steel bars</p> <p><b>Column spacing:</b> 8.4m×8.4m</p> <p><b>Main beam:</b> RC 500mm×200mm</p> <p><b>External Wall:</b> AAC block</p> <p><b>Floor:</b> 100mm cast-in-place RC</p> <p><b>Roof:</b> 120mm cast-in-place RC</p> <p><b>Area ratio of window to wall (overall):</b> 0.70</p>
HR-RCF-SW/T	<p><b>Columns:</b> 500mm×500mm, C25 concrete + 12mm steel bars</p> <p><b>Column spacing:</b> 6.6m×6.6m</p> <p><b>Shearing wall:</b> 250mm thickness, C40 concrete + steel bars, located in each corner and in-between corners</p> <p><b>Main beam:</b> RC 500mm×200mm</p> <p><b>External Wall:</b> AAC block</p> <p><b>Floor:</b> 100mm cast-in-place RC</p> <p><b>Roof:</b> 120mm cast-in-place RC</p> <p><b>Area ratio of window to wall (overall):</b> 0.30</p>	<p><b>Columns:</b> 375mm×375mm, C25 concrete + 12mm steel bars</p> <p><b>Column spacing:</b> 8.4m×8.4m</p> <p><b>Shearing wall:</b> 180mm thickness, C40 concrete + steel bars, located in each corner</p> <p><b>Main beam:</b> RC 500mm×200mm</p> <p><b>External Wall:</b> AAC block</p> <p><b>Floor:</b> 100mm cast-in-place RC</p> <p><b>Roof:</b> 120mm cast-in-place RC</p> <p><b>Area ratio of window to wall (overall):</b> 0.70</p>
HR-SF-SW/T	<b>Steel columns:</b>	<b>Steel Columns:</b>



	<p>200mm×250mm, Q235 steel, H-shape  <b>Column spacing:</b> 9m×9m  <b>Tube structure:</b>  250mm thickness, C40 concrete + steel bars, located in center of building  <b>Main beam:</b>  Q235 steel, 200mm×150mm  <b>External Wall:</b> AAC block  <b>Floor:</b> 100mm cast-in-place RC  <b>Roof:</b> 120mm cast-in-place RC  <b>Area ratio of window to wall (overall):</b> 0.30</p>	<p>200mm×250mm, Q235 steel, H-shape  <b>Column spacing:</b> 10m×12m  <b>Tube structure:</b>  200mm thickness, C40 concrete + steel bars, located in center of building  <b>Main beam:</b>  Q235 steel, 200mm×150mm  <b>External Wall:</b> AAC block  <b>Floor:</b> 80mm cast-in-place RC  <b>Roof:</b> 120mm cast-in-place RC  <b>Area ratio of window to wall (overall):</b> 0.70</p>
--	---	--

By using the “maximum effective thickness” method corresponding to ISO 13786 [118], the key building elements that directly contact the internal air and significantly affect the building mass are considered for the thermal mass, in which the light-weight partition wall, windows and decoration layer are not included. For the key building elements, 0.1m of thickness from the internal surface are counted in the thermal mass calculation. The  $A_m$  and  $C_m$  are generated for the higher and lower thermal mass example of each office building type, by using Eqs. 3.1 and 3.2. The relationship between  $A_m$ ,  $C_m$  and the conditioned floor area  $A_f$  are outlined in Figure 3.5 and Figure 3.6.

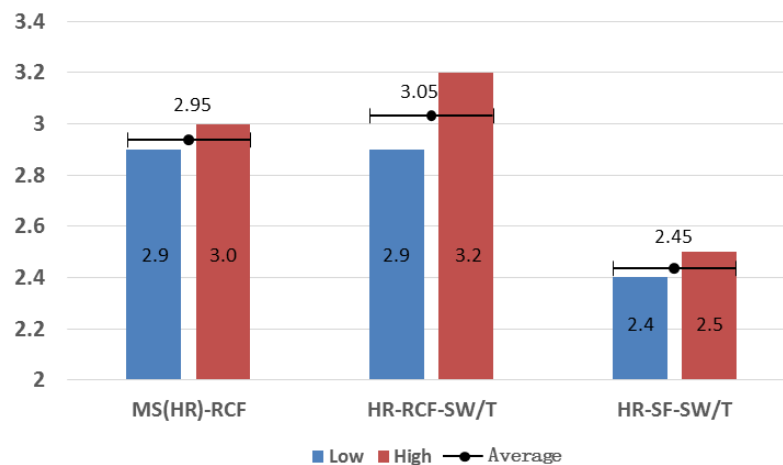


Figure 3.5:  $A_m$  per m<sup>2</sup> conditioned floor area of example buildings from each structure type:

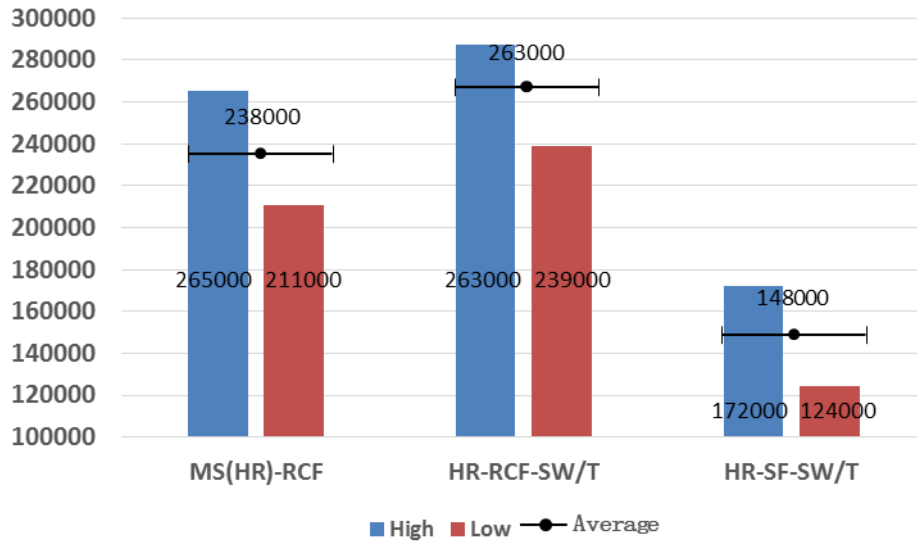


Figure 3.6:  $C_m$  per  $m^2$  conditioned floor area of example buildings from each structure type

The average value of  $A_m/m^2$  and  $C_m/m^2$  are used to represent the value of each building type. The adjustment factor  $m$  and  $n$  are introduced to reflect the simplified relationship between average  $A_m$ ,  $C_m$  and the conditioned floor area  $A_f$ , expressed in Eqs. 3.25 and 3.26 below.

$$A_m = mA_f \quad (3.25)$$

$$C_m = nA_f \quad (3.26)$$

Where: the adjustment factor  $m$  and  $n$  can be taken from Table 3.2 below.

Table 3.2: Adjustment factor for  $A_m$  and  $C_m$

Structure type	$m$	$n$
Multi-story RCF(<6F), High-rise RCF(7F-9F)	2.95	238000
High-rise RCF-SW/T(10F-25F)	3.05	263000
High-rise SF-SW/T(10F-25F)	2.45	148000

### 3.4.3 The refined and China-focused model for transparent windows and glazing curtain walls.

The thermal transfer through transparent windows and the glazed curtain wall (GCW) are jointly discussed in this section. Instead of the data collection from the product catalogues, heat transfer rates of the transparent windows or walls,  $H_{tr,w}$ , are calculated by using a simplified method which is dedicated to China application.

The heat transfers within the framed-supported GCW and the GCW with semi-exposed

frame are treated the same as to normal windows, whereas the heat transfer of the hidden frame GCW will only be affected by the glazing layer which is the only component exposed to external air. For all these transparent or semi-transparent elements, the single glazing, double glazing and triple glazing structure with different filled gaps and functional coating layers, are considered. Together with the frames, the heat transfer coefficient of transparent windows and the GCW are computed by Eq.3.27:

$$H_{tr,w,j} = A_j[U_g + F_F(U_f - U_g)] \quad (3.27)$$

Where:  $A_j$  is the area of windows/curtain wall, in  $m^2$ ;  $F_F$  is the frame ratio;  $U_g$  and  $U_f$  are the U-value of glazing part and the frame part respectively, in  $W/m^2.K$ .

The data for typical frames in China is outlined in Table 3.3, while the U-value of the glazing part are discussed as follows:

Table 3.3: The dataset for typical windows/GCW frames in China

Type	Aluminium frame without thermal break	Aluminum frame with thermal break (PA66 insulation)	PVC frame	Wood frame
$U_f$ ( $w/m^2k$ )	6.21	3.72	1.91	2.37
$F_F$ -windows	0.25	0.25	0.28	0.28
$F_F$ frame supported GCW	0.25	0.25	N/A	N/A
$F_F$ semi-exposed faming GCW	0.15	0.15	N/A	N/A

The whole  $U_g$  for the common glazing structure (single, double and triple glazing with/without low-e coating or gas filling) is the reciprocal of the sum of thermal resistances of the inner and outer surfaces, glass layers, and air gaps (if there are any), and calculated using Eqs. 3.28 and 3.29. The position of components that variables refer to can be seen in the schematic drawing in Figure 3.7.

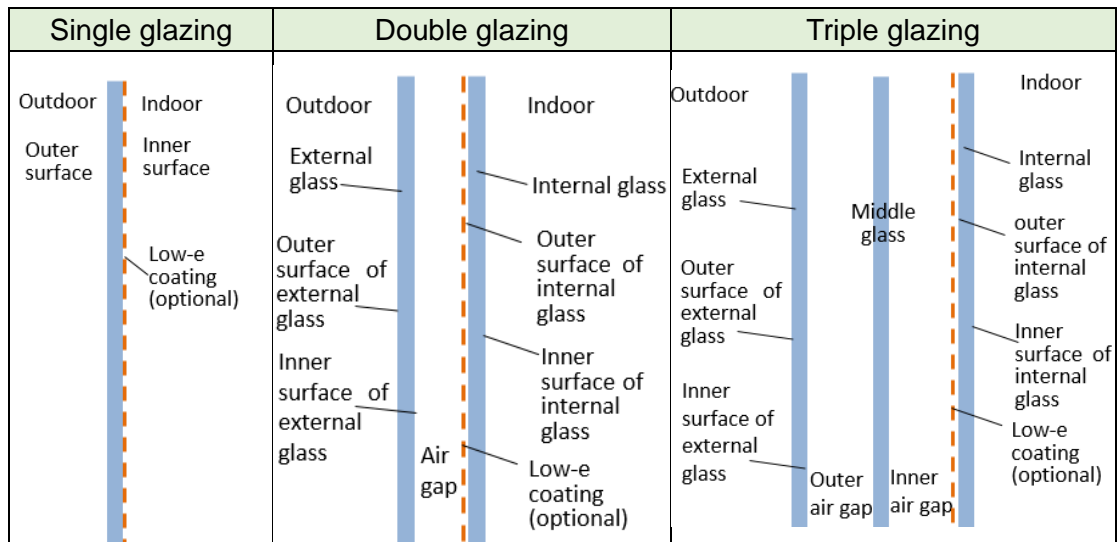


Figure 3.7: Schematic drawing of the glazing layers

$$U_g = \begin{cases} 1 / \left[ \frac{1}{(6.12\varepsilon_{in} + 3.6)} + \frac{D}{\lambda} + \frac{1}{(6.12\varepsilon_{out} + 17.9)} \right], & \text{Single glazing} \\ 1 / \left[ \frac{1}{(6.12\varepsilon_{in,in} + 3.6)} + \sum \frac{D_m}{\lambda_m} + \sum R_{gap,n} + \frac{1}{(6.12\varepsilon_{out,ext} + 17.9)} \right], & \text{Multiple glazing} \end{cases} \quad (3.28)$$

Where,  $\varepsilon_{in}$  and  $\varepsilon_{out}$  are the heat emissivity from the inner or outer surface of glass;  $\varepsilon_{in,in}$  and  $\varepsilon_{out,ext}$  are the heat emissivity from the inner surface of internal glass and from the outer surface of external glass;  $\varepsilon$  is considered as 0.84 for the normal glass surfaces, and 0.06 for the glass with a low-e coating;  $D_m$  and  $\lambda_m$  are the thickness and heat conductivity of glass layer, in m, detailed in Appendix I for the common types;  $R_{gap,n}$  is the R-value of the air gap layer  $n$ , expressed in Eq. 3.17.

$$R_{gap} = \frac{1}{\frac{6.12}{\left[ \left( \frac{1}{\varepsilon_{in,gap}} \right) + \left( \frac{1}{\varepsilon_{out,gap}} \right) - 1 \right]} + \frac{\lambda_{air}}{D_{air}}} \quad (3.29)$$

Where,  $\varepsilon_{in,gap}$  and  $\varepsilon_{out,gap}$  are the heat emissivity from the inner and outer surface of two glass between the air gap;  $D_{air}$  and  $\lambda_{air}$  are the thickness and heat conductivity of air/gas within the air gap, while  $\lambda_{air}$  is 0.024 W/m.K for air and 0.016 W/m.K for argon filling.

For the  $H_{tr,w,j}$  of the hidden frame GCW, no frame's heat transfer is considered in ideal conditions, the frame ratio  $F_F$  is taken as 0, and then the same method as to normal GCW is applied, indicated in Eqs. 3.27 to 3.29.

### 3.4.4 The refinement and China-focused model for the opaque walls and roofs.

#### 3.4.4.1. Simplified model for the opaque walls and roofs

The structure of the external opaque wall is considered as a 4-layer-model for thermal performance evaluation. From the external to internal, the external wall is constructed by (1) an external finishing layer, (2) insulation layer, (3) major structure layer and (4) internal decoration layer. Each layer is assembled and sealed by cement-sand mortar, but for the external wall with dry-hanging external finishing layer (type 2), there is a gap behind that layer. The schematic drawing for the 4-layer-model of the opaque wall is shown in Figure 3.8.

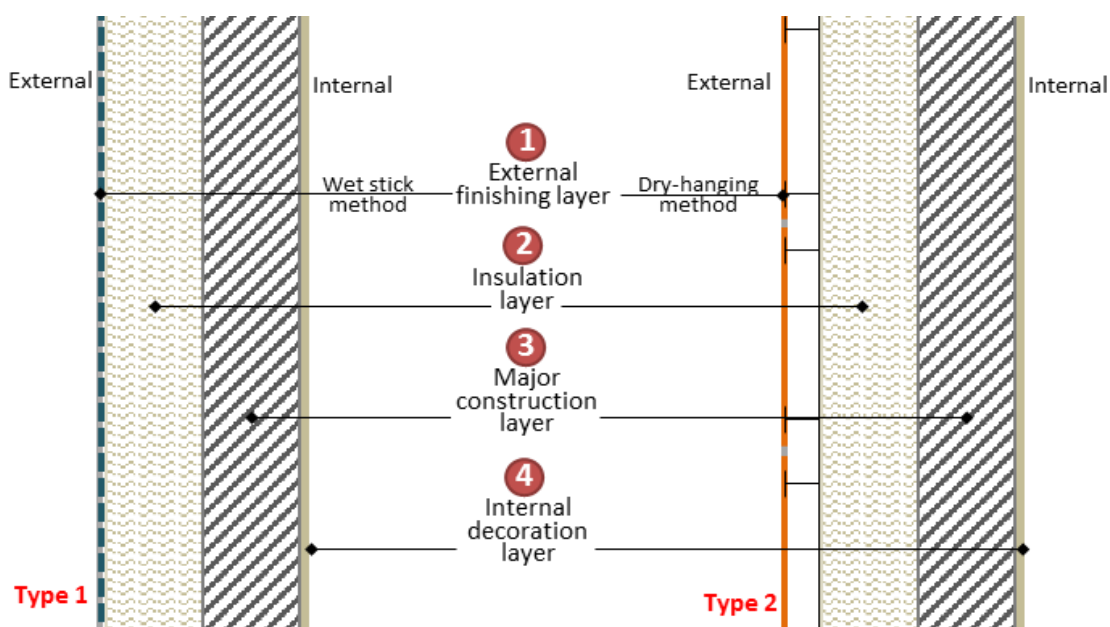


Figure 3.8: Schematic drawing of the 4-layer external wall structure

Similar to the opaque wall, the roof is simplified to a 4-layer-model as well, including (1) green roof layer (optional), (2) protection and waterproof layer, (3) insulation layer, (4) load-bearing roof slab. The schematic structure drawing for the 4-layer-model of roof is displayed in Figure 3.9 below.

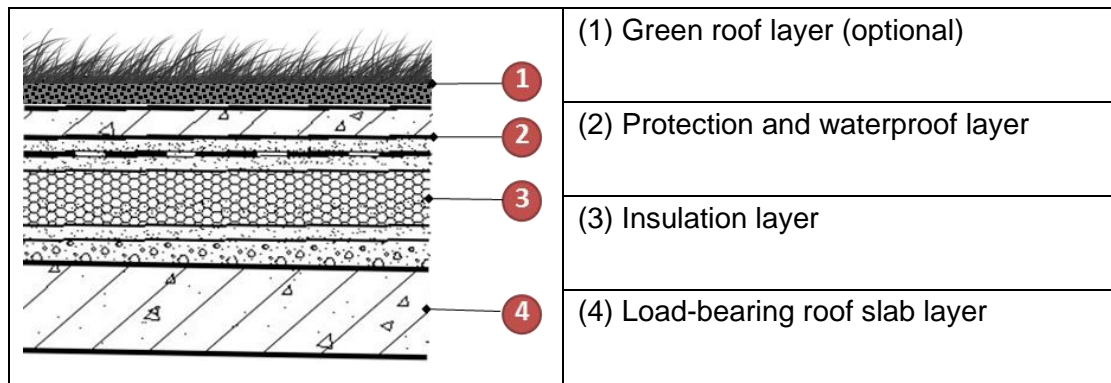


Figure 3.9: The schematic structure drawing for the 4-layer-model of roof

The thermal transfer efficiency  $H_{tr,op,j}$  for the whole 4-layer-model of wall  $j$  or roof  $j$ , in  $w/k$ , are generated by Eq. 3.30 below.

$$H_{tr,op,j} = A_j \left( \frac{1}{R_{Si} + R_1 + R_2 + R_3 + R_4 + R_{So}} \right) \quad (3.30)$$

Where:  $A_j$  is the area of the opaque wall  $j$ ;  $R_1$  to  $R_4$  is the heat resistance of layer 1 to layer 4 respectively; the  $R_{Si}$  and  $R_{So}$  are the external and internal heat resistance value, according to CIBSE guide, common values are taken, where  $R_{Si} = 0.04 \text{m}^2\text{K/w}$ ,  $R_{So} = 0.13 \text{m}^2\text{K/w}$ .

#### 3.4.4 B. The China-focused dataset for the materials applied to opaque walls and roofs

The China available materials and their technical specifications for the 4-layers opaque wall structure are collected and presented in Table 3.4. For the external wall with dry-hanging external finishing layer, the thermal resistance of the finishing layer is considered as nil, as the gap between the finishing layer and insulation layer are freely ventilated. The detailed thermal properties for materials of this table are shown in Appendix I.

Table 3.4: China-focused typical material dataset for the opaque walls

Layers	Specifications for the material options	Thermal resistance (R)
(1) External finish layer	<p><b>a. Glazed facing tile decoration (wet stick)</b> Glazed facing tile + 15mm cement lime mortar with building adhesive + 9mm cement lime mortar + 3mm special cement mortar</p> <p><b>b. Stone material curtain wall decoration (dry-</b></p>	<p><b>a.</b> The overall <math>R=0.162 \text{ Wm}^2/\text{k}</math></p>

	<b>hanging)</b> Marble + steel-frame and hanging component	<b>b. R=0</b>
(2) Insulation layer	<b>a. XPS</b> <b>Thickness:</b> 0.01m 0.02m 0.025m 0.03m 0.04m 0.05m 0.075m 0.1m 0.12m 0.15m <b>b. EPS</b> <b>Thickness:</b> 0.01 m 0.02m 0.025m 0.03m 0.04m 0.05m 0.075m 0.1m 0.12m 0.15m <b>c. Glasswool</b> <b>Thickness:</b> 0.03m 0.05m 0.08m 0.1m <b>d. Rockwool</b> <b>Thickness:</b> 0.03m 0.05m 0.08m 0.1m	The thermal performance details can be seen in Appendix I
(3) Major structure layer	<b>a. AAC</b> <b>Thickness Options:</b> 0.1m 0.12m 0.15m 0.18m 0.2m 0.25m 0.3m <b>b. CHB</b> <b>Thickness Options:</b> 0.09m 0.115m 0.14m 0.19m <b>c. CSB</b> <b>Thickness Options:</b> 0.14m 0.19m <b>d. CCHB</b> <b>Thickness Options:</b> 0.14m 0.19m	
(4) Internal decoration layer.	<b>Lime mortar plaster inside decoration</b> 1mm wall paint + 5mm cement lime mortar screed + 8mm cement lime mortar + 3mm special surface treatment lime mortar	The overall R=0.22 Wm <sup>2</sup> /k

The China-focused materials and their specifications for the opaque roofs are collected and presented in Table 3.5. The typical extensive green roof design is used to reflect the specifications of the green roof layer, which has a 100mm earth that is the major source of the thermal resistance. A thermal resistance assessment method for growing medium (earth) layer is applied in this research, in correspondence with Wong's research [119] on DOE-2 simulation (described in the literature review, Chapter 2.4.3), the increasingly growing medium (soil) will bring a certain amount of thermal resistance which is 0.4 m<sup>2</sup>K/W per 100mm dry earth and 0.063 m<sup>2</sup>K/W per 100mm 40% moisture earth. The latter is more close to natural clay conditions, its thermal resistance contributes to the main part of the thermal resistance of a typical green roof layer.

Table 3.5: China-focused typical material dataset for the opaque roof.

Layers	Specification for localised options	Heat resistance (R)
(1) green roof layer (optional)	<b>Extensive Green Roofs</b> 100mm Engineered soil with plantings + Filter fabric + Drainage layer + Root barrier	The overall R=0.09Wm <sup>2</sup> /k
(2) Protection and waterproof layer	waterproof membrane + 20mm cement mortar	The overall R=0.03Wm <sup>2</sup> /k

(3) Insulation layer	<b>a. XPS</b> <b>Thickness:</b> 30mm 40mm 50mm 60mm 70mm <b>b. EPS</b> <b>Thickness:</b> 30mm 40mm 50mm 60mm 70mm	The thermal performance details can be seen in Appendix I
(4) Load-bearing roof slab layer	20mm cement mortar + 30mm light aggregate concrete + 120mm cast-in-place reinforced concrete roof slab + 5mm cement lime mortar screed + 8mm cement lime mortar + 3mm special surface treatment lime mortar	The overall $R=0.25$ $Wm^2/k$

By applying the simplified 4-layer-model and China-focused material dataset, the heat transfer coefficient  $H_{tr,op}$  for any opaque external wall and roof can be easily generated with relatively good accuracy and this can be applied to the 5R1C model.

### 3.4.5 The refined and localised model for underground space.

#### 3.4.5 A. Simplified model for the basement

The thermal heat transfer coefficient from the unconditioned basement to conditioned aboveground space,  $H_g$ , between the internal environment and external underground soil, through the basement, is effected by two parts in the simplified model, which are the thermal transmittance of the floor between the ground floor and the basement and the thermal transmittance of the basement as a whole. The two parts heat transfer approach and parameter definition are displayed in Figure 3.10.

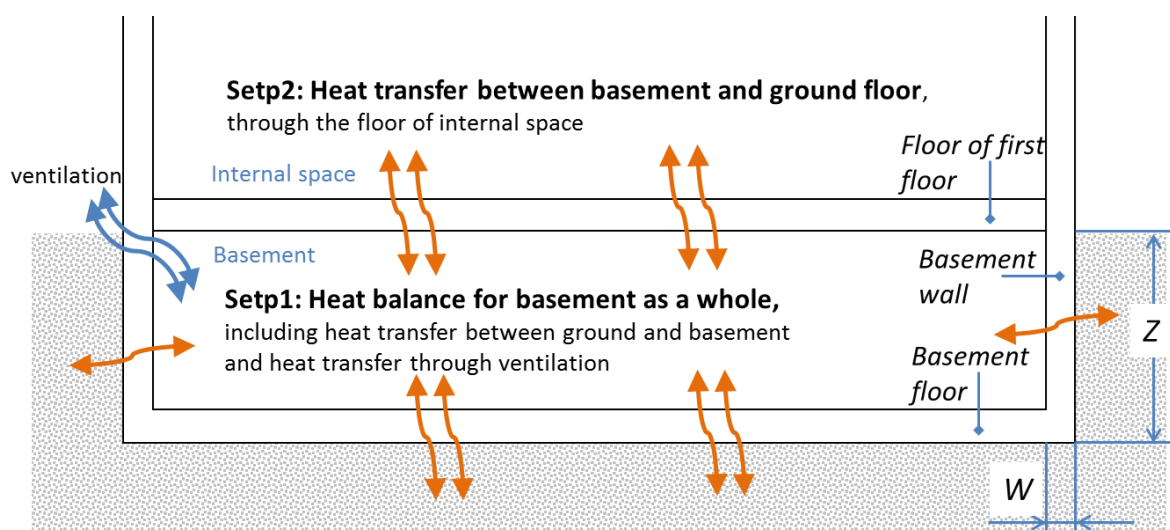


Figure 3.10: The heat transfer approach and parameter definition for basement



The simplified  $H_g$  is generated by Eq. 3.31.

$$H_g = A / \left( \frac{1}{U_{fl}} + \frac{A}{AU_{bf} + zPU_{bw} + 0.33nV} \right) \quad (3.31)$$

Where  $A$  is the basement floor area;  $U_{fl}$  is the thermal transmittance of the floor between first floor and basement.  $Z$  is the depth of the basement under the ground level;  $P$  is the exposed perimeter of the floor;  $n$  is the ventilation rate of the basement, in the ACH model;  $V$  is the volume of the basement;  $U_{bf}$  and  $U_{bw}$  are the thermal transmittance of the basement's floor and wall respectively, generated in Eqs. 3.32 and 3.33 in Table 3.6 below.

Table 3.6: the calculation of  $U_{bf}$  and  $U_{bw}$  for basement heat transfer

$$U_{bf} = \frac{\lambda}{0.457 \left( \frac{A}{0.5P} \right) + d_t + 0.5z} \quad (3.32)$$

$$U_{bw} = \frac{2\lambda}{\pi z} \left( 1 + \frac{0.5d_t}{d_t + z} \right) \ln \left( \frac{z}{d_w} + 1 \right) \quad (3.33)$$

Where:  $\lambda$  is the thermal conductivity of the ground (soil & rock) in W/mK;  $d_t$  and  $d_w$  is the equivalent thickness for basement floor and wall respectively, in m, including any insulation effect from soil & rock, generated in Eqs.3.36 and 3.37:

$$d_t = w + \lambda(R_{si} + R_f + R_{se}) \quad (3.34)$$

$$d_w = \lambda(R_{si} + R_w + R_{se}) \quad (3.35)$$

Where:  $R_{si}$  and  $R_{se}$  are the surface heat resistance of the internal and external basement surface respectively, in  $m^2.K/W$ ;  $R_f$  and  $R_w$  are the heat resistance of the basement floor and wall respectively, in  $m^2.K/W$ .

The above ground heat transfer coefficient,  $H_g$ , is actually related to the temperature difference of the internal space and the ground, rather than the external air temperature. The ground temperature is affected by depth and external air temperature with a certain delay.

In order to establish the relationship between the basement heat flow rate and internal and external air temperature, a monthly mean ground heat transfer coefficient,  $H_{g,m}$ , is introduced to this research, which is generated using the mean internal and external air temperature by Eq. 3.36 below.

$$H_{g,m} = \frac{\Phi_m}{\theta_{i,m} - \theta_{e,m}} \quad (3.36)$$

Where:  $\theta_{i,m}$  and  $\theta_{e,m}$  are the monthly internal and external mean air temperatures for the month  $m$ ;  $\Phi_m$  is the monthly mean ground heat flow rate for the month  $m$ , in  $W$ , expressed in Eqs. 3.37 to 3.39 in Table 3.7 below.

Table 3.7: the calculation of  $\Phi_m$  for basement heat transfer

$\Phi_m = H_g(\bar{\theta}_i - \bar{\theta}_e) - H_{pi}(\bar{\theta}_i - \theta_{i,m}) + H_{pe}(\bar{\theta}_e - \theta_{e,m}) \quad (3.37)$
<p>Where: <math>\bar{\theta}_i</math> and <math>\bar{\theta}_e</math> are the yearly average internal and external air temperature; <math>\theta_{i,m}</math> and <math>\theta_{e,m}</math> are the monthly average internal and external air temperature; <math>H_{pi}</math> and <math>H_{pe}</math> are the internal and external periodic heat transfer coefficient, in <math>W/K</math>, expressed in Eq.3.40 and 3.41 below.</p>
$H_{pi} = 1 / \left( \frac{1}{AU_{fl}} + \frac{1}{(A+zP)\lambda/\delta + 0.33nV} \right) \quad (3.38)$
$H_{pe} = AU_{fl} \frac{0.37P\lambda(2 - e^{-z/\delta}) \ln\left(\frac{\delta}{d_t} + 1\right) + 0.33nV}{(A+zP)\lambda/\delta + 0.33nV + AU_{fl}} \quad (3.39)$
<p>Where, <math>\delta</math> is the periodic penetration depth for specific ground type, in m, and <math>e</math> is the Euler number (2.71828).</p>

#### 3.4.5 B. The localised data set for the basement material and related parameters.

In this research, the typical structure and material specification are used to represent the commonly localised basement design. The thickness of insulation layers for the basement floor and wall are designed to provide different types of thermal resistance. This allows the design to match the requirement of local building energy saving standards (“Design standards for energy efficiency of public buildings” GB 50189 [51]) for different climate regions. The typical thermal resistance and thickness for the basement envelope are listed in Table 3.8 below.

Table 3.8: The dataset for typical basement envelope

Position	Specification for localized design	Parameters
(1) Floor between the internal space and basement	<p><b>Facing layer</b> ceramic tile + 15mm cement lime mortar with building adhesive + 10 mm cement lime mortar</p> <p><b>Insulation layer</b> 30mm XPS</p> <p><b>Construction layer</b></p>	The overall R: 1.09 $Wm^2/k$

	15mm cement lime mortar + 100mm cast-in-place RC slab + 10 mm cement lime mortar	
(2) The Basement floor	<p><b>Facing layer</b> ceramic tile + 15mm cement lime mortar with building adhesive + 10 mm cement lime mortar</p> <p><b>Insulation layer</b> A. Severe cold zone: 75mm XPS B. Cold zone: 50mm C. Hot summer cold winter zone: 40mm D. Hot summer warm winter, temperate zone: 30mm</p> <p><b>Construction layer</b> 15mm cement lime mortar + 100mm cast-in-place RC slab + 10mm special surface treatment lime mortar + waterproof membrane + 20mm cement mortar + 10mm sand cement mortar</p>	<p>The overall R for</p> <p>A zone: 2.60 Wm<sup>2</sup>/k B zone: 1.76 Wm<sup>2</sup>/k C zone: 1.43 Wm<sup>2</sup>/k D zone: 1.10 Wm<sup>2</sup>/k</p>
(3) Basement wall	<p><b>Facing layer</b> wall paint + 5mm cement lime mortar screed + 10mm special surface treatment lime mortar + 10 mm cement lime mortar</p> <p><b>Insulation layer</b> A. Severe cold zone: 75mm XPS B. Cold zone: 50mm C. Hot summer cold winter zone: 40mm D. Hot summer warm winter, temperate zone: 30mm</p> <p><b>Construction layer</b> 15mm cement lime mortar + 80mm cast-in-place RC + 10mm cement lime mortar screed + 10mm special surface treatment lime mortar + waterproof membrane + 20mm cement mortar</p>	<p>The overall R for</p> <p>A zone: 2.58 Wm<sup>2</sup>/k B zone: 1.74 Wm<sup>2</sup>/k C zone: 1.41 Wm<sup>2</sup>/k D zone: 1.08 Wm<sup>2</sup>/k</p>

The thermal properties of the ground vary from one location to another. In this research, the sand and gravel are the properties' values, which are laid in the middle of common ground materials values that are used to represent the general condition of the Chinese office building design. Besides, the general value for the surface thermal resistance of different heat flow directions for basement elements are defined, corresponding to the UK BRE's guide [120] and China's "Thermal Design Code for Civil Building" [121]. The thermal properties and other localised input values are listed in Table 3.9 below.

Table 3.9: The China-focused input dataset for basement related parameters

Typical ground thermal conductivity	The ground periodic penetration depth	Surface thermal resistance for basement wall	Surface thermal resistance for basement floor	Surface thermal resistance for floor of first floor
$\lambda=2.0\text{W/mk}$	$\delta=3.2\text{m}$	$R_{si}=0.13\text{m}^2\text{K/W}$ $R_{se}=0\text{ m}^2\text{K/W}$	$R_{si}=0.17\text{m}^2\text{K/W}$ $R_{se}=0\text{ m}^2\text{K/W}$	$R_{si}=0.17\text{m}^2\text{K/W}$ $R_{se}=0.04\text{ m}^2\text{K/W}$

### 3.4.6 The simplified and localised model to generate the HVAC electricity demand.

As described in section 3.3.3 above, the heating or cooling energy demand,  $\Phi_{HC,nd,ac}$ , generated by the original EN ISO13790 is only for the theoretical value of the heat that is supplied or removed from the space rather than the actual electricity needed from the HVAC system. In this section, the simplified model for the energy estimation of the HVAC system using the energy efficiency ratio (EER) will be added to the CN13790, to enable an energy assessment for the “real” HVAC demand.

The electricity demand for whole HVAC system is generated by the Eq.3.40 below:

$$\Phi_{HVAC,i} = \Phi_{HC,nd,ac,i}/EER_i \quad (3.40)$$

Where: the  $\Phi_{HVAC,i}$  is the actual electricity demand of the whole HVAC system for a given hour  $i$ ; the  $\Phi_{HC,nd,ac,i}$  is the heating/cooling load for the given hour generated by the 5R1C heat balance model as shown in section 3.3.3; the  $EER_i$  is the energy efficiency ratio of whole HVAC system including the chiller and fan etc, The typical value is given below;

**The localised representation of EER used in the Chinese office building is selected below.**

The EER varies according to with many factors in HVAC design, but the value from an example of the Daikin water cooled HVAC system is given to represent the general situation in the Chinese office building approach. Daikin is the world’s leading HVAC manufacturer with a high market share that is able to represent the common product used in China. The EER varies depending on outdoor temperature and is described in Table 3.10 below.

Table 3.10: The typical EER from the Daikin HVAC system

	$T_1$	$T_2$	$T_3$	$T_4$	$T_5$
External Temp. range	>30°C	20°C–30°C	10°C–20°C	0°C–10°C	<0°C
$EER_i$ for cooling	4.3	5.3	5.6	5.9	5.9
$EER_i$ for heating	6.6	6.6	6.2	5.9	4.8

### The whole year`s HVAC electricity demand is generated as follows.

Through the calculation above, the hourly HVAC electricity demand,  $\Phi_{HVAC,i}$ , is generated. In order to obtain the whole year`s data, this process needs to be iterated for 8760 times (the building mass temperature  $\theta_{m,t}$  is used as  $\theta_{m,t-1}$  for the next iteration, see section 3.3.3). For a given period, the total heating or cooling demand,  $Q_{HVAC,tot}$ , the heating demand,  $Q_{H,tot}$ , and the cooling demand,  $Q_{C,tot}$ , are expressed in kWh, and calculated through Eq. 3.41 and 3.42 below.

$$Q_{HVAC,tot} = \sum_i^j |\Phi_{HVAC,i}| / 1000 \quad (3.41)$$

$$\begin{cases} Q_{H,tot} = \sum_n^m \Phi_{HVAC,i} / 1000, & \Phi_{HVAC,i} > 0 \\ Q_{C,tot} = \sum_n^m \Phi_{HVAC,i} / 1000, & \Phi_{HVAC,i} < 0 \end{cases} \quad (3.42)$$

Where: the  $\Phi_{HC,nd,ac,i}$  is the hourly heating/cooling power needed for a given hour  $i$ , expressed in W;  $m$  is the starting hour for a particular period;  $n$  is the ending hour for that period. The heating or cooling demand can be simply obtained by the sum of all the positive or negative values of the heating or cooling power;  $m$  and  $n$ , taken from Table 3.11 below.

Table 3.11: The starting and ending hour of each month

	Jan	Feb	Mar	Apr	May	Jun	Jul	Aug	Sep	Oct	Nov	Dec	Annual
$m$	1	745	1417	2161	2881	3625	4345	5089	5833	6553	7397	8017	1
$n$	744	1416	2160	2880	3624	4344	5088	5832	6552	7296	8016	8760	8760

### 3.5 The Validation of the CN 13790 HAVC module for the Chinese office building.

The accuracy of any building energy estimation method depends highly on the detail level of the boundary condition input and the tolerance of the heat balance method (e.g. the ability to keep accuracy in various external/internal condition while dealing with different building structure). Since the EN ISO13790, which is the basement of the HAVC module of the CN 13790, is designed for building energy demand for EU countries, its adaptability and accuracy for the Chinese office building strategy needs to be validated.

The HAVC module validation includes **(1)** the accuracy assessment for various office building designs in China, and **(2)** the adaptability verification for applying the HAVC module to different climatic regions in China.

### **3.5.1 The accuracy assessment of CN13790 HAVC module**

The improvement of the CN13790 to EN ISO13790, includes the “one-zone” model without the consideration of the inter-zone heat transfer, the simplified model for windows, glazing walls and underground space heat transfer. It also involves the simplified and localised model for the external wall and roof. These changes will respectively affect the heat transfer characteristics by degrees on specific building components, and therefore bring certain changes to the heat balance of the whole building. Thus, the accuracy of the CN13790 HAVC module needs to be monitored and checked.

#### **A. The Methodology for accuracy validation of the CN13790 HAVC module.**

In order to validate the accuracy of the CN13790 HAVC module, numerous comparative studies have been carried out. A set of office building cases is modelled to represent the variation of key design factors. Their heating and cooling demands are estimated one-by-one by different methods, including the CN13790 method, the widely recognised dynamic simulation tools, EnergyPlus and ESP-r and the manual rough calculation method degree-day method. This is intended to provide the comparable information from both “modern” and “traditional” estimation methods respectively.

There are 4 key design factors that are able to significantly affect the heating or cooling energy demand. They are the heavy-light weighted structure (focusing on the effect of building thermal mass), the high-low glass wall ratio (the effect of building solar heat gain and windows heat transfer), the high-low internal gain, and the high-low natural ventilation rate (the effect of ventilation heat transfer). Firstly, a standard office building is modelled to represent the typical office building design with intermediate values for all key design factors (e.g. the intermediate structure weight, the intermediate windows-wall ratio, etc.). 4 pairs of office building cases are modelled with similar geometric designs as the standard case, but each pair of the buildings reflects a design difference on one key design factor (e.g. a pair of cases with high and low insulation levels respectively). In total, 9 cases are modelled. The difference of the heating or cooling estimation results among these models and among these estimation methods are analysed to reflect the

accuracy and ability of the CN13790 HVAC module when dealing with buildings having different key design features. The principle of the accuracy assessment procedure can be seen in Figure 3.11.

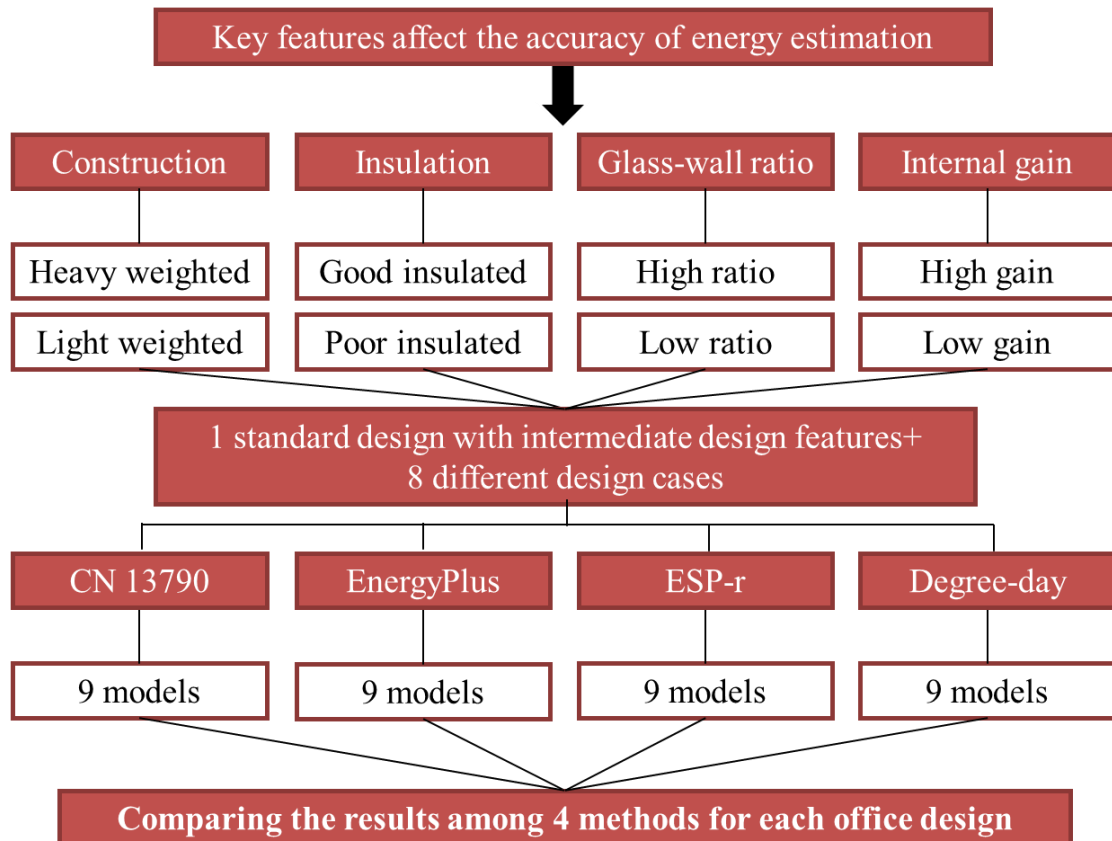


Figure 3.11: Flow chart for the principal of accuracy assessment.

## B. Model establishing and boundary condition equivalencing

For each building model of same building case, the boundary conditions that highly affect the results are ensured to be the same. The results generated from any method are for the basic monthly and annual heating or cooling need only. No building service systems are considered in the analysis.

### Definition of location and weather conditions.

To undertake the energy estimation for heating and cooling, the building cases must be located in a region where the environmental temperature is far from the comfort zone during summer and/or winter. Shanghai is an ideal city as it lies in the “Hot Summer and

Cold Winter Zone.” This region has a humid subtropical climate and four distinct seasons. The annual average temperature is 15.7°C, whereas the average temperature for summer and winter are 30°C and 1°C, with the highest and lowest temperature of 40.8°C and -10.1°C respectively. The average heating or cooling time is 78 days and 55 days respectively. The weather file, based on 20 years’ statistics from DOE, is used in this research.

#### Modelling for the standard office building.

A standard office building model, representing the most common design with an intermediate value for all key design factors, is established for 4 estimation methods. The standard office building has 10 above ground storeys (air-conditioned) and 1 underground basement (none air-conditioned), each story has 2400 m<sup>2</sup>, the total gross floor area is 24000 m<sup>2</sup>. The model is designed as a simple cuboid, facing the south, with a 60m length and a 40m width. The height of each story is 4.5m and the total height is 45m. Apart from the geometry, the definitions for 4 key design factors are described in Table 3.12.

Table 3.12: Specifications for the standard office building case

<b>Building structure</b>	<b>Columns:</b> 500mm×500mm C25 RC, 6.6m×6.6m, 12mm steel bars <b>Columns spacing:</b> 8.4m×8.4m <b>shear wall:</b> 200mm C40 RC
<b>Insulation</b>	<b>External Wall:</b> 50mmEPS panel + 120mm AAC block <b>Roof:</b> 20mm concrete + 50mmEPS panel <b>Windows:</b> double glazing window + 10mm air gap + + aluminum frame <b>Door:</b> Wooden fire resistance door <b>Basement:</b> 20mm concrete + 7.5 mm XPS panel
<b>Windows-wall ratio</b>	<b>Overall windows-wall ratio:</b> 0.4
<b>Internal heat gain</b>	<b>People:</b> 10 m <sup>2</sup> /person- 8 W/m <sup>2</sup> <b>Lighting:</b> CFL- 9W W/m <sup>2</sup> <b>Others:</b> Printer & others- 18W W/m <sup>2</sup>



### Modelling for 8 different office cases

The basic geometry for 8 office building cases is the same as the standard office building, but the key design factors are different for each case to reflect the energy consumption related design variations.

For the weight of the building structure, the reinforced concrete frame with a shear wall structure is used to represent the heavy-weight structure, whereas the steel frame with tube structure is used to reflect the light-weight structure.

For the windows-wall ratio, the upper and lower limited values in building regulation (Design standard for energy efficiency of public buildings. GB 50189 [51]) are used to represent the high and low windows-wall ratio. Same glass is used in traditional windows and the glazing curtain wall.

For internal heat gain, an office building with high and low occupation and equipment density are used to represent the high and low internal gain of the office building case, which is designed according to the combination of the CIBSE guide A [122] and the “China design standard for energy efficiency of public buildings” [51].

Abbreviations are given for each case to make the discussion clear and easier, such as case “H-W” for high-weighted structure cases, and case “L-I” for low insulated cases.

The specification of the design difference can be seen in Table 3.13.

Table 3.13: The specification for 8 office cases.

<b>Case Abbr.</b>	<b>Description</b>	<b>Design difference from standard case - Specification</b>
H-W	Heavy-weighted structure	<b>Columns:</b> 375mm×375mm C25 RC, 12mm steel bars <b>Columns spacing:</b> 6.6m×6.6m <b>shear wall:</b> 220mm C40 RC
L-W	Low-weight structure	<b>Columns:</b> 200mm×150mm Q235 steel H-beam <b>Columns spacing:</b> 10m×12m <b>shear wall:</b> 180mm C40 RC
H-I	High insulation level	<b>External Wall:</b> 70mmEPS panel + 120mm AAC block <b>Roof:</b> 20mm concrete + 70mmEPS panel <b>Windows:</b> Low-e double glazing window + 10mm air gap + thermal breaking aluminium frame

		<b>Door:</b> Wooden fire resistance door <b>Basement:</b> 20mm concrete + 7.5 mm XPS panel
L-I	Low insulation level	<b>External Wall:</b> 30mmEPS panel + 120mm AAC block <b>Roof:</b> 20mm concrete + 30mmEPS panel <b>Windows:</b> single glazing window + aluminium frame <b>Door:</b> Wooden fire resistance door <b>Basement:</b> 20mm concrete + 7.5 mm XPS panel
H-WR	High windows-wall ratio	<b>Overall windows-wall ratio:</b> 0.8 (Glazing curtain wall)
L-WR	Low windows-wall ratio	<b>Overall windows-wall ratio:</b> 0.2
H-IG	High internal gain	4m <sup>2</sup> /person: 20W/m <sup>2</sup> + CFL: 12W/m <sup>2</sup> + others: 25W W/m <sup>2</sup>
L-IG	Low internal gain	20m <sup>2</sup> /person: 4W/m <sup>2</sup> + LED: 6W/m <sup>2</sup> + others: 10W W/m <sup>2</sup>

### Boundary condition equivalencing for the 4 estimation methods

The equivalent boundary condition is ensured for 4 models of any building cases, including the building operation schedule, external weather and ground conditions. The calculation for the CN13790 and Degree day method are based on Visual studio coding with textual input and output, whereas ESP-r models are based on the input in its own interface, and the EnergyPlus models are established using SketchUp OpenStudio plugin. With the help of the visualised modelling process of the OpenStudio plugin, the EnergyPlus models are used to represent the appearance of 9 building cases and can be seen in Figure 3.12.

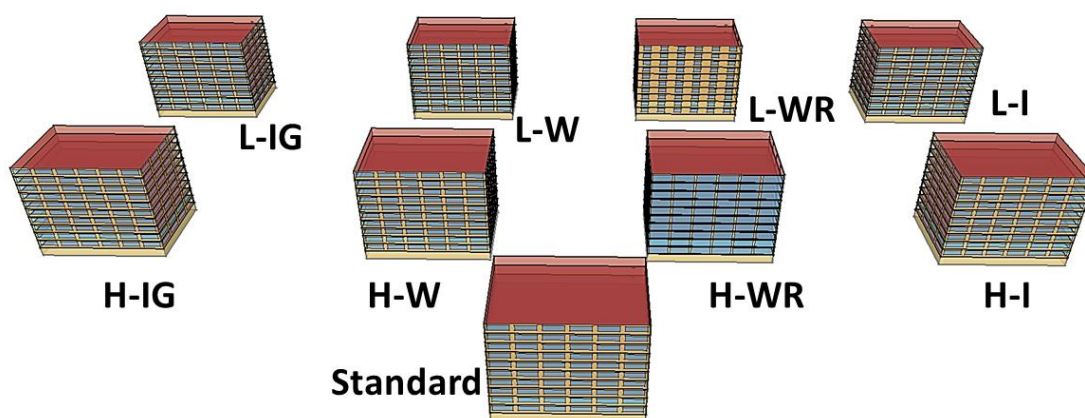


Figure 3.12: the appearance of the 9 building cases (EnergyPlus OpenStudio model)

## C. Results and discussion

The heating or cooling energy demand calculated by using the 4 methods is presented in kWh/m<sup>2</sup>. The detailed results are listed in Appendix IV. The energy demand estimation

accuracy of the CN13790 is assessed by comparing the results from various calculation methods, and discussed for the heating and cooling demand separately.

#### The accuracy on annual space heating.

The results of the annual space heating demand, estimated by different methods are compared in Figure 3.13 below. For all the cases, the CN13790 produced results are slightly higher than the results from the EnergyPlus and ESP-r, while the results generated by the degree day method are significantly higher than the other 3 methods. For all calculation methods, the insulation level has the most obvious effect on heating demand, followed by the windows-wall ratio. As the typical thermal capacity values are used, the standard case and H-W case have the same thermal capacity value, thus generating the same energy demand.

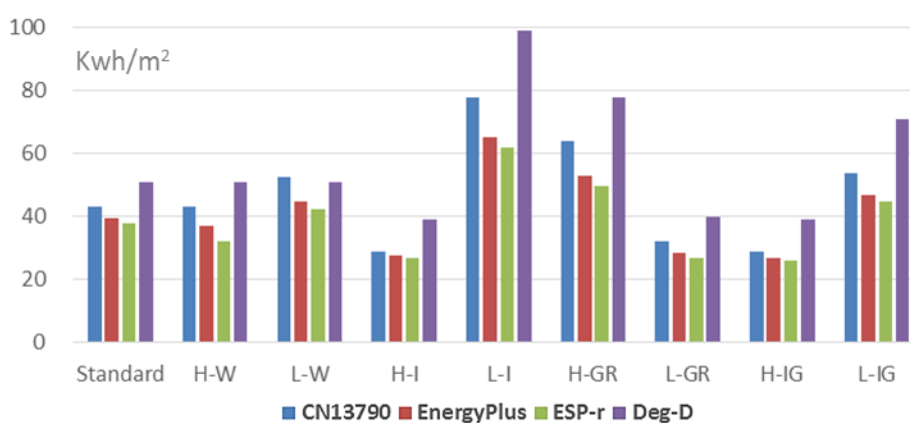


Figure 3.13: The annual heating demand from each calculation method

The results from the EnergyPlus and ESP-r are very close for all cases, their average value is named as the dynamic simulation value and used as the benchmark value in accuracy analysis. The numerical difference between the results from the CN13790 module and from degree-day method and the benchmark value can be seen in the scatter chart in Figure 3.14. The black solid line is the dynamic simulation value, the blue and red dash line are the approximate distribution range for the CN13790 and the degree-day method respectively. The CN13790 heating demand is proportionally distributed with an average of 14% higher than the benchmark value (19% for the maximum case), while the degree-day method is about 30% higher than the benchmark line.

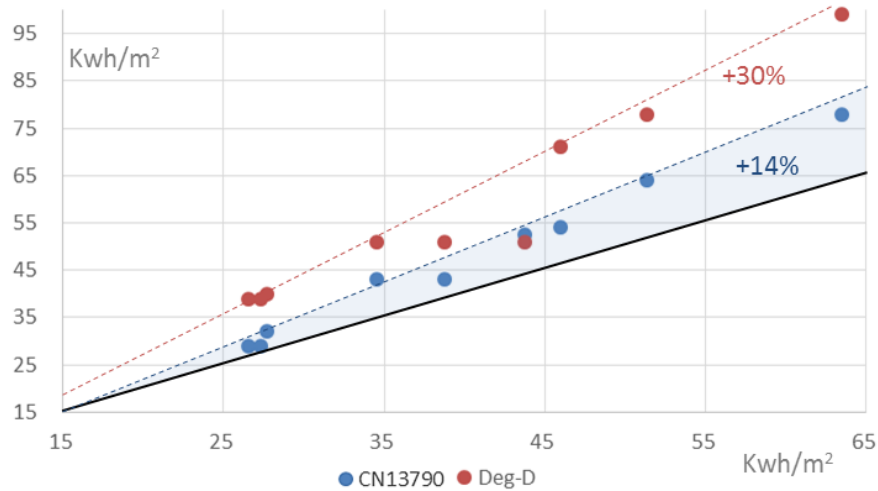


Figure 3.14: The difference between the heating demand from the CN13790, from a degree-day method and the benchmark value.

The accuracy on annual space cooling

The difference of the cooling demand results between 4 calculation methods is similar to the heating demand. For all cases, the CN13790 results are higher than the dynamic simulation software but dramatically lower than the Degree day method. The annual cooling demand from each calculation method can be seen in Figure 3.15.

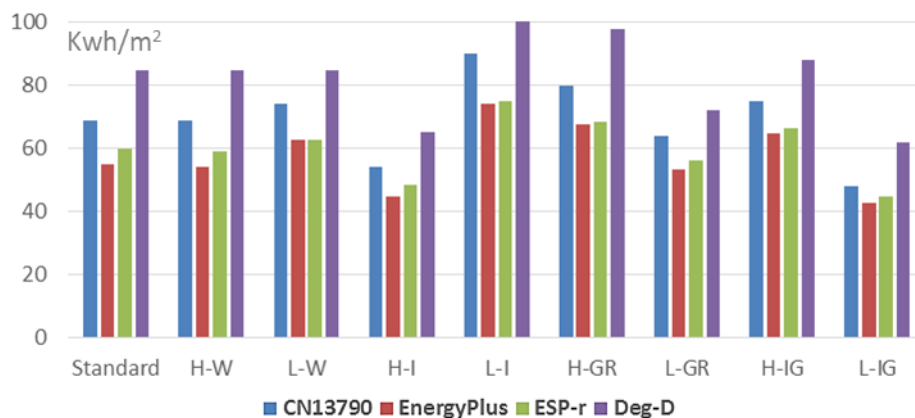


Figure 3.15: The annual cooling demand from each calculation method.

Similar to the above section, a benchmark value is used to represent the average value of the EnergyPlus and ESP-r generated results. The results from the CN13790 and the degree-day method and the benchmark line are scattered in Figure 3.16. The CN13790's result is also proportionally distributed with an average of 15% higher (18% for the maximum case) than the benchmark value, while the degree-day method is about 35%

higher than the benchmark line. The results distribution of the degree-day method for the cooling demand is worse than the heating demand, with compared irregular and distant indicators to the benchmark line. It is obvious that the CN13790's cooling demand estimation accuracy is more reliable and predictable than the degree-day method, as the difference ratio of the CN13790 is much closer to the average trend blue dash line.

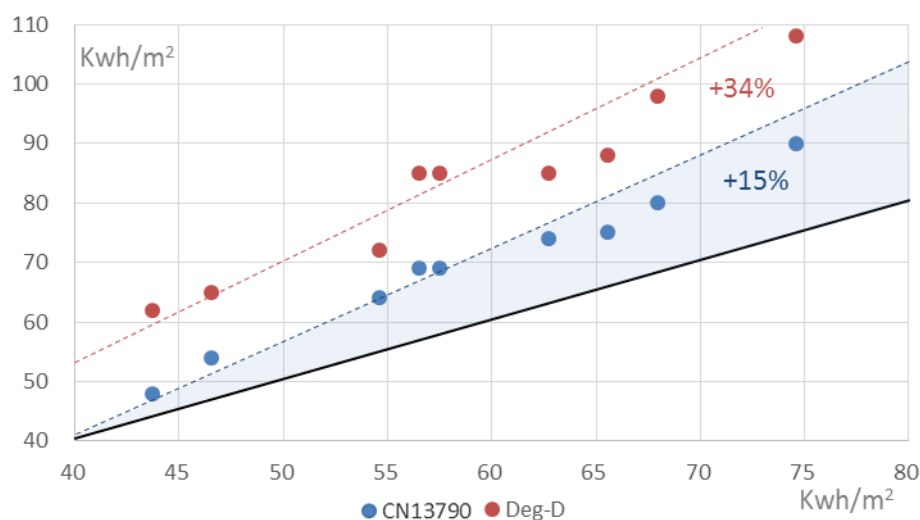


Figure 3.16: The difference between the cooling demand from the CN13790, from degree-day method and the benchmark value.

It is clear that, compared to the manual degree-day calculation method, the results from the CN13790 method are much closer to dynamic simulation tools. Although the CN13790's energy estimation is about 15% higher than the dynamic simulation tools in most cases for both the heating and cooling demand. The difference for most cases has a constant linear growth, the results still lie in a reasonable and predictable range.

### 3.5.2 The verification of climate adaptability for different climate regions in China

The basic heat balance model of the CN13790 method is referred to the EN ISO13790, which is mainly used in EU countries. Although the energy estimation accuracy of the CN13790 is assessed in the above section based on the Shanghai climate, its adaptability for other Chinese climate regions still needs to be verified. The climate adaptability of the CN13790 is tested and analysed in this section.

### A. The Methodology for adaptability verification.

The adaptability verification is based on the “China building climate zone”, 5 cities (each one for each climate zone) are selected to represent the climate condition of each zone. The heating / cooling energy estimation ability of the CN13790 under the climate condition of each city is assessed respectively, by using the standard building model (see above section). The selected cities` location and their monthly average temperature distribution can be seen in Figure 3.17.

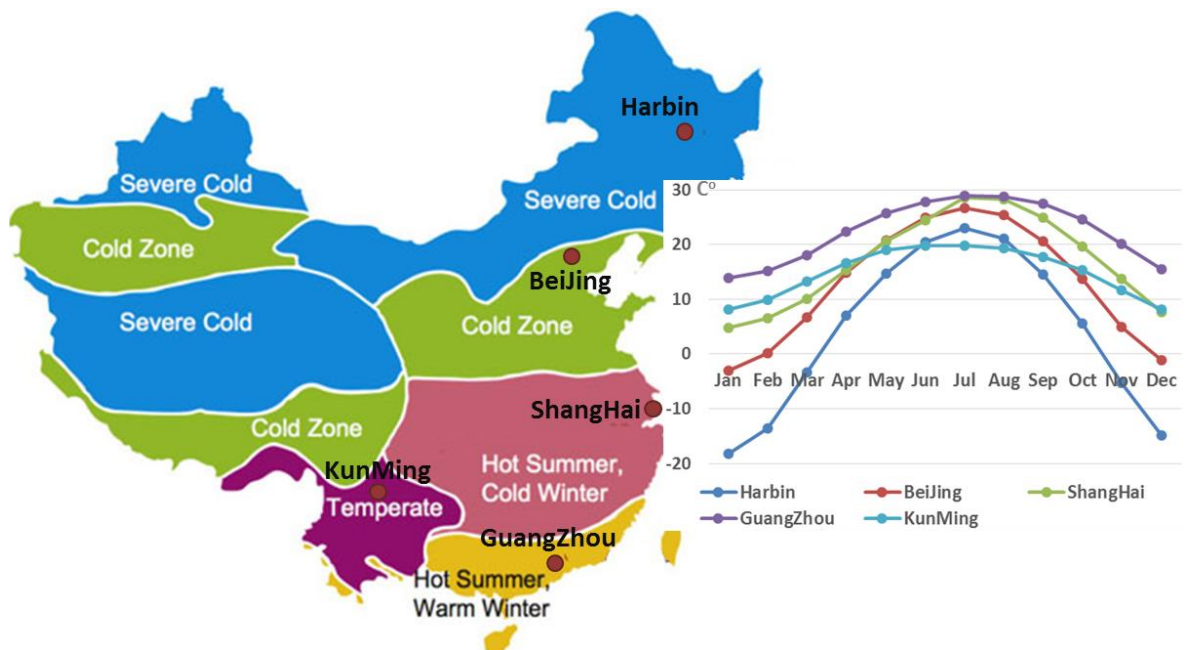


Figure 3.17: The selected cities` location and monthly average temperature distribution.

The representative city of the most severe cold climate zone, Harbin, has the coldest and longest winter, while in the summer months its average temperature is still higher than the comfortable temperature zone. Thus, both heating and cooling buildings are needed in this city. As well as Beijing and Shanghai, representing the cold zone and the hot summer and cold winter zones respectively, heating and cooling are both required. But for the representative city of the hot summer and warm winter climate zone, Guangzhou, no heating is needed as the temperature is higher than the heating setpoint for almost the whole year. For Kunming, which is in the temperate climate zone, the temperature is laid within the comfort zone for most months of the year, only cooling is required for few weeks in the summer.

The heating / cooling energy of the standard building case in each city is calculated by using the 4 estimation method respectively. The whole model and boundary condition setup is the same. The only difference is the variety of external climate conditions represented by DOE`s hourly weather files of each city.

## B. Results and discussion

According to the energy estimation results from the 4 methods, the CN13790`s result (both heating and cooling) is slightly higher than the dynamic simulation results in all the climate zones, while the difference between 2 dynamic simulation tools is very small. Similar as the results in the above section, for all climate zones, the results from the Degree day method are significantly higher than from others. The estimation results for heating and cooling can be seen in Figure 3.18 where “(H)” and “(C)” represent the name of the city with the energy demand for heating and cooling respectively.

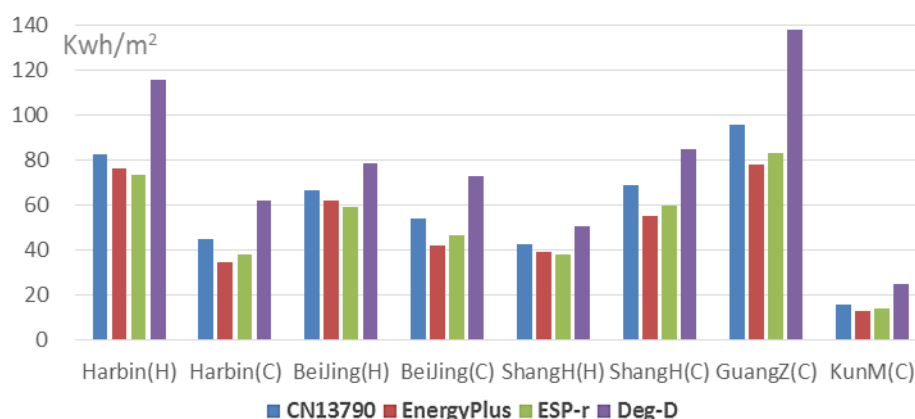


Figure 3.18: The heating and cooling demand from each calculation method for the 5 cities.

In terms of different rates, the results from the CN13790 has an average of 15% higher than that from the dynamic simulation tools. The CN13790 has the best estimation accuracy for heating demand in Beijing, showing a 9% difference. The maximum difference exists in the estimation of the cooling demand in Harbin (19%), followed by the cooling demand in Beijing (18%). Thus, by the effect of climate difference, there is a 10% fluctuation on estimation accuracy. The degree-day method has far worse estimation accuracy than the CN13790, its average difference is 37%. By considering the effect of climate difference, the fluctuating range of estimation accuracy for the

degree-day method is 21%. The different rate distribution of the CN13790 and degree-day method can be seen in Figure 3.19.

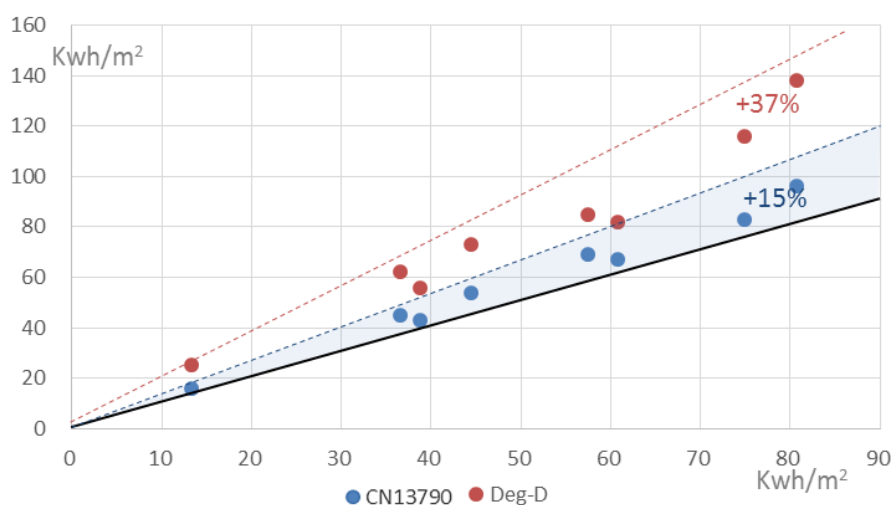


Figure 3.19: The difference between the results from the CN13790, from the degree-day method and the benchmark value.

It is clear that, compared to the manual degree-day calculation method, the CN13790 method has a more stable accuracy rate with less fluctuation in the different climate zones of China. As same to the two dynamic simulation tools, the CN13790 method has good adaptability in China.

### 3.5.3 The assessment of computing time for the CN13790 method.

The reduced requirement of calculation time is another key advantage of the CN13790 method since the quick feedback is a crucial factor in building early design stage. The benefit from the simplified heat transfer models and single thermal zone definition show that when computed, the load is dramatically reduced than in the detailed dynamic method.

**Assessment method.** The computing time using the EnergyPlus, ESP-r and the CN13790 method is recorded, including the calculation for the 9 example building model (used in section 3.5.1) and for the standard model in the 5 climate region (used in section 3.5.2). The computing time for the rough manual calculation is not compared here, as it is highly dependent on the proficiency level of people and the computer tool they use,



for example excel or Matlab. For EnergyPlus, the computing time is displayed on its monitor window, whereas it is recorded by using a stopwatch for the ESP-r and CN13790 method. The computing is operated by a computer equipped with Intel i7 6700 CPU and 16G RAM.

**Results and discussion.** The average computing time for each method can be seen in Table 3.14 below.

Table 3.14: The average computing time from the EnergyPlus, ESP-r and the CN13790 method.

	EnergyPlus	ESP-r	CN13790
Computing time (second)	152	185	<1

According to the average computing time for the 14 building cases, the dynamic methods consumed around 3 mins to generated a whole year`s data (8760 hours), while the CN13790 method (based on the Visio Basic.net coding) completed the process within 1 second. The 168 times average efficiency improvement was achieved by using the CN13790 method. It is very important for the early design stage as the trial and error process exists in the selection of every design feature which needs vast repeated trials for energy estimation.

### **3.6 Adding the additional energy consumption module and renewable energy generation module to the CN13790.**

The energy estimation method for the main energy consumption, HVAC system, has been established and validated in the HVAC module above, but there are other energy consumptions from buildings which are estimated by additional energy consumption modules. Besides, the energy saving effect caused by renewable energy technologies is estimated by using the renewable energy generation module. The two modules are added to the CN13790 in this section.

### 3.6.1 The Development of the additional energy consumption module for the other regular energy consumption

The additional energy consumption module work on the estimation of other regular energy consumption like lighting, office appliance, and hot water supply, in the Chinese office building, is described below.

#### **The estimation of lighting and office equipment energy.**

This is based on the suggested design values in relation to the building's floor area taken from the "China design standard for energy efficiency of public buildings" [51]. A LED option is added to the suggestion value for the new green building design, the LED efficiency refers to DOE's research on LED lighting products [123]. The energy estimation for the additional energy consumption is listed in Table 3.15 below:

Table 3.15: the typical value for other energy consumers is used in the CN13790 (per m<sup>2</sup>)

Lighting	Office appliance	Overall
CFL lighting - 9W LED lighting (optional) – 7W	18 W	27W Or 25W(optional)

#### **The hot water supply for office building is optional.**

The design value is taken from the CIBSE guide A [122], and converted to 1.1L/ m<sup>2</sup>· day. According to the energy saving regulation in public buildings in china [51], hot water cannot be generated directly from a boiler. Thus, the air-source heat pump is normally preferred in the Chinese green building scheme and assumed to be the preferred option in this research.

The electricity demand for hot water is generated by a simplified method based on daily demand, similar to the "HVAC electricity demand" in section 3.4.5, daily electricity demand for hot water ( $q_{hw,d}$ ) is also calculated by using daily average energy efficiency ratio ( $EER_d$ ) and expressed in Eq. 3.43 below.

$$q_{hw,d} = \frac{1.1C_p(T_{f0}-T_{fi})}{EER_d} \quad (3.43)$$

Where:  $C_p$  is the specific heat of water, in J/(kg·K);  $T_{f0}$  is the outlet water temperature,

taken  $55^{\circ}\text{C}$ ;  $T_{fi}$  is the inlet water temperature equal to the daily average outdoor air temperature, in  $^{\circ}\text{C}$ ;  $EER_d$  is the daily average energy efficiency ratio of the air-source heat pump, by using the daily average air temperature, the value can be taken from the Table 3.16 below.

Table 3.16: the typical EER for typical air-source heat pump

	$T_1$	$T_2$	$T_3$	$T_4$	$T_5$
External Temp. range	$>30^{\circ}\text{C}$	$20^{\circ}\text{C}-30^{\circ}\text{C}$	$10^{\circ}\text{C}-20^{\circ}\text{C}$	$0^{\circ}\text{C}-10^{\circ}\text{C}$	$<0^{\circ}\text{C}$
$EER_i$ for heating	6.6	6.6	6.2	5.9	4.8

### 3.6.2 The Development of the renewable energy generation module for additional energy saving from renewable energy systems

The PV and solar thermal system is integrated in office building in many ways on different positions. The typical models are developed with simplified system setups and energy estimation methods to reflect the typical energy saving ability.

#### **For BIPV system, the typical model is described as follows:**

- (1) All PV models are mounted on the roof of the office building. They are all south oriented with a tilt angle,  $\beta$ , equals to the  $5^{\circ} + \varphi$  ( $\varphi$  is the local latitude), which is the approximate optimized installation angle that is widely used in practice.
- (2) The total area of PV panels ( $A_{PV}$ ) is assumed as 80% of the insulation roof area ( $A_{rf,ins}$ ), in order to avoid the shading between panels.
- (3) In order to avoid the effect of electric demand fluctuation, the PV array assumes a grid connection, the generated electricity will be directly sent to the grid rather than used in the building. The energy saving result has no difference from the total society energy respect point of view, but a highly simplified calculation.

The definition of the simplified BIPV model can be seen in Figure 3.20.

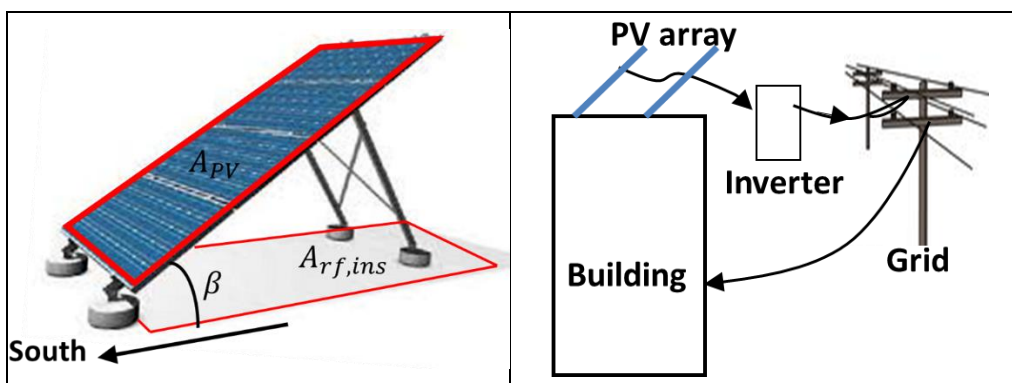


Figure 3.20: the definition of the simplified BIPV model

The simplified method is used to estimate the daily electricity energy saving from the BIPV, expressed in Eq. 3.44.

$$E_{pv,d} = 0.8A_{rf,ins}\bar{H}_d\eta_p(1 - \lambda_a)(1 - \lambda_c)\eta_{inv} \quad (3.44)$$

Where:  $A_{rf,ins}$  is the roof area planned to install the PV array;  $\bar{H}_d$  is the daily total solar radiation energy per  $m^2$  on the PV panel, generated by the commonly used Hay's method [115] using the solar data of the weather file.  $\eta_p$  is the performance ratio of the PV panel;  $\lambda_a$  is the rate of miscellaneous array losses;  $\lambda_c$  is the rate of power conditioning losses, and  $\eta_{inv}$  is average inverter efficiency. The typical parameter of BIPV in China [124] are summarised in Table 3.17.

Table 3.17: The typical parameter for BIPV in China

$\eta_p$	$\lambda_a$	$\lambda_c$	$\eta_{inv}$
17%	17%	1%	90%

**For the solar thermal collector, the typical model is described as follow:**

- (1) The orientation and title angle for the solar thermal collector installation is a default the same as the PV arrays. The total area of the solar thermal collector ( $A_{sol}$ ) is assumed as 80% of the insulation roof area.
- (2) In order to avoid the mismatch of peak hot water load and generation, the water heated by solar thermal collector is stored in insulated hot water tank, the volume of tank is not considered.

The daily electricity saving by replacing the usage of air-source heat pump water heater

with solar thermal collector is expressed in Eq. 3.45.

$$q_{sol,d} = 0.8A_{rf,ins}(1 - \lambda_L)\bar{H}_d(\eta_0 - U\frac{\bar{T}_i - \bar{T}_a}{\bar{H}_d})/EER_d \quad (3.45)$$

Where:  $\eta_0$  is the instantaneous efficiency of collector;  $U$  is the overall U-value for the insulated case of collector, in  $W/(m^2 \cdot ^\circ C)$ ;  $\bar{T}_i$  is the water temperature in the collector, equal to temperature of water tank;  $\bar{T}_a$  is the daily average outdoor temperature for day time;  $\lambda_L$  is the rate of total system heat loss; The typical parameter of the solar thermal collector in China [125] are listed in Table 3.18.

Table 3.18: The typical parameter for solar thermal collector in China

$\eta_0$	$\lambda_L$	$U$ (w/)	$\bar{T}_i$
0.7573	10%	5.153	55°C

### 3.7 Chapter Conclusion

The existing energy estimation tool applicable to green building design is either a complicated dynamic computing tool or an inaccurate manual calculation system; both are unsuitable for the early stage building conceptual design. To fill this gap, a novel building operational energy estimation method, namely CN13790, which comprised of three modules, has been developed. This method, owing to the limited inputs need and light computing load, is ideally suitable for the use in early conceptual design stage, in terms of the building's operational energy estimation.

The HVAC module of CN13790 has been established by refining and updating the existing ENISO13790 method. Six simplified models for specific building elements / systems are established to suit the specific requirement of the Chinese office buildings, and the general parametrical inputs are outlined referring to building standards and materials applicable to China. Through the simplification and China-focused refinement, the HVAC module is well applicable to energy estimation at the earlier conceptual stage of the building design. Compared to the complex dynamic simulation tools used in the final stage building design, the simplified HVAC module has much less input variable number and faster computational speed. Meanwhile, the module can achieve more accurate and reliable outputs than the traditional manual calculation method.

The energy estimation accuracy for the new HAVC module has also been tested in this chapter. Nine building cases are selected to represent the four common design variations that mostly affect the energy demand of the Chinese office buildings. The validation result shows that, with the similar efficient and convenient input, the CN13790 model is capable of providing more accurate energy estimation ability than traditional manual degree-day calculation methods in all climate zones in China. In both heating and cooling demand calculation, the results difference of the CN13790 and existing dynamic simulation method is reasonable and predictable (around 15%), whereas the calculation speed is 168 times faster.

The other energy demand is estimated by the additional energy consumption module, while the energy saving is calculated by using the renewable energy generation module. The overall operational energy demand of office buildings is the sum of the energy consumption (or generation) from three modules. The benefit from the simplification and localization is based on the Chinese conditions, the CN13790 is preferred for the heating/cooling demand estimation work for the Chinese office building context. It can replace the traditional manual degree-day calculation method to provide a more reliable result, with sample input requirements that are suitable for the conceptual design stage.

The overall energy demand of the building operational stage generated by CN13790 method provides an important data for the life-cycle embodied energy and pollutant emissions as will be discussed in Chapter 4. They are used as criteria in the “multiple criteria based on green design assessment and selection tool” in Chapter 6.

**Chapter 4. Development of the simplified life-cycle energy and pollutants assessment method applicable to conceptual design of the buildings**

## 4.1 Introduction

The life-cycle energy consumption (LCE) and life-cycle pollutant emissions (LCP) are the key factors used to assess the performance of office buildings. To judge and select the most appropriate conceptual design solution, the LCE and LCP need to be assessed at the early design stage. Previous studies have already provided certain assessment methods for LCE and LCP, which, owing to the need for detailed design information that is unavailable at the early design stage, or with less comprehensive targets (i.e. energy or CO<sub>2</sub> alone) and limited applicable regions, is inapplicable to the earlier conceptual design stage of Chinese office buildings.

**The aim of this chapter is to develop a series of simplified methods for the assessment of the LCE and LCP of the Chinese office buildings at the earlier conceptual design stage.** These involve the estimation of the energy consumption and the emission of 4 main pollutants (i.e. CO<sub>2</sub>, SO<sub>2</sub>, NO<sub>x</sub> and PM) during the whole life-cycle period of an office building in China. The process includes the analysis of statistical data, the development of the mathematical correlations between the design parameters and LCE & LCP, as well as the establishment of China-focused LCE& LCP datasets.

**The advantage of the new assessment method is that** the input of the method is highly simplified, removing the consideration of the internal partition and other design details that are unavailable during the conceptual design stage. The estimation method is based on the common formulation dedicated for Chinese office buildings, which were developed by investigating of the Chinese office buildings and individual case studies. This method, connected to the established local dataset, is becoming simpler and faster than the existing methods.

To achieve this target, the LCE & LCP models are divided into 4 major phases of building life cycles (i.e. material, on-site construction, building operation and demolition) which are detailed in Sections 4.3 to 4.6 respectively. For each phase, the characteristics of the LCE and LCP from Chinese office buildings are studied first, followed by the



establishment of associated mathematical equations for the LCE & LCP prediction. In the end, the conclusions are drawn to address the practicality and impact of this method.

## 4.2 Methodology

### 4.2.1 Research scope for different phases and time scopes for the LCE & LCP

The Cradle-to-Grave life cycle analysis is employed in this study, covering four phases from resource extraction (“Cradle”) to disposal (“Grave”). These are (1) the building material/component extraction and production phase, (2) the building construction phase, (3) the building operation phase, and (4) the building demolition phase. These phases operate as a cycle, as shown in Figure 4.1. It should be noted that some materials will be recycled in the last phase and reused in the first phase.

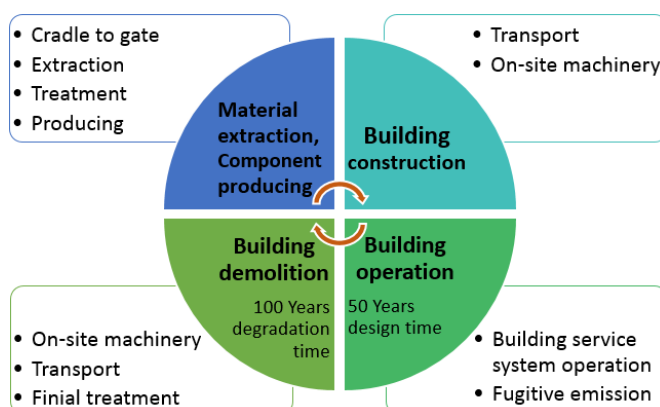


Figure 4.1: Four-phase cycle and their sources for building LCE&LCP

The building operational phase period is considered at 50 years, which is the designed service life for the common office building in China. Although in China the average service life for the office building was only 24 years due to the rapid extension of the urban area and changes in city planning, a well-designed and maintained building should service at least 50 years to reduce the environmental impacts from the rebuild. The time span for the building demolition phase is 100 years. According to the IPCC's (The Intergovernmental Panel on Climate Change) model [22], during the final treatment process, any energy or pollutant emission regarding building waste within a 100 year degradation time will be considered in this research.

#### 4.2.2 Research scope for energy sources and pollutant emissions

The energy resources involved in this research are electricity (for building service system especially HVAC and lighting), gas (mainly for heating), and heat (e.g. solar thermal for heating), as well as diesel and petrol (for transportation and on-site machinery). These energy sources are taken into account during the LCE and LCP assessment.

The pollutants considered in this research are CO<sub>2</sub> equivalents (CO<sub>2</sub>e), SO<sub>2</sub>, NO<sub>x</sub> and PM (Figure 4.2), which are mainly from the direct emissions of on-site construction machinery operation, refrigerant fugitive emissions, and indirect emissions of energy generation that are consumed by buildings themselves. In reality, there are other pollutants generated by an office building, e.g. water, noise and light pollution. However, these pollutants are usually ignored owing to the shortage of the available building standards or accurate measurement methods. As a result, four types of air pollution (i.e. CO<sub>2</sub>, SO<sub>2</sub>, NO<sub>x</sub> and PM), are the only parameters considered in this study.

CO<sub>2</sub>e represents 6 greenhouse gases (GHG): including (1) CO<sub>2</sub>, CH<sub>4</sub>, N<sub>2</sub>O that are mainly from the contribution of fossil fuel combustion, and (2) HFCs, PFCs, SF<sub>6</sub> that are directly from the fugitive emission of refrigeration and air-conditioning (RAC) equipment. All the GHGs emissions are converted to the CO<sub>2</sub> equivalent for a comparable result by using the specific global warming potential (GWP) factor from UNEP-SBCI [13]. NO<sub>x</sub> is a generic term for the mono-nitrogen oxides NO and NO<sub>2</sub>. They are produced from the reaction of nitrogen, oxygen and even hydrocarbons during combustion. The amount of emissions for both NO and NO<sub>2</sub> are accounted in the NO<sub>x</sub> to simplify the calculation. PM (particulate matter), represented by the most harmful and deadly types -- PM<sub>2.5</sub> and PM<sub>10</sub> in this research, is the microscopic solid or liquid matter suspended in the atmosphere. They have impacts on climate and precipitation that adversely affects human health, while SO<sub>2</sub> represents the chemical compound Sulphur dioxide itself.

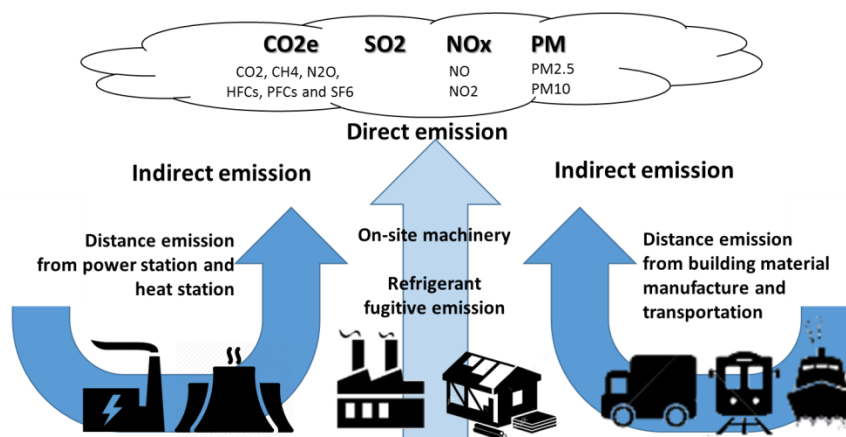


Figure 4.2: Direct and indirect emission sources for LCP [13]

### 4.2.3 Research scope relating to the building materials, components and systems

It is impossible to investigate all types of building materials and components used in the real-world practice, since it is a huge number. Only the ones that are commonly used and certainly decisive in LCE and LCP, are involved in this research. Based on their replaceability, they are divided into two sections for further calculation, those are: the fixed main structure (FMS) section and the variable components (VC) section. The schematic diagram of the two sections can be seen in Figure 4.3.

- The fixed main structure (FMS) section is the fabric of the building; the design of which is largely dependant upon the type of the building structure type and the national codes for the building design. Thus, it has the relatively fixed effect to building`s LCE and LCP. The FMS contains the whole load-bearing structure, the basic structure and the essential accessories for the fabric structure, including the floor and the ceiling, the pillars, the load-bearing layer of the roof, basement and foundation, and the most basic pipelines and wiring. These are studied through the 4 commonly used office building structures.
- On the contrary, the building variable components (VC) section is relatively flexible with a lot of alterable options. It contains everything for the building envelope, including glass / stone curtain walls (4 types), a solid wall with building blocks (4 types), insulation(4 types) and decoration (2 types) layers, windows (4 glass types and 4 frame types), and functional layers (e.g. insulation, green roof) above the load

bearing structure of the roof. The VC section also includes the building service system, involving HVAC (3 types), lighting (2 types), PV and solar thermal system. The selection of the VC section will crucially affect the building's thermal and energy performance, thus bringing a significant impact to the LCE and LCP.

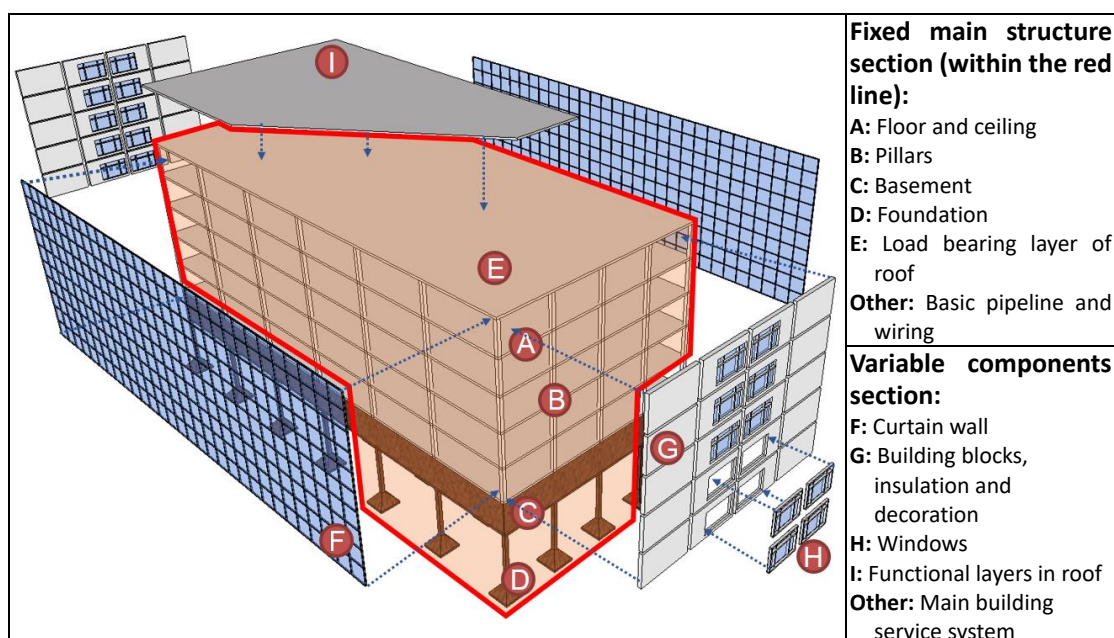


Figure 4.3: Schematic diagram of two sections and their components

- Other components (i.e. light internal partition, elevator, IT / security system and office appliance) are not be considered in this study, as they are customised for specific occupancy and often change during the building operation stage in real-word.

#### 4.2.4 The principles of the assessment method for a building's LCE and LCP

The principle for assessment of the LCE and LCP is illustrated below, which is the basic framework of this research. The overall assessment method for building LCE and LCP is based on the process-based cycle (4 phases), expressed as:

$$LCE = E_M + E_{Con} + E_{Op} + E_{De} \quad (4.1)$$

$$LCP_j = P_{M,j} + P_{Con,j} + P_{Op,j} + P_{De,j} \quad (4.2)$$

Where,  $E_M$  and  $P_{M,j}$  are the embodied energy (MJ) and pollutant  $j$ 's emission (kg) from building material exploitation and producing phase; Similarly,  $E_{Con}$  and  $P_{Con,j}$  are them from the building construction phase;  $E_{Op}$  and  $P_{Op,j}$  are the them during building

operation phase;  $E_{De}$  and  $P_{De,j}$  are them from the building demolition phase.

#### A. The assessment method for the embodied energy and pollutant emissions from building material exploitation and production phase (first phase)

With regard to the material's wastage and service life, the embodied energy consumption ( $E_M$ ) and pollutant  $j$ 's emission ( $P_{M,j}$ ) from building material exploitation and producing is given as:

$$E_M = \sum_{i=1}^n m_i(1 + \delta_i)EF_{M,i}[t_B/t_i] \quad (4.3)$$

$$P_{M,j} = \sum_{i=1}^n m_i(1 + \delta_i)PF_{M,i,j}[t_B/t_i] \quad (4.4)$$

Where:  $m_i$  is the usage (kg) of the specific building material  $i$ ;  $\delta_i$  is the wastage ratio of building material  $i$ ;  $EF_{M,i}$  is the embodied energy consumption factor (MJ/kg) of the specific material  $i$ ;  $PF_{M,i,j}$  is the emission factor (kg/kg) of the embodied pollutants  $j$  for specific material  $i$ ;  $t_B$  is the service life for building (50 year in this research);  $t_i$  is the service life for building material / component  $i$ ;  $[t_B/t_i]$  is the ceiling of  $t_B/t_i$ .

#### B. The assessment method for the embodied energy and pollutant emissions from building on-site construction phase (second phase)

The embodied energy consumption ( $E_{Con}$ ) and pollutant emissions ( $P_{Con,j}$ ) from construction process consist of three sources, they are given as:

$$E_{Con} = E_{Con-T} + E_{Con-O} + E_{Con-L} \quad (4.5)$$

$$P_{Con,j} = P_{Con-T,j} + P_{Con-O,j} + P_{Con-L,j} \quad (4.6)$$

Where:  $E_{Con-T}$  and  $P_{Con-T,j}$  are the embodied energy (MJ) and pollutant  $j$ 's emission (kg) from material transportation (from factory to building site) process; the  $E_{Con-O}$  and  $P_{Con-O,j}$  are them from on-site construction work;  $E_{Con-L}$  and  $P_{Con-L,j}$  are them from the change of land use.

#### C. The assessment method for the embodied energy and pollutant emissions from building operation phase (third phase)

The embodied energy consumption ( $E_{Op}$ ) and pollutant emissions ( $P_{Op,j}$ ) from building

operation phase are related to the operation of building service system and the fugitive emissions. These are expressed as:

$$E_{Op} = E_{Op-ser} + E_{Op-fug} \quad (4.7)$$

$$P_{Op, j} = P_{Op-ser, j} + P_{Op-fug, CO2e} \quad (4.8)$$

Where: the  $E_{Op-ser}$  and  $P_{Op-ser, j}$  are the energy consumption (MJ) and pollutant  $\hat{j}$ 's emission (kg) from the operation of building service system; The  $E_{Op-fug}$  and the  $P_{Op-fug, CO2e}$  are the embodied energy and equivalent carbon emission from the fugitive emission of refrigerants in building RAC (Refrigeration and Air-Conditioning) system.

D. The assessment method for the embodied energy and pollutant emissions from building demolition and follow-on treatment phase (fourth phase)

The energy consumption and pollutant emissions in this phase are mainly from the on-site demolition work, the building wastes transportation, and their final treatment; these are expressed as:

$$E_{De} = E_{De-On} + E_{De-T} + E_{De-Treat} \quad (4.9)$$

$$P_{De, j} = P_{De-On, j} + P_{De-T, j} + P_{De-Treat, j} \quad (4.10)$$

Where: the  $E_{De-On}$ ,  $E_{De-T}$  and  $E_{De-Treat}$  are respectively the energy consumption (MJ) caused by the on-site demolition work, waste transportation, and waste final treatment processes; the  $P_{De-On, j}$ ,  $P_{De-T, j}$  and  $P_{De-Treat, j}$  are the pollutant  $\hat{j}$ 's emission (kg) from those process respectively.

#### 4.2.5 The approaches for the simplified LCE and LCP assessment methods

The simplification and localization of the LCE and LCP assessment for Chinese office buildings are carried out in this research. This is achieved by generating the regression model, the simplified model (from statistical data and typical case analyses), and summarizing the localized dataset. The methods used to generate the simplified estimation models in each phase are shown in Table 4.1 below.

Table 4.1: The method used to generated the simplified and localised estimation models

Phases	Sub-items	Simplification and localisation method
<b>Material</b>	Fixed main structure (FMS) section	Establishing the regression models for the relationship of building features and LCE/LCP through analysing the statistical data, addressed in section 4.3.2.
	Variable component (VC) section	(1) Generating the simplified model and dataset by studying the material usage for building bricks, insulation layer, decoration layer, HVAC and lighting systems; (2) Establishing the regression models for the relationship of glass curtain wall's features and LCE/LCP; addressed in section 4.3.3.
<b>Building construction</b>	Material transport	Simplified model for relationship of statistical distance, vehicle and LCE/LCP, addressed in section 4.4.1
	On-site construction	Establishing the Simplified model for the relationship of LCE&LCP and floor area, addressed in section 4.4.2
	Change of land use	The dataset for 4 typical land types, addressed in section 4.4.3.
<b>Building operation</b>	Building service system operation	The "CN13790" operational energy estimation tool is employed, with the localized dataset of emission factor, addressed in section 4.5.1
	Fugitive emissions	Generating the default fugitive rate for 3 typical RAC systems, addressed in section 4.5.2
<b>Building demolition</b>	On-site demolition	Establishing model for relationship of LCE&LCP and floor area, addressed in section 4.6.1
	Waste transporting	Simplified model and dataset for the relationship of statistical distance, vehicle and LCE/LCP, addressed in section 4.6.2
	Building waste final treatment	Simplified model for the relationship of waste amount and LCE&LCP, and dataset for typical treatment method, addressed in section 4.6.3

### 4.3 The development of the simplified assessment method for the building material phase`s embodied energy ( $E_M$ ) and pollutant emissions ( $P_{M,j}$ )

#### 4.3.1 The general description of the simplified assessment method for $E_M$ and $P_{M,j}$

The  $E_M$  and  $P_{M,j}$  in this phase include the "cradle to gate" scope, which account the energy and pollutants from raw materials extraction, treatment, manufacturing and packing, up to the factory`s gate. The simplified assessment methods for  $E_M$  and  $P_{M,j}$  are discussed respectively for the fixed main structure (FMS) section and variable component (VC) section.

For both FMS section and VC section, the general material`s wastage ratio ( $\delta_i$ ) and service life ( $t_i$ ) for Chinese office building will be investigated using Eqs. 4.3 and 4.4.

The localised dataset for wastage ratio ( $\delta_i$ ) and material service life ( $t_i$ ). The wastage

ratio vary depend upon the design and management level, a dataset contents the average wastage ratio [126] for Chinese building construction is generated (Table 4.2) through the investigation for previous statistics. As previously addressed, the building life is assumed to 50 years in China. Generally, the main structure part, pipe, cable and ventilation ducts are able to serve the whole life span of building, but most windows, waterproof material and external decoration need to be replaced when it can't meet the working/safety standards. The localized dataset for the average service time of the building materials is generated, as shown in Table 4.3.

Table 4.2: Wastage ratio for building materials in this research [126]

Categories	Materials	Wastage Ratio
Basic materials	Steel; cement; concrete; mortar; sand	0.05
All block / brick for building envelop	Concrete brick (CHB, AAC, CBS, CCHB)	0.10
Decoration	Gypsum	0.10
	Stone (marble, etc.); painting	0.05
Others	Electric cable; wire; steel and plastic raceways, air duct and pipes	0.03

Table 4.3: Designed service lift for building components in this research

Building components	Materials contents	Service life
Structure part, pipes, cords, ducts	Steel, cement, concrete, mortar, sand, envelope block and brick, Electric cable, wire, raceways, pipes, ducts.	Same life with building (50 years)
Other envelope components, decorative panels and tiles	decorative stone, decorative tiles, doors, windows, glass curtain wall	30 years
Waterproof layer material	Waterproofing coating and roll	20 years
Building service and renewable energy systems	HVAC, PV and solar thermal	15 years
Others	Internal gypsum surface or decoration, decorative painting	10 years

The material usage  $m_i$ , the energy consumption factor of material phase  $EF_M$  and pollutant emissions factor of this phase  $PF_{M,j}$  and discussed by the FMS section and VC section separately in sections below.

#### 4.3.2 Generating the regression models for $E_M$ and $P_{M,j}$ from the fixed main structure (FMS) section

Through characterization of the  $E_M$  and  $P_{M,j}$  from fixed main structure (FMS) section,



regression models are generated to simplify the assessment for the  $E_M$  and  $P_{M,j}$  from (FMS) section.

- In step A: The energy consumption factors ( $EF_M$ ) and the pollutant emissions factors ( $PF_{M,j}$ ) of this phase for the materials of FMS section are discussed first;
- In step B: The material usage  $m_i$  of FMS section is investigated by case study;
- In step C:  $E_M$  and  $P_{M,j}$  for the selected samples are analyzed;
- In step D: Based on these, the regression equations for the assessment of the  $E_M$  and  $P_{M,j}$  from FMS section are generated.

#### **Step A: Generate the general $EF_M$ and $PF_{M,j}$ for FMS section of Chinese office building**

Investigation of the  $EF_M$  and  $PF_{M,j}$  by the summarizing different data sources through literature review. In China, although the building material related energy and pollutants were widely investigated, there is still no general database containing the data for most commonly building materials. Besides, as the great regional economical and technology difference, the results of same building material from different researches are always distinct.

- For energy consumption factor and CO<sub>2</sub> emission factor, Li Rui's research [127] (i.e. the integration of carbon emission from building materials) and Y. Song's [128] research (i.e. embodied energy from building materials), together with other research results [129] [130] [131], are adopted in this research.
- For emission factor of SO<sub>2</sub>, NO<sub>x</sub> and PM, the lower limit value from "Iron and steel industry cleaner production evaluation index system"(2014) [132] are used for any steel material; the emission standard for new capacity in "The specific requirement for main pollutant emission reducing in 12<sup>th</sup> 5 year plan" [133] are used as the emission source for cement, copper and aluminum; the limitation from "Emission standard of pollutants for petroleum chemistry industry" [134] are used as emission data for anything made of plastic material. For any building material that contains more than one raw material, the emission is calculated by the proportion of contents

(such as ready-mixed concrete) or using the dominant content's emission factor (such as using copper's data instead of electricity wire). Any data that is missing in the data source or not reasonable, a world average or UK's data is used instead of the original one.

The localised dataset for  $EF_{M,i}$  and  $PF_{M,i,j}$  of FMS section is generated and presented in Table 4.4. The data source and reference data are presented in Table 4.5.

Table 4.4:  $EF_M$  and  $PF_{M,j}$  for the buildings with fixed structure

Material		Unit	$EF_M$ MJ/Unit	$PF_{M,CO_2e}$	$PF_{M,SO_2}$	$PF_{M,NO_x}$	$PF_{M,PM}$
Steel bar		kg	22.83	3.744	0.0008	0.00016	0.0006
Other steels		kg	29	3.003	0.0008	0.00016	0.0006
Cement		kg	4.5	0.92	0.311	0.00175	0.0027
Sand		kg	0.6	0.21	0.0002	0.0028	0.00002
Gravel		kg	0.9	0.0052	0.000005	0.00007	0.0000004
Ready-mixed concrete	RC 25/30	m <sup>3</sup>	2293.42	332.10	135.281	0.761	1.174
	RC 28/35		2483.54	363.38	148.025	0.833	1.284
	RC 32/40		2743.44	411.55	167.647	0.943	1.454
Ready-mixed mortar		m <sup>3</sup>	1955	314.67	128.2	0.722	1.12
Electric wires		m	8.14	4.43	0.002	--	--
Plastic raceways		m	3.73	0.35	0.012	0.006	--
Electric cable		m	8.14	4.43	0.002	--	--
Steel cable raceways		m	19.41	1.32	0.004	-	0.0003
Steel air duct		m <sup>2</sup>	357	24.31	0.006	0.0013	0.0049
Steel pipe for electric wire		m	747.2	45.48	0.013	0.0026	0.0096
Steel pipe-other purpose		m	747.2	45.48	0.013	0.0026	0.0096
Water supply pipes-copper		m	52.5	3.39	0.023	--	--
Water drain pipe-PVC		m	27.7	1.325	0.052	0.026	--
Water supply pipes-PPR		m	27.7	1.325	0.052	0.026	--
Water supply pipes-UPVC		m	27.7	1.325	0.052	0.026	--

Table 4.5: Data source description for  $EF_M$  and  $PF_{M,j}$

Material		Data source & Notes
Steel bar & Other steels		Energy and CO <sub>2</sub> emission refer to [128] and [127], others from [132].
Cement		Energy and CO <sub>2</sub> emission refer to [128] and [127], others from [133].
Sand		Energy data converted from [127]; CO <sub>2</sub> from UK ICE's data [135], other's converted from standard diesel drive machinery's emission.
Gravel		
Ready mixed concrete	RC 25/30	Energy and CO <sub>2</sub> emission refers to [127]. For RC 25/30: 0.953 MJ/kg and 0.138 kgCO <sub>2</sub> /kg and 2406.53kg/m <sup>3</sup> . For RC 28/35: 1.032 MJ/kg and
	RC 28/35	

	<b>RC 32/40</b>	0.151 kgCo <sub>2</sub> /kg, 2406.53kg/m <sup>3</sup> . For RC 32/40: 1.14 MJ/kg and 0.171kgCo <sub>2</sub> /kg, 2406.53kg/m <sup>3</sup> .
<b>Ready mixed mortar</b>		Converted from [136]
<b>Electric wires &amp; Electric cable</b>		No data available, using UK ICE's cooper's data [135]: 69.02 MJ/kg and 37.52 kgCo <sub>2</sub> /kg; Weight: 0.118 kg/m, Data represented by size AWG 6.
<b>Plastic raceways</b>		Energy and CO <sub>2</sub> are converted from [136] PVC's data: 15.3 MJ/kg and 1.45kgCo <sub>2</sub> /kg; Other pollutants from [134]. Representing by Sourcingmap 1.9 Ft product.
<b>Steel cable raceways</b>		Converted from [132]and [127]steel's data: 44.1 MJ/kg, 3.003 kgCo <sub>2</sub> e/kg; Weight: 0.44k kg/m, representing by Wiremold 500 Series 10 ft [137].
<b>Steel air duct &amp; Steel pipe for electric wire &amp; Steel pipe-other purpose</b>		Converted from [132]and [127]steel's data: 44.1 MJ/kg, 3.003 kgCo <sub>2</sub> e/kg; For air duct: 8.09 kg/m <sup>2</sup> , thickness: 0.0375 inches; For pipes: 16.06 kg/m representing by: pipe size 4 inches, nominal thickness: 0.24 inches [138]
<b>Water supply pipes-copper</b>		Energy and CO <sub>2</sub> are converted from UK ICE copper pipe's data [135]. 1.25 kg/m; Data represented by: Pipe size 1 inches, nominal thickness: 0.065 inches [139] data, SO <sub>2</sub> from [133].
<b>Water drain pipe-PVC PPR UPVC</b>		Converted from [128]and [134]'s data: 22.16 MJ/kg, 1.06 kgCo <sub>2</sub> e/kg, Weight: 1.25 kg/m; Data represented by: pipe diameter 50mm [140].

Generation of the simplified overall  $EF_M$  and  $PF_{M,j}$  for ready-mixed concrete. Although the  $EF_M$  and  $PF_{M,j}$  for every specific grades of ready-mixed concrete is generated in Table 4.4, it is still not practical to sum them up, as at the conceptual design stage only the total concrete usage is predictable rather than the detailed concrete usage of each concrete grade. Thus, the overall embodied energy consumption factor and embodied pollutant emission factors for each office building types are needed. As previously mentioned, four office building types are selected in this research, which are multi-storage with reinforced concrete frame structure (MS-RCF), high-rise with reinforced concrete frame structure (HR-RCF), high-rise with reinforced concrete frame shearing wall/tube structure (HR-RCF-SW/T) and the high-rise with steel frame shearing wall/tube structure (HR-SF-SW/T). According to the analysis of concrete usage in research samples (71 samples out of 93 samples have the specific grade usage data), concrete grades RC 25/30, RC 28/35 and RC 32/40 takes up 94% of the total concrete usage. The weighted average usage proportion of concrete grades ( $R$ ) is calculated as follow:

$$R = (\sum_{i=1}^n M_i r_i) / (\sum_{i=1}^n M_i) \quad (4.11)$$

Where:  $R$  is weighted average usage proportion for a specific concrete grades in an office building type;  $n$  is the number of samples with 3 concrete grade's data for this office building type;  $M_i$  is the total concrete usage for all grades in sample  $i$ ;  $r_i$  is the

proportion of usage for the specific concrete grade in sample  $i$ .

The calculation results of weighted average usage proportion ( $R$ ) for each office building type are listed in Table 4.6. Based on the  $R$  and the energy consumption factor ( $EF_M$ ) and pollutants emission factors ( $PF_{M,j}$ ) of each concrete grades, the overall  $EF_M$  and ( $PF_{M,j}$ ) of the ready-mixed concrete for each structure type of office building can be seen in Table 4.7.

Table 4.6: The weighted average usage proportion ( $R$ ) for each office building type

Office building structure type:		MS-RCF	HR-RCF	HR-RCF-SW/T	HR-SF-SW/T
Samples with concrete grades usage data / total number of statistic samples		10/12	17/23	25/31	19/27
Weighted average usage proportion ( $R$ )	RC 25/30	0.38	0.35	0.26	0.12
	RC 28/35	0.6	0.63	0.5	0.61
	RC 32/40	0.02	0.02	0.15	0.27

Table 4.7: Overall  $EF_M$  and  $PF_{M,j}$  of the ready-mixed concrete for each office building types

Construction	$EF_M$ MJ/ m <sup>3</sup>	$PF_{M,CO_2e}$	$PF_{M,SO_2}$	$PF_{M,NO_x}$	$PF_{M,PM}$
		kg/ m <sup>3</sup>			
MS-RCF	2407.49	350.87	142.927	0.804	1.240
HR-RCF	2416.99	352.44	143.567	0.808	1.246
HR-RCF-SW/T	2474.99	362.78	147.779	0.831	1.282
HR-SF-SW/T	2519.99	370.73	151.017	0.850	1.311

### Step B: Collect the material usage from the FMS section of Chinese office building

Generate the material usages for the main fixed structure (FMS) section by investigating the building material usage statistic. In total, 93 example buildings are investigated in this research, including all common structural types that are situated in 7 cities among 4 China building climates zone (in which most Chinese cities and population exist). The information of these buildings was taken from local authorities and building research institution (e.g. Shanghai Department of Construction & Construction Material Industry Administration). Thus the selected example buildings can represent the common condition office building in China. The information and distribution of samples can be seen in Table 4.8 and Figure 4.4 below.

Table 4.8: The information and distribution of samples

Structure types of building samples	12 MS-RCF office buildings, 23 HR-RCF office buildings, 31 HR-RCF-SW/T office buildings and 27 HR-SF-SW/T office buildings
Build time	From 1996 to 2015
Location (cities) of building samples	Harbin, Changchun, Beijing, Tianjin, Shanghai, Guangzhou and Shenzhen
Location (China building climate zones) of building samples	Severe cold zone, Cold zone, Hot summer cold winter zone, Hot summer warm winter zone

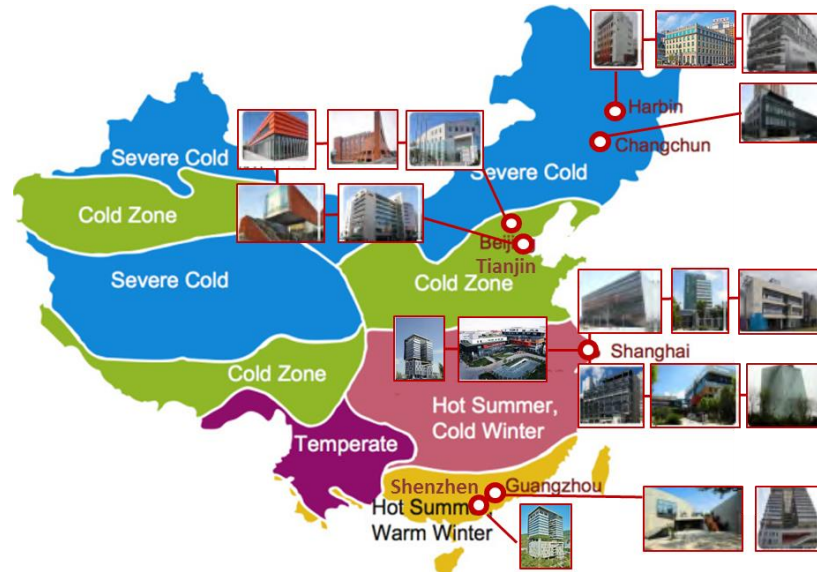


Figure 4.4: Building samples distribution and appearance of the selected samples.

**Step C: Generation of the  $E_M$  and  $P_{M,j}$  for the FMS section of example buildings**

By applying the  $EF_M$  &  $PF_{M,j}$ , and specific material usage data in to equations 4.3-4.4. The  $E_M$  and  $P_{M,j}$  from FMS section for every single example buildings are calculated. A calculation result for  $E_M$  and  $P_{M,j}$  for one of the example buildings is given (Table 4.9), the FMS section's  $E_M$  and  $P_{M,j}$  is respectively 6,043 MJ/m<sup>2</sup>, 720 kgCO<sub>2</sub>e/m<sup>2</sup>, 56.523 kgSO<sub>2</sub>/m<sup>2</sup>, 53.325 kgNO<sub>x</sub>/m<sup>2</sup> and 0.86 kgPM/m<sup>2</sup>. Most  $E_M$  and  $P_M$  in this case are from few key materials (e.g. steel bar and concrete).

Table 4.9: Calculation table for a six-storage sample office building

<b>Example building:</b> 6 story office building with 2 elevators, GFA 7675 m <sup>2</sup>							
<b>Type:</b> Reinforced concrete frame structure							
<b>Unit:</b> $EF_M$ --MJ/Unit; $CF_M$ --kgCO <sub>2</sub> e/ Unit; $E_M$ -- MJ; $C_M$ -- kgCO <sub>2</sub> e							
Material	Unit	Usage /100m <sup>2</sup>	$E_M$ MJ/ m <sup>3</sup>	$P_{M,CO_2e}$ kg/ m <sup>3</sup>	$P_{M,SO_2}$ kg/ m <sup>3</sup>	$P_{M,NO_x}$ kg/ m <sup>3</sup>	$P_{M,PM}$ kg/ m <sup>3</sup>
Steel bar	kg	6362	145244	23819	5.090	1.018	3.817
Other steels	kg	159.3	4620	478	0.127	0.025	0.096

Cement	kg	-	-	-	-	-	-
Sand	kg	-	-	-	-	-	-
Gravel	kg	3112	2801	16	0.016	0.218	0.001
Ready - made concrete	m <sup>3</sup>	36.9	89187	13005	45.977	5297.66	29.815
Ready - made mortar	m <sup>3</sup>	43.62	85277	13726	5592.08	31.494	48.854
Electric wires	m	954.5	7770	4229	1.909	0.000	0.000
Plastic raceways	m	9.8	37	3	0.118	0.059	0.000
Electric cable	m	63.1	514	279	0.126	0.000	0.000
Steel cable raceways	m	13.76	267	18	0.055	0.000	0.004
Steel air duct	m <sup>2</sup>	40.5	14451	984	0.243	0.053	0.198
Steel pipe-electric wire	m	259.4	193824	11798	3.372	0.674	2.490
Steel pipe-other purpose	m	79.1	59133	3599	1.029	0.206	0.760
Water supply pipes-copper	m	0.36	19	1	0.008	0.000	0.000
Water supply pipes-PPR	m	20.5	567	27	1.065	0.532	0.000
Water supply pipes-UPVC	m	-	-	-	-	-	-
Water drain pipe-PVC	m	20.2	560	27	1.050	0.525	0.000
<b>Total:</b> (Whole building)			<b>46377753</b>	<b>5526807</b>	<b>433812</b>	<b>409267</b>	<b>6603</b>
<b>Total:</b> (Per m <sup>2</sup> )			<b>6043</b>	<b>720</b>	<b>56.523</b>	<b>53.325</b>	<b>0.860</b>

The 93 example buildings are calculated in the same way. The building materials are classified into 3 major groups (i.e. Concrete & Mortar group, Steel group, and Wire, Pipe, Others group), while their specifications are listed in Table 4.10. For each building sample, each material group's contribution to  $E_M$  and  $P_{M,j}$  are analyzed, and the mean value ( $\mu$ ) of each group's contribution are obtained for all typical structures (addressed in Figure 4.5- Figure 4.7). In order to validate the effectiveness of the mean value, the coefficient of variation (CV), also known as relative standard deviation (RSD), are checked in Table 4.11. Following the 'rule of thumb' criteria for precision values, RSD less than 25%, 18%, and 10% for 2, 3 to 6 and over 6 samples respectively, are considered low variation. The RSDs in Table 4.11 are all below 10% thus the  $\mu$  are all valid.

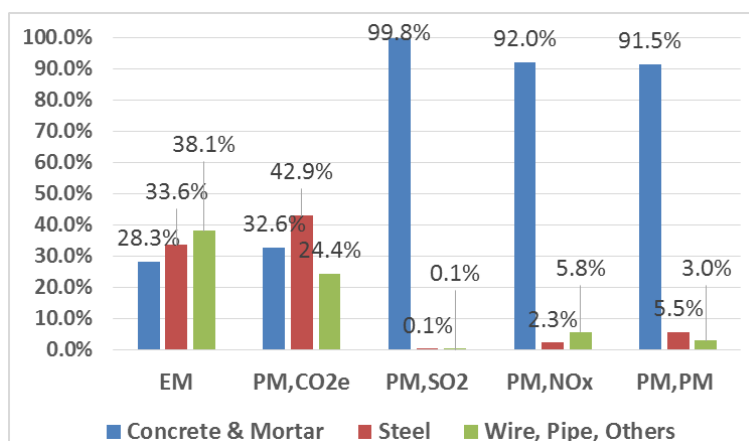
Table 4.10: the specification of 3 major materials groups in FMS

Major groups	Concrete&Mortar	Steel	Wire, Pipe, Others
Included materials Specification	cement, sand, gravel, ready-made concrete ready-made mortar	steel bar, other steels	electric wires, electric cable, cable raceways -- Plastic/steel steel air duct steel pipe--electric wire/other purposes water supply pipes -- copper / PPR / UPVC / PVC

Table 4.11: RSD checking Table for each material group of typical structures

Material catalogues in 3 building types		RSD of samples for specific items				
		$E_M$	$P_{M,CO_2e}$	$P_{M,SO_2}$	$P_{M,NO_x}$	$P_{M,PM}$
MS-RCF & HR-RCF (35 samples)	Concrete & Mortar	6.0%	7.1%	7.1%	6.9%	7.1%
	Steel	9.3%	9.3%	9.3%	9.3%	9.3%
	Wire, Pipe, Others	8.7%	7.5%	4.1%	7.4%	9.1%
HR-RCF-SW/T (31 samples)	Concrete & Mortar	4.2%	4.0%	3.8%	4.4%	3.8%
	Steel	7.9%	7.3%	7.6%	7.6%	7.6%
	Wire, Pipe, Others	9.8%	9.1%	8.5%	8.4%	9.8%
HR-SF-SW/T (27 samples)	Concrete & Mortar	4.6%	4.0%	4.1%	4.8%	3.8%
	Steel	7.7%	8.0%	8.3%	7.9%	7.7%
	Wire, Pipe, Others	9.8%	9.5%	9.2%	8.7%	9.3%

Note: 12 MS-RCF samples and 23 HR-RCF samples are analyzed together as they both belonging to the reinforced concrete frame structure.

Figure 4.5: The group's contribution to  $E_M$  and  $P_{M,j}$  for MS-RCF & HR-RCF structure buildings

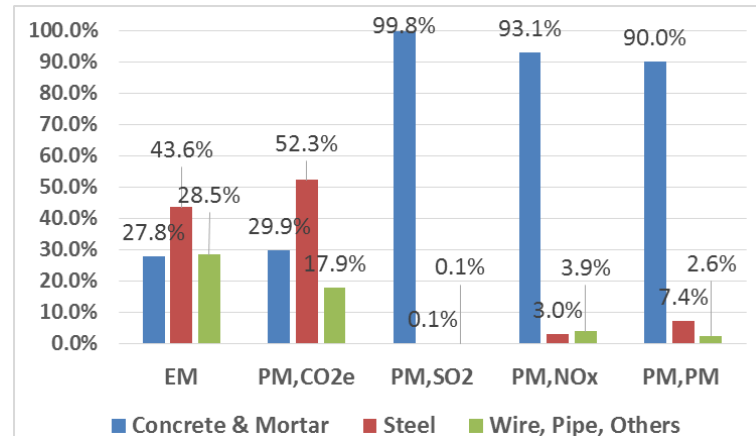


Figure 4.6: The group's contribution to  $E_M$  and  $P_{M,j}$  for the HR-RCF-SW/T structure buildings

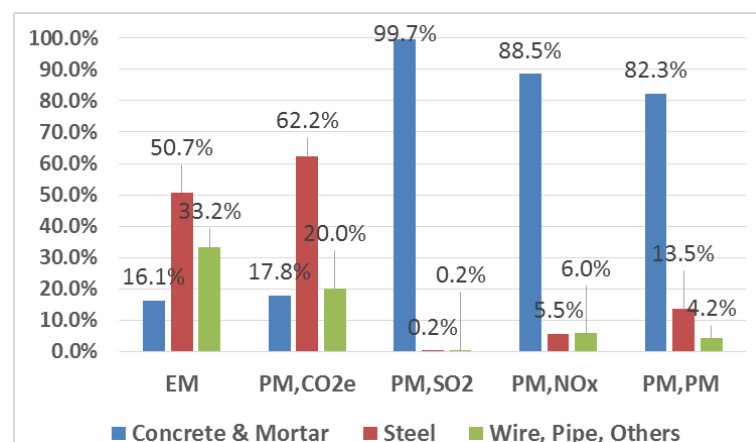


Figure 4.7: The group's contribution to  $E_M$  and  $P_{M,j}$  for the HR-SF-SW/T structure buildings

#### Analysing the characteristics of $E_M$ and $P_{M,j}$ from three material groups.

- For  $E_M$  in FMS section: the percentage of  $E_M$  from concrete & mortar material group are similar in the MS-RCF & HR-RCF building type and HR-RCF-SW/T building type, but it is 8% less in HR-SF-SW/T type, because the structure is relatively lighter with help of load bearing by steel frame. In contrast, the steel material group contributes more than 50% of  $E_M$  in HR-SF-SW/T structure, most of which are from the load-bearing steel frame. The  $E_M$  from steel is 10% higher in HR-RCF-SW/T structure than in MS-RCF & HR-RCF structure, as the latter type have higher load-bearing requirement and steel bar usage in structural column and shear wall. It is worth noticing that although material usage of the wire, pipe and other material group is not as much as concrete or steel, they still significantly contribute to the  $E_M$ . This is because they are deep-processed products from metal



and petrochemicals, which have higher  $EF_M$  and  $PF_{M,j}$ .

- For  $P_{M,CO_2e}$  in FMS section: The distribution of  $CO_2e$  is similar to the energy consumption. The concrete & mortar materials group contributes 32.6% to 17.8%  $CO_2e$  emission among all structure types. The percentage of  $P_{M,CO_2e}$  from steel material group is higher in every construction types compare to its contribution of energy consumption, owing to metal's high emission factor.
- For  $P_{M,SO_2}$ ,  $P_{M,NO_x}$  and  $P_{M,PM}$  in FMS section: More than 90% of  $SO_2$ ,  $NO_x$  and PM emission are from concrete material group, especially for  $SO_2$ , caused by the compared low manufacturing technology level in China cement industry, this value are reducing with the application of high standard de-sulfurizing and dust removing facilities. The upgrading of China cement industry will help greatly decrease the  $SO_2$ ,  $NO_x$  and PM simultaneously.

#### **Step D: Generation of the mathematic estimation method for the $E_M$ and $P_{M,j}$ from FMS section**

The 93 example buildings' overall  $E_M$  and  $P_{M,j}$  from FMS section are computed to analysis the relations between them and the number of building storeys for typical construction types. The calculation results are first validated by RSD checking, the following regression functions are then developed for the estimation of  $E_M$  and  $P_{M,j}$  from FMS section.

**For MS-RCF and HR-RCF structure office building**, the mean values ( $\mu$ ) of FMS section's  $E_M$  and  $P_{M,j}$  for 35 example buildings are computed, then validated by RSD check (Table 4.12). The maximum (worst) RSD is 9.9% for 7 storeys building (7 samples)'s  $P_{M,PM}$ , which is still lower than the 10% limited, therefore, the  $\mu$  is appropriate to represents the  $E_M$  and  $P_{M,j}$  for this structure type.

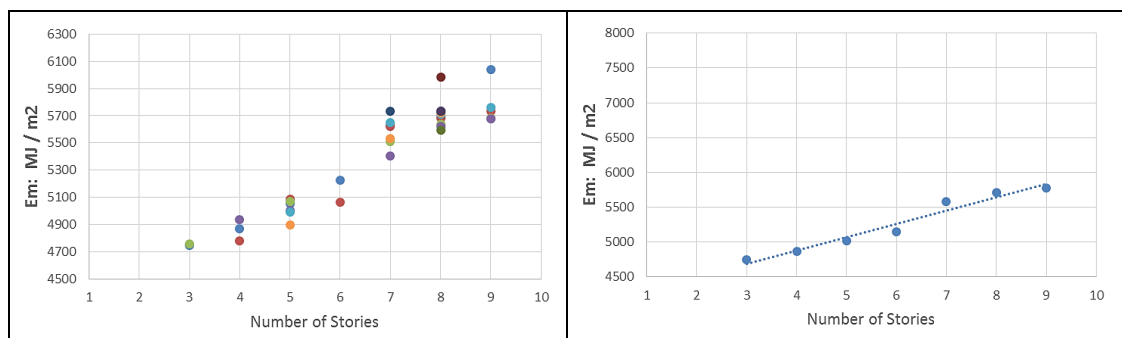
Table 4.12: Basic descriptive statistics of  $E_M$  and  $P_{M,j}$  from MS-RCF and HR-RCF samples

Number of Stories		3	4	5	6	7	8	9
Number of samples		2	3	6	2	7	10	5
$E_M$	$\mu$	4753.3	4862.8	5016.7	5146.8	5583.3	5710.7	5780.0
	RSD	0.1%	1.3%	1.3%	1.5%	1.8%	1.8%	2.3%
$P_{M,CO2}$	$\mu$	634.3	631.1	652.7	662.7	682.9	671.9	716.6
	RSD	0.3%	3.5%	1.3%	0.1%	2.0%	2.3%	1.2%
$P_{M,SO2}$	$\mu$	63.55	74.43	85.28	97.05	92.76	108.26	107.08
	RSD	3.6%	4.0%	3.6%	1.6%	6.3%	5.6%	6.6%
$P_{M,NOx}$	$\mu$	0.405	0.447	0.528	0.532	0.530	0.645	0.627
	RSD	6.2%	6.6%	3.6%	1.9%	8.3%	6.1%	8.7%
$P_{M,PM}$	$\mu$	0.540	0.642	0.700	0.705	0.929	0.966	0.938
	RSD	3.7%	7.8%	3.6%	1.7%	9.9%	6.1%	8.7%

Based on the above, the linear regression functions (represent the relationship between  $E_M$ ,  $P_{M,j}$  and the number of storeys) are obtained by using mean values. The functions and their coefficient of determination ( $R^2$ ) are given in Table 4.13. According to  $R^2$ , the data are close enough to the fitted regression line (Figure 4.8). The  $E_M$  and  $P_{M,j}$  (Y in equation) can be estimated for each possible value of building storeys (X in equation).

Table 4.13: Regression functions and key indicators for FMS of MS-RCF and HR-RCF office building

Y	Function	$R^2$	p-value
$E_M$	$Y=190.8X+4120$	0.958	0.044
$P_{M,CO2}$	$Y=12.818X+587.7$	0.871	0.041
$P_{M,SO2}$	$Y=7.347X+45.69$	0.9182	0.038
$P_{M,NOx}$	$Y=0.038X+0.303$	0.8956	0.036
$P_{M,PM}$	$Y=0.074X+0.330$	0.9003	0.041



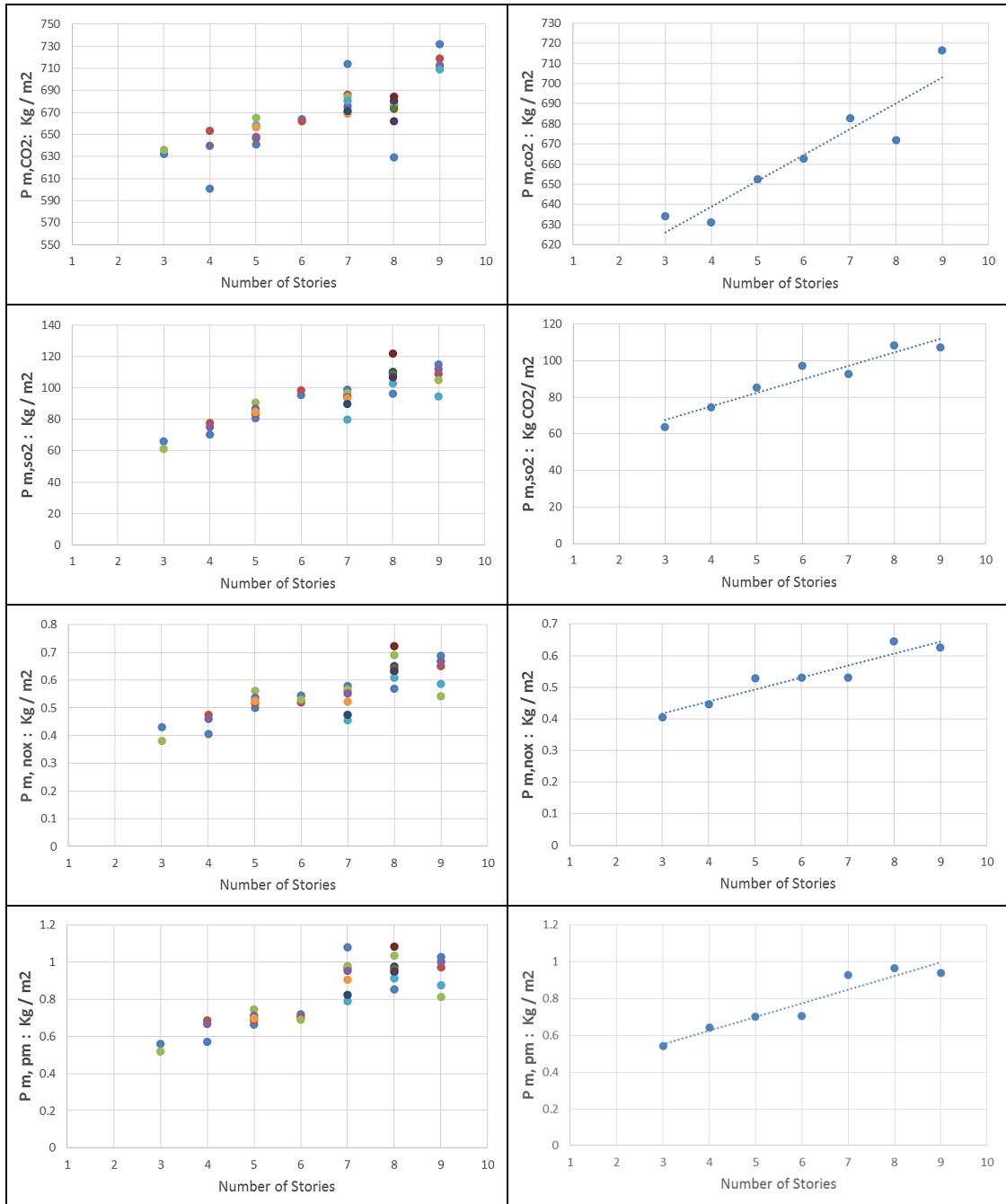


Figure 4.8: Scatter plot and the regression line of  $E_M$  and  $P_{M,j}$  and building stories numbers for the FMS of MS-RCF and HR-RCF office building

**For the HR-RCF-SW/T structure office building,** the process is similar. The  $\mu$  and RSDs of  $E_M$  and  $P_{M,j}$  for 31 example buildings with different storeys are computed (Table 4.14). The maximum (worst) RSD is 13.3%, which is still lower than the 18% limitation. Therefore, the  $\mu$  is appropriate to obtain the linear regression functions for  $E_M$  and  $P_{M,j}$  (Table 4.15). According to  $R^2$ , for all regression functions the data are close enough to the fitted regression lines (Figure 4.9). The  $E_M$  and  $P_{M,j}$  (Y in equation) can

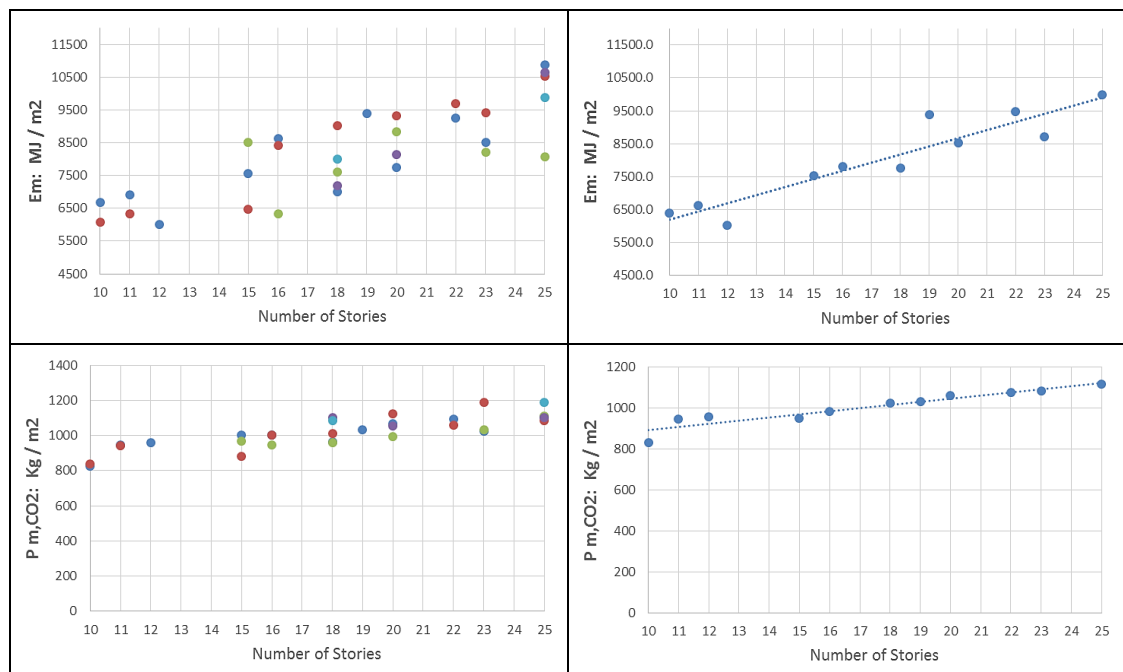
be estimated for each possible value of building storeys (X in equation) using the equations given in Table 4.15.

Table 4.14: Basic descriptive statistics of  $E_M$  and  $P_{M,j}$  from the HR-RCF-SW/T samples

Storage number	10	11	12	15	16	18	19	20	22	23	25	
Sample number	2	2	1	3	3	5	1	4	2	3	5	
$E_M$	$\mu$	6380.7	6626.7	6019.6	7523.4	7798.7	7764.0	9386.5	8515.7	9483.7	8712.2	9895.8
	RSD	4.7%	4.3%	--	11.1%	13.3%	9.2%	--	7.2%	2.3%	5.8%	10.2%
$P_{M,CO2}$	$\mu$	833.6	945.6	958.9	950.7	985.5	1024.9	1031.7	1061.0	1076.2	1083.1	1119.4
	RSD	0.8%	0.2%	--	5.5%	2.6%	5.8%	--	4.4%	1.7%	6.9%	3.3%
$P_{M,SO2}$	$\mu$	107.52	101.39	109.34	107.61	117.98	122.35	131.19	119.15	140.14	137.57	152.75
	RSD	2.8%	1.5%	--	5.4%	12.2%	11.6%	--	5.6%	7.8%	8.2%	4.0%
$P_{M,NOx}$	$\mu$	0.73	0.621	0.663	0.723	0.793	0.777	0.779	0.83	0.773	0.850	0.865
	RSD	1.2%	2.6%	--	10.9%	11.5%	12.3%	--	4.4%	0.9%	11.6%	6.6%
$P_{M,PM}$	$\mu$	1.079	1.096	1.104	1.130	1.132	1.206	1.161	1.199	1.241	1.217	1.271
	RSD	0.7%	1.2%	--	8.0%	5.2%	4.8%	--	5.4%	1.8%	0.8%	6.1%

Table 4.15: Regression functions and key indicators for FMS of HR-RCF-SW/T office building

Y	function	R <sup>2</sup>	p-value
$E_M$	$Y=246.68X+3735.5$	0.872	0.031
$P_{M,CO2}$	$Y=15.404X+738.9$	0.897	0.033
$P_{M,SO2}$	$Y=3.008X+70.227$	0.918	0.035
$P_{M,NOx}$	$Y=0.038X+0.303$	0.870	0.033
$P_{M,PM}$	$Y=0.0132X+0.5336$	0.767	0.041



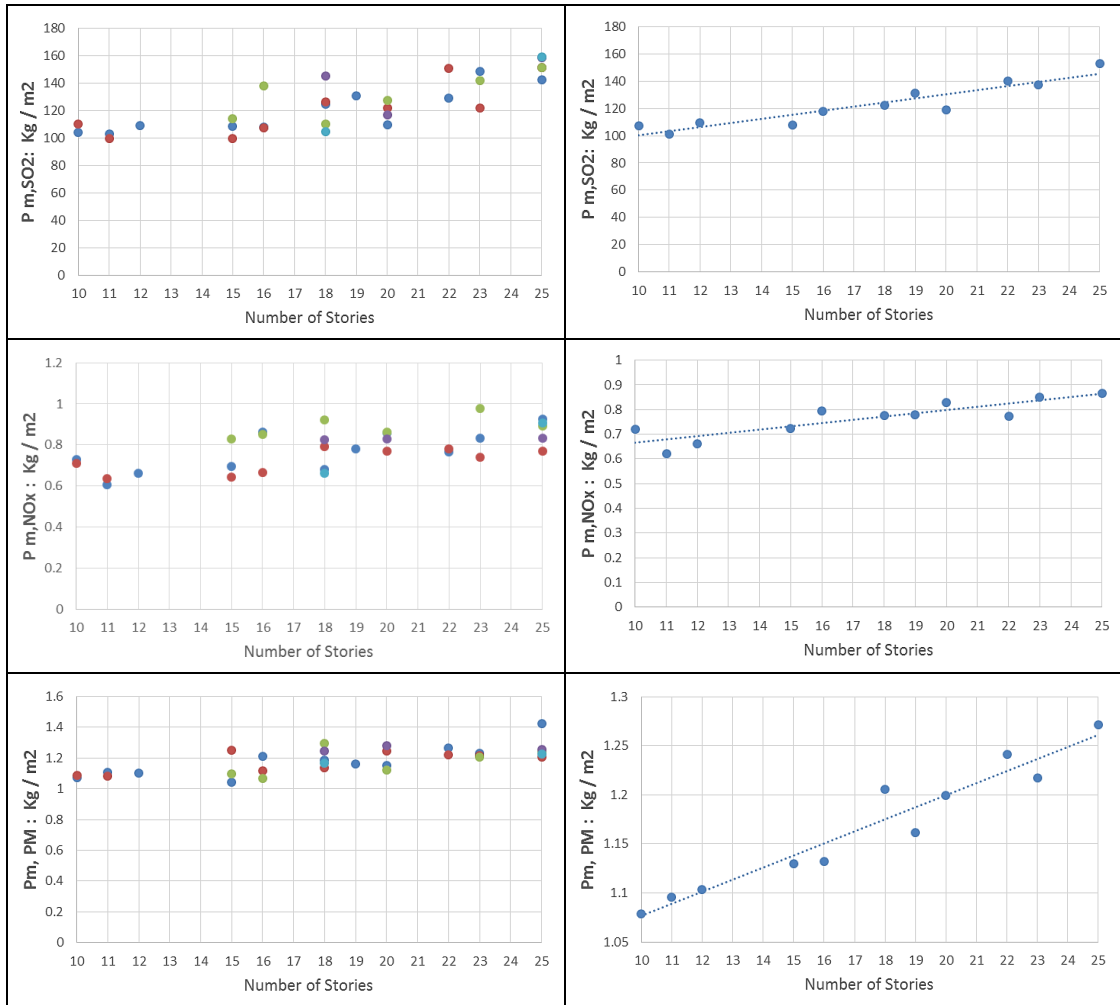


Figure 4.9: Scatter plot and the regression line of  $E_M$  and  $P_{M,j}$  and building stories numbers for FMS of HR-RCF-SW/T office building.

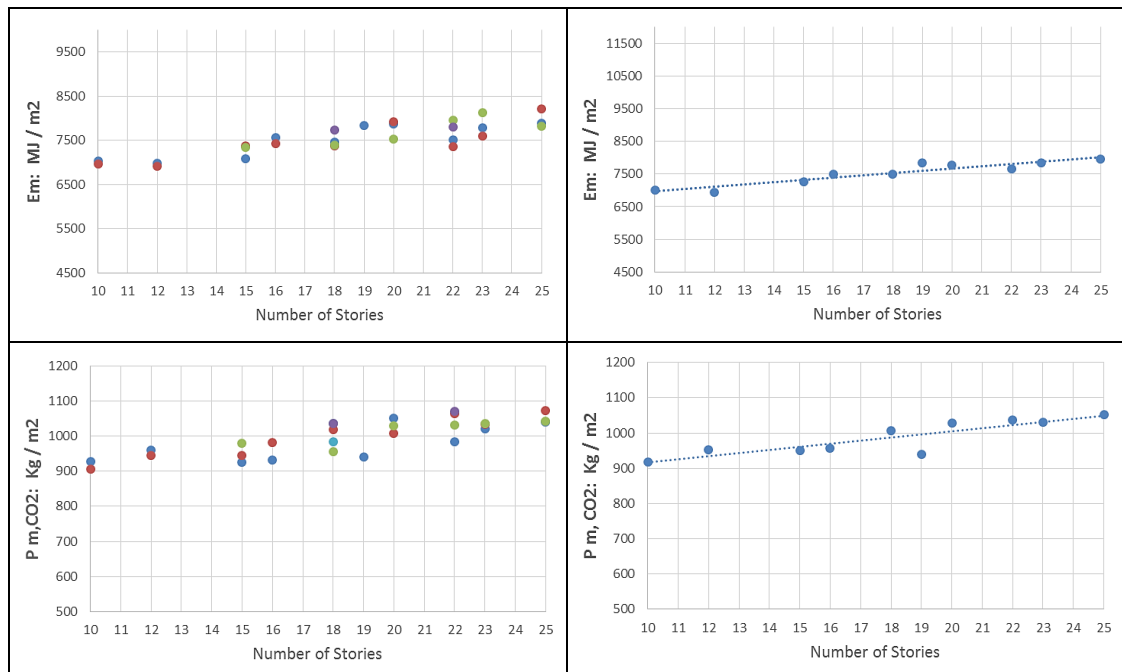
**For HR-SF-SW/T structure office building,** the process is similar. The  $\mu$  and RSDs of  $E_M$  and  $P_{M,j}$  for 27 example buildings with different storeys are computed (Table 4.16). The maximum (worst) RSD is 5.2 %, which is still lower than the 18% limitation. Therefore, the  $\mu$  is appropriate to obtain the linear regression functions for  $E_M$  and  $P_{M,j}$  (Table 4.17). According to  $R^2$  for each function, the data are close enough to the fitted regression lines (Figure 4.10). The  $E_M$  and  $P_{M,j}$  (Y in equation) can be estimated for each possible value of building storeys (X in equation) using the equations given in Table 4.17.

Table 4.16: Basic descriptive statistics of  $E_M$  and  $P_{M,j}$  from HR-SF-SW/T samples

Number of Stories	10	12	15	16	18	19	20	22	23	25	
Number of samples	2	2	3	2	4	1	3	4	3	3	
$E_M$	$\mu$	7000.6	6942.5	7264.3	7494.9	7492.4	7836.5	7779.5	7653.3	7835.4	7969.1
	RSD	0.6%	0.4%	1.7%	1.0%	2.0%	0.0%	2.3%	3.1%	2.8%	2.2%
$P_{M,CO2}$	$\mu$	917.2	952.9	949.8	956.4	1005.5	940.0	1028.8	1036.9	1029.7	1051.7
	RSD	1.1%	0.8%	2.3%	2.6%	3.2%	0.0%	1.7%	3.3%	0.6%	1.5%
$P_{M,SO2}$	$\mu$	61.23	68.50	66.72	69.85	69.20	73.56	71.91	74.64	75.00	79.67
	RSD	3.6%	5.1%	3.5%	0.1%	3.3%	0.0%	2.7%	2.7%	3.0%	5.2%
$P_{M,NOx}$	$\mu$	0.43	0.45	0.46	0.48	0.48	0.52	0.53	0.51	0.51	0.52
	RSD	3.2%	1.4%	3.9%	4.2%	3.8%	0.0%	0.3%	4.2%	2.2%	3.6%
$P_{M,PM}$	$\mu$	0.672	0.677	0.747	0.736	0.748	0.724	0.729	0.785	0.798	0.827
	RSD	3.3%	0.6%	1.0%	2.2%	3.8%	0.0%	2.9%	3.3%	3.4%	3.9%

Table 4.17: Regression functions and key indicators for FMS of HR-SF-SW/T office building

Y	function	R <sup>2</sup>	p-value
$E_M$	$Y=69.842X+6269.7$	0.878	0.032
$P_{M,CO2}$	$Y=8.837X+827.83$	0.768	0.029
$P_{M,SO2}$	$Y=0.9998X+53.032$	0.879	0.031
$P_{M,NOx}$	$Y=0.0064X+0.3745$	0.823	0.038
$P_{M,PM}$	$Y=0.0094X+0.5754$	0.835	0.037



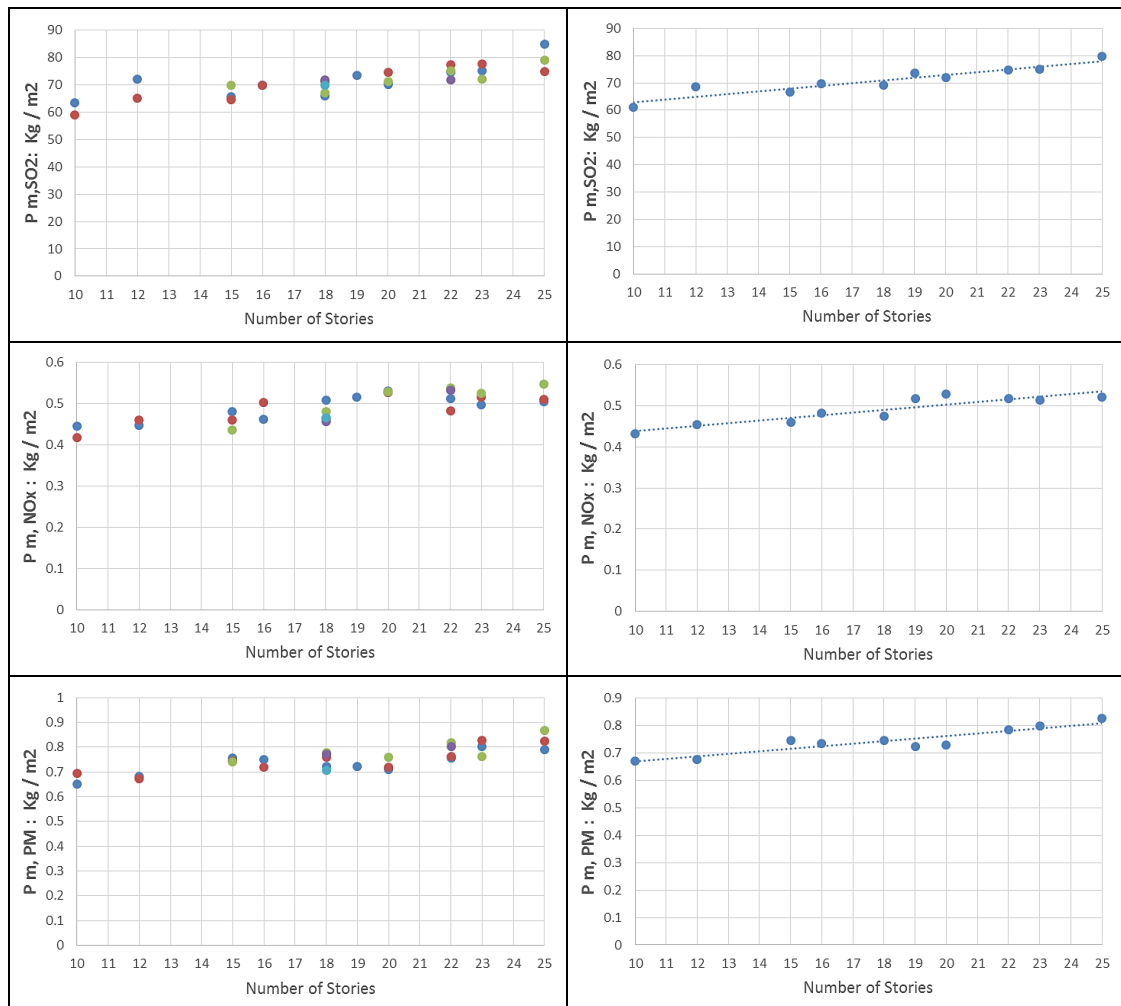


Figure 4.10: Scatter plot and the regression line of  $E_M$  and  $P_{M,j}$  and building stories numbers for FMS of HR-SF-SW/T office building.

**In summary**, the  $E_M$  &  $P_{M,j}$  increased with the number of building storeys, and the linear increasing trend exists in all structural types. For the MS-RCF & HR-RCF structure type, there's a 3% increasing rate of  $E_M$  &  $P_{M,j}$  for adding one single storey. Similar increasing rate are shown in HR-RCF-SW/T structure building. However, for the 9-storey (with MS-RCF & HR-RCF structure) to 10-storeys building (with HR-RCF-SW/T structure), 10% increase in  $E_M$  &  $P_{M,j}$  is found, owing to the significant change in the type of the structure. The shearing wall in the latter structure contains large amount of high-grade concrete in order to bearing the load from high-rising building.

Comparison between the HR-RCF-SW/T and HR-SF-SW/T structure indicated that the latter structure has about 10% higher in  $E_M$  &  $P_{M,j}$  for lower building. However, the latter has significantly lower  $E_M$  &  $P_{M,j}$  values than the former structure when the

building height is increasing. The obvious advantage of the steel frame is that the load-bearing structure is light-weighted, and less load-bearing. Therefore, the material usage of the load-bearing part will have a much reduced increase rate than that for the heavy-weighted structure types. Benefiting from this reduced increasing rate, a 25 storeys office building with HR-SF-SW/T structure will have 24% lower energy consumption and SO<sub>2</sub>, NO<sub>x</sub>, and PM emission than the HR-RCF-SW/T building with the same height. It is worth to emphasize that the same trend doesn't exist in CO<sub>2e</sub> emission, owing to the high CO<sub>2e</sub> emission factor of steel.

#### 4.3.3 Generation of the simplified assessment method for $E_M$ and $P_{M,j}$ from the variable components (VC) section

As mentioned in the methodology, the variable components (VC) section of office building includes all components of building envelope and also the key building service systems. Each component of the VC section has various options in real-world practice, which will bring significantly different thermal performance, energy usages and pollutant emissions. The  $E_M$  &  $P_{M,j}$  are discussed respectively for the building block/brick and insulation layer (section A), the decoration layers (section B), the windows/glass curtain wall (section C), the HVAC system (section D) and the lighting system (section E).

##### **A. The simplified assessment method for the $E_M$ and $P_{M,j}$ from the building block/brick and insulation layer**

In this research, four typical blocks/bricks and four typical wall insulation materials are investigated; these are AAC (autoclaved aerated concrete), CHB (concrete hollow blocks), CSB (concrete solid block), CCHB (ceramsite concrete hollow block) and XPS (extruded polystyrene), EPS (expanded polystyrene), Glasswool, Rockwool. The  $E_M$  &  $P_{M,j}$  in above components consist of two sources which are the main material itself (e.g. EPS panel) and the additional material/accessories (e.g. agglutinant and hanging frame for EPS panel); these are expressed as.

$$E_{M,i} = EF_{M,i,mai}A_i d_i \rho_i + E_{M,i,add} \quad (4.12)$$









$$P_{M,j,i} = PF_{M,j,i}A_i d_i \rho_i + P_{M,j,i,add} \quad (4.13)$$



Where: the  $EF_{M,i,mai}$  and  $PF_{M,j,i}$  are respectively the energy consumption factor (MJ/kg) and pollutants  $\hat{j}$ 's emission factor (kg/kg) for building material phase from main material  $i$  of building block and insulation;  $A_i$  is the application area (m<sup>2</sup>) of material  $i$  (e.g. EPS panel);  $d_i$  is the thickness (m) of material  $i$ ;  $\rho_i$  is the density (kg/m<sup>3</sup>) of material  $i$ ;  $E_{M,i,add}$  and  $P_{M,j,i,add}$  are respectively the energy consumption (MJ) and pollutants  $\hat{j}$ 's emission (kg) of building material phase from additional material/accessories.

The calculation method and dataset for the main materials of the building block and the insulation layer. The  $EF_{M,i,mai}$  and  $PF_{M,j,i,mai}$ , as well as other specification (i.e. thickness, density) of main materials are summarized into the China localized dataset based on the market investigation and standard review; and presented in Table 4.18.

Table 4.18: Options of Block/brick and insulation layer for building envelope and their specification [131] [141] [142] [143] [144]

Block/brick and insulation layer for building envelope				
	AAC	CHB	CSB	CCHB
Type:				
$EF_M$ & $PF_{M,j}$	$EF_M$ : 9.79MJ/kg $PF_{M,CO2e}$ :0.86kg/kg $PF_{M,SO2}$ :0.311kg/kg $PF_{M,NOx}$ :0.0018kg/kg $PF_{M,PM}$ :0.0027kg/kg	$EF_M$ : 2.59/kg $PF_{M,CO2e}$ :0.301kg/kg $PF_{M,SO2}$ :0.082kg/kg $PF_{M,NOx}$ :0.0005kg/kg $PF_{M,PM}$ :0.0007kg/kg	$EF_M$ : 2.28MJ/kg $PF_{M,CO2e}$ :0.243kg/kg $PF_{M,SO2}$ :0.072kg/kg $PF_{M,NOx}$ :0.0004kg/kg $PF_{M,PM}$ :0.0006kg/kg	$EF_M$ : 2.28MJ/kg $PF_{M,CO2e}$ :0.243kg/kg $PF_{M,SO2}$ :0.072kg/kg $PF_{M,NOx}$ :0.0004kg/kg $PF_{M,PM}$ :0.0006kg/kg
Options specification	Type: A3.5 B06 600kg/m <sup>3</sup> Thickness Options: 0.1 m 0.12 m 0.15 m 0.18 m 0.2 m 0.25 m 0.3 m	Type 1: Single hole 800kg/m <sup>3</sup> , Type 2: Double hole 780kg/m <sup>3</sup> , Thickness Options: 0.09 m 0.115 m 0.14 m 0.19 m	Thickness Options: 0.14 m 0.19 m Density: 1760kg/m <sup>3</sup> ,	Thickness Options: 0.14 m 0.19 m Density: 600kg/m <sup>3</sup> ,
	XPS	EPS	Glasswool	Rockwool
Type:				

<b><math>EF_M</math> &amp; <math>PF_{M,j}</math></b>	$EF_M$ : 13.99MJ/kg $PF_{M.CO2e}$ : 1.191kg/kg $PF_{M.SO2}$ : 0.05kg/kg $PF_{M.NOx}$ : 0.0246kg/kg $PF_{M.PM}$ : 0.0052kg/kg	$EF_M$ : 13.99MJ/kg $PF_{M.CO2e}$ : 1.191kg/kg $PF_{M.SO2}$ : 0.05kg/kg $PF_{M.NOx}$ : 0.0246kg/kg $PF_{M.PM}$ : 0.0052kg/kg	$EF_M$ : 12.47MJ/kg $PF_{M.CO2e}$ : 1.29kg/kg $PF_{M.SO2}$ : 0.0006kg/kg $PF_{M.NOx}$ : 0.0054kg/kg $PF_{M.PM}$ : 0.0052kg/kg	$EF_M$ : 2.6MJ/kg $PF_{M.CO2e}$ : 0.33kg/kg $PF_{M.SO2}$ : 0.0006kg/kg $PF_{M.NOx}$ : 0.0054kg/kg $PF_{M.PM}$ : 0.0052kg/kg
<b>Options specification</b>	<b>Thickness:</b> 0.01 m 0.02 m 0.025 m 0.03 m 0.04 m 0.05 m 0.075 m 0.1 m 0.12 m 0.15 m <b>Density:</b> 30kg/m <sup>3</sup> ,	<b>Thickness:</b> 0.01 m 0.02 m 0.025 m 0.03 m 0.04 m 0.05 m 0.075 m 0.1 m 0.12 m 0.15 m <b>Density:</b> 25kg/m <sup>3</sup> ,	<b>Thickness:</b> 0.03m 0.05m 0.08m 0.1m <b>Density:</b> 24kg/m <sup>3</sup>	<b>Thickness:</b> 0.03 m 0.05 m 0.08 m 0.1 m <b>Density:</b> 200kg/m <sup>3</sup> ,

The calculation method and dataset for the energy consumption ( $E_{M,i,add}$ ) and pollutant emissions ( $P_{M,j,i,add}$ ) for the additional materials. The  $E_{M,i,add}$  and  $P_{M,j,i,add}$  of the additional materials (e.g. adhesives and cement) and accessories (e.g. nails) for the installation of building block and insulation layers are discussed separately.

- The  $E_{M,i,add}$  and  $P_{M,j,i,add}$  of additional materials for the building block/brick are expressed as:

$$E_{M,i,add} = EF_{M,i,add} A_i d_i \quad (4.14)$$

$$P_{M,j,i,add} = PF_{M,j,i,add} A_i d_i \quad (4.15)$$

Where: the  $EF_{M,i,add}$  and  $PF_{M,i,add}$  respectively are the energy factor (MJ/m<sup>3</sup>) and pollutant  $j$ 's emission factor (kg/m<sup>3</sup>) for additional materials of building block;  $A_i$  and  $d_i$  are the application area (m<sup>2</sup>) and thickness (m) of building block.

According to statistics for the construction process in China, the general  $EF_{M,i,add}$  and  $PF_{M,i,add}$  of block/brick is represented by the energy and emission data from the M5 cement mortar used in the installation of 1m<sup>3</sup> AAC bricks (Table 4.19)

Table 4.19: Additional material and accessories dataset for building block/brick per m<sup>3</sup>

Material and usage	$EF_{M,i,add}$	$PF_{M.CO2e, i,add}$	$PF_{M.SO2, i,add}$	$PF_{M.NOx, i,add}$	$PF_{M.PM, i,add}$
Cement mortar M5 (0.397 m <sup>3</sup> )	776.1	124.9	50.90	0.2866	0.4446

- The  $E_{M,i,add}$  and  $P_{M,j,i,add}$  of additional materials for insulation layer are expressed as:

$$E_{M,i,add} = EF_{M,i,add} A_i \quad (4.16)$$

$$P_{M,j,i,add} = PF_{M,j,i,add} A_i \quad (4.17)$$

Where: the  $EF_{M,i,add}$ ,  $PF_{M,i,add}$  and  $A_i$  respectively are the energy factor (MJ/m<sup>2</sup>)

and pollutant  $j$ 's emission factor ( $\text{kg}/\text{m}^2$ ), and application area ( $\text{m}^2$ ) for additional materials of insulation layer.

The general  $EF_M$  and  $PF_{M,j}$  for the additional materials are summarized according to the statistics for the construction process in China. The typical dataset is established for the data of the additional material of insulation layers, addressed in Table 4.20.

Table 4.20: Additional material and accessories dataset for insulation layer per  $\text{m}^2$

Material and usage	$EF_{M,i,add}$	$PF_{M,CO_2e,i,add}$	$PF_{M,SO_2,i,add}$	$PF_{M,NO_x,i,add}$	$PF_{M,PM,i,add}$
Polymer adhesive mortar (4kg)	11.64	1.874	0.763	0.004	0.007
Polymer overlay mortar (6kg)	17.46	2.810	1.145	0.006	0.010
Low alkali cloth mesh (1.1 $\text{m}^2$ )	6.897	0.352	-	-	-
Nails (0.25kg)	7.875	0.75	0.00028	0.00003	0.0002
<b>Total</b> (General data $EF_{M,i,add}$ and $PF_{M,j,i,add}$ of insulation layer)	<b>43.9</b>	<b>5.8</b>	<b>1.91</b>	<b>0.010</b>	<b>0.017</b>
Note: I .The $EF_M$ and $PF_{M,j}$ for Polymer adhesive mortar and Polymer Overlay mortar are assumed as high as 5 times of normal M5 mortar's data. II . The $EF_M$ and $PF_{M,j}$ for felt underlay from ICE2.0 are used for Low alkali cloth mesh felt underlay					

## B. The simplified assessment method for the $E_M$ and $P_{M,j}$ from the internal and external decoration layers of building envelope

There are vast of selections for the decoration layers of the internal and external surface of the building envelope. They are relatively insignificant for the thermal performance of the façade. Hence, only one typical decoration for the internal surface (i.e. glazed facing tile decoration) and two for the external surface (i.e. dry hanging stone decoration and lime mortar plaster decoration) are studied in this research. Their  $E_{M,i}$  and  $P_{M,j,i}$ , including the main decoration material and additional materials/accessories, are expressed as:

$$E_{M,i} = EF_{M,i}A_i \quad (4.18)$$

$$P_{M,j,i} = PF_{M,j,i}A_i \quad (4.19)$$

Where: the  $EF_{M,i}$ ,  $PF_{M,i}$ , and  $A_i$  respectively are the energy factor ( $\text{MJ}/\text{m}^2$ ) and pollutant  $j$ 's emission factor ( $\text{kg}/\text{m}^2$ ), and application area ( $\text{m}^2$ ) for decoration layer.

The general  $EF_M$  and  $PF_{M,j}$  are summarized according to statistics for the construction

process in China, three typical datasets are established to represent the  $EF_M$  and  $PF_{M,j}$  for each decoration type; these are presented in Table 4.21- 4.23.

Table 4.21: Dataset for the general  $EF_M$  and  $PF_{M,j}$  of glazed facing tile external decoration

Material and usage	$EF_M$	$PF_{M,CO_2e}$	$PF_{M,SO_2}$	$PF_{M,NO_x}$	$PF_{M,PM}$
Glazed facing tile (30kg)	11.64	1.874	0.763	0.004	0.007
15mm 1 : 0.3 : 1.5 cement lime mortar with adhesive	54.5	7.3	3.576	0.020	0.031
9mm 1 : 1 : 6 cement lime mortar					
3mm surface treatment mortar					
<b>Total</b> (General value for $EF_M$ & $PF_{M,i}$ of glazed facing tile decoration)	<b>43.9</b>	<b>5.8</b>	<b>1.91</b>	<b>0.010</b>	<b>0.017</b>

Note:  
 I .A total  $Em$  and  $Pm,j$  for cement lime mortar with adhesive, cement lime mortar and surface treatment mortar are used in the table, the result is not accurate but stands for the common value.  
 II . The  $EF_M$  and  $PF_M$  date for glazed facing tile is taken from [145].

Table 4.22: Dataset for the general  $EF_M$  and  $PF_{M,j}$  of dry hanging stone external decoration

Material and usage	$EF_M$	$PF_{M,CO_2e}$	$PF_{M,SO_2}$	$PF_{M,NO_x}$	$PF_{M,PM}$
Marble (50 kg)	250.8	15.8	-	-	-
Steel-frame and hanging component (9.2kg)	266.8	27.63	0.007	0.001	0.006
<b>Total</b> (General value for $EF_M$ & $PF_{M,i}$ of dry hanging stone decoration)	<b>517.6</b>	<b>43.43</b>	<b>0.007</b>	<b>0.001</b>	<b>0.006</b>

Note:  
 The weight of marble: 2500kg/m<sup>3</sup>, the thickness of marble board is 0.02m, referring to ICE2.0 [135].

Table 4.23: Dataset for the general  $EF_M$  and  $PF_{M,j}$  of lime mortar plaster internal decoration

Material and usage	$EF_M$	$PF_{M,CO_2e}$	$PF_{M,SO_2}$	$PF_{M,NO_x}$	$PF_{M,PM}$
5mm 1 : 0.5 : 2.5 cement lime mortar	44.3	6.02	2.451	0.013	0.022
8mm 1 : 1 : 6 cement lime mortar					
3mm surface treatment mortar					
<b>Total</b> (General value for $EF_M$ & $PF_{M,i}$ of lime mortar plaster decoration)	<b>44.3</b>	<b>6.02</b>	<b>2.451</b>	<b>0.013</b>	<b>0.022</b>

Note:  
 A total  $EF_M$  and  $PF_M$  for cement lime mortar, cement lime mortar and surface treatment mortar are used in the table, the result is not accurate but stands for the common value.

### C. The simplified assessment method for the $E_M$ and $P_{M,j}$ from the windows and glass curtain wall

The windows and glass curtain walls have significant  $E_M$  &  $P_{M,j}$  contribution to office building, owing to the large application area and relatively high energy and emission factors. The calculation of energy consumption ( $E_{M,i}$ ) and pollutant  $j$ 's emission ( $P_{M,i,j}$ ) for windows/curtain wall type  $i$  include two parts, i.e. the glass and the frame and accessories; these are expressed as:

$$E_{M,i} = EF_{M,i,gla}F_gA_i + E_{M,i,fra} \quad (4.20)$$

$$P_{M,j,i} = PF_{M,i,j,gla}F_gA_i + P_{M,j,i,fra} \quad (4.21)$$

Where: the  $EF_{M,i,gla}$  (MJ/m<sup>2</sup>) and  $PF_{M,i,j,gla}$  (kg/m<sup>2</sup>) are the energy consumption factor and pollutant emission factor for the glass part; the  $F_g$  is the area factor of glass part; the  $A_i$  (m<sup>2</sup>) is the application area of window type  $i$ . The  $E_{M,i,fra}$  (MJ) and  $P_{M,j,i,fra}$  (kg) are respectively the energy consumption and pollutant emission for the frame and accessories part.

For the specifications of the glass part, according to the investigation of building glass market, the 6mm and 9mm glasses (with/without low-E coating) are normally used in normal windows, while only the toughened glass can be applied on glass curtain wall as the requirement of the safety standard. 0.75m<sup>2</sup> of glass will be consumed during the factory manufacturing process for 1m<sup>2</sup> of window ( $F_g=0.75$ ), while  $F_g=0.75$  for the glass curtain wall (on-site assembled). The  $EF_{M,i,gla}$  and  $PF_{M,i,j,gla}$  for glass are summarized into the localized dataset, as shown in Table 4.24.

Table 4.24: The localized dataset for general  $EF_{M,i,gla}$  and  $PF_{M,i,j,gla}$  of building glass

Glass	$EF_M$	$PF_{M,CO2e}$	$PF_{M,SO2}$	$PF_{M,NOx}$	$PF_{M,PM}$
6mm clear	239.8	14.5	0.091	0.091	0.024
6mm Low-E	251.4	15.3	0.095	0.095	0.025
9mm clear	359.7	21.8	0.135	0.135	0.036
9mm Low-E	377.1	22.5	0.141	0.139	0.037
9mm toughened (for glass curtain wall)	563.6	30.5	0.211	0.189	0.056
9mm toughened Low E (for glass curtain wall)	590.7	31.2	0.222	0.192	0.059

Note:

I . Clear glass's  $EF_{M,i}$  and  $PF_{M,i,j}$  are converted from typical data for Chinese glass industry [146], others are taken from the average data of "Emission Standard of pollutants for domestic glass industry" [147]. The density of 2500kg/m<sup>3</sup> is used in conversion.

II . Typical sample from NSG Group [148] is used to represent the s  $EF_{M,i}$  and  $PF_{M,i,j}$  for Low-E glass.

The estimation method and dataset for the energy consumption ( $E_{M,i,fra}$ ) and pollutant emission ( $P_{M,j,i,fra}$ ) of frame and accessories. In term of structure, there are significant difference between the windows frame and frame of glass curtain wall. The former is installed within a wall thus only bears the weights of the glass and itself, while the latter is designed to support the weight of whole curtain wall as well as wind load. The  $E_{M,i,fra}$

and  $P_{M,j,i, fra}$  for the frame and accessories of windows or glass curtain wall are expressed as:

$$E_{M,i, fra} = EF_{M,i, fra} A_i \quad (4.22)$$

$$P_{M,j,i, fra} = PF_{M,i,j, fra} A_i \quad (4.23)$$

Where: the  $EF_{M,i, fra}$  (MJ/m<sup>2</sup>) and  $PF_{M,i,j, fra}$  (kg/m<sup>2</sup>) are the energy consumption factor and pollutant emission factor for frame type  $i$ ;  $A_i$  is the whole windows / glass curtain wall area (m<sup>2</sup>). The  $EF_{M,i, fra}$  and  $PF_{M,i,j, fra}$  for the frame of window or glass curtain wall are discussed respectively as follow:

- The  $EF_{M,i, fra}$  and  $PF_{M,i,j, fra}$  for the windows frame are generated by analyzing the material usage of typical windows product in Chinese market.

Three most commonly used frame types, including the aluminium frame (AF), thermally broken aluminium frame (TBAF) and PVC frame (PVCF), are investigated in this research, while the double glazing option is available for the last two types. For each frame type, the material usage per unit window area is basically fixed. Then based on the statistic of main material usage, the energy and emission factor of the windows frame are summarised into the localised dataset (Table 4.25).

Table 4.25: The localized dataset for general  $EF_{M,i, fra}$  and  $PF_{M,i,j, fra}$  of window frame

Windows frame types	Main material usage	$EF_M$	$PF_{M,CO_2e}$	$PF_{M,SO_2}$	$PF_{M,NO_x}$	$PF_{M,PM}$
Single Glazed AF	Aluminum Usage: 8.98kg,	1615.4	93.6	0.0575	0.054	0.0465
Double Glazed AF with 9mm air gap	Aluminum Usage: 10.14kg	1825.2	105.8	0.065	0.061	0.053
Double Glazed AF with 12mm air gap	Aluminum Usage: 10.66kg	1917.5	111.1	0.068	0.064	0.0555
Double Glazed TBAF with 9mm air gap	Aluminum Usage: 10.14kg, Rubber usage: 1.5kg	1961.7	110.1	0.0675	0.0635	0.0605
Double Glazed TBAF with 12mm air gap	Aluminum Usage: 10.66kg, Rubber usage: 1.5kg	2054	115.4	0.071	0.0665	0.063
Single Glazed PVCF	PVC usage: 16.69kg, Steel usage: 9.88kg	656.5	47.4	0.029	0.027	0.086
Double Glazed PVCF with 9mm air gap	PVC usage: 18.25kg, Steel usage: 10.31kg	703.4	50.3	0.031	0.029	0.095
Double Glazed PVCF with 12mm air gap	PVC usage: 18.92kg, Steel usage: 10.31kg	718.3	51.0	0.031	0.029	0.099
Argon filling	9 mm	0.945	0.003	0.002	0.0005	0.003
	12 mm	1.26	0.004	0.003	0.001	0.004

Note:

I . The material usage refers the products sheet of Langshi windows [149], and converted to kg/m<sup>2</sup>.

- II. The emission factors of aluminium, steel and rubber are taken from the industry emission standard [132] [150].
- III. The  $EF_M$  of argon filling is 0.672MJ/Litre, this is used to convert the  $P_{M,j}$  by the national electricity emission factor of China.
- IV. For the argon filled double glazed frame, the  $EF_M$  and  $P_{M,j}$  of argon filling should be added.

- The  $E_{M,i,fra}$  and  $P_{M,j,i,fra}$  for the frame of glass curtain wall vary from the curtain wall's height to design wind load level. Through analyzing the material usage of typical glass curtain wall in China, the usage of executed aluminum frame will increase with the building height and design wind load. However, the usage of other accessories (e.g. sealant and fastener) is almost invariable (listed in Table 4.26).

Table 4.26: Dataset for typical material usage,  $E_M$  (MJ) and  $P_{M,j}$  (kg) from accessories per 1m<sup>2</sup> glass curtain wall

Material and usage	$E_M$	$P_{M,CO2e}$	$P_{M,SO2}$	$P_{M,NOx}$	$P_{M,PM}$
Galvanized Connector (2.56 kg)	112.89	7.69	0.004	0.0006	0.003
Structural Adhesive (1.57 kg)	177.63	32.97	0.254	0.682	--
Silicone Sealant (2.31 kg)	224.07	41.58	0.320	0.860	--
Stainless Steel Fasteners (1 kg)	110	7.54	0.004	0.0003	0.003
Insulation layer (0.1 m <sup>2</sup> )	34.98	2.68	0.050	0.055	--
Total $E_M$ & $P_{M,j}$	659.6	92.5	1.568	1.597	0.632

For buildings no more than 10 storeys (40 meters), material usage of typical glass curtain wall shows that the usage of the executed aluminium frame is approximately 10kg/m<sup>2</sup> f. The  $EF_{M,i,fra}$  and  $PF_{M,i,j,fra}$  of curtain wall's frame for lower buildings ( $\leq 10$  storeys) are generated (Table 4.27) by adding up the data of accessories and executed aluminum frame together.

Table 4.27: Dataset for  $EF_{M,i,fra}$  and  $PF_{M,i,j,fra}$  of curtain wall's frame for lower buildings ( $\leq 10$  storeys)

$EF_M$	$PF_{M,CO2e}$	$PF_{M,SO2}$	$PF_{M,NOx}$	$PF_{M,PM}$
2557	202	0.723	1.691	0.08

For the buildings with above 10 storeys, statistic [136] shows that the average usage of executed aluminium increases with the design wind load. The materials usage and  $E_M$  &  $P_{M,j}$  of frame and accessories together are generated for each design wind load level, as shown in Table 4.28. The simple linear regression equations for the relationship of wind load (represented by X) and  $E_{M,i,fra}$  &  $P_{M,j,i,fra}$  (represented

by Y) are developed and presented in Table 4.29.

Table 4.28: The materials usage and  $E_M$  &  $P_{M,j}$  of frame and accessories for each wind load level

Design wind load (KPa)	Aluminium frame usage (kg/m <sup>2</sup> )	Accessories usage	$EF_{M,i, fra}$ and $PF_{M,i, fra}$ for frame and accessories together				
			$EF_M$	$PF_{M,CO_2e}$	$PF_{M,SO_2}$	$PF_{M,NO_x}$	$PF_{M,PM}$
<2	10	Fixed usage as in Table 4.26	2459.6	196.8	0.720	1.679	0.077
2-2.5	12		2819.6	217.6	0.732	1.691	0.087
2.5-3	14		3179.6	238.5	0.745	1.703	0.098
3-3.5	16		3539.6	259.3	0.758	1.715	0.108
3.5-4	18		3899.6	280.2	0.771	1.727	0.118
>4	20		4259.6	301.1	0.784	1.739	0.129

Table 4.29: linear regression equations for design wind load and  $E_{M,i, fra}$  &  $P_{M,j,i, fra}$

Y	Regression equations	R <sup>2</sup>
$EF_M$	Y=830.8X+867.3	0.98
$PF_{M,CO_2e}$	Y=48.1X+104.5	0.98
$PF_{M,SO_2}$	Y=0.0297X+0.663	0.99
$PF_{M,NO_x}$	Y=0.012X+1.667	0.99
$PF_{M,PM}$	Y=0.024X+0.031	0.98

The relationship of building height and wind load is studied by a simplified method. According to the “load code for the design of building structures” [151] which provides the default wind loads for 4 typical Chinese cities (i.e. Beijing-0.5KN/m<sup>2</sup>, Tianjin-0.6KN/m<sup>2</sup>, Shanghai-0.6KN/m<sup>2</sup> and Guangzhou-0.8KN/m<sup>2</sup>), for safety and simplification 1 KN/m<sup>2</sup> is used as default wind load for China cities in this calculation. The gust fact [152] is set to 3 in this research in order to keep sufficient safety margins. The actual design wind load is the product of the default wind load, height adjusts factor for specific building height [151] (Table 4.30) and gust factor.

Table 4.30: Height adjust factor for urban area

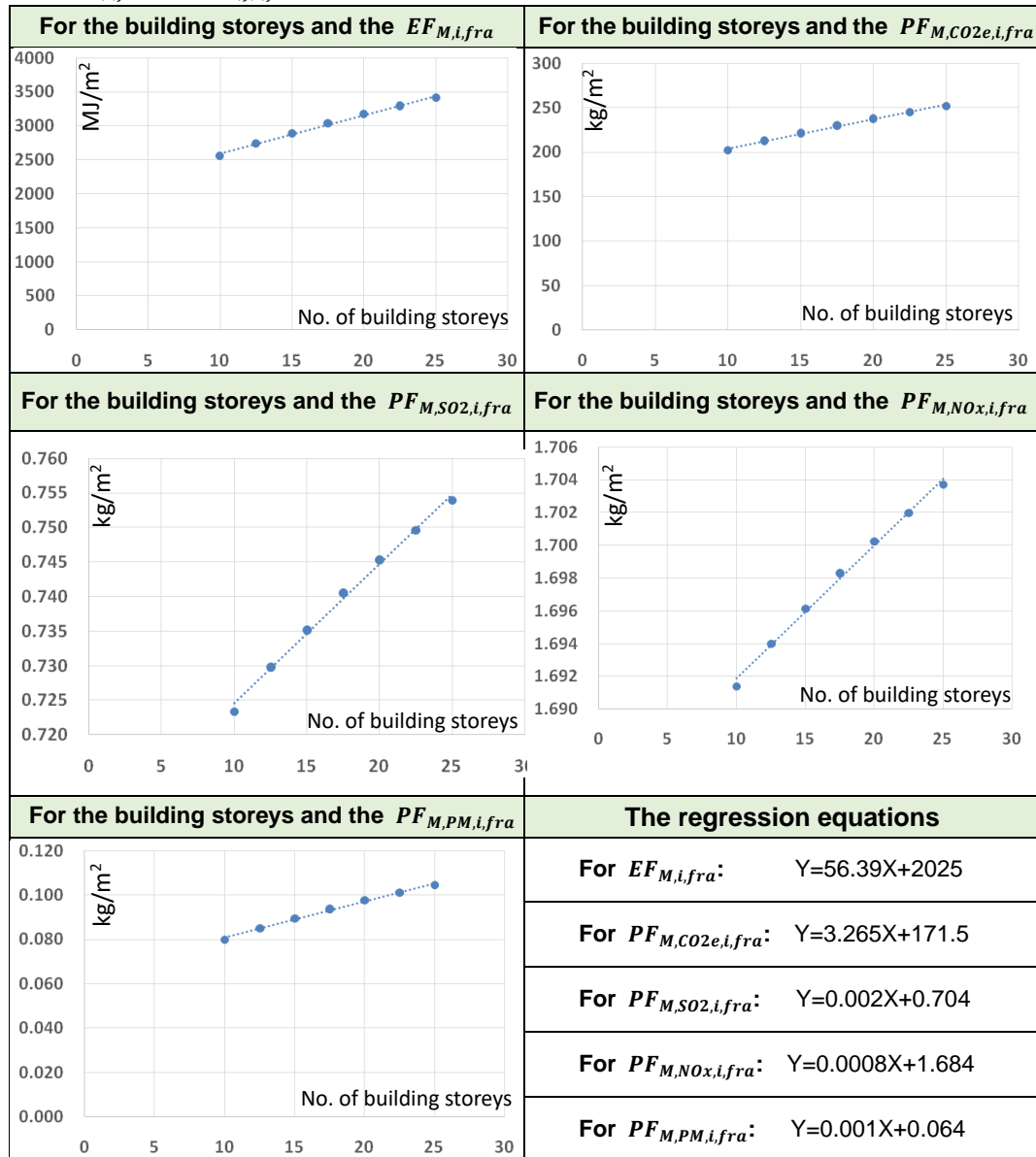
Height(m)	40	50	60	70	80	90	100
Adjust factor	1.13	1.25	1.35	1.45	1.54	1.62	1.70

Through the above analyses, the material usage and the  $E_{M,i, fra}$  &  $P_{M,j,i, fra}$  for seven building heights (i.e. 40m-100m as height in Table 4.30) can be calculated. By replacing the building height with the number of building storeys (default floor height=4m), the scatter plots and the regression equations for the relationship of building storeys (represented by X) and the  $EF_{M,i, fra}$  &  $PF_{M,j,i, fra}$  (represented by Y) are established, as shown in



Table 4.31.

Table 4.31: the scatter plots and the regression equations for the relationship of building storeys and the  $EF_{M,i, fra}$  &  $PF_{M,j,i, fra}$  for 10-25 storey buildings



#### D. The simplified assessment method for the $E_M$ and $P_{M,j}$ from the building HVAC system

Three typical HVAC systems applicable to Chinese office buildings are investigated in this research, including the VRV/VRF system, air-cooled chilled water system (ACCW) and water-cooled chilled water system (WCCW). The material phase's energy consumption ( $E_M$ ) and pollutant emission ( $P_{M,j}$ ) of HVAC system are calculated as follow:

$$E_{M,HVAC,i} = EF_{M,HVAC,i} P_i \quad (4.24)$$

$$P_{M,HVAC,j,i} = PF_{M,HVAC,i,j}P_i \quad (4.25)$$

Where: the  $EF_{M,HVAC,i}$  (MJ/kW) and  $PF_{M,HVAC,i,j}$  (kg/kW) are the energy consumption factor and pollutant emission factor for HVAC type  $i$ ;  $P_i$  is the design heating/cooling power of HVAC type  $i$  (kW).

The dataset for the general energy consumption factor ( $EF_{M,HVAC,i}$ ) and pollutant emission factor ( $PF_{M,HVAC,i,j}$ ) of typical HVAC systems. The key materials usage of each HVAC type are studied, through the investigation of the Chinese market-leading products, these are detailed below:

For VRV/VRF (Variable Refrigerant Volume/Flow) system, according to the statistic from industrial data source in 2005 [153], the key material consumed in the HVAC manufacturing are steel, copper, aluminum and ABS plastic, the general proportion of each material in the system (including outdoor condensing unit, indoor unit and pipes) are outlined in Table 4.32. Meanwhile, through investigation of ten outdoor VRV units model and nine indoor unit model from the market leading brand Daikin [154], the average weight factors (weight of HVAC unit per cooling/heating power) are generated (Table 4.33). By adding the average weight of the outdoor unit, indoor unit and refrigerant pipes together, the total weight of a typical system (addressed in Table 4.33) by cooling/heating capacity is 11.88kg/kW. By multiplying this figure with the proportion of materials usage, the materials usage of VRV system is calculated and presented in Table 4.34.

Table 4.32: The average material usage proposition in VRV system. [153]

	Steel	Aluminum	Copper	ABS
<b>Material usage proportion in VRV/VRF system</b>	61.6%	7.8%	16%	15.1%

Table 4.33: The investigated VRV units and their typical weight by cooling capacity [154]

	Investigated models	Average weight by cooling capacity (kg/kW)
<b>Outdoor unit</b>	REYQ8T, REYQ10T, REMQ5T, REYQ10T, REMQ12T, REYQ12T, REYQ14T, REYQ16T, REYQ18T, REYQ20T	6.48
<b>Indoor unit</b>	FXFQ20A, FXFQ25A, FXFQ32A, FXFQ40A, FXFQ50A, FXFQ63A, FXFQ80A, FXFQ100A, FXFQ125A	2.4
<b>Pipes</b>	Normal copper refrigerant pipes	3

<b>Total</b>	11.88
Note: I . A typical system is assumed in the calculation, in which 10 indoor units are installed for each outdoor unit, the average distance between indoor and outdoor unit is 60m. II . For the investigated outdoor unit the capacity range is from 22kW to 56kW; For the investigated indoor unit the capacity range is from 2.2kW to 14kW.	

Table 4.34: the average materials` weight by cooling capacity in VRV system.

Material	Steel	Aluminum	Copper	ABS
<b>Weight by cooling capacity (kg/kW)</b>	7.26	1.9	0.93	1.79

For the WCCW and ACCW systems, a similar method is applied. The average materials usage for the WCCW system and ACCW systems are obtained by previous research [155]. The typical ACCW system has the weight factor of 11.1kg/kW while the figure of WCCW is 5.75 kg/kW. The specific proportion of materials usage and materials` weight is presented in Table 4.35.

Table 4.35: The materials` average proportion and weight by cooling capacity of ACCW and WCCW HVAC type. [155]

		Steel	Aluminum	Copper	Total
<b>ACCW HVAC</b>	Proportion of materials	80.55%	5.2%	14.3%	100%
	Weight by cooling capacity (kg/kW)	8.94	0.58	1.59	11.1
<b>WCCW HVAC</b>	Proportion of materials	75.53%	0.7%	23.77%	100%
	Weight by cooling capacity (kg/kW)	4.34	0.04	1.37	5.75

By multiplying the materials` usage with the materials` energy consumption factor and emission factor, the  $EF_{M,HVAC,i}$  (MJ/kW) and  $PF_{M,HVAC,i,j}$  (kg/kW) of typical HVAC systems are calculated and presented in Table 4.36.

Table 4.36: The general energy consumption factor and pollutant emission factor for 4 types of HVAC

	$EF_{M,HVAC}$	$PF_{M,HVAC,CO2e}$	$PF_{M,HVAC,SO2}$	$PF_{M,HVAC,NOx}$	$PF_{M,HVAC,PM}$
<b>VRV/VRF</b>	700.2	59.2	0.016	0.003	0.012
<b>ACCW</b>	409.2	46.2	0.012	0.002	0.009
<b>WCCW</b>	166.2	20.6	0.005	0.001	0.004

### **E. The simplified assessment method for the $E_M$ and $P_{M,j}$ from the building lighting system**

For the most Chinese office buildings, the compact fluorescent lamps (CFL) lighting system and light emitting diodes (LED) lighting system are usually adopted, and the general  $E_M$  and  $P_{M,j}$  for the lighting systems can be calculated as follow:

$$E_{M,light,i} = EF_{M,light,i}E_vAt \quad (4.26)$$

$$P_{M,light,j,i} = PF_{M,light,j,i}E_vAt \quad (4.27)$$

Where:  $EF_{M,light,i}$  (MJ/Million-Limen-Hours) and  $PF_{M,light,j,i}$  (kg/Million-Limen-Hours) are the energy consumption factor and emission factor for the specific lighting system  $i$ ;  $E_v$  is the designed luminance level (Lux) of building space;  $A$  is the lighting area ( $m^2$ ); and  $t$  is the designed light operation time (hours) during the whole building life-cycle.

The  $EF_{M,light,i}$  and  $PF_{M,light,j,i}$ , in form of MJ/Million-Limen-Hours and kg/Million-Limen-Hours, represent the material phase's energy consumption and pollutant emissions from the lamps which can provide 1 Million Lumen-Hours together. The typical CFL lamp (i.e. 15watt lamp, 900 lumens and 8500 hours lifetime [156]) and LED lamp (i.e. 12.5 Watt 5 LED package lamp, 800 lumens and 25000 hours lifetime [123]) are selected in the analysis, the former is 2.6 times as high as the latter in term of "Limen-Hours". According to DOE [156], in term of weight, CFL lamp contents 40.78% of glass, 22.76% of plastic, and LED lamp contents [123] 44.7% of aluminum and 13% of glass. Combine the materials' energy and emission factor and the Limen-Hours, the  $EF_{M,light,i}$  and  $PF_{M,light,j,i}$  of typical lighting system is generated in dataset (Table 4.37).

Table 4.37: the general  $EF_{M,light,i}$  and  $PF_{M,light,j,i}$  for typical lighting systems

	$EF_{M,Light}$	$PF_{M,Light,CO2e}$	$PF_{M,Light,SO2}$	$PF_{M,Light,NOx}$	$PF_{M,Light,PM}$
<b>CFL</b>	8.5	0.607	0.00023	0.00003	0.0002
<b>LED</b>	6.6	0.401	0.00018	0.00002	0.0001

#### 4.4 The development of the simplified assessment method for the on-site construction phase's embodied energy ( $E_{Con}$ ) and pollutant emissions ( $P_{Con,j}$ )

The embodied energy consumption and pollutant emissions from construction process consist of three sources (i.e. the material transportation between factory and building site, on-site construction, and change of land use). The first source depends on the building materials' weight and transportation method, the second one related to the structure type and technology level, the third one depends on the original land condition. The simplified assessment for the energy and emission from three sources are respectively

investigated below.

#### 4.4.1 Development of the simplified assessment method for the energy consumption ( $E_{Con-T}$ ) and pollutant emissions ( $P_{Con-T,j}$ ) from the material transportation between factory and building site

For any building materials, the  $E_{Con-T}$  and  $P_{Con-T,j}$  are the product of the materials' usage, transportation distance and the energy factor and emission factors of transportation method. These can be calculated as follow:

$$E_{Con-T} = \sum_{i=1}^n m_i EF_{Con-T} D_i \quad (4.28)$$

$$P_{Con-T,j} = \sum_{i=1}^n m_i PF_{Con-T,j} D_i \quad (4.29)$$

Where,  $m_{i,r}$  is the usage (Tonne) of building material  $i$ ;  $EF_{Con-T}$  is the energy consumption factor (MJ/km) for dedicated transportation mode;  $PF_{Con-T,j}$  is the pollutant  $j$ 's emission factor (kg/km) for dedicated transportation mode;  $D_i$  is the transport distance (km) for material  $i$ .

The  $EF_{Con-T}$  and  $PF_{Con-T}$  are mainly for road vehicles (e.g.HGV and vans) as the most building materials in China are transported by them. Thus, the  $EF_{Con-T}$  and  $PF_{Con-T,j}$  consist of two source, including them from fuels combustion in transportation vehicle and them from fuel's production, refining and distribution. The first source is converted from the national average energy consumption for freighting good by diesel HGV (3.038 MJ/Tonne.km) [157], by using the vehicle emission standard (China national emission standard-stage 4, equivalent to "Euro Four emissions criteria"). The second source is actually happens during the the WTT (Well-to-Wheel) process [158], as China still don't have a completed research on this area, the overall WTT data for EU [159] is used instead. The overall  $EF_{Con-T}$  and  $PF_{Con-T,j}$ , including the first and second sources are calculated in dataset (Table 4.38).

Table 4.38: The  $EF_{Con-T}$  &  $PF_{Con-T,j}$  for China building material transportation

	$EF_{Con-T}$	$PF_{Con-T, Co2e}$	$PF_{Con-T, SO2}$	$PF_{Con-T, NOx}$	$PF_{Con-T, PM}$
Combustion	3.038	0.947	0.001	0.013	0.00007

WTT	0.608	0.047	--	--	--
Overall	3.646	0.994	0.001	0.013	0.00007

The transported distance for building material ( $D_i$ ) from factory to building site is summarized from the previous statistical studies [128]. The average distance for each typical building material is summarised in dataset (Table 4.39)

Table 4.39: The average transportation distance ( $D_i$ ) for typical building materials in China

Materials	$D_i$ (km)	Material	$D_i$ (km)	Materials	$D_i$ (km)
Steel bar	122.72	Other steels	122.72	Building blocks/bricks	57.75
Cement	65.57	Sand	89.99	Windows	128.08
Gravel	89.99	Ready - made concrete	30	Decoration glazing tile	106.38
Ready - made mortar	30	electric wires	76.22	Decoration Stone	57.75
Plastic raceways	76.22	electric cable	76.22	Insulation panels	57.75
steel cable raceways	122.72	steel air duct	122.72	Glass— for curtain wall	98.84
steel pipe-electric wire	122.72	steel pipe-other purpose	122.72	Aluminum — for curtain wall	71.32
water supply pipes-copper	76.22	water supply pipes-PPR	76.22		
water supply pipes-UPVC	76.22	water drain pipe-PVC	76.22		
Note:					
To simplify the model, some small accessories such as nail or sealant are not include					

#### 4.4.2 Generating the simplified assessment method for the energy consumption ( $E_{Con-o}$ ) and pollutant emissions ( $P_{Con-o,j}$ ) from the on-site construction work

The energy consumption and emission from on-site construction are highly dependent on the structure type and construction method. For example, prefabricated construction requires less on-site assembly energy than it of on-site build construction. For the comparability in this research, all building structure types are assumed as on-site build structure and for the same structure type, the construction method and main engineering machinery used in construction site are similar. The  $E_{Con-o}$  and  $P_{Con-o,j}$  are generated as follow:

$$E_{Con-o} = EF_{Con-o,i} * A \quad (4.30)$$

$$P_{Con-o,j} = PF_{Con-o,i,j} * A \quad (4.31)$$

Where:  $EF_{Con-o, j}$  (MJ/m<sup>2</sup>) and  $PF_{Con-o,i,j}$  (kg/m<sup>2</sup>) are the energy consumption factor and pollutant  $j$ 's emission factor of on-site construction process for structure type  $i$ ;  $A$  (m<sup>2</sup>) is the gross floor area of the office building.

The general  $EF_{Con-o, j}$  is summarized from previous studies, then the  $PF_{Con-o,i,j}$  is derivable. The average energy consumption factor ( $EF_{Con-o,i}$ ) for 4 structure types is obtained (Table 4.40) by previous statistics [160], assuming that the common construction method and average engineering machinery level are applied. Through these, the emission factors ( $PF_{Con-o,i,j}$ ) are then derivable by using the proportions of specific energy sources and their emission factors. Through previous statistics, the common energy sources applied in on-site construction work are diesel (54.62%), petrol (2.46%) and electricity (42.92%). The overall emissions data for unit energy consumption are calculated in Table 4.41 by multiply the proportion of energy usage and specific emission factor of each energy source.

Table 4.40: The general  $EF_{Con-o,i}$  for on-site construction work of typical structure types

	MS-RCF & HR-RCF	HR-RCF-SW/T	SF-SW/T
$EF_{Con-o, j}$ (MJ/m <sup>2</sup> )	305.1	326.3	272.7

Table 4.41: The emissions data for unit energy consumption (kg/MJ) of 3 energy sources

	CO2 (kg/MJ)	SO2 (kg/MJ)	NOx (kg/MJ)	PM (kg/MJ)
Diesel	0.0728	0.0003	0.0038	2.177E-05
Petrol	0.0726	0.0003	0.0011	2.177E-05
Electricity	0.2094	0.0006	0.0005	0.0001
<b>Overall</b> (weighted average)	0.1314	0.0004	0.0023	5.77E-05
Note: I . The emission factors for diesel and petrol are obtained by adding WTT part and combustion part (addressed in 4.4.2) together II . The electricity emission factor in China refers to the IPCC's data [13].				

Through multiply the overall emissions data for unit energy consumption to the energy consumption factor of each construction type, the emission factors can be generated.

The general  $EF_{Con-o,i}$  (MJ/m<sup>2</sup>) and  $EP_{Con-o,i,j}$  (kg/m<sup>2</sup>) for each structure type are

Table 4.42: The general energy factor (MJ/m<sup>2</sup>) and emission factor (kg/m<sup>2</sup>) of each construction type

	$EF_{Con-o,i}$	$EP_{Con-o,i,CO2}$	$EP_{Con-o,i,SO2}$	$EP_{Con-o,i,NOx}$	$EP_{Con-o,i,PM}$
MS-RCF & HR-RCF	305.1	40.1032	0.1291	0.7093	0.0176

HR-RCF-SW/T	326.3	42.8898	0.1381	0.7586	0.0188
SF-SW/T	272.7	35.8445	0.1154	0.6340	0.0157

#### 4.4.3 Generating the simplified assessment method for the energy consumption ( $E_{Con-L}$ ) and pollutant emissions ( $P_{Con-L, j}$ ) from change of land use

The embodied energy consumption and pollutant emissions from the change of land use are defined from the view of ecological compensation. For example, energy is “consumed” when changing the land use from wind-farm to building site. The  $E_{on-L}$  and  $P_{Con-L, j}$  are expressed as follow:

$$E_{Con-L} = A(EF_{Aft,i} - EF_{Bef,i})t_B \quad (4.32)$$

$$P_{Con-L, j} = A(PF_{Aft,i,j} - PF_{Bef,i,j})t_B \quad (4.33)$$

Where:  $A$  is the land area ( $m^2$ ) covered by the building; The  $EF_{Bef,i}$  and the  $PF_{Bef,i,j}$  are the energy factor ( $kWh/m^2$ year) and pollutant  $j$ 's emission factor ( $kg/m^2$ year) for the original land use before building is constructed; the  $EF_{Aft,i}$  and  $PF_{Aft,i,j}$  are the energy factor ( $kWh/m^2$ year) and pollutant  $j$ 's emission factor (pollutants absorbing ability,  $kg/m^2$ year) for the land use after building is constructed. The  $t_B$  is the designed service life for the whole building (50 years in this research).





In this research, only the land covered by building itself is counted in  $A$ , while any other land covered by road or car park may vary and not considered in the calculation. Based on the actual situation in China, it is rare to build office building on a land with energy generation capacity (e.g. wind-farm or PV-farm), thus, both  $EF_{Bef,i}$  and  $EF_{Aft,i}$  are zero. The default value of  $E_{Con-L}$  is zero in this research.

In order to generate the  $PF_{Aft,i,j}$  and  $PF_{Bef,i,j}$ , the land use is classified into 4 categories (i.e. Forest Land, Agroforestry Land, Rangeland/Grassland, Peri-Urban Land), in which only the last one are covered by artificial pavement or concrete. By review the research results from IPCC [22] and LCBM [161], only the  $CO_2$  reduction by plants are widely and



quantitatively studied. The emission factor (pollutants absorbing ability) of original land use ( $PF_{Bef,i,j}$ ) are summarized to dataset (). The default value of emission factor after building is constructed ( $PF_{Aft,i,j}$ ) is zero as the land changed to Peri-Urban Land type.

Table 4.43: The emission factor of original land use ( $PF_{Bef,i,j}$ )

	Forest Land	Agroforestry Land	Rangeland/Grassland	Peri-Urban Land
land use classification				
$PF_{Bef,i,i}$ (kgCO <sub>2</sub> /m <sup>2</sup> year)	-30	-10	-4	0

#### 4.5 The development of the simplified assessment method for the building operation phase's embodied energy ( $E_{Op}$ ) and pollutant emissions ( $P_{Op, j}$ )

The  $E_{Op}$  and  $P_{Op, j}$  consist of two source, including the operation of building service system and the fugitive emissions due to the use of refrigerants in building RAC (Refrigeration and Air-Conditioning) system. They are investigated respectively below.

##### 4.5.1 Generating the simplified assessment method for the energy consumption ( $E_{Op-ser}$ ) and pollutant emissions ( $P_{Op-ser, j}$ ) caused by the operation of building service system

The HVAC and lighting systems in office building contribute over 90% of energy use and pollutant emission of all building service systems. Thus, other systems (e.g. building intelligent control and elevator) are not considered in this research. The  $E_{Op-ser}$  and  $P_{Op-ser, j}$  are generated as follow:

$$E_{Op-ser} = \sum_{i=1}^n E_i t_B \quad (4.34)$$

$$P_{Op-ser, j} = \sum_{i=1}^n \sum_{r=1}^m E_{i, r} PF_{r, j} t_B \quad (4.35)$$

Where,  $E_i$  (MJ) is the annual energy consumption of system  $i$ ;  $t_B$  is the service time of building (50 years);  $E_{i, r}$  (MJ) is the energy source  $r$ 's annual energy consumption by system  $i$ ;  $PF_{r, j}$  (kg/MJ) is the pollutant  $j$ 's emission factor of energy source  $r$ .

The annual energy consumption of specific systems ( $E_i$ ) are provided by the "CN13790

energy estimation tool for Chinese office building” addressed in Chapter 3. The local emission factors for energy resources ( $PF_{r, j}$ ) are summarized to dataset ().

Table 4.44 The local emission factors for energy resources ( $PF_{r, j}$ )

	CO <sub>2</sub>	SO <sub>2</sub>	NO <sub>x</sub>	PM
Electricity	0.2094	0.0006	0.0005	0.0001
Gas	0.0564	--	0.0008	--

Note:  
 I . The emission factors for Electricity refers to IPCC`s data [13];  
 II . The emission factors for Gas consists of its lifecycle impact, including the production and transportation process [162]. The performance of Chinese typical gas boiler is used in the calculation.

#### 4.5.2 Generating the simplified assessment method for the energy consumption ( $E_{Op-fug}$ ) and CO<sub>2</sub>e emission ( $P_{Op-fug, CO2e}$ ) from the fugitive emissions

The fugitive emissions refer to the fugitive from the refrigerants in building RAC system. The embodied energy of fugitive refrigerants ( $E_{Op-fug}$ ) is considered as zero as the amount of fugitive refrigerant is very small. Whereas, since the refrigerants have significant GWP (global warming potential), the equivalent CO<sub>2</sub> emission ( $P_{Op-fug, CO2e}$ ) is considered in this research. The  $P_{Op-fug, CO2}$  is calculated as follow:

$$P_{Op-fug, CO2e} = \sum_{i=1}^n \left( M_{C,i} R_{ins} \left\lceil \frac{t_B}{t_i} \right\rceil + M_{S,i} R_a t_B + (M_{C,i} R_{ins} - M_{S,i} R_a t_B) R_d \left\lceil \frac{t_B}{t_i} \right\rceil \right) CF_i \quad (4.36)$$

Where: the  $M_{C,i}$  (kg) is the mass of refrigerants charged in installation stage for RAC unit  $i$ ; the  $R_{ins}$  is the installation fugitive rate; the  $t_B$  is the service life of building (50 years);  $t_i$  is the service life of RAC unit  $i$  (15 years);  $\lceil t_B/t_i \rceil$  is the ceiling of  $t_B/t_i$ ; the  $M_{S,i}$  (kg) is the mass of refrigerants stored in RAC unit  $i$ ; the  $R_a$  is the annual leakage rate; the  $R_d$  is the disposal fugitive rate; the  $CF_i$  is the embodied equivalent CO<sub>2</sub> emission factor for refrigerants used in RAC unit  $i$ .

The dataset for the average installation fugitive factor ( $R_{ins}$ ), annual fugitive factor ( $R_a$ ), disposal fugitive factor ( $R_d$ ) and mass of initial refrigerants per RAC unit ( $M_{C,i}$ ) is generated. The specification of typical RAC unit applied in this research (Table 4.45) refers to IPCC`s data [13].

Table 4.45: General specification of RAC unit applied in this research

$M_{C,i}$ (kg)	$R_{ins}$	$R_a$	$R_d$
49.75	0.6%	3%	25%

The dataset for the emission factors ( $CF_i$ ) for the general refrigerant used in 3 typical RAC units is generated (Table 4.46) by investigate the market-leading products in China.

Table 4.46: The emission factors ( $CF_i$ ) for the general refrigerant used in 3 typical RAC

Options	VRV/VRF	Air-cooled chilled water system	Water-cooled chilled water system
Refrigerant	R410A	HFC134a	HFC134a
$CF_i$ (GWP) kgCo <sub>2</sub> e/kg	1725	1300	1300

#### 4.6 The development of the simplified assessment method for the building demolition phase`s embodied energy ( $E_{De}$ ) and pollutant emissions ( $P_{De,j}$ )

The energy consumption and pollutant emissions in this phase mainly come from 3 sources, including the on-site demolition work (e.g. excavator and other machinery), the transportation of building wastes, and the final treatment of building wastes. They are investigated respectively below.

##### 4.6.1 Generating the simplified assessment method for the energy consumption ( $E_{De-on}$ ) and pollutant emissions ( $P_{De-on,j}$ ) from the on-site demolition work

A simplified method is applied here, the average energy factor and emission factor are used for the on-site demolition work. The  $E_{De-on}$  and  $P_{De-on,j}$  are generated by Eq. 4.37-Eq.4.38:

$$E_{De-on} = EF_{De-on}A \quad (4.37)$$

$$P_{De-on,j} = PF_{De-on,j}A \quad (4.38)$$

Where: the  $EF_{De-on}$  (MJ/m<sup>2</sup>) and  $PF_{De-on,j}$  (kg/m<sup>2</sup>) are the energy consumption factor and pollutant  $j$ 's emission factor respectively.  $A$  (m<sup>2</sup>) is the demolished building area (equivalent to building`s GFA).

According to previous statistics [163], the majority of demolition engineering machinery are powered by diesel engine, in which averagely 0.8 litre diesel will be consumed for every m<sup>2</sup> of building demolition work. Thus, the general  $EF_{De-on}$  and  $PF_{De-on,j}$  are

calculated ( $E_{De-T}$ ), by using diesel's embodied energy and emission factor (combine them from WTT and combustion stages together, addressed in section 4.4.2).

Table 4.47: The  $EF_{De-On}$  and  $PF_{De-On,j}$  for on-site demolition work

$EF_{De-On}$ (kg/m <sup>2</sup> )	$PF_{De-On,CO2}$ (MJ/m <sup>2</sup> )	$PF_{De-On,SO2}$ (MJ/m <sup>2</sup> )	$PF_{De-On,NOx}$ (MJ/m <sup>2</sup> )	$PF_{De-On,PM}$ (MJ/m <sup>2</sup> )
34.56	2.5160	0.0090	0.1316	0.0008

#### 4.6.2 Generating the simplified assessment method for the energy consumption ( $E_{De-T}$ ) and pollutant emissions ( $P_{De-T,j}$ ) from transportation of building demolition waste

The estimation method for energy and emission caused by demolition waste transportation are as same as them caused by building material transportation. The  $E_{De-T}$  and  $P_{De-T,j}$  are generated by Eq.4.39-Eq.4.40:

$$E_{De-T} = \sum_{i=1}^n \sum_{r=1}^n m_i p_{i,r} EF_{De-T,r} D_r \quad (4.39)$$

$$P_{De-T,j} = \sum_{i=1}^n \sum_{r=1}^n m_i p_{i,r} PF_{De-T,j,r} D_r \quad (4.40)$$

Where:  $m_i$  is the weight (Tonne) of building waste  $i$ ;  $p_{i,r}$  is the proportion (%) of demolition waste  $i$  that be processed by treatment method  $r$ ;  $EF_{De-T,r}$  (MJ/km) and  $PF_{De-T,j,r}$  (MJ/km) are the energy consumption factor and emission factor of pollutant  $j$  for dedicated transportation mode;  $D_r$  is the transportation distance (km) for waste treatment mode  $r$ .

The energy factor ( $EF_{De-T}$ ) and emission factor ( $PF_{De-T,j}$ ) of diesel vehicles (addressed in section 4.4.2 in Table 4.38) are applied, as the majority of the building demolition waste is transported by diesel road vehicles.

The transported distance ( $D_r$ ) for waste from building site to treatment/recycle plant various depend on the local waste treatment arrangement. No localized data for China is previously studied, thus, UK's statistic data for 2009 [164] is applied in this research, in Which the average transport distance for landfill, incineration and recycle method are 26km, 46km and 46km respectively.

The mass of building waste ( $m_i$ ) is gathered from building material usage statistic, as same as the new building material (material for FMS only, addressed in section 4.3.2)

The global default value for the proportion of building waste treated by method  $r$  ( $p_{i,r}$ ) is applied in this research [161]. The proportions of landfill ( $p_{i,LF}$ ), incineration ( $p_{i,I}$ ) and recycle ( $p_{i,Re}$ ) for each waste types are summarized in dataset (Table 4.48).

Table 4.48: The proportions of material waste in each treatment method [161]

Material	$p_{i,LF}$	$p_{i,I}$	$p_{i,Re}$	Material	$p_{i,LF}$	$p_{i,I}$	$p_{i,Re}$
Steel bar	25%		75%	Other steels	25%		75%
Cement	45%		55%	Sand	45%		55%
Gravel	45%		55%	Ready - made concrete	45%		55%
Ready-made mortar	45%		55%	electric wires	25%		75%
Plastic raceways	70%	20%	10%	electric cable	25%		75%
steel cable raceways	25%		75%	steel air duct	25%		75%
steel pipe-electric wire	25%		75%	steel pipe-other purpose	25%		75%
water supply pipes-copper	25%		75%	water supply pipes-PPR	70%	20%	10%
water supply pipes-UPVC	70%	20%	10%	water drain pipe-PVC	70%	20%	10%
Building blocks/bricks	45%		55%	Insulation panels	25%		75%
Aluminium in curtain wall & windows	25%		75%	Glass in curtain wall & windows	30%		70%
Decoration glazing tile	45%		55%	Decoration Stone	45%		55%
<p>Note:</p> <p>I . The cement, sand and gravel do not exist in the real building waste they are have already became mortar and concrete. But they are listed and calculated separately as same as the original building material usage statistic table for the convenience of calculation.</p> <p>II . The aluminium and glass from windows and glass curtain wall are listed separately, their mass per m<sup>2</sup> windows/curtain wall are obtained from section 4.3.3 part C.</p>							

#### 4.6.3 Generating the simplified assessment method for the embodied energy consumption ( $E_{De-Tr}$ ) and pollutant emissions ( $P_{De-Tr, j}$ ) from final treatment of building demolition waste

In this research, three waste treatment methods (i.e. landfill, incineration and recycle/reuse) are investigated. In which the  $E_{De-Tr}$  and  $P_{De-Tr, j}$  are expressed by Eq.4.41 – Eq. 4.42:

$$E_{De-Tr} = \sum_{i=1}^n (M_i p_{i,LF} EF_{i,LF} + M_i p_{i,I} EF_{i,I} + M_i p_{i,Re} EF_{i,Re}) \quad (4.41)$$

$$P_{De-Tr, j} = \sum_{i=1}^n (M_i p_{i,LF} PF_{i,LF,j} + M_i p_{i,I} PF_{i,I,j} + M_i p_{i,Re} PF_{i,Re,j}) \quad (4.42)$$

Where: the  $M_i$  is the mass (Tonne) of demolition waste  $i$ ; The  $p_{i,LF}$ ,  $p_{i,I}$  and  $p_{i,Re}$  are the proportion (%) of demolition waste  $i$  that treated by landfill, incineration and recycle/reuse method respectively; The  $EF_{i,LF}$ ,  $EF_{i,I}$  and  $EF_{i,Re}$  are the energy consumption factor (MJ/Tonne) for waste  $i$  being processed by method of landfill, incineration and recycle/reuse respectively; The  $PF_{i,LF,j}$ ,  $PF_{i,I,j}$  and  $PF_{i,Re,j}$  pollutants  $j$ 's emission factor (kg/Tonne) of those process method respectively.

The  $M_i$  and  $R_{i,LF}$  are obtained from the waste transportation section (section 4.6.3)

The  $EF_{i,LF}$ ,  $PF_{i,LF,j}$  and the  $EF_{i,Re}$ ,  $PF_{i,Re,j}$  are all zero in this research. All the landfilled wastes are inorganics which will not release air pollutant after be landfilled for a long term. The energy consumption factor and emission factor of the reused/recycled process have already involved in those of new material that have recycled contents.

The  $EF_{i,I}$  and  $PF_{i,I,j}$  are negative figures, as certain energy can be generated from the incineration plants. In this research, a typical incineration plant [165] using fossil origin waste (e.g. plastics) with 75% heat recovery efficiency are selected to represent general  $EF_{i,I}$  and  $PF_{i,I,j}$ . Averagely, 9GJ/Tonne electricity are generated from the waste incineration, the net pollutant emissions reduction is the difference of the offset emission for 9GJ electricity (using Chinese electricity emission factor) and the emission from waste incineration. The calculation results of the (negative) energy consumption factor and net pollutants emission factor are listed in dataset (Table 4.49).

Table 4.49: The general  $EF_{i,I}$  and  $PF_{i,I,j}$  for typical waste incineration plants in China

$EF_{i,I}$ (9GJ/Tonne)	$PF_{i,I,CO2}$ (kg/Tonne)	$PF_{i,I,S02}$ (kg/Tonne)	$PF_{i,I,NOx}$ (kg/Tonne)	$PF_{i,I,PM}$ (kg/Tonne)
-9	-13.7	-0.04	-0.03	-0.01

## 4.7 Conclusions

In this chapter, the simplified assessment method for the life-cycle energy consumption and pollutant emission of the China office building is established. The new method,

capable of overcoming the shortages of previous methods (e.g. that highly rely on the detailed design information or building material statistics list from the late design stage), can briefly estimate the LCE and LCP of the Chinese office building at the conceptual design stage with no need for the detailed design input, thus enabling the enhancement of the “green performance” of buildings at the earlier design stages.

The assessment methods for four different building life-cycle phases (i.e. material, on-site construction, building operation and demolition) are established through the characterization of the LCE and LCP of the actual building systems and building cases. The mathematic correlation between the LCE, LCP and building characteristics are established, while the dataset applicable to China is also summarized to provide the general parameters of the common Chinese office buildings.

Through the characterization of the LCE and LCP, the energy and emissions caused by materials for building fixed main structure (FMS), have a linear relationship to the building height, while the slopes of lines depend upon the structure of the building. The energy and emissions caused by on-site construction depend highly upon the types of structure and Chinese diesel vehicle and machinery emissions. The energy and emissions from the demolition stage are relatively stable as they rely on the building material usage as well as the national waste treatment arrangements (e.g. the proportion of treatment, the efficiency of incineration plant etc.).

By applying this new method, the LCE and LCP of Chinese office buildings can be easily assessed at the earlier stage of the building’s design. The assessment results (i.e. embodied energy and four embodied air pollutants) give useful information to the designers in verifying the design concept, which, as an earlier warning in the building design process can prevent potential hazards to the environment brought about by unimproved office design.

**Chapter 5. Development of a general environmental impact assessment system  
associated with the office buildings` pollutant emissions**



## 5.1 Introduction

The pollutants emitted from the full life-cycle of Chinese office buildings, including the CO<sub>2</sub> equivalents (e.g. CH<sub>4</sub>, N<sub>2</sub>O, HFCs, PFCs and SF<sub>6</sub>), NO<sub>x</sub>, SO<sub>2</sub> and PM (e.g. PM<sub>2.5</sub> and PM<sub>10</sub>), can be estimated by using “CN13790” and “life-cycle embodied pollutant emissions estimation” method described in Chapters 3 and 4. However, the environmental impact of a building at its earlier conceptual design stage, cannot be assessed by the individual emission volumes of the above named pollutants alone. In principle, a “traditional” green building is designed that way to minimize the volume of a single pollutant, e.g. reducing CO<sub>2</sub> emission to achieve the low carbon target. However, since the other pollutants are also discharged simultaneously, they may affect the emission level of the selected pollutant (e.g. CO<sub>2</sub>). An overall environmental assessment system that addresses the inter-relationship of numerous pollutants is required to give a subjective evaluation to the performance of the building in terms of its environmental impact. To give an example, if an earlier-stage building design solution indicates a 20% reduction in CO<sub>2</sub> emission, and a 5% increase in NO<sub>x</sub> emission compared to the other design solution, the overall performance of the two design solutions are still non-comparable owing to the shortage of the overall index in the context of the environmental impact. The environmental assessment system to be established in this chapter will be the solution to solving this problem.

**The aim of this chapter is to generate an environmental impact assessment system that enables the subjective evaluation of the performance of a building. This system, is indicated by the innovative metric, namely the pollutant equivalent (PE) that considers four types of pollutants in a combined way, and allows the measurable, reportable and verifiable (MRV) environmental performance assessment in the green building designs.** The PE is a dimensionless figure that is based on the discharge amount of each pollutant type and the resultant importance on

the environmental impact (represented by the monetization environmental cost) among them. On the basis of the result of the comparison importance generated by the analytic hierarchy process (AHP) based method, the weights, which allow the PE to be generated, are assigned to each of them.

In this chapter, **(1)** PE is firstly defined, as shown in Section 5.2; **(2)** the system development methodology is described, as shown in Section 5.3; **(3)** the environmental impact from each pollutant is analyzed and the relevant data are collected from various sources and stored in a dataset, as shown in Section 5.4; and **(4)** the relative importance (weight) of each pollutant is calculated using an AHP based method, and consequently the PE of the system is obtained, as shown in Section 5.5. Finally **(5)** a case study is carried out to examine the effectiveness of the environmental impact assessment system, as shown in Section 5.6. The life-cycle environmental impacts from the current and improved design of a typical office building are analyzed using PE as the indicative metric. The environmental impact characteristic of this building is observed in order to understand the whole life environmental impact and to test the practicalities of the PE metric.

## 5.2 Definition of the general environmental impact metric

PE (pollutant equivalent) is defined as the general environmental impact metric, which reflects the comprehensive building environmental impact from four air pollutants. The PE can be converted from pollutants' emission using Eq. 5.1 and can have the units of PE/m<sup>2</sup> or PE/year etc.

$$PE = F_{CO_2}Emi_{CO_2} + F_{NO_x}Emi_{NO_x} + F_{SO_2}Emi_{SO_2} + F_{PM}Emi_{PM} \quad (5.1)$$

Where:  $F_{CO_2}$ ,  $F_{SO_2}$ ,  $F_{NO_x}$  and  $F_{PM}$ , are the converter factors for CO<sub>2</sub>, SO<sub>2</sub>, NO<sub>x</sub> and PM respectively, generated by the comparison importance level on the environmental impact among them;  $Emi_{CO_2}$ ,  $Emi_{SO_2}$ ,  $Emi_{NO_x}$  and  $Emi_{PM}$  are the emission amounts (kg) for each pollutant.

To define the converter factor for pollutants, the environmental impact of each pollutant and the relationship between them needs to be studied. There are many aspects that should be considered in the assessment of pollutant environmental impact, (e.g. environment damage, economic damage and civil health harm). For each pollutant, the mechanism of the environmental impact is different. In that case, the emission amounts can't be directly used as the comparable value for impact assessment and PE calculation. The most commonly used method for representing and comparing pollutant impacts is the conversion of the impact to a **monetization environmental cost**. Many types of monetization costs are widely used (e.g. the environmental remediation cost, the civil hospital cost and the pollutant emission ticket cost from the government) as it is easy to compare among each other and can be calculated directly with other cost data. The approach for recognizing the environmental impact from pollutants is illustrated in Figure 5.1.

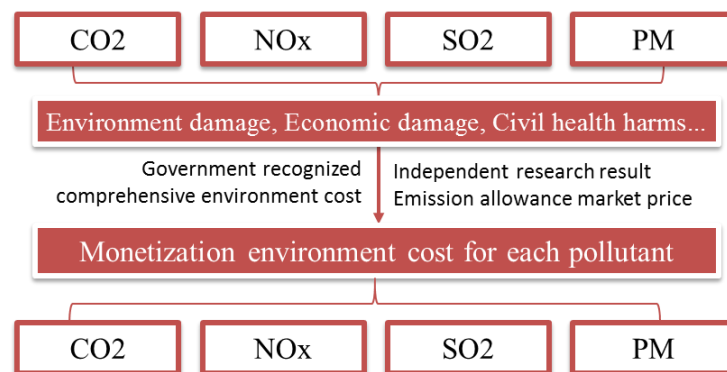


Figure 5.1: Approach to recognizing the environmental impact from pollutants

### 5.3 Methodology

#### 5.3.1 The overall methodology

In order to generate the general environmental impact metric: PE and the weights for each pollutant used in PE, the harm from each pollutant is studied and the environmental impact data is collected to a dataset. The dataset is then analyzed by using an AHP method to derive the weight of each pollutant that is used to compose the PE. After this, the practicality of PE is proven through a case study. The research processes are shown in Figure 5.2.

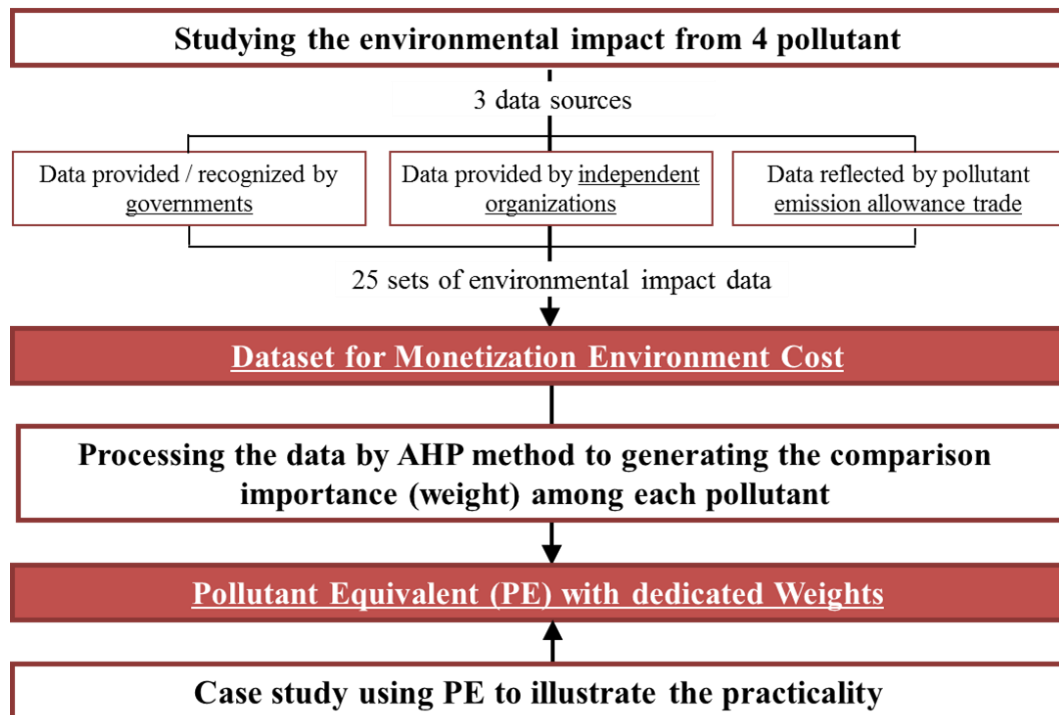


Figure 5.2: The research processes of Chapter 5

**For the study of the environmental impact** from each pollutant (section 5.3.2), the environmental impact is quantified by using the monetization environmental cost, which is collected from 3 types of data sources (e.g. governments, independent organisations and the market price for emission allowance trade) through the use of literature / policy reviews and market price gathering.

**For the data processing and weight generation**, an AHP based method is used, in which the pairwise matrix for the importance of criteria is generated by mathematic analyses, and the ranking of criteria priorities (weights) is derived by using the eigenvector solution method [166]. The principle of the AHP based method is described in section 5.3.2 below.

**For the case study to illustrate the practicality of the PE method**, a typical office building is selected and the PE from each stage of its life-cycle is studied. By using a comparison study, the environmental impact results that are unique from the existing single metric (i.e. CO<sub>2</sub>e) illustrate the value of the PE method.

### 5.3.2 The Principle of the AHP method - the mathematical foundation for the weights of the PE.

The conversion factors for each pollutant (i.e.  $F_{CO_2}$ ,  $F_{SO_2}$ ,  $F_{NO_x}$  and  $F_{PM}$ ) are generated by comparing the relevant importance of environmental impacts among each other. The more environmental impact one pollutant has, the higher the conversion factor will be given to it. It is similar to a weighting system that assigns weight to each criterion to reflect its importance, then an overall value can be generated by using the weights and values of each criterion. The conversion factor (weight) for each pollutant is calculated through an AHP based method, the principle of the AHP method and the conversion factor generation process will be described below.

The analytic hierarchy process (AHP) is a systematic and structured technique for organizing and analyzing complex decision making. It is based on mathematics and psychology by using both qualitative and quantitative criteria [167]. The AHP was developed by Thomas L. Saaty in the 1970s [168] and has been widely used in the research and industry fields, until now a lot of improvement and refining has been applied to AHP when applied to specific problem-solving. The principle of AHP is as follows, firstly a hierarchical model will be established (not necessarily for this research since 4 pollution belongs to the same level for the problem solving), then there is the factor comparison/judgment matrix, and the priority vector which will be calculated followed by the consistency test. In the last step the combined priority vector will be generated and the consistency test will be applied to them.

**The calculation process is provided by using an example to illuminate the weight assignment process in the decision-making system.** Assuming three criteria ( $C_1$ ,  $C_2$ ,  $C_3$ ) relevant to building design that are able to impact the environment, the approaches of their environmental impact are quite distinct. Meanwhile, there are more than one methods to assess the environmental impact of different pollutants and the importance among them. Three steps are arranged, as below:

### **Step 1 - Establishment of the pairwise matrix for the importance of criteria.**

According to research on the importance between two criteria by self-calculating or organizing/summarizing the literature, for each assessment method, the relative importance of one criterion over another can be expressed separately. For example, by assuming that based on a dedicated assessment method,  $C_1$  is 2 times as important as  $C_2$ ,  $C_2$  is 3 times as important as  $C_3$ , and  $C_1$  is 5 times as important as  $C_3$ , the relative importance among three criteria are listed in Table 5.1. The number in Position a-b (abbreviated as  $P_{a-b}$ ) is the ratio of  $C_a$  to  $C_b$ .

Table 5.1: Pairwise relative importance of criteria

Pairwise importance comparison	$C_1$		$C_2$		$C_3$	
$C_1$	$P_{1-1}$	1	$P_{1-2}$	2	$P_{1-3}$	5
$C_2$	$P_{2-1}$	1/2	$P_{2-2}$	1	$P_{2-3}$	3
$C_3$	$P_{3-1}$	1/5	$P_{3-2}$	1/3	$P_{3-3}$	1

Based on the importance comparison given above,  $P_{1-2}$ ,  $P_{2-3}$  and  $P_{1-3}$  are filled with 2, 3 and 5, and their reciprocal value 1/2, 1/3 and 1/5 are filled in  $P_{2-1}$ ,  $P_{3-2}$  and  $P_{3-1}$ ;  $P_{1-1}$ ,  $P_{2-2}$  and  $P_{3-3}$  are filled with 1 as they are equal to themselves. Significantly, (1) the comparison should be pairwise, reflecting the importance between two criteria; (2) in this example,  $C_1=2C_2$ ,  $C_2=2C_3$  and  $C_1=5C_3$ , values are not consistent, they are allowed to be inconsistent as long as their consistency ratio is less than a specific value (This will be explained in following part). The pairwise matrix for the importance of criteria can be converted from the content of Table 5.1 to matrix C and the fraction in the pairwise matrix are converted to decimals, as shown in the matrix (5.2).

$$C = \begin{bmatrix} 1 & 2 & 5 \\ 1/2 & 1 & 3 \\ 1/5 & 1/3 & 1 \end{bmatrix} \rightarrow \begin{bmatrix} 1 & 2 & 5 \\ 0.5 & 1 & 3 \\ 0.1667 & 0.3333 & 1 \end{bmatrix} \quad (5.2)$$

**Step 2 - Validation of the consistency.** According to the principle of APH, the consistency of importance comparison needs to be tested, for the consistency ratio less than 10%, the consistency of importance values is usable for making judgments in this method. The consistency rate is computed by Eq. (5.3).

$$CR = |(\lambda_{max} - n)/(n - 1) / RI| \quad (5.3)$$

Where, CR is the consistency ratio, which should be less than 10%;  $\lambda_{max}$  is the eigenvalue for matrix C (addressed in 5.2); n is the number of criteria; RI is the average random consistency index of sample size 500 matrix which was provided by Prof. Thomas L. Saaty [167] and the value of the RI are listed in Table 5.2.

Table 5.2: Random consistency index (RI)

N	1	2	3	4	5	6	7	8	9	10
RI	0	0	0.58	0.9	1.12	1.24	1.32	4.41	1.45	1.49

For our example, CR is calculated below using Eq. 5.3, in which the consistency of the example pairwise comparison is acceptable.

$$CR = |(2.9457 - 3)/(3 - 1) / 0.58| = 4.7\% < 10\%$$

### **Step 3 - Ranking of the criteria priorities.**

Following the mathematical study made by Prof. Thomas L. Saaty [167], the eigenvector solution is the best approach for priorities ranking from a pairwise matrix. In order to get the eigenvector, the pairwise matrix needs to be squared and the row sums are then calculated and normalized. After that, it is important to iterate the squaring and normalizing calculation process until the absolute value of the differences rate ( $\epsilon$ ) between these sums in two consecutive calculation is less than 1% for any row sums.

For our example, to derive the ranking of criteria priorities, the matrix (5.2) are squared to the matrix (5.4), and then calculated using the row sums and normalizing them by dividing the row sum by the row totals, the results are the eigenvector of this matrix, as shown in Eq. 5.5.

$$\begin{bmatrix} 2.8335 & 5.6665 & 16 \\ 1.5001 & 2.9999 & 8.5 \\ 0.50005 & 1 & 2.8334 \end{bmatrix} \quad (5.4)$$

$$\begin{bmatrix} 2.8335 & + & 5.6665 & + & 16 \\ 1.5001 & + & 2.9999 & + & 8.5 \\ 0.50005 & + & 1 & + & 2.8334 \end{bmatrix} = \begin{bmatrix} 24.5 \\ 13 \\ 4.33345 \end{bmatrix} \rightarrow \begin{bmatrix} 0.585656 \\ 0.310756 \\ 0.103588 \end{bmatrix} \quad (5.5)$$

As a follow-on measure, a repetition of the last step and calculation of the differences between the eigenvectors in two consecutive calculations is made. The squared matrix are shown in the matrix (5.6) and the new eigenvector is listed in Eq. 5.7. The difference rates ( $\epsilon$ ) between eigenvectors in two consecutive calculation is shown in Eq. 5.8, which is less than 1%. In this circumstance, the iterations are finished.

$$\begin{bmatrix} 224.52984 & 49.05496 & 138.8357 \\ 13.00111 & 25.99972 & 73.58465 \\ 4.333833 & 8.666833 & 24.52896 \end{bmatrix} \quad (5.6)$$

$$\begin{bmatrix} 24.52984 & + & 49.05496 & + & 138.8357 \\ 13.00111 & + & 25.99972 & + & 73.58465 \\ 4.333833 & + & 8.666833 & + & 24.52896 \end{bmatrix} = \begin{bmatrix} 212.4205 \\ 112.5855 \\ 37.52962 \end{bmatrix} \rightarrow \begin{bmatrix} 0.58593 \\ 0.31055 \\ 0.10352 \end{bmatrix} \quad (5.7)$$

$$\begin{bmatrix} 0.585656 \\ 0.310756 \\ 0.103588 \end{bmatrix} - \begin{bmatrix} 0.58593 \\ 0.31055 \\ 0.10352 \end{bmatrix} = \begin{bmatrix} -0.00027 \\ 0.00021 \\ 0.00007 \end{bmatrix} \rightarrow \epsilon = \begin{matrix} 0.05\% \\ 0.07\% < 1\% \\ 0.07\% \end{matrix} \quad (5.8)$$

Thus, the eigenvectors from the final step is the basis for criteria priorities and can be assigned to the criteria as their weights in the example judgment problem. The weights for C1, C2 and C3 are 58.593%, 31.055% and 10.352% respectively.

This AHP based weight assignment process will be used in the following section 5.5 to judge the importance and assignment of weights for each pollutant type.

#### 5.4 Recognizing the environmental impact from pollutants and collecting related data.

In this section, the monetization environmental cost is studied for each pollutant in typical reigns. Obviously, the cost will be varied between reigns, but the importance ratio between each pollutant can still be summarized. The environmental cost of SO<sub>2</sub>, NO<sub>x</sub> and PM are discussed reign by reign as the damage is highly dependent upon the location and emission sources, while the costs from CO<sub>2e</sub> are almost same in all the world. If no specific regional data is in existence for CO<sub>2e</sub>, the average price in the same year for the EU emissions trading market will be assigned to the CO<sub>2e</sub>'s environmental



cost as it is a mature market price which can basically reflect its environmental cost.

The three types of data sources for the monetization environmental cost are studied in this research. These include the comprehensive environmental cost provided or recognized by the government and the comprehensive environmental cost calculated by independent researchers/organizations and the market price for the pollutant emission allowance.

### **The comprehensive environmental cost provided / recognized by the government:**

The environmental cost data recognized by the government of the UK, US and China are involved in this research, they represent the technology and environmental level of Europe, America and Asia, and also the majority of other countries in terms of relevant building activity.

In the UK, the Department of the Environment, Food and Rural Affairs (DEFRA) carried out research on the damage cost that included remediation costs and direct health costs. These were used to assess the national policies and environmental protection projects. As NO<sub>x</sub> can be partly converted into PM or facilitate PM generation, based on the DEFRA's data [169], the NO<sub>x</sub> damage cost value of both NO<sub>x</sub> and PM were caused by NO<sub>x</sub>. Damage costs from the energy supply industry are used to represent damage from building as most of the pollution discharged in the building sector is energy-related, either during building material manufacturing or building operations. The cost for SO<sub>2</sub>, NO<sub>x</sub> and PM are £1,956, £1,263 and £2,906 respectively per tonne, which are listed in Table 5.3.

In the US, there are also environmental cost data that are recognized by the government and used to measure the environmental impact of construction. For example, the cost recognized by New York State and assigned to the energy price for CO<sub>2e</sub> and SO<sub>2</sub> are £0.68 and £1352 respectively per tonne, whereas, in Massachusetts, the government recognized costs for CO<sub>2e</sub> and SO<sub>2</sub> are £15.9 and £4686 respectively per tonne [170]. In the state of Washington, the government recommended environmental cost data used

for the “final environmental impact statement” in the city integrated resource plan for CO<sub>2</sub>e, SO<sub>2</sub>, NO<sub>x</sub> and PM are £15.2, £1491, £1658 and £2951 respectively per tonne [171].

In China, the government recognized environmental costs are summarized in the 2012 annual statistical report on the environment [172] by the Ministry of Environmental Protection of China, in which the comprehensive cost for SO<sub>2</sub>, NO<sub>x</sub> and PM are £1,217, £1,258 and £20,459 respectively per tonne.

### **The comprehensive environmental cost provided by independent organizations:**

For the independent research's data, three sources are involved in this research. Firstly, the DG environment has carried out a research on the marginal external costs of pollutants. The results have been used in the Clean Air for Europe Programme (CAFE) [173]. The damage data per ton of pollutants account for variations in the site of emissions by providing estimates for each country in the main EU countries. The damage, including aspects from PM mortality (mean estimates of the value of the statistical life method), O<sub>3</sub> mortality (mean estimates of the value of a life year method), direct and indirect health impacts and impacts to materials and crops. Furthermore, Mike Holland and Paul Watkiss have studied the pollutant cost for the European Commission in the benefits table database (BeTa) [174] and generated the overall value for 15 EU countries, which are involved in the comparison as well. Apart from the above, Tsinghua University carried out a study to the comprehensive cost in China [175], leading to the results shown in Table 5.3.

### **The market price for the pollutant emission allowance:**

In the UK, the European Union Emission Trading Scheme (or EU ETS), which is the largest multi-national greenhouse gas emissions trading scheme in the world, is used to carry out the CO<sub>2</sub> emission trading. However, there is no existing trading system for NO<sub>x</sub> and SO<sub>2</sub> up to date, although proposals are being considered for using trading to control their emission. Only the price for CO<sub>2</sub> is meaningless since no cost comparison

information among the pollutants is in existence. In this case, the market price for the UK is not used in the analysis.

In the US, the emission allowance is tradable since the set of the SO<sub>2</sub> trading system under the framework of the Acid Rain Program of the 1990 Clean Air Act in the U.S [176] was introduced. The national SO<sub>2</sub> trading program was challenged in 2004 and replaced in the 2011 Cross-State Air Pollution Rule (CSAPR) [177]. Four separate trading groups for SO<sub>2</sub> and NO<sub>x</sub> are open to the market under the CSAPR. Meanwhile, the CO<sub>2</sub> emission price fluctuates with the “EU ETS” price and is affected by regional regulations. The price from the emission allowance auction under CSAPR can reflect the environmental cost. The average auction price for 2008-2010 [178] is listed in Table 5.3.

In China, the pollutant allowance trade market has partly been opened in a few provinces, recently. In November 2011, China approved pilot tests of carbon trading in several provinces and cities, including Beijing, Chongqing, Shanghai, Shenzhen, Tianjin as well as ShanXi Province, Guangdong Province and Hebei Province, in which different prices are applied. As its national trading is expected to start in 2016, the prices from the Shaanxi province and Hebei province [172], as shown in Table 5.3, are used to represent the price in the current stage.

Table 5.3: Monetization environmental cost statistic dataset by type and region

		Monetization environmental cost (£/tonne)				
Data Type	Data Source & NO.	CO <sub>2</sub> e	SO <sub>2</sub>	NO <sub>x</sub>	PM	
<b>Type-1:</b> Government recognized comprehensive environmental cost	UK-DEFRA (1)	5.46	1956	1263	2906	
	US-New York State (2)	9.68	1352	-	-	
	US-Massachusetts State (3)	15.9	4686	-	-	
	US-Washington State (4)	15.2	1491	1658	2951	
	China Centre Gov. (5)	3.97	1217	1258	20459	
<b>Type-2:</b> Independent research result	CAFE Programme data from DG environment	Belgium (6)	15.6	24180	10920	140400
		Czech Republic (7)	15.6	17940	15600	70980
		Denmark (8)	15.6	11700	9438	37440
		France (9)	15.6	17940	16380	101400
		Finland (10)	15.6	3978	1560	12480
		Greece (11)	15.6	3120	1482	19500
		Germany (12)	15.6	24960	20280	109200

	Italy ( 13 )	15.6	14040	12480	75660
	Poland (14)	15.6	12480	7800	64740
	Spain (15)	15.6	9360	5616	42120
	Sweden (16)	15.6	6318	4602	26520
	UK (17)	15.6	14820	7800	85800
	Ireland (18)	15.6	10920	8580	32760
	BeTa`s EU data (19)	15.6	4056	3276	10920
	China-Tsinghua University (20)	7	630	1450	-
<b>Type-3:</b> Emission allowance price	US- 2008 average (21)	20.4	171.8	497.9	-
	US- 2009 average (22)	9.6	50.03	287.70	-
	US- 2010 average ( 23 )	9	10.19	27.55	-
	China - ShaanXi ( 24 )	9	1063	790	-
	China – Hebei ( 25 )	9	500	500	-

The dataset of the monetization environmental cost in Table 5.3 is analyzed to generate the weights for each pollutant in PE, by using the comparison importance from an AHP based method (described methodology) in the section below.

### 5.5 Generating the conversion factor (weight) for the PE by an AHP based method

As mentioned above, four criteria are involved in the judgment of the environmental impact of the building. The emission amount of four pollutants is computed by the method explained in Chapter 4. As criteria, the 4 pollutants, i.e., CO<sub>2</sub>e, SO<sub>2</sub>, NO<sub>x</sub> and PM, are represented by A1, A2, A3 and A4 respectively. According to the data presented in Table 5.3, the pairwise comparison of the environmental cost for every single data source can be computed, and are listed in Table 5.4.

Table 5.4: The pairwise comparison result for the monetization environmental cost from 25 data sources

NO.	A11	A12	A13	A14	A21	A22	A23	A24	A31	A32	A33	A34	A41	A42	A43	A44
1	1	0.0028	0.0043	0.0019	358.2	1	1.55	0.67	231	0.65	1	0.43	532	1.49	2.30	1
2	1	0.0072	-	-	139.6	1	-	-	-	-	1	-	-	-	-	1
3	1	0.0034	-	-	294.7	1	-	-	-	-	1	-	-	-	-	1
4	1	0.0102	0.0092	0.0052	98.1	1	0.90	0.51	109	1.11	1	0.56	194	1.98	1.78	1
5	1	0.0033	0.0032	0.0002	306.6	1	0.97	0.06	317	1.03	1	0.06	5153	16.81	16.26	1
6	1	0.0006	0.0014	0.0001	1550	1	2.21	0.17	700	0.45	1	0.08	9000	5.81	12.86	1
7	1	0.0009	0.0010	0.0002	1150	1	1.15	0.25	1000	0.87	1	0.22	4550	3.96	4.55	1
8	1	0.0013	0.0017	0.0004	750	1	1.24	0.31	605	0.81	1	0.25	2400	3.20	3.97	1
9	1	0.0009	0.0010	0.0002	1150	1	1.10	0.18	1050	0.91	1	0.16	6500	5.65	6.19	1
10	1	0.0039	0.0100	0.0013	255	1	2.55	0.32	100	0.39	1	0.13	800	3.14	8.00	1

11	1	0.0050	0.0105	0.0008	200	1	2.11	0.16	95	0.48	1	0.08	1250	6.25	13.16	1
12	1	0.0006	0.0008	0.0001	1600	1	1.23	0.23	1300	0.81	1	0.19	7000	4.38	5.38	1
13	1	0.0011	0.0013	0.0002	900	1	1.13	0.19	800	0.89	1	0.16	4850	5.39	6.06	1
14	1	0.0013	0.0020	0.0002	800	1	1.60	0.19	500	0.63	1	0.12	4150	5.19	8.30	1
15	1	0.0017	0.0028	0.0004	600	1	1.67	0.22	360	0.60	1	0.13	2700	4.50	7.50	1
16	1	0.0025	0.0034	0.0006	405	1	1.37	0.24	295	0.73	1	0.17	1700	4.20	5.76	1
17	1	0.0011	0.0020	0.0002	950	1	1.90	0.17	500	0.53	1	0.09	5500	5.79	11.00	1
18	1	0.0014	0.0018	0.0005	700	1	1.27	0.33	550	0.79	1	0.26	2100	3.00	3.82	1
19	1	0.0038	0.0048	0.0014	260	1	1.24	0.37	210	0.81	1	0.30	700	2.69	3.33	1
20	1	0.1187	0.0410	-	8.42	1	0.345	-	24.4	2.89	1	-	-	-	-	1
21	1	0.0501	0.0173	-	19.9	1	0.35	-	57.9	2.90	1	-	-	-	-	1
22	1	0.1919	0.0511	-	5.21	1	0.27	-	19.6	3.75	1	-	-	-	-	1
23	1	0.8832	0.3267	-	1.13	1	0.37	-	3.06	2.70	1	-	-	-	-	1
24	1	0.0054	0.0114	-	184.8	1	2.11	-	87.8	0.48	1	-	-	-	-	1
25	1	0.0180	0.0180	-	55.6	1	1.00	-	55.6	1.00	1	-	-	-	-	1

After completing the pairwise comparison among 25 data sources, the overall pairwise comparison for each data source type can be computed separately by normalizing and averaging the results of Table 5.4. Thus, the overall pairwise comparison matrix for each data source type can be established and their consistency ratio can be tested.

The overall average normalized results for 3 data source types and their consistency ratio are listed in Table 5.5. It is worth noticing that some comparisons are not available from data no.2 and no.3, so they are replaced by the average value from data no.1, no.4 and no.5 when calculating the overall average data for the data source type 1. Owing to the incomplete PM's data from the last 5 data sources, the data source type 3 has only 3 criteria.

Table 5.5: The overall average normalized results

Data source type 1 (from government provided / recognized data)							
A11	A12	A13	A14	A21	A22	A23	A24
0.000862	0.000006	0.000006	0.000003	0.156958	0.000862	0.000932	0.000434
A31	A32	A33	A34	A41	A42	A43	A44
0.140964	0.000843	0.000862	0.000410	0.690123	0.002921	0.002952	0.000862
Eigenvalue=3.9738; CR = 0.97% < 10%							
Data source type 2 (from independent research results)							
A11	A12	A13	A14	A21	A22	A23	A24
0.0005203	0.0000033	0.0000026	0.0000002	0.1746588	0.0005203	0.0006048	0.0000809

A31	A32	A33	A34	A41	A42	A43	A44
0.1530864	0.0006991	0.0005203	0.0000532	0.6653874	0.0012281	0.0021140	0.0005203
Eigenvalue=3.8573; CR = 5.28% < 10%							
Data source type 3 (from emission allowance price)							
A11	A12	A13	A21	A22	A23	A31	A32
0.0323944	0.0126011	0.0046407	0.3199533	0.0323944	0.0162284	0.4638184	0.0855748
A33	A32	A33	A34	A41	A42	A43	A44
0.0323944	N/A	N/A	N/A	N/A	N/A	N/A	N/A
Eigenvalue=3.1089; CR = 9.4% < 10%							

Based on the results given in above Table 5.5, all the consistency ratio of the pairwise comparison for 3 data source types are less than 10%, therefore, they are all consistent and can be used to derive the weight of the criteria. The ranking (weight) of the criteria can be derived by using the eigenvector solution method. For each data source type, after 2 iterations, the absolute value of the differences rate ( $\epsilon$ ) between sums in two consecutive calculation, are all less than 1%. The ranking of criteria for each data source type (including the converted data for data source type 3) and their difference rate are listed in Table 5.6. It is worth pointing out that the weights of data sources 3 don't include, thus, the average weight for PM from the data source type 1 and 2 (66.469%) is given to data source 3. The rest of the weights (100%-66.469%=33.531%) in data source 3 are assigned to the other 3 criteria based on their calculated comparison importance.

Table 5.6: The ranking of criteria for each data source type

Data source type	Iteration time	Differences rate ( $\epsilon$ )	Criteria's weight			
			CO <sub>2</sub> e	SO <sub>2</sub>	NO <sub>x</sub>	PM
1	2	0.07% < 1%	0.134%	19.674%	18.401%	61.792%
2	2	0.01% < 1%	0.046%	17.457%	11.349%	71.147%
3	2	0.09% < 1%	6.964%	32.422%	60.614%	N/A
3 (converted)	-	-	2.335%	10.871%	20.325%	66.469%

The overall weights for 4 criteria are the mean value of weight from 3 data source types. The overall weights for 4 criteria are the mean value of weight from the 3 data source types. On this basis, the global weights for the 4 criteria are calculated and the results are presented in Table 5.7. The weight for pollutants is used as the conversion factor in PE. By integrating the weights to Eq. 5.1, the PE for any office building can be generated using Eq. 5.9.

Table 5.7: Overall weights for 4 criteria

Criteria`s weight (convert factor)			
CO <sub>2</sub> e	SO <sub>2</sub>	NO <sub>x</sub>	PM
0.838%	16.001%	16.691%	66.469%

$$PE = 0.838\%Emi_{CO_2} + 16.001\%Emi_{SO_2} + 16.691\%Emi_{NO_x} + 66.469\%Emi_{PM} \quad (5.9)$$

## 5.6 The case study and results discussion: using PE in the office building designs comparison.

After the PE method is defined and the weights are determined, the environmental impact of a typical office building represented by the PE metric is studied in this section. The PE from the original and improved design of this office building are analyzed, the environmental impact improvements, PE source and characteristic are observed in this section. Through this case study, the applicability and practicality of PE metrics are tested and discussed in the last section.

### 5.6.1 A description of an example building (original and improved design).

An office building designed to be located in Shanghai China is selected as the example building to apply PE metrics. The example building, as can be seen in Figure 5.3 (in the red box) and 5.4, is the office building for people who work for a large-scale data centre. It is a 3 story reinforced concrete frame structure building with a gross building area of 9600m<sup>2</sup>. The basic information of its original design is presented in Table 5.8.

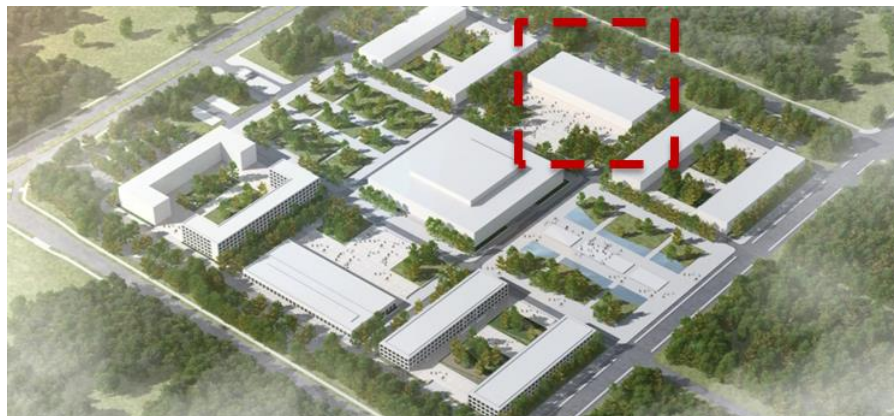


Figure 5.3: An architectural rendering of the large-scale data centre

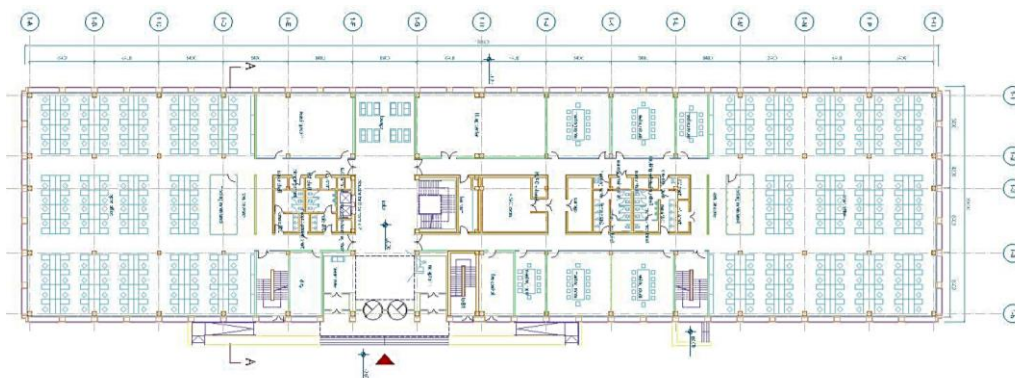


Figure 5.4: The layout for the ground floor of the example office building

Table 5.8: Basic information for the original design

Components	Specification
Structure type	reinforced concrete frame structure
Wall	External: Hollow concrete block + 25mmEPS panel + marble curtain wall Internal: Autoclaved aerated concrete block
Roof	Waterproofing mortar + concrete panel +10mmEPS panel
Windows	8mm Single glazing window with aluminium frame
HVAC	Water cooled air conditioning with screw chillers
Lighting	CFL lighting system

The example building is fully air-conditioned in the day-time, and natural ventilation will be operated during the night for cooling in summer in order to reduce the cooling needs for the next day. The typical EER for the water-cooled air conditioning system defined in Chapter 3 is used in the calculation of the HVAC electricity demand. The lighting and office equipment are also defined by using the typical dataset in Chapter 3. No hot water supply is designed and no renewable energy technology is integrated.

In the follow-up building design process, for the purpose of enhancing building energy saving, an improved design plan was provided which mainly focused on the improvement of passive green building strategies. In the improved design, the insulation layer for the external wall and roof has been enhanced. High performance windows are used instead of single glazing one. The specifications of design improvements are presented in Table 5.9.



Table 5.9: Specifications for improved design

Components	Specification
Wall	External: Hollow concrete block + 40mmEPS panel + marble curtain wall
Roof	Waterproofing mortar + precast ceramic concrete +20mmEPS panel
Windows	Double glazing window Low-E coating and thermal breaking aluminium frame

### 5.6.2 Calculating the life-cycle PE for the original and improved design of example building

The life-cycle energy and emission assessment method described in Chapter 4 are applied to estimate the emission for the original and improved design of the example building. The building material usage is derived from the “building material usage estimation” of the construction budget sheet in the real design. According to material usage and the relevant default value (e.g. transporting distance, waste ratio, recycling ratio, etc.) in Chapter 4, the pollutants` emission from the 4 building life phases (i.e. material producing, on-site construction, operation and demolition) are calculated. All pollutant emissions are converted to the PE by using Eq. 5.9. The detailed emission data and environmental impact data reflected by the PE are presented in .

Table 5.10: Pollutant and environmental cost for original and improved design

		Pollutants				PE
		CO <sub>2e</sub>	SO <sub>2</sub>	NO <sub>x</sub>	PM	
Material (Original)	Emission (Tonne)	10,886	1,007.90	8	9.7	260,282
	Envir. impact (PE)	91224.7	161274	1335.3	6447.5	
Material (Improved)	Emission (Tonne)	11016.1	1018.9	8.5	9.8	263,275
	Envir. impact (PE)	92314.7	163032	1416.1	6512.0	
Construction phase	Emission (Tonne)	262.6	0.2	3.5	0.02	2,830
	Envir. impact (PE)	2200.6	32.0	584.2	13.3	
Operation Phase (Original)	Emission (Tonne)	48,150	146.868	116.215	24.2668	462,527
	Envir. impact (PE)	403499.	23500.3	19397.5	16129.9	
Operation Phase (Improved)	Emission (Tonne)	33,673.4	102.708	81.2712	16.9708	323,463
	Envir. impact (PE)	282183	16434.3	13565.0	11280.3	
Demolition Phase	Emission (Tonne)	167.8	0.2	2.2	0.01	1,812
	Envir. impact (PE)	1406.2	32.0	367.2	6.6	
SUM (Original)	Emission (Tonne)	59,467	1,155	130	34	727,450
	Envir. impact (PE)	498330	184838	21684	22597	
SUM (Improved)	Emission (Tonne)	45,120	1,122	95	27	591,380
	Envir. impact (PE)	378104	179530	15932	17812	

### 5.6.3 Analyzing the environmental impact reflected by the PE in example building design.

The environmental impact characteristics of the example building (reflected by the PE) is analyzed and the environmental impact reduction by design modification is discussed in this section.

#### Analyzing the PE for the whole life-cycle of the example building

In the original design, the whole life-cycle emission for CO<sub>2</sub>e, SO<sub>2</sub>, NO<sub>x</sub> and PM is 59466 tonne, 1155 tonne, 129 tonnes and 34 tonnes respectively, in which CO<sub>2</sub>e takes over 97% in 4 pollutants. However, in terms of the environmental impact, CO<sub>2</sub>e contributes 68% of the PE, SO<sub>2</sub> contributes around 28% of the PE although its emission volume is only 1.9% of the total emission; while NO<sub>x</sub> and PM together contribute around 6% of the total PE, although their emission weight is only around 1%.

Through the improvement of the design solution, reduction in CO<sub>2</sub>e emission of 14,346 tonne (24%), SO<sub>2</sub> emission of 33 tonne (2.8%), NO<sub>x</sub> emission of 34 tonne (26%) and PM emission of 7 tonne (21%) will be achieved throughout the 50 years' building's life-cycle period. , thus leading to a reduction of PE by 136,070 (18.7%). The reason for the less PE reduction compared to the overall emission reduction is the smaller reduction of SO<sub>2</sub> emission (2.8%) which, however, has a higher environment hazard rate, owing to the increased usage of high-performance building material in the improved design. The emission and PE figures derived from each pollutant and their respective percentage in the original and improved designs are shown in Figure 5.5.

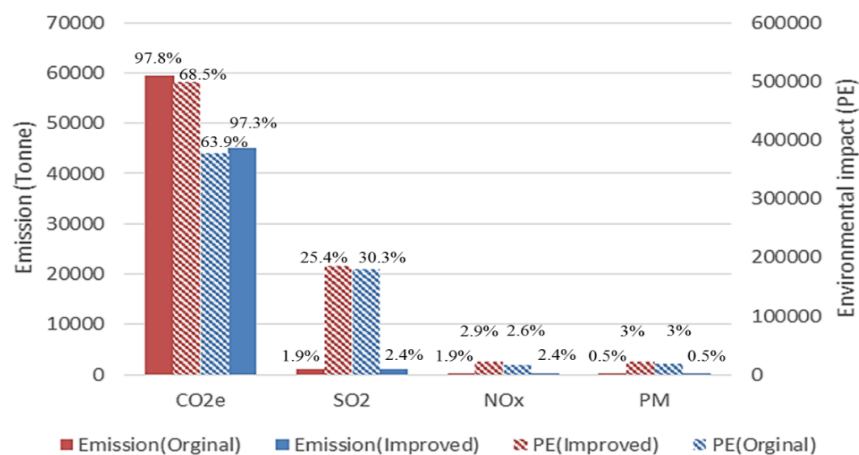


Figure 5.5: The emission and PE figures for each pollutant

### **Analyzing the PE for each stage of building life-cycle.**

In terms of emission amounts, in both the original and improved design, around 70%-90% of CO<sub>2</sub>e, NO<sub>x</sub> and PM are discharged in the building operational stage, whereas about 90% of SO<sub>2</sub> are from the material manufacturing stage due to the high SO<sub>2</sub> emission factor in the main material manufacture process, especially for cement and steel. In terms of the environmental impact, the major PE source is from the building operational stage, which contributes 63.6% and 57.4% of the whole life-cycle PE respectively in the original and improved design. The following PE source is the building's operational stage, the numbers are 35.8% and 44.5% in the two designs. The primary PE source is the CO<sub>2</sub>e emission for all building stages, except for the material manufacture stage, in which the environmental hazards are mainly from SO<sub>2</sub> emissions. The PE value distribution among building life stages and the detailed PE sources are presented in Figure 5.6.

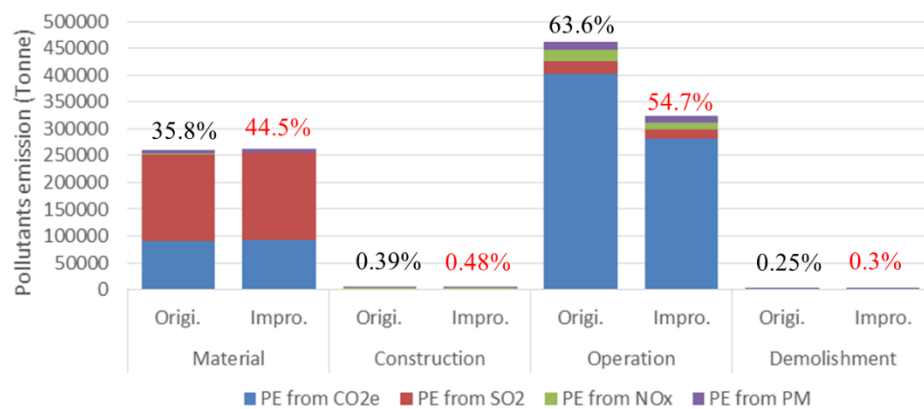


Figure 5.6: The PE distribution among building life stages and source specification

### **Analyzing the PE for the effect on building design improvement**

Comparison between the original and improved designs indicates that the life-cycle environmental impact can be reduced by 18.7% (136070 PE), through improving the building's thermal performance. To be specific, 30.1% of PE from the operational stage can be reduced owing to the operational energy saving led by the improvement of the design, whereby the PE at the material manufacture stage increases by 1.2%, owing to the higher material usage and application of material with better thermal performance. In the aspect of the whole life-cycle, the improved design will effectively decrease the

environmental impact, the slight PE increase from building materials can be easily offset by only 1.67 years of PE reducing from operation stage. In this example, the main building construction does not change in design improvement, thus, the process and workload changing in the on-site construction stage and demolition stage are very small. For this reason, the PE changes in the above two stages are not considered. The changing in PE and its source specifications are presented in Figure 5.7.

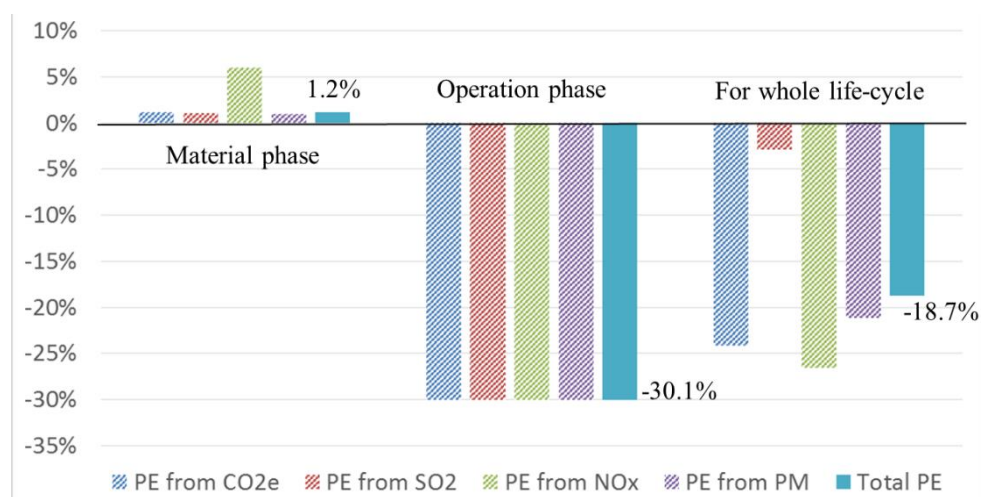


Figure 5.7: The changing in PE and its sources specification

## 5.7 The chapter conclusion

In this chapter, a novel environmental impact assessment system, presented by the PE metric, is established to evaluate the environmental performance of buildings in a measurable, reportable and verifiable way. To allow solution of the weights of each pollutant in the PE, the comparison importance regarding environmental damage among pollutants is studied by investigating 25 sets of the monetization environmental cost data from 3 types of data sources and processing them using an AHP based method. At the end of the chapter, PE metric's practicability is examined by a dedicated case study into a real office design. It is found that:

**PE has great advantage and unique characteristics compared to other existing metrics.** Compared to other pollution metrics (e.g. CO<sub>2</sub>e), the PE presents an obvious difference for different building design solutions at any stage of the building's life-cycle. To give an example, with the improved design solution, the SO<sub>2</sub> emission is reduced by

around 1.9% the corresponding PE reduction is around 28%, reflecting a significant reduction in the environmental impact of the design solution. It is therefore concluded that the use of the PE in building's environmental performance analysis can provide a clear image in justification of the "green" performance of the design solution. It is also found that:

**PE has the ability to reflect the comprehensive environmental impact.** Unlike the existing metrics that reflect the emission volume of a single pollutant, PE is able to provide a macro image for the comprehensive environmental impact of the design solution. In the selected case study, the overall environmental impact can be represented and assessed by using the PE, without considering the complex changing and relationships between each indicator.

It is worth pointing out that unlike emission data for a single pollutant, the PE is not an all-time accurate indicator. The value of PE reflecting the degree of environmental hazards for a specific time scope, region and research scope, can be assessed since the fundamental data of weight are related to them. The PE used in this research is only a general metric that reflects the globe value. It, by referring to the previously reviewed research outcomes, can be re-calculated when being used in the assessment of another specific purpose.

By taking the advantages of the PE metric, the comprehensive environmental impact of office building can be assessed. For this reason, the PE, together with embodied energy consumption (addressed in chapter 4) and building cost (addressed in Appendix III), are considered as the most important criteria that can be broadly used in comparison and selection of the green building design solutions.

**Chapter 6. Establishment of the multiple criteria based green design assessment and  
selection system**

## 6.1 Chapter Introduction

Owing to the multiple criteria applied to the decision making process for building design, it seems to be difficult to sort out the all-beneficial design solution at the early conceptual design stage. To obtain a so-called 'optimum' solution, trade-offs among the multiple conflicting objectives (e.g. energy saving and cost, building embodied energy and operational energy) may be needed. In fact, the 'best' design solution that meets all the desired objectives positively is none existent. In order to sort out the most favourite (i.e. optimum) design solution, a comprehensive green design assessment system should be developed to take the appropriate trade-offs among the multiple objectives so as to rank the design solutions in terms of the overall performance index and eventually select the best one.

**The aim of this chapter is to develop a green building design assessment and selection method (GBAS) in order to quantify the trade-offs to satisfy the different green design objectives, as well as to find the optimized design solution for the particular preferences of decision makers.** The TOPSIS (the technique for order of preference by similarity to ideal solution) based methods are applied in the GBAS to identify the appropriate green building design solution. Meanwhile, the preferences of the building's decision makers are considered via a survey of a range of building experts. The results of survey will be analyzed using an AHP based method and then applied to the TOPSIS system as the relevant weights to reflect the scenarios for different design's preferences.

In this chapter, the criteria considered in green office building design and the scenarios for different design preferences with related criteria are discussed. The methodology for the green building design assessment and selection using the TOPSIS method and AHP method together is described. A building expert survey is conducted and the result is analyzed to identify the importance of each criterion in different design preference scenarios. Furthermore, the mathematical function and method to assess the design solutions is generated for each preference scenario, by which the most appropriate

design solution can be selected.

The GBAS is a flexible and effective green building design solution assessment tool based on simple mathematical calculations. The design solution can be selected in a quantitative way, rather than a qualitative analysis in the traditional building design process. This ensures the selection of most appropriate design solutions at the conceptual design stage. Meanwhile, it is crucial to highly improve the design efficiency by avoiding the trial and error process.

## 6.2 Criteria and decision-making scenarios involved in the GBAS

### 6.2.1 Criteria involved in the GBAS

The criteria involved in the GBAS are the factors that are most commonly considered in green building design, including the energy consumption, the environmental impact and the cost of building. Under those tier 1 criteria, there are tier 2 criteria for each of them. The criteria in the GBAS are presented in Figure 6.1.

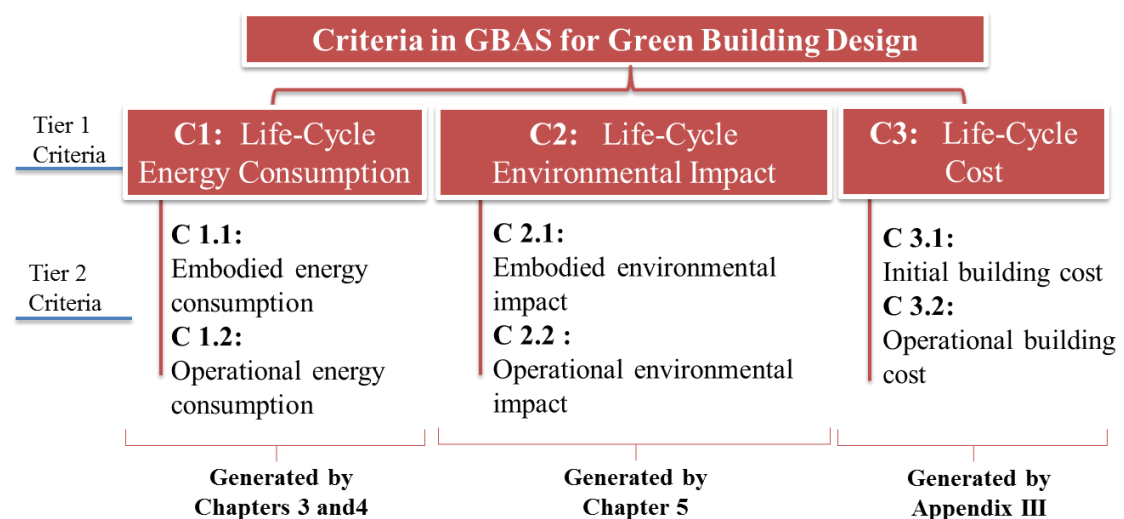


Figure 6.1: Criteria in GBAS

All criteria in GBAS can be generated by the calculation methods developed in previous Chapters, described below:

- C1.1 and C1.2 as the embodied and operational energy consumption, in MJ/m<sup>2</sup>, can



be generated by an embodied energy estimation model in chapter 4 and operational energy estimation model in chapter 3 respectively;

- C2.1 and C2.2 as the embodied and operational environmental impact, in k PE/m<sup>2</sup>, can be generated by the general environmental impact metric as discussed in chapter 5;
- C3.1 and C3.2, is the one-off construction cost and operational cost, in k £/m<sup>2</sup>. It can be generated by the “simplified general life-cycle office building cost estimation method” (addressed in Appendix III), which is based on the cost-area ratio of each building component, the cost-energy ratio of the each building’s service / renewable energy systems and its typical cost dataset.

### **6.2.2 The decision-making scenarios in the GBAS.**

The objectives for every specific green office building design vary, for instance, energy saving will be the main objective for energy-hungry regions whereas environmental impact reduction is the main objective for environmentally fragile regions with strict emission rules. The design decision-making scenarios are summarized to reflect the designers’ and decision-makers’ subjective preferences. The priority ranks of design objectives are defined in each decision-making scenario and described in this section.

By considering the common factors in green building design (i.e. energy saving, environment protection and cost effectiveness), the decision-maker’s subjective preferences are summarized into 3 groups including a total of 12 preference scenarios. The scenario-groups and scenarios in GBAS can be seen in Figure 6.2, the details of decision-maker’s preferences for each scenario group are discussed as follow:

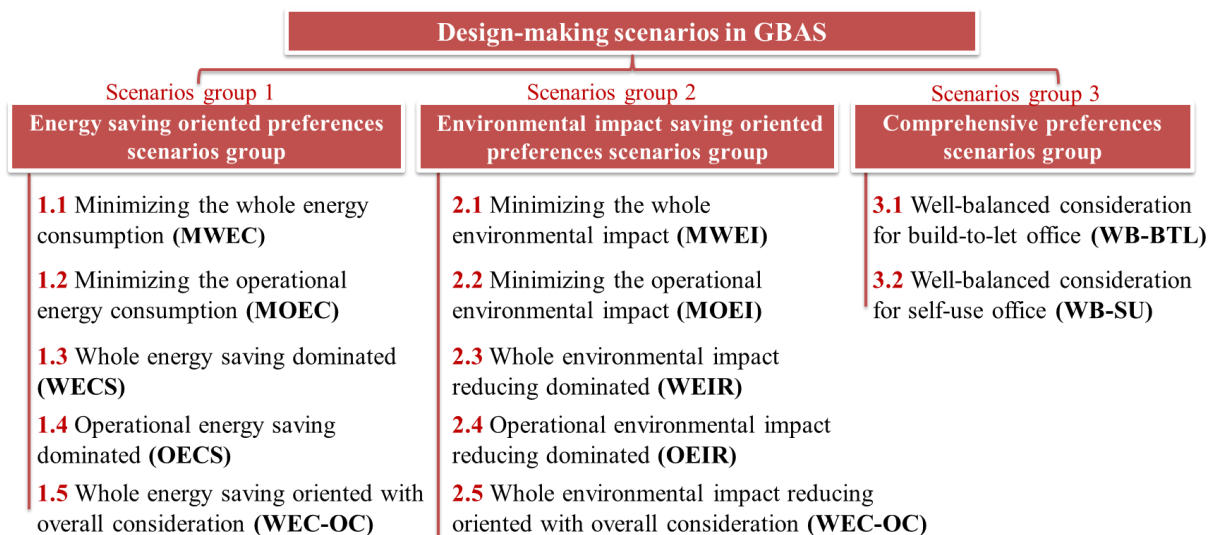


Figure 6.2: The scenarios group and scenarios in GBAS

**Energy saving oriented preference scenarios group (Group1):**

5 designer`s preferences scenarios are involved group 1, they are described in Table 6.1. Two optimized design solutions (ODS) will be generated from 1.3(WECS) and 1.4(OECS), to represent the differences between general office building and the high-grade office buildings with adequate investments. Also, apart from the ODS, 2 reference design solutions (RDS) will be given from the 1.5 WEC-OC to provide additional information to decision-makers.

Table 6.1: The Energy saving oriented preferences scenarios group

Group 1: Energy saving oriented preference scenarios group		
Preferences scenarios	Decision-maker`s preferences	Output
1.1 Minimizing the whole energy consumption (MWECE)	Designer prefers to exploit the full potentialities of energy saving in the whole life-cycle of a building.	ODS1.1
1.2 Minimizing the operational energy consumption (MOEC)	Designer prefers to exploit the full potentialities of energy saving in the operational stage of a building	ODS1.2
1.3 Whole energy saving dominated (WECS)	Designer prefers to maximize energy saving while enabling a certain feasibility level in design practice. It is suitable for <b>(1)</b> the region that has a strict building energy saving policy and an eco-material application incentive policy; <b>(2)</b> The designer is willing to claim points from “materials and resources” category of LEED/BREEAM	ODS1.31 for <u>general office building</u> ; ODS1.32 for <u>high-grade office building</u> with adequate initial investment
1.4 Operational energy saving dominated (OECS)	Designer prefers to maximize operational energy saving while enabling a certain feasibility level in design practice. It is suitable	ODS1.41 for <u>general office building</u> ;

	for the region that has a strict building operational energy saving policy but no overall society energy reducing / eco-material application policies are available	ODS1.42 for <u>high-grade office building</u> with adequate initial investments.
1.5 Whole energy saving oriented with overall consideration (WEC-OC)	Designer prefers the building to meet the building energy saving standard. Only considering other criteria as long as the energy consumption is low enough.	ODS1.5 RDS1.51 RDS1.52

### **Environmental impact oriented preference scenarios group (Group2):**

5 designer`s preferences scenarios are involved group 2, they are described in Table 6.2.

The same principle is applied to each preference scenario as shown in group 1.

Table 6.2: The Environmental impact oriented preferences scenarios group

<b>Group 2: The Environmental impact oriented preference scenarios group</b>		
<b>Preferences scenarios</b>	<b>Decision maker`s preferences</b>	<b>Output</b>
2.1 Minimizing the whole environmental impact (MWEI)	Designer prefers to exploit the full potentialities of environmental impact reducing in the whole life-cycle of a building.	ODS2.1
2.2 Minimizing the operational environmental impact (MOEI)	Designer prefers to exploit the full potentialities of environmental impact reducing in the operational stage of a building	ODS2.2
2.3 Whole environmental impact reducing dominated (WEIR)	Designer prefers to minimize the environmental impact while enabling a certain feasibility level in design practice. It is suitable for <b>(1)</b> building projects under strict long-term environmental protection policies; or <b>(2)</b> for designers with the research purpose of exploring the environmental protection potentialities.	ODS2.31 for <u>general office building</u> ; ODS2.32 for <u>high-grade office building</u> with an adequate initial investment
2.4 Operational environmental impact reducing dominated (OEIR)	Designer prefers to minimize the building operational environmental impact while enabling a certain feasibility level in design practice. It is suitable for the region that has a strict environmental protection policy on building operations rather than the overall social environmental impact.	ODS2.41 for <u>general office building</u> ; ODS2.42 for <u>high-grade office building</u> with an adequate initial investment
2.5 Whole environmental impact reducing oriented with overall consideration (WEC-OC)	Designer prefers the building to meet the building environmental protection standards. Only considering other criteria as long as the environmental impact is low enough.	ODS2.5 RDS2.51 RDS2.52

### **Comprehensive preference scenario group (group3):**

2 designer`s preferences scenarios are involved group 3, they are described in Table 6.3.

The same principle is applied to each preference scenario as to group 1.

Table 6.3: The comprehensive considered preference scenarios group

Group 3: The comprehensive preference scenario group		
Preferences scenarios name	Decision maker`s preferences	Output
3.1 Well-balanced consideration for build-to-let offices (WB-BTL)	Designer prefers to minimize the whole life-cycle energy consumption, whole environmental impact and initial cost as having the same importance	OSD3.1
3.2 Well-balanced consideration for self-use office (WB-SU)	Designer prefers to minimize the whole life-cycle energy consumption, whole environmental impact and whole life-cycle cost as having the same importance	OSD3.2

### 6.3 The methodology of green building design assessment and selection

#### 6.3.1 The overall methodology for green building design assessment and selection.

To select the appropriate office building design solution for each decision maker`s preferences scenario, GBAS is developed by using the TOPSIS based method with the help of the varying weighting system that reflects the preferences of scenarios. The varying weight is determined by the AHP technique using the relative importance among different criteria.

The possible office building design solutions are the input of **the TOPSIS based process, in which the performances of each design solution are assessed by their geometric distance from “best” and “worst” points in the coordinating system. Meanwhile, different weights are assigned to the criteria in TOPSIS to reflect the designer`s willingness for each preference scenario. The weights are generated by an AHP method based on the feedback from expert surveys.** By using the TOPSIS method, the appropriate design solutions for each preference scenario will be selected from the vast number of possible design solutions. The overall method for design solution assessment and selection in GBAS can be seen in Figure 6.3.

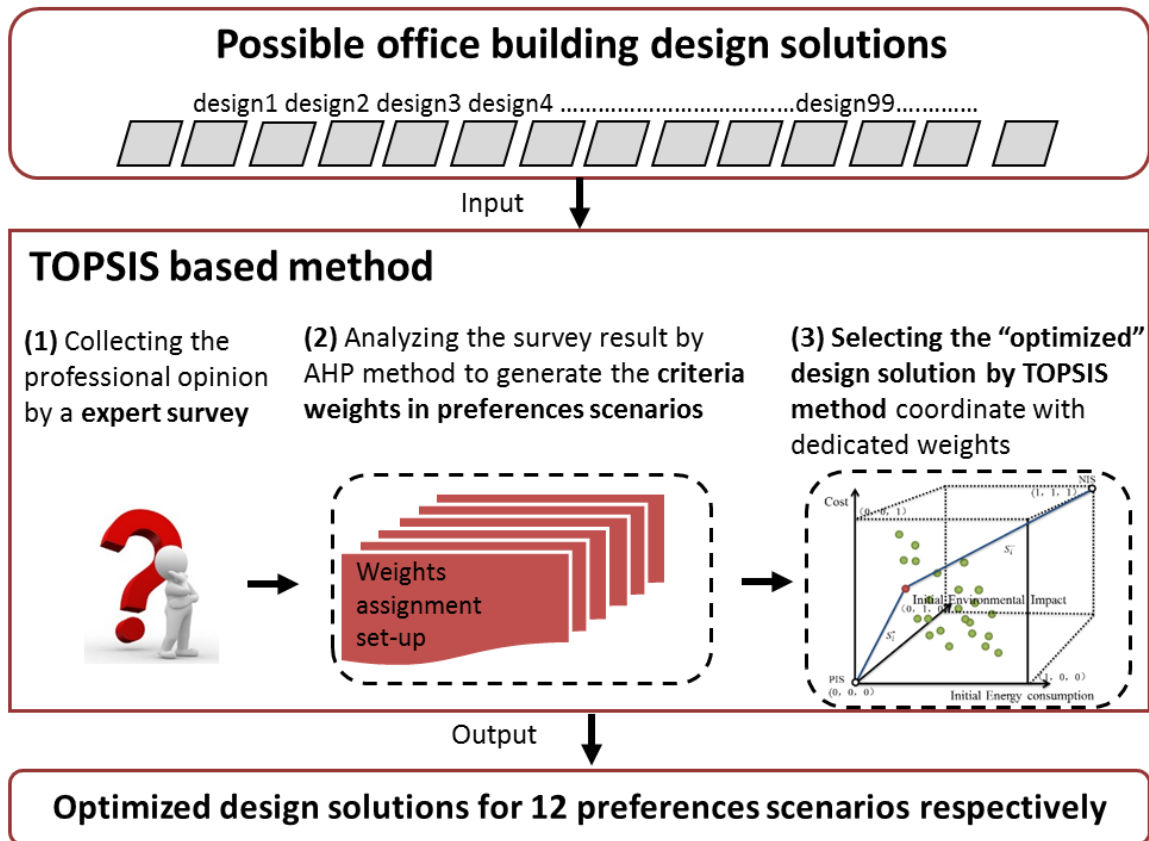


Figure 6.3: The overall method for design solution assessment and selection in GBAS

### 6.3.2 The principle of the TOPSIS based method in the GBAS

The TOPSIS (the technique for order of preference by similarity to ideal solution) is a multi-criteria decision analysis approach, which was originally developed by Hwang and Yoon in 1981 [179]. The TOPSIS is based on the concept that the chosen alternative should have the shortest geometric distance from the positive ideal solution (PIS) and the longest geometric distance from the negative ideal solution (NIS). The GBAS `s design solution selection process is described below:

Assuming that  $m$  design solutions (the number will be far more than 4 in practice) were prepared and the  $n$  criteria are considered in the assessment.  $X_{ij}$  is the value for criteria  $j$  in solution  $i$ , then, the solution matrix  $V$  can be seen in matrix 6.1.

$$V = \begin{bmatrix} X_{11} & X_{12} & \dots & X_{1n} \\ X_{21} & X_{22} & \dots & X_{2n} \\ \dots & \dots & \dots & \dots \\ X_{i1} & \dots & X_{ij} & \dots \\ \dots & \dots & \dots & \dots \\ X_{m1} & X_{m2} & \dots & X_{m} \end{bmatrix} \tag{5.1}$$

By using Eq. 6.2, the units of each criterion are removed and a normalized decision matrix  $V'$  6.3 can be calculated and listed below. According to normalizing process, all criteria's value are converted to a figure between 0 and 1 while the original ranking remains.

$$X'_{ij} = X_{ij} / \sqrt{\sum_{i=1}^m x^2_{ij}} \quad i = 1, 2, \dots, m, \quad j = 1, 2, \dots, n \quad (6.2)$$

$$V' = \begin{bmatrix} X'_{11} & X'_{12} & \dots & X'_{1n} \\ X'_{21} & X'_{22} & \dots & X'_{2n} \\ \dots & \dots & \dots & \dots \\ X'_{i1} & \dots & X'_{ij} & \dots \\ \dots & \dots & \dots & \dots \\ X'_{m1} & X'_{m2} & \dots & X'_{mn} \end{bmatrix} \quad (6.3)$$

Assuming that there's a positive ideal solution (PIS)  $V^* = (V^*_1, V^*_2, \dots, V^*_n)$  and a negative ideal solution (NIS)  $V^- = (V^-_1, V^-_2, \dots, V^-_n)$  that reflects the best and worst solutions respectively. For any design solution, the separation from the PIS and NIS, represent by  $S_i^*$  and  $S_i^-$  respectively, are calculated using the geometrical distance equations, which are shown as follows:

$$S_i^* = \sqrt{\sum_{j=1}^n w_j (V'_{ij} - V_j^*)^2} \quad i = 1, 2, \dots, m \quad (6.4)$$

$$S_i^- = \sqrt{\sum_{j=1}^n w_j (V'_{ij} - V_j^-)^2} \quad i = 1, 2, \dots, m \quad (6.5)$$

Where,  $W_j$  is the weight for criteria  $j$ , which is calculated respectively for different preferences scenarios to reflects the design's preferences and willingness. The method of weight assignment is illustrated in Section 6.3.3.

As all criteria in this research have negative values that need to be minimized to achieve the optimal design solution (ODS) (e.g. the less energy consumption the better), the PIS can be set as  $V^* = (0, 0, 0, \dots, 0)$ , and the NIS can be set as  $V^- = (1, 1, 1, \dots, 1)$ .

Finally, the selection of the ideal solution  $k$  can be calculated using Eq. 6.6. The solution  $k$ , with smallest  $C_i^*$ , is the most optimized design solution (ODS) for the specific designer's preferences scenarios.

$$\begin{cases} C_k^* = \min\{C_i^*\} \\ C_i^* = S_i^* / (S_i^* + S_i^-) \end{cases} \quad (6.6)$$

An example is provided to illustrate the solution selection process of the GBAS. Assuming that 24 design solutions (the number will be far more than 4 in practice) were prepared and the criteria applied are the initial energy consumption (C1), initial environmental impact (C2) and initial cost (C3), which are already catered for through specialized computing models. The designer's preference 1 has the balanced consideration to all criteria; whereas the designer's preference 2 mainly focuses on C1. The weight for criteria and criteria for each solution are presented in Table 6.4.

Table 6.4: Weight of criteria and criteria for each solution

Design options	C1 (Mwh/m2)	C2 (k PE/m2)	C3 (k £/m2)
Weight for designer's preferences 1	$W_1=1$	$W_2=1$	$W_3=1$
Weight for designer's preferences 2	$W_1=5$	$W_2=2$	$W_3=1$
Solution 1	120	4050	2.4
Solution 2	150	4200	1.9
....	....	....	....
Solution 24	110	3020	2.7

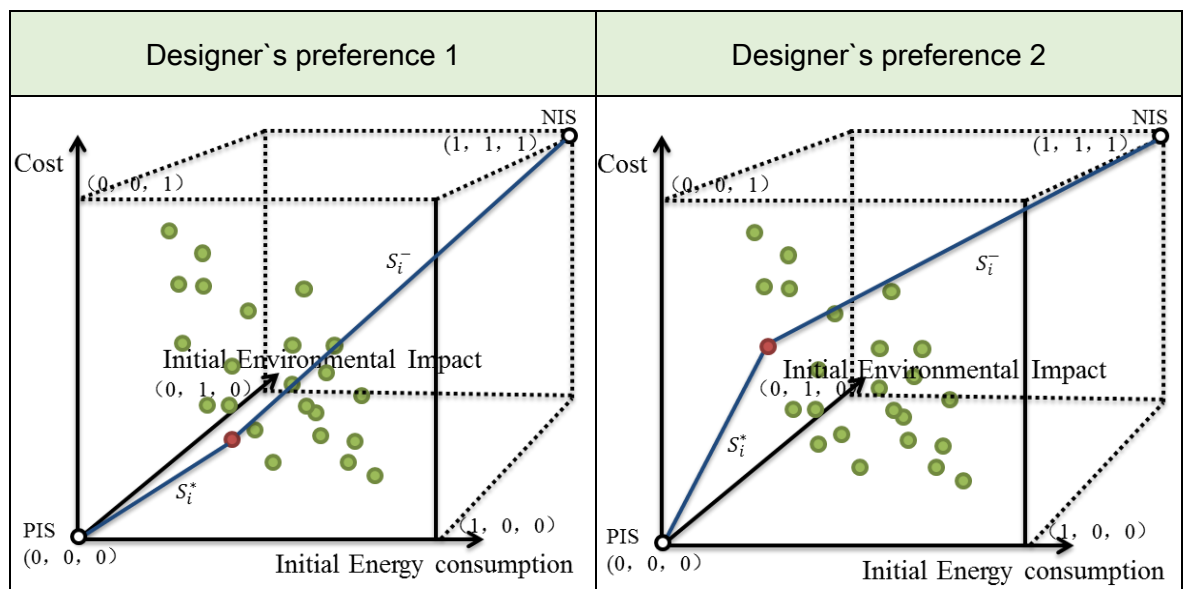


Figure 6.4: 3-dimension coordination systems of the GBAS for the two designers' preferences.

The matrix for criteria can be established and the geometric distance between the PIS and NIS can be computed using Eqs 6.1 to 6.5. As shown in Figure 6.4, all the design

solutions can be observed in a c; each is represented by a point, while the  $S_i^*$  and  $S_i^-$  are indicated by the blue lines. From the calculation using the Eq. 6.6, it is shown that the red point has the smallest  $C_i^*$ , and thus the design solution represented by the red point is considered the optimized solution according to the designer's preference.

According to the effect of weight assignment, the optimized solutions for two different designers' preferences can reflect the designers' willingness. Thus, the weight assignment is very important to exactly reflect the preference scenarios. The method for an appropriate weight assignment for 7 preference scenarios is discussed in Section 6.3.3 below.

### **6.3.3 The weight assignment method for “subjective” preference scenarios by an expert survey and AHP method.**

To use TOPSIS based method in this research, the weights in each preference scenarios are recognized by the method below:

**For all “objective” preferences** including 1.1-MWEC, 1.2-MOEC, 2.1-MWEI and 2.2-MOEI, there is the one and the only clear and definite criterion to optimize (minimize or maximize). In this case weight assignment for those “objective” scenarios is not needed.

**However, for the “subjective” preference scenarios** including 1.3-WECS, 1.4-OECS, 1.5-WEC-OC, 2.3-WEIR, 2.4-OEIR, 2.5-WEI-OC, 3.1-WB-BTL and 3.2-WB-SU, more than one criteria are included. In this case, extra consideration for the weight assignment is needed.

**In order to generate the rational weights for those above the “subjective” scenarios, professional options are collected through expert surveys and processed using the AHP based method.**

**The expert selection:** A total of 24 building experts are selected and invited to participate in this research, including 6 building owners / shareholders, 6 architects (2



LEED AP), 6 MEP engineers (3 LEED AP), 3 building environment researchers and 3 end user / occupant representatives (if not the owners). The expertise of these people who are the investors, designers and end users are able to cover the key processes of the green building design and operation.

**The questionnaire design:** A questionnaire is designed to collect the experts` opinions. The full set of questions (8 pages) for all the preference scenarios are included in Appendix 2. The principle and relative emphasis of each preference scenario are clearly described to the experts. Based on the full understanding of the target and usage of each preference scenario, 3 key criteria that are largely relevant to the key performance and can reflect the purpose of this scenario need to be selected by the experts. The judgment for pair-wise comparison importance within the key criterion is required and the results are thus generated and recorded in the provided tables separately for each preference scenario. An example pilot questionnaire is provided in Figure 6.5 (only illustrate the example pages).

Dear Sir / Madam,

This questionnaire is used for a research on green building design optimization, carried out by PhD candidate Zishang Zhu in University of Hull. Your expertise and professional opinion is quite precious and valuable. Thank you very much for your time.

**Part 1: Personal information** (You can ignore the optional questions if concerning privacy)

Name (optional): Miss Gao Organization (optional): CABR

Organization status (tick):  
 Industrial / Company     Education     Research institute  
 Other: None

Occupation/position (tick):  
 Architect     MEP Engineer  
 Building owner / shareholder / investor     Building occupant / tenant only

Do you have experience or certificate on green building design/operation?  
 Yes     No

If yes, how many year experience do you have? 4

Type of certificate: Work on LEED certified certificate

**Part 2: Subjective judgment for 10 building design scenario**

The following tables (table 1 - table 10) are prepared respectively for different green building design preference scenario, each design preference scenario is set to achieving dedicate design purpose. For each table, could you please select no more than 3 key criterion (from options below) that you believe significantly relevant to the key performance and purpose of this preference scenario? The selection should base on the aim and usage scenario of each preference scenario that described in each table.

After select the key criterion, please judge the importance among each criteria for specific scenario. Please use the fundamental verbal scale 1 to 9 (see table 11) to representing the pairwise importance.

Table 3

Preference scenarios 3: Operational energy consumption saving dominated scenarios A									
Preference scenarios description									
Principle: This scenario mainly focus on building energy consumption in building's operational stage. The optimized design solutions should contribute to maximized operational energy saving meanwhile keep certain feasibility level in real design practice.									
Purpose of building: The building will be used as general office building for investor /owner self-use or build-to-let purpose.									
Policy and other consideration: This scenario is for building site that have strict building energy saving policy, but no social energy reducing / eco-material application policy available.									
Key criterion (pick from A to I)	Criteria 1			Criteria 2			Criteria 3		
	A11	A12	A13	A21	A22	A23	A31	A32	A33
Pairwise criterion importance	1	5	7	0.2	1	2	0.14	0.5	1

Table 4

Preference scenarios 4: Operational energy consumption saving dominated scenarios B									
Preference scenarios description									
Principle: This scenario mainly focus on building energy consumption in building's whole life-cycle. The optimized design solutions should contribute to maximized energy saving meanwhile keep certain feasibility level in real design practice.									
Purpose of building: The building is a high-grade office building with relative high investment budget. No limit for owner self-use or building-to-let purpose.									
Policy and other consideration: This scenario is for building site that have strict building energy saving policy, but no social energy reducing / eco-material application policy available.									
Key criterion (pick from A to I)	Criteria 1			Criteria 2			Criteria 3		
	A11	A12	A13	A21	A22	A23	A31	A32	A33
Pairwise criterion importance	1	1	7	0.2	1	3	0.14	0.33	1

Figure 6.5: The example pages of the questionnaire

The experts` subjective judgment for pair-wise importance is assigned in the form of importance scores ranging from 1 to 9, based on the common fundamental verbal scale [167] shown in Table 6.5.

Table 6.5: Fundamental verbal scale for pair-wise importance

Importance	Definition	Explanation
1	Equally important	Two activities contribute equally to the objective
2	Weakly or slightly important	
3	Moderately more important	Experience and judgment slightly favour one activity over another
4	Moderately plus important	
5	Strongly important	Experience and judgment strongly favour one activity over another
6	Strongly plus important	
7	Very strong or demonstrably important	An activity is favoured very strongly over another; its dominance demonstrated in practice
8	Very, very strongly important	
9	Absolutely or extremely important	The evidence favouring one activity over another is the highest possible order of affirmation

### Data processing using the AHP method:

Similar to the AHP method addressed in Chapter 5, the refined AHP process in the GBAS for weight generation is as follows: **(1)** Based on professional judgment, a criterion importance comparison matrix will be established and normalized; **(2)** its consistency will be tested by calculating its eigenvalue [166]; and **(3)** the priority ranking (weight) can be derived by computing its eigenvector [166].

By using the above-illustrated method, the expert survey feedback is analyzed by using the AHP. The weight set-up for each reference scenario is generated and described in Section 6.3.

### 6.4 Weight assignment for the energy consumption saving oriented preference scenarios

#### (Group 1).

There are five scenarios considered in this group. They are: minimized overall energy consumption (1.1-MWEC), minimized operational energy consumption (1.2 - MOEC), the overall energy saving (1.3-WECS), the operational energy saving (1.4-OECS) and the overall energy saving oriented with an overall consideration (1.5-WEC-OC). The weight assignments for different scenarios are discussed respectively as follows:

#### 6.4.1 The reliability testing to the survey results.

To ensure the reliability of the survey results, the Cronbach's alpha values of the survey results are tested using SPSS 20 for the survey feedback of each question. Their Cronbach's alpha responses are all above 0.7 and the overall Cronbach's alpha is 0.77, which gives an acceptable internal consistency according to the common rule of the psychometrics theory [180]. The survey results analysis and weight assignment for each preference scenario are then discussed respectively in Section 6.3.

#### 6.4.2 Weight assignment for “subjective” scenarios: 1.1-MWEC and 1.2-MOEC

For 1.1 - Minimizing whole energy consumption and 1.2 - Minimizing operational energy consumption preference scenarios, the decision-maker would like to exploit the full potentialities of energy saving for the whole life-cycle or operational stage of a building.

**For 1.1 - MWEC**, only the whole life-cycle energy consumption criterion (C1) is considered, thus the solution selection becomes a simple one criteria ranking problem, the optimized design solution (ODS)  $k$  can be selected by using Eq. 6.7.

$$C1_k = \min \{ C1_i \} \quad (6.7)$$

**For 1.2 - MOEC**, only the operational energy consumption criterion (C1.2) is considered. The ODS selection method is expressed as follows:

$$C1.2_k = \min \{ C1.2_i \} \quad (6.8)$$

#### 6.4.3 Weight assignment for the “objective” scenarios: 1.3-WECS and 1.4-OECS

The 1.3 “Whole energy consumption saving dominated” scenario and the 1.4 “Operational energy consumption saving dominated” scenario mainly focus on building energy consumption in the whole life-cycle and operational stage respectively. For each scenario, two ODSs will be generated, namely, 1.31 - WECS and 1.32 - WECS, 1.41 -

OECS and 1.42-OECS respectively. The weights used in the TOPSIS for each ODS are generated by expert survey results coordinated with an AHP method described below.

**Step 1 - the key criteria that are largely relevant to the key performance and purpose of this scenario are selected by experts.** According to the expert survey, 21 out of 24 experts choose the following criterion, as displayed in Table 6.6, for scenarios 1.3 - WECS and 1.4 - OECS as their key criterion.

Table 6.6: The selected key criteria in 1.3 - WECS and 1.4 - OECS scenarios

Key criterion Selected by expert		Criteria 1	Criteria 2	Criteria 3
<b>1.3 WECS</b>	ODS 1.31	life-cycle energy consumption (C1)	life-cycle environmental impact (C2)	life-cycle cost (C3)
	ODS 1.32	life-cycle energy consumption (C1)	life-cycle environmental impact (C2)	operational cost (C3.2)
<b>1.4 OECS</b>	ODS 1.41	operational energy consumption (C1.2)	life-cycle environmental impact (C2)	life-cycle cost (C3)
	ODS 1.42	operational energy consumption (C1.2)	life-cycle environmental impact (C2)	operational cost (C3.2)

### Step 2 - Analyzing the pair-wise importance among the key criteria

The average importance score of pair-wise comparison from 21 experts for scenarios 1.3-WECS and 1.4-OECS are presented in Table 6.7. For example, in the table A1 - 3.2 represents the comparison importance of C1 to criteria C3.2.

Table 6.7: The pair-wise comparison among criterion for 1.3 - WECS and 1.4 - OECS preference scenarios

ODS	Pairwise comparison	A11	A12	A13	A21	A22	A23	A31	A32	A33
<b>1.31</b>	Importance value	1	4.9	6.6	0.2	1	3	0.14	0.32	1
	Pairwise comparison	A11	A12	A1 (3.2)	A21	A22	A2 (3.2)	A (3.2) 1	A (3.2) 2	A (3.2) (3.2)
<b>1.32</b>	Importance value	1	5	7.2	0.2	1	3.1	0.14	0.32	1
	Pairwise comparison	A(1.2) (1.2)	A(1.2) 2	A(1.2) 3	A2(1.2)	A22	A23	A3(1.2)	A32	A33
<b>1.41</b>	Importance value	1	4.9	6.6	0.2	1	3	0.14	0.32	1
	Pairwise comparison	A(1.2) (1.2)	A(1.2) 2	A(1.2) (3.2)	A2(1.2)	A22	A2 (3.2)	A (3.2) (1.2)	A (3.2) 2	A (3.2) (3.2)

1.42	Importance value	1	5	7.2	0.2	1	3.1	0.14	0.32	1
------	------------------	---	---	-----	-----	---	-----	------	------	---

It is worth noting that owing to the similarity between the 1.3 WECS and 1.4 OECS (the only difference is that 1.4 - OECS using C1.2 operational energy consumption rather than the C1 whole life-cycle energy consumption), the average importance score distribution for 1.4 - OECS are the same as 1.3 - WECS.

### Step 3 - generation of the criteria's weights for each ODS in 1.3-WECS and 1.4-OECS scenarios

According to the AHP method, the following steps are carried out to generate the weight for each ODS. **(1)** The pair-wise comparisons of the average importance value are converted into comparison matrices; **(2)** Their consistency ratios (CR) are tested, leading to less than 10% of discrepancy; **(3)** the weights for the three criteria are obtained by computing the eigenvector solution. For the final eigenvector, the absolute value of differences rate ( $\epsilon$ ) between sums in the two consecutive calculations is checked until it is less than 1%.

The calculation results for 1.3 - WECS and 1.4 - OECS are presented in Table 6.8, including the values for the consistency ratio (CR), the differences rate ( $\epsilon$ ) and weight of criteria. In the table, the contents between parentheses are for 1.4 OECS scenarios.

Table 6.8: Weight assignment for 1.3 WECS and 1.4 OECS scenarios

ODS 1.31 / (ODS 1.41)	CR	Eigenvalue=3.12; $CR =  (3.12 - 3)/(3 - 1) / 0.58  = 7.0\% < 10\%$		
	E	Iteration times = 2; $\epsilon = 0.04\%$		
	Criteria	C1	C2	C3 / (C3.2)
	Weight	72.33%	19.28%	8.39%
ODS 1.32 / (ODS 1.42)	CR	Eigenvalue=3.11; $CR =  (3.11 - 3)/(3 - 1) / 0.58  = 6.5\% < 10\%$		
	$\epsilon$	Iteration times = 2; $\epsilon = 0.04\%$		
	Criteria	C1 / (C1.2)	C2	C3.2
	Weight	73.21%	18.91%	7.88%

The results show that, in both scenarios the experts would like to put the minimization of

the building's energy consumption (C1 / C1.2) as the top priority and treat the environmental impact (C2) as secondary. Meanwhile, they give a certain consideration to the building's cost (C3 / C3.2) in order to prevent the solution with the excessive cost.

**Step 4 - The weights are assigned into the TOPSIS method and the equation for ODS derivation is given.** According to the TOPSIS method, by assigning the weight to Eqs 6.4 to 6.6, the ODSs generated in 1.3 - WECS and 1.4 - OECS scenarios can be selected by calculating the  $C_i^*$ . The mathematic Eqs 6.9- 6.12 for the OSDs selection is generated below.

**For the OSD1.31**, the design solution  $k$ , with the smallest  $C_i^*$ , is the OSD1.31 for the preference scenario 1.3 - WECS.

$$\begin{cases} C_k^* = \min \{C_i^*\} \\ C_i^* = \frac{\sqrt{0.7233V'_{i,C1}{}^2 + 0.1928V'_{i,C2}{}^2 + 0.0839V'_{i,C3}{}^2}}{\sqrt{0.7233V'_{i,C1}{}^2 + 0.1928V'_{i,C2}{}^2 + 0.0839V'_{i,C3}{}^2} + \sqrt{0.7233(V'_{i,C1} - 1)^2 + 0.1928(V'_{i,C2} - 1)^2 + 0.0839(V'_{i,C3} - 1)^2}} \end{cases} \quad (6.9)$$

**For OSD - 1.32**, the design solution  $k$ , with the smallest  $C_i^*$ , is the OSD - 1.32 for preference scenario 1.3 - WECS.

$$\begin{cases} C_k^* = \min \{C_i^*\} \\ C_i^* = \frac{\sqrt{0.7233V'_{i,C1}{}^2 + 0.1928V'_{i,C2}{}^2 + 0.0839V'_{i,C3.2}{}^2}}{\sqrt{0.7233V'_{i,C1}{}^2 + 0.1928V'_{i,C2}{}^2 + 0.0839V'_{i,C3.2}{}^2} + \sqrt{0.7233(V'_{i,C1} - 1)^2 + 0.1928(V'_{i,C2} - 1)^2 + 0.0839(V'_{i,C3.2} - 1)^2}} \end{cases} \quad (6.10)$$

**For OSD - 1.41**, the design solution  $k$ , with the smallest  $C_i^*$ , is the OSD1.41 for preference scenario 1.4 - OECS.

$$\begin{cases} C_k^* = \min \{C_i^*\} \\ C_i^* = \frac{\sqrt{0.7233V'_{i,C1.2}{}^2 + 0.1928V'_{i,C2}{}^2 + 0.0839V'_{i,C3}{}^2}}{\sqrt{0.7233V'_{i,C1.2}{}^2 + 0.1928V'_{i,C2}{}^2 + 0.0839V'_{i,C3}{}^2} + \sqrt{0.7233(V'_{i,C1.2} - 1)^2 + 0.1928(V'_{i,C2} - 1)^2 + 0.0839(V'_{i,C3} - 1)^2}} \end{cases} \quad (6.11)$$

**For OSD - 1.42**, the design solution  $k$ , with the smallest  $C_i^*$ , is the OSD1.41 for preference scenario 1.4 OECS.

$$\begin{cases} C_k^* = \min\{C_i^*\} \\ C_i^* = \frac{\sqrt{0.7233V'_{i,C1.2}{}^2 + 0.1928V'_{i,C2}{}^2 + 0.0839V'_{i,C3.2}{}^2}}{\sqrt{0.7233V'_{i,C1.2}{}^2 + 0.1928V'_{i,C2}{}^2 + 0.0839V'_{i,C3.2}{}^2 + \sqrt{0.7233(V'_{i,C1.2} - 1)^2 + 0.1928(V'_{i,C2} - 1)^2 + 0.0839(V'_{i,C3.2} - 1)^2}}} \end{cases} \quad (6.12)$$

Where:  $K$  is the optimized design solution in solutions set;  $V'_{i, c1}$ ,  $V'_{i, c2}$ ,  $V'_{i, c3}$  and  $V'_{i, c1.2}$ ,  $V'_{i, c3.2}$  are the normalized value of criteria C1, C2, C3 and C1.2, C3.2 respectively for design solution  $i$  in the solutions set.

#### 6.4.4 Weight assignment for the 1.5 WEC-OC scenario:

The 1.5 “Whole energy consumption saving oriented with overall consideration” preference scenario focuses on the whole life-cycle energy saving with an overall consideration, but other criteria are considered only if the building design solution has already met the building energy saving standards. The continuous variable weights are applied to the criteria in order to reflect their continuous changing importance during the changing of the design solution’s energy saving performance. This scenario will determine the design option that can meet the building’s energy standards first, thus achieving other performances as high as possible.

**Key criteria are directly assigned as the same as the 1.31 WECS:** Because this scenario is also mainly for whole life-cycle energy saving, which is the same as the 1.31 - WECS scenario. Thus, in the survey the same key criteria are given to building expert for importance judgment. The key criteria are the whole life-cycle energy consumption (C1), whole life-cycle environmental impact (C2) and whole life-cycle cost (C3). Besides, although the operational energy consumption (C1.2) is not the key criterion, it is also monitored as the indicator of energy saving performance of each design solution, in order to judge the continuous variable weights of key criterion.

#### **The continuous variable weights of the key criteria are separated into three phases.**

Based on the building’s energy performance (indicated by the operational energy consumption (C1.2)), the weights are defined in three phases:

Phase A: The operational energy consumption (C1.2) is better (lower) than the dedicated lower-point of green building standards requirement;

Phase B: The C1.2 is just between the dedicated higher-point and lower-point of green building standards requirement;

Phase C: The C1.2 is worse (higher) than the dedicated higher-point of green building standards requirement.

Defining the higher-point and lower-point for separation of phases. The higher-point and lower-point are defined corresponding to the updated building energy standard, namely the “Standard for Energy Consumption of Buildings” [181], in which the mandatory energy consumption limitation and suggested energy consumption value are provided for office buildings and used as the higher-point and lower-point in this research. The higher-point and lower-point definition for different regions in China are presented in Table 6.9.

Table 6.9: The higher-point and lower-point definition for different regions in China

<b>Climate Zones</b>	<b>Higher-point</b> (Mandatory energy consumption limitation)	<b>Lower-point</b> (Suggested energy consumption)
Severe cold & Cold Exp. Beijing, Tianjin	80 (kWh/m <sup>2</sup> -year)	60 (kWh/m <sup>2</sup> -year)
Hot summer cold winter Exp. Shanghai, Nanjing	110 (kWh/m <sup>2</sup> -year)	80 (kWh/m <sup>2</sup> -year)
Hot summer warm winter Exp. Guangzhou, Shenzhen	100 (kWh/m <sup>2</sup> -year)	75 (kWh/m <sup>2</sup> -year)

Only those design solutions with C1.2 within phase B (just meeting the green building standard) are considered in the ODS selection. However, the two reference design solutions (RDSs) in phases A and C are still discussed in order to provide some useful information.

**Weight assignment for design solutions with C2.1 within phase A.** As the operational energy consumption for design solutions have already been better (lower) than the lower-point (e.g. lower than 80 kWh/m<sup>2</sup>-year in Shanghai), the importance level



of C1 is no longer the first priority. The weight for C1, C2 and C3 are judged by 24 experts, and analyzed by AHP method as described above. The average importance values of the pair-wise importance among key criterion are presented in Table 6.10, and the consistency ratio (CR), differences rate ( $\epsilon$ ) and weights are generated in Table 6.11.

Table 6.10: The pair-wise comparison among criteria in the 1.5 WEC-OC scenario

1.5 WEC-OC	Pair-wise comparison	A11	A12	A13	A21	A22	A23	A31	A32	A33
	Importance value	1	0.217	0.233	4.6	1	1.2	4.3	0.83	1

Table 6.11: Weight assignment for 1.5 WEC-OC scenarios

1.5 WEC-OC	CR	Eigenvalue=3.01; $CR =  (3.01 - 3)/(3 - 1) / 0.58  = 5.7\% < 10\%$		
	$\epsilon$	Iteration times = 2; $\epsilon = 0.03\%$		
	Criteria	C1	C2	C3
	Weight	10.07%	46.19%	44.74%

As the weights for C2 and C3 are similar, to simplify the calculation, the weights of 10%, 45%, and 45% are assigned to C1, C2 and C3 respectively.

**Weight assignment for design solutions with C2.1 within phase C.** For design solution with C2.1 higher (worse) than the higher-point (e.g. higher than 110 kWh/m<sup>2</sup>-year in Shanghai), the minimization of C1 is the one and only aim. In this case, the weights for C1, C2 and C3 are 100%, 0% and 0% respectively.

**Weight assignment for design solutions with C2.1 within phase B.** As the energy consumption of design solutions in this phase have already met the green building standard's mandatory requirement, this is still worse than the suggested value (e.g. between 80-110 kWh/m<sup>2</sup>-year in Shanghai), more attention will be given to the environment (C2) and cost (C3) criterion..

Thus, when selecting the ODS, the importance of C1 will be decreased with the decrease in C2.1. Meanwhile, the importance level of C2 and C3 will increase with the decrease in C1.

The changeable weight of C1 in phase B ( $w_{c1, B}$ ) is linear and can be computed by Eq. 6.13 below; meanwhile the weight for C2 ( $w_{c2, B}$ ) and C3 ( $w_{c3, B}$ ) in phase B are the same, both linearly changed with the opposite trend of C1`and given in Eq. 6.14.

$$w_{c1, B} = 100\% - \frac{E_{Hi} - OPE}{E_{Hi} - E_{Lo}} * (w_{c1, C} - w_{c1, A}) \tag{6.13}$$

$$w_{c2, B} = w_{c3, B} = (100\% - w_{c1, B})/2 \tag{6.14}$$

Where,  $E_{Hi}$  is the mandatory energy consumption value for a specific climate zone (addressed in Table 6.9);  $E_{Opt}$  is the specific design option`s operational energy consumption (C2.1);  $E_{Lo}$  is the suggested energy consumption value for a specific climate zone (addressed in Table 6.9);  $w_{c1, A}$  and  $w_{c1, C}$  is C1`s weight in phase A and phase C, in this case  $w_{c1, C}=100\%$  and  $w_{c1, A}=10\%$ .

**Overall, the continuous variable weights for criteria in scenario 1.5 WEC-OC are illustrated in Figure 6.6 to 6.8.**

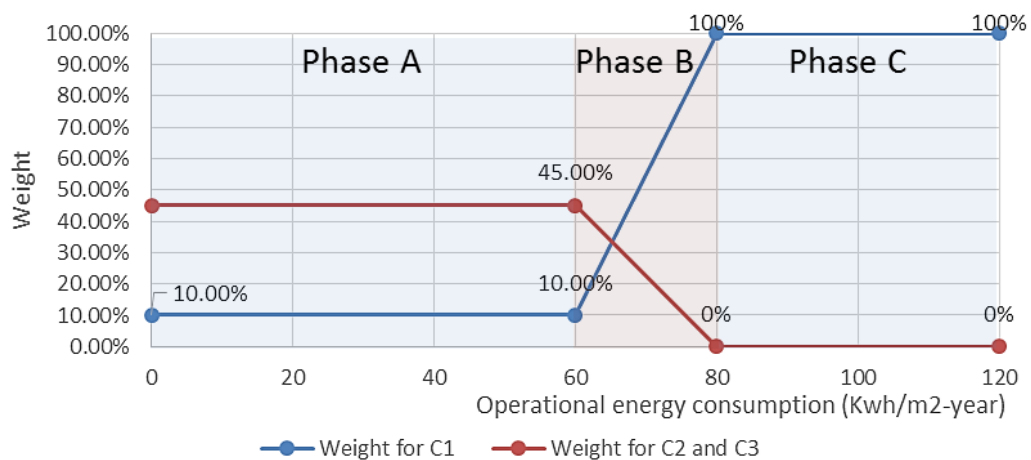


Figure 6.6: Variable weight for severe cold & cold climate zones

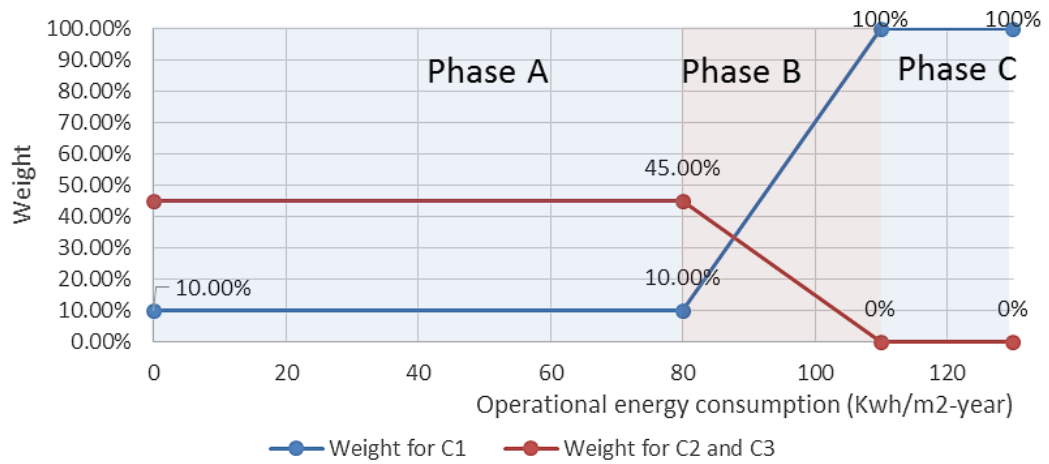


Figure 6.7: Variable weight for hot summer cold winter climate zone

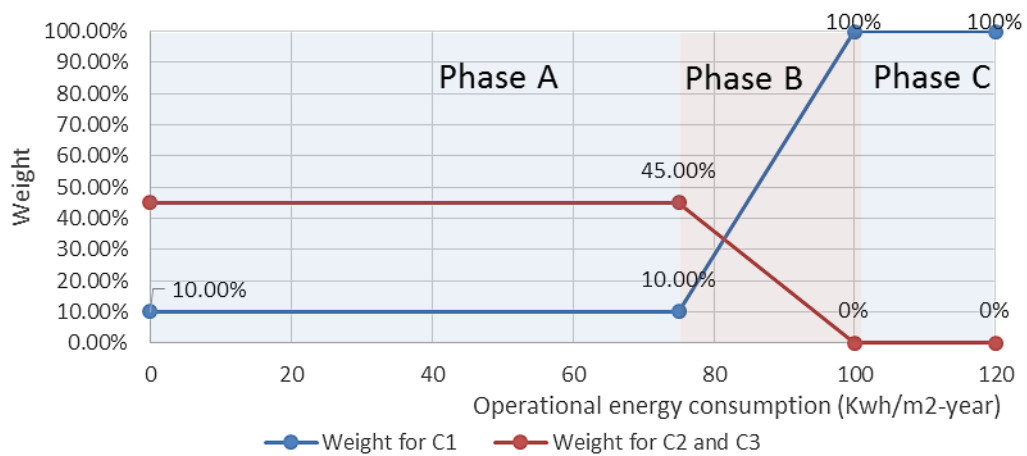


Figure 6.8: Variable weight for hot summer warm winter climate zone

By assigning weights into Eqs. 6.4 to 6.6, the mathematical equation for ODS derivation is generated, as well as the reference design solutions (RDS1.51 and RDS1.52).

**For OSD1.5**, only the design solutions with C1.2 in Phase B are considered in this selection. The design solution  $k$ , with the smallest  $C_i^*$ , is the ODS1.5 for scenario 1.5WEC-OC:

$$\begin{cases} C_K^* = \min \{C_i^*\} \\ C_i^* = \frac{\sqrt{w'_{C1,B} V'_{i,C1}{}^2 + w'_{C2,B} V'_{i,C2}{}^2 + w'_{C3,B} V'_{i,C3}{}^2}}{\sqrt{w'_{C1,B} V'_{i,C1}{}^2 + w'_{C2,B} V'_{i,C2}{}^2 + w'_{C3,B} V'_{i,C3}{}^2} + \sqrt{w'_{C1,B} (V'_{i,C1} - 1)^2 + w'_{C2,B} (V'_{i,C2} - 1)^2 + w'_{C3,B} (V'_{i,C3.2} - 1)^2}} \end{cases} \quad (6.15)$$

**For RDS1.51**, the design solutions with C1.2 which lies in Phase A are considered in the selection. The design solution  $k$ , with the smallest  $C_i^*$ , is the selected RDS1.51:

$$\begin{cases} C_K^* = \min \{C_i^*\} \\ C_i^* = \frac{\sqrt{0.1V_{i,C1}'^2 + 0.45V_{i,C2}'^2 + 0.45V_{i,C3}'^2}}{\sqrt{0.1V_{i,C1}'^2 + 0.45V_{i,C2}'^2 + 0.45V_{i,C3}'^2} + \sqrt{0.1(V_{i,C1}' - 1)^2 + 0.45(V_{i,C2}' - 1)^2 + 0.45(V_{i,C3.2}' - 1)^2}} \end{cases} \quad (6.16)$$

**For RDS1.52**, the design solutions with C1.2 which lies in Phase C are considered in selection. It becomes a simple single-object minimization problem as criterion C1 has 100% of weight. The design solution  $k$ , with the smallest  $C_i^*$ , is the selected RDS1.52:

$$C1_K = \min \{C1_i\} \quad (6.17)$$

Where:  $K$  is the optimized design solution in solutions set;  $w_{c1, B}$ ,  $w_{c2, B}$  and  $w_{c3, B}$  are the continuous variable weights for criteria C1, C2 and C3 respectively, already calculated by Eqs. 6.13 and 6.14;

## 6.5 Weight assignment for environmental impact reducing oriented scenarios (Group 2)

There are five scenarios involved in this scenarios group. These are (1) the minimization of the whole environmental impact (2.1MWEI), (2) the minimization of the operational environmental impact (2.2MOEI), (3) the whole environmental impact reduction dominated (2.3WEIR), (4) the operational environmental impact reduction dominated (2.4OEIR), and (5) whole environmental impact reduction oriented with an overall consideration (2.5WEI-OC). The principle of scenarios in this group 2 are similar to those in group 1, the only difference in weight assignment is that it is using the environmental impact related criteria instead of energy consumption related criteria.

### 6.5.1 Weight assignment for 2.1-MWEI, 2.2-MOEI, 2.3-WEIR and 2.4-OEIR scenarios:

**For 2.1 - MWEI and 2.2 - MOEI preference scenarios**, the selection of ODS is same as 1.1-MWEC and 1.2-MOEC in the scenarios groups 1, which are actually the simple single-object minimization problem. The ODS is represented by design solution  $k$ , respectively for 2.1-MWEI and 2.2-MOEI and can be selected by using Eqs. 6.18 and

6.19:

$$C2_k = \min\{C2_i\} \quad (6.18)$$

$$C2.1_k = \min\{C2.1_i\} \quad (6.19)$$

**For 2.3-WEIR and 2.4-OEIR preference scenarios**, the selection of ODSs is the same as 1.3-WECS and 1.4-OECS in the scenarios group 1. The professional opinions from expert surveys are analyzed by an AHP method, in order to generate the criterion's weights for the 2 preference scenarios. By using the TOPSIS method using weight, the mathematical equations for the ODSs selection are derived.

According to the expert survey, 21 out of 24 experts chose the following criterion, as displayed in Table 6.12, as the key criterion for scenarios 2.3-WEIR and 2.4-OEIR.

Table 6.12: The selected key criteria in 2.3-WEIR and 2.4-OEIR scenarios

Key criterion Selected by expert		Criteria 1	Criteria 2	Criteria 3
<b>2.3 WEIR</b>	ODS 2.31	life-cycle energy consumption (C1)	life-cycle environmental impact (C2)	life-cycle cost (C3)
	ODS 2.32	life-cycle energy consumption (C1)	life-cycle environmental impact (C2)	operational cost (C3.2)
<b>2.4 OEIR</b>	ODS 2.41	operational energy consumption (C1)	life-cycle environmental impact (C2.2)	life-cycle cost (C3)
	ODS 2.42	operational energy consumption (C1)	life-cycle environmental impact (C2.2)	operational cost (C3.2)

The pair-wise importance among the key criteria from experts' surveys is analyzed by an AHP method. The average importance values are listed in Table 6.13. The consistency ratio (CR), differences rate ( $\epsilon$ ) and weights of criteria can be calculated and the results are presented in Table 6.14.

Table 6.13: The pairwise comparison among criteria in 2.3WEIR and 2.4OEIR scenario

ODS	Pairwise comparison	A11	A12	A13	A21	A22	A23	A31	A32	A33
<b>2.31</b>	Importance value	1	0.2	2.8	4.5	1	6.7	0.3571	0.1492	1
	Pairwise comparison	A11	A12	A1(3.2)	A21	A22	A2(3.2)	A(3.2)1	A(3.2)2	A(3.2)(3.2)
<b>2.32</b>	Importance value	1	0.2	3.5	5	1	7.3	0.143	0.333	1

ODS 2.41	Pairwise comparison	A11	A1(2.2)	A13	A(2.2)1	A(2.2)(2.2)	A(2.2)3	A31	A3(2.2)	A33
	Importance value	1	0.2	2.8	4.5	1	6.7	0.3571	0.1492	1
ODS 2.42	Pairwise comparison	A11	A1(2.2)	A1(3.2)	A(2.2)1	A(2.2)(2.2)	A(2.2)(3.2)	A(3.2)1	A(3.2)(2.2)	A(3.2)(3.2)
	Importance value	1	0.2	3.5	5	1	7.3	0.143	0.333	1

Table 6.14: Weight assignment for 2.3WEIR and 2.4OEIR scenarios

ODS 2.31 / (ODS 2.41)	CR	Eigenvalue=3.02; CR =  (3.04 - 3)/(3 - 1) / 0.58  = 2.4% < 10%		
	E	Iteration times = 2; ε = 0.02%		
	Criteria	C1	C2 / (C2.2)	C3 / (C3.1)
	Weight	19.27%	71.99%	8.74%
ODS 2.32 / (ODS 2.42)	CR	Eigenvalue=3.11; CR =  (3.15 - 3)/(3 - 1) / 0.58  = 8.4% < 10%		
	E	Iteration times = 2; ε = 0.07%		
	Criteria	C1	C2 / (C2.2)	C3.2 / (C3.1)
	Weight	19.53%	73.00%	7.47%

By assigning the weights into the TOPSIS method, the equation for the ODS derivation is given. The mathematical equations for deriving the ODSs are listed as below.

For OSD2.31, the design solution  $k$ , with the smallest  $C_i^*$  in Eq. 6.20, is the ODS2.31:

$$\begin{cases} C_k^* = \min \{C_i^*\} \\ C_i^* = \frac{\sqrt{0.1927V_{i,C1}'^2 + 0.7199V_{i,C2}'^2 + 0.0874V_{i,C3}'^2}}{\sqrt{0.1927V_{i,C1}'^2 + 0.7199V_{i,C2}'^2 + 0.0874V_{i,C3}'^2} + \sqrt{0.1927(V_{i,C1}' - 1)^2 + 0.7199(V_{i,C2}' - 1)^2 + 0.0874(V_{i,C3}' - 1)^2}} \end{cases} \quad (6.20)$$

For OSD2.32, the design solution  $k$ , with the smallest  $C_i^*$  in Eq. 6.21, is the ODS2.32:

$$\begin{cases} C_k^* = \min \{C_i^*\} \\ C_i^* = \frac{\sqrt{0.1927V_{i,C1}'^2 + 0.7199V_{i,C2}'^2 + 0.0874V_{i,C3.2}'^2}}{\sqrt{0.1927V_{i,C1}'^2 + 0.7199V_{i,C2}'^2 + 0.0874V_{i,C3.2}'^2} + \sqrt{0.1927(V_{i,C1}' - 1)^2 + 0.7199(V_{i,C2}' - 1)^2 + 0.0874(V_{i,C3.2}' - 1)^2}} \end{cases} \quad (6.21)$$

For OSD2.41, the design solution  $k$ , with the smallest  $C_i^*$  in Eq. 6.22, is the ODS2.41:

$$\begin{cases} C_k^* = \min \{C_i^*\} \\ C_i^* = \frac{\sqrt{0.1953V'_{i,C1}{}^2 + 0.73V'_{i,C2.2}{}^2 + 0.747V'_{i,C3}{}^2}}{\sqrt{0.1953V'_{i,C1}{}^2 + 0.73V'_{i,C2.2}{}^2 + 0.747V'_{i,C3}{}^2 + \sqrt{0.1953(V'_{i,C1} - 1)^2 + 0.73(V'_{i,C2.2} - 1)^2 + 0.0747(V'_{i,C3} - 1)^2}}} \end{cases} \quad (6.22)$$

For **OSD2.42**, the design solution  $k$ , with the smallest  $C_i^*$  in Eq. 6.23, is the ODS2.42:

$$\begin{cases} C_k^* = \min \{C_i^*\} \\ C_i^* = \frac{\sqrt{0.1953V'_{i,C1}{}^2 + 0.73V'_{i,C2.2}{}^2 + 0.747V'_{i,C3.2}{}^2}}{\sqrt{0.1953V'_{i,C1}{}^2 + 0.73V'_{i,C2.2}{}^2 + 0.747V'_{i,C3.2}{}^2 + \sqrt{0.1953(V'_{i,C1} - 1)^2 + 0.73(V'_{i,C2.2} - 1)^2 + 0.0747(V'_{i,C3.2} - 1)^2}}} \end{cases} \quad (6.23)$$

Where:  $K$  is the optimized design solution in solutions set;  $V'_{i, C1}$ ,  $V'_{i, C2}$ ,  $V'_{i, C3}$  and  $V'_{i, C2.2}$ ,  $V'_{i, C3.2}$  are the normalized value of criteria C1, C2, C3 and C2.2, C3.2 respectively for design solution  $i$  in solutions set.

### 6.5.2 Weight assignment for the 2.5 WEI-OC scenario:

The “Whole environmental impact reducing orientation with an overall consideration” preference scenario (2.5WEI-OC) focuses on the whole life-cycle environmental impact with an overall consideration by using the continuous variable weight method. This scenario is described in a simple way as its` s principle is similar to the 1.5 WEC-OC.

#### **The Key criteria are directly assigned as the same as 2.31 WEIR.**

Three key criteria are considered in the assessment, these are the whole life-cycle energy consumption (C1), the whole life-cycle environmental impact (C2) and the whole life-cycle cost (C3) of proposed office buildings. Besides, although the operational environmental impact (C2.2) is not the key criteria, it is also monitored as the indicator of the environmental impact of each design solution. This is done in order to judge the continuous variable weights of key criteria.

#### **The continuous variable weights of key criteria are separated into three phases.**

**Phase A:** The C2.2 is better (lower) than the dedicated lower-point of the green building

standards requirement; **Phase B:** The C2.2 is just between the dedicated higher-point and the lower-point of the green building standards requirement; **Phase C:** The C2.2 is worse (higher) than the dedicated higher-point of green building standard requirements.

Defining the higher-points and lower-points for separation of phases by converting existing statistical data. By now, most countries don't have comprehensive regulations for pollutant emission in the building sector, only a few counties have the limitation rules for operational CO<sub>2</sub> emissions. Therefore, in this section, a suggested range for the operational environmental impact (C2.2), in the form of PE (comparable pollution equivalent), is developed to separate C2.2 of the emissions into 3 phases.

The suggested range for C2.2 is generated from the statistical data (sourced from Tsinghua University [182]) for the green office building (at least rated as “one star”) in China, including the operational energy consumption for average and excellent cases, the proportion of energy sources and the emission factor for different energy sources [183] [184], as shown in Table 6.15 and 6.16. The suggested range of higher and lower points of PE are calculated by using methods given Chapter 5 and presented in Table 6.17.

Table 6.15: Energy consumption and proportion of each energy source

	Severe cold & Cold	Hot summer cold winter	Hot summer warm winter
Green building average operational energy consumption (kWh/m <sup>2</sup> yr)	87	72.3	77.4
Green building excellent operational energy consumption (kWh/m <sup>2</sup> yr)	50	52	50
Electricity (%)	79.3	75	100
District heat - nature gas (%)	20.7	-	-
Distributed heat- nature Gas (%)	-	25	-

Table 6.16: Typical emission factors for each energy source

Emission factor (kg/kWh)	CO <sub>2</sub>	SO <sub>2</sub>	NO <sub>x</sub>	PM
Electricity	0.754	0.0023	0.00182	0.00038
District heating - nature gas	0.19855	0.00006	0.00005	0.00003
Distributed heating - nature gas	0.203		0.00277	



Table 6.17: Suggested environmental impacts at the operational stage

	Severe cold & Cold	Hot summer cold winter	Hot summer warm winter
Low-point for operational environmental impact (EP/m <sup>2</sup> yr)	26.5	21.6	28.0
High-point for operational environmental impact (EP/m <sup>2</sup> yr)	15.2	15.5	18.1

**Weight assignment for design solutions with C2.1 within phase A.** As a similar method as to 1.5 WEC-OC. The weights for C1, C2 and C3 are judged by 24 experts, and analyzed by the use of an AHP method, giving the weights of C2, C1 and C3 of 10%, 45% and 45% respectively.

**Weight assignment for design solutions with C2.1 within phase C.** The minimization of C2 is the sole aim of the work. In this case, the weights for C1, C2 and C3 are 0%, 100%, and 0% respectively.

**Weight assignment for design solutions with C2.1 within phase B.** As the energy consumption of design solutions in this phase have already met the higher-point of the suggested PE range but still being worse than the lower-point, much attention will be given to the energy (C1) and cost (C3) criteria.

The weight of C2 in phase B ( $w_{c2, B}$ ) is linearly varying and can be computed by Eq. 6.24 below; meanwhile the weights for C1 ( $w_{c1, B}$ ) and C3 ( $w_{c3, B}$ ) in phase B are the same, both linearly varying with the opposite trend of C2` and this is given in Eq. 6.25:

$$w_{c2, B} = 100\% - \frac{EI_{Hi} - OP\_PE}{EI_{Hi} - EI_{Lo}} 90\% \quad (6.24)$$

$$w_{c1, B} = w_{c3, B} = (100\% - w_{c2, B})/2 \quad (6.25)$$

Where:  $EI_{Hi}$  is the higher-point of operational PE for specific climate zones (see Table 6.17);  $OP\_PE$  is the specific design solution`s operational EI (C2.2);  $EI_{Lo}$  is the lower-point operational PE for specific climate zone (see Table 6.17);  $w_{c2, C}$  and  $w_{c2, A}$  is C2`s weight in phase C and phase A, in this case  $w_{c2, C}=100\%$  and  $w_{c2, A}=10\%$ .

**Overall, the continuous variable weights for the criterion in the scenario 2.5 WEI-OC are illustrated in Figure 6.9 to 6.11.**

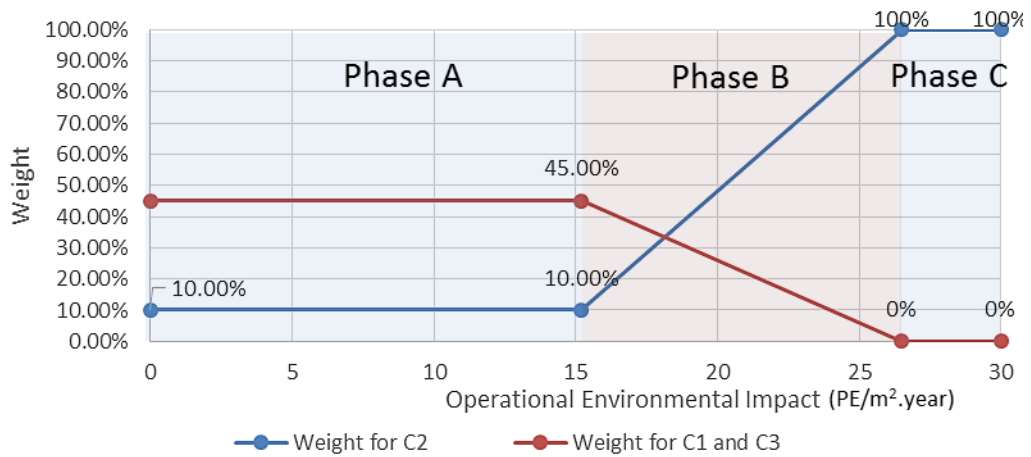


Figure 6.9: Variable weight for severe cold & cold climate zones.

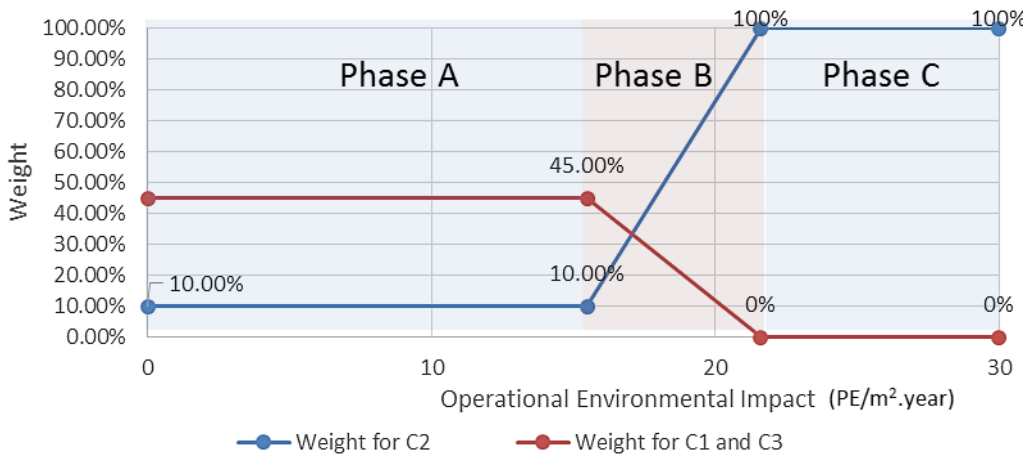


Figure 6.10: Variable weight for hot summer cold winter climate zone

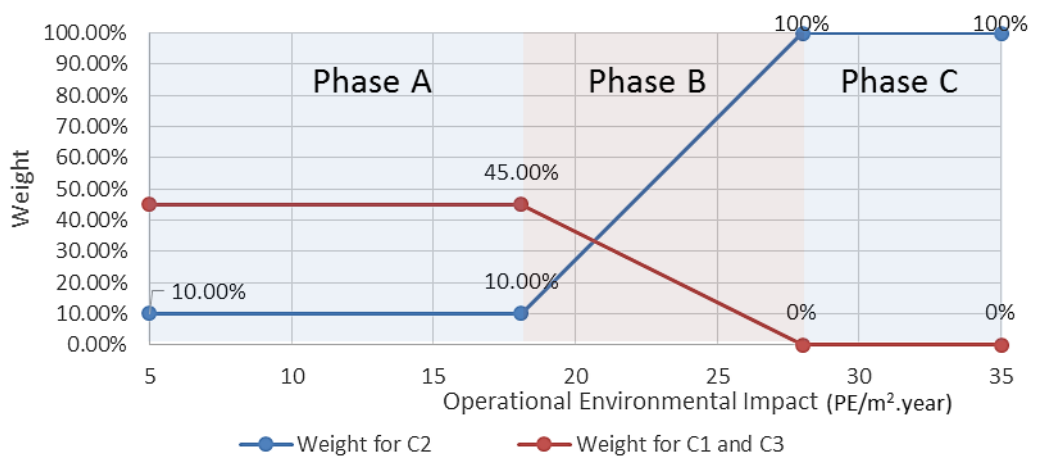


Figure 6.11: Variable weight for hot summer warm winter climate zone

By assigning weights into Eqs. 6.4 to 6.6, the mathematical equations for ODS derivation as well as the reference design solutions (RDS2.51 and RDS2.52) can be derived as follow:

In 2.5 - WEI-OC scenario, the ODS can only be selected from design solutions with an operational environmental impact (C2.2) within Phase B. Two RDSs where C2.2 lies in Phase A and Phase C are also selected for information. The mathematical equation for OSD2.5, RDS2.51 and RDS2.52 can be derived by assigning the weights into Eqs. 6.4 to 6.6. The mathematical expressions are derived exactly same as Eqs. 6.15 to 6.17 addressed in previous section 6.3.4 for 1.5 WEC-OC scenario.

### **6.6 Weight assignment for the comprehensive preference scenarios group (Group 3).**

In the preference scenarios of this group, the energy, environmental impact and cost criteria are considered as equally important in order to select a well-balanced design solution. Two scenarios are involved in this group, the design's preference is based on the target user of the building.

#### **6.6.1 Weight assignment for the 3.1 WB-BTL scenario:**

In a well-balanced consideration for build-to-let offices (3.1WB-BTL) preference scenario, the designer would like to find a design solution that treats the energy and environmental impact and cost as of equal importance. For a build-to-let office building project, the designer, in accordance with the building owner's wishes, prefers to control the initial construction cost rather than the operational cost. The energy bill and further environmental saving responsibility normally need to be paid by the tenant or user instead of the building owner.

Therefore, 3 criteria are considered in the WB-BTL preference scenario. These are the whole life-cycle energy consumption (C1), the whole life-cycle environmental impact (C2) and the initial construction cost (C3.1). The same weights (33.3%) are assigned to all criterion,

Assigning the weight to Eqs. 6.4 to 6.6 of the TOPSIS method, the ODS 3.1 is the design solution  $k$ , with the smallest  $C_i^*$  expressed as follow:

$$\begin{cases} C_k^* = \min \{C_i^*\} \\ C_i^* = \frac{\sqrt{0.333V'_{i,C1}{}^2 + 0.333V'_{i,C2}{}^2 + 0.333V'_{i,C3.1}{}^2}}{\sqrt{0.333V'_{i,C1}{}^2 + 0.333V'_{i,C2}{}^2 + 0.333V'_{i,C3.1}{}^2 + \sqrt{0.333(V'_{i,C1} - 1)^2 + 0.333(V'_{i,C2} - 1)^2 + 0.333(V'_{i,C3.1} - 1)^2}}} \end{cases} \quad (6.26)$$

Where:  $K$  is the optimized design solution in solutions set;  $V'_{i, C1}$ ,  $V'_{i, C2}$ , and  $V'_{i, C3.1}$  are the normalized value of criteria C1, C2 and C3.1 respectively for the design solution  $i$ .

### 6.6.2 Weight assignment for 3.2 - WB-SU scenario:

The designer's preference in a well-balanced consideration for the self-use office (3.2WB-SU) preference scenario is similar to that in 3.1 - WB-BTL. The difference is that for a self-using office building project, the designer, in accordance with the building owner's wishes, prefers to reduce the whole life-cycle cost including the initial construction cost and the operational cost, as they will be responsible for further energy bills and environmental saving responsibilities.

Therefore, three criteria are considered in the WB-BTL preference scenario, these are the whole life-cycle energy consumption (C1), the whole life-cycle environmental impact (C2) and the whole life-cycle cost (C3). The same weights of (33.3%) are assigned to all criteria.

Assigning the weight to Eqs 5.4, 5.5 and 5.6 of the TOPSIS method, the ODS 3.1 is the design solution  $k$ , with the smallest  $C_i^*$  expressed as follow:

$$\begin{cases} C_k^* = \min \{C_i^*\} \\ C_i^* = \frac{\sqrt{0.333V'_{i,C1}{}^2 + 0.333V'_{i,C2}{}^2 + 0.333V'_{i,C3}{}^2}}{\sqrt{0.333V'_{i,C1}{}^2 + 0.333V'_{i,C2}{}^2 + 0.333V'_{i,C3}{}^2 + \sqrt{0.333(V'_{i,C1} - 1)^2 + 0.333(V'_{i,C2} - 1)^2 + 0.333(V'_{i,C3} - 1)^2}}} \end{cases} \quad (6.27)$$

Where:  $K$  is the optimized design solution in solutions set;  $V'_{i, C1}$ ,  $V'_{i, C2}$ , and  $V'_{i, C3.1}$  are the normalized value of criteria C1, C2, and C3.1 respectively for design solution  $i$ .

## 6.7 Conclusion

In this chapter, a green building design assessment and selection method (GBAS) was developed to deal with the overall “best” design solution finding problem with trade-off of the various objectives. Through the design solution selection using GBAS, the conflicting objectives of green buildings (i.e. energy saving, environment protection and cost reducing) will be balanced based on the designer’s preference for different building design projects. For the generation of the GBAS, three parts of works have been completed, as briefed as follows:

Twelve designer preference scenarios under three scenario groups (i.e. energy saving oriented, environmental impact reducing oriented and comprehensive) and their key criteria are outlined. Those preference scenarios are able to represent the designer’s willingness / preference for most of the green building design situations in the real world. The key criteria for each preference scenario are selected based on the expert survey. It’s worth mentioning that the criteria selected by experts are similar for same preference scenario. Whereas they are very distinct from the different scenario.

The dedicated criteria’s weights for each preference scenario are generated by an AHP method based on experts’ survey. The criteria weight for each preference scenario are derived from analysis of the criteria’s relative importance (based on the expert survey) by using the AHP method. Through the expert survey, the importance of main criterion has similar distribution rule for the different orientated scenario, e.g. weight for energy is 73.33% in ODS1.31 (energy-saving oriented), the weight for environmental impact is 71.99% in ODS2.31 (environmental impact oriented). Also, the weights distribution rules are similar between two preference scenarios with continuous variable weights.

The mathematical method for appropriate design solution selection of each designer preference scenarios is defined, based on the TOPSIS method using criteria weights. Sixteen sets of mathematical equations for selecting the optimized design solution (ODS) and reference design solution (RDS) for each preference scenario (12 ODSs and 4RDSs

in total), were generated, using the principle of the TOPSIS method accompanied by criteria weights.

The innovated GBAS method selects the optimized design solution by both “subjective” (e.g. the preference scenarios definition) and “objective” (e.g. mathematic calculation) approaches, which make GBAS very flexible for different green building design cases and meanwhile being very effective with a reduced calculation-load. By using GBAS, the green building design solution can be selected in a very design-orientated quantitative way, rather than an inaccurate qualitative analysis in the traditional building design process.

In this Chapter, the mathematical foundation of GBAS is completed, base on which, a computerized selection tool is programmed by VB.net in the next Chapter to enable the easy-use and validation of the GBAS method. The program also integrates the life-cycle building energy and environmental impact estimation method (as shown in Chapter 3 and 4), and the simplified building cost estimation method (as shown in Appendix III) to provide the key criteria`s value to GBAS.

**Chapter 7. Development of an integrated computer-aided tool to enable fast and convenient green design optimization and selection**

## 7.1 Introduction

The estimation methods for the life-cycle energy consumption, the environmental impact and the cost of the Chinese office building have already been developed in Chapter 3 to Chapter 5 as well as in Appendix III. These provide the elementary “green performance” data in the GBAS method (addressed in Chapter6) to assess the building design solutions and select the optimized one for building designers. These works, though leading to the development of the simplified methods and China-focused building components dataset, still partly rely on the manual processing by the building designers and thus non-intuitive and inconvenient.

**The aim of this Chapter is to develop a computer-aided tool for the Chinese office building design that integrates the energy and environmental impact estimation methods with the GBAS method. The tool is functioned to be able to directly generate all the possible design solutions** (based on the design requirement from the input) **with “green performance” data, and select the optimized one in an efficient way.** The obvious advantage of the computer tool is that it highly improves the working efficiency and avoids the trial and error process by providing suggestions for the design solution selection. Furthermore, the integrated China-focused building components datasets will provide a practical reference to the earlier stage conceptual design.

In this Chapter, a dedicated computer-aided tool is illustrated, including its principle and structure, interface, input and output method. The application of this computer tool is demonstrated and its applicability and feasibility are tested through a case study.

## 7.2 Development of the computer-aided tool

The computer-aided tool is developed by using the Basic language of the MS Visio Studio Express for desktop 2012. The tool, able to operate on the Windows platform, has three functional modules: **(1)** the possible design solutions module; **(2)** the “green performance” estimation module; and **(3)** the design solution selection module. These functions are



detailed below

**(1) The possible design solutions module will generate hundreds or thousands of possible design solutions based on the input of the design requirement.** The requirements for the design factors are entered from the tool interface in the form of a fixed value or range, while the supporting data (e.g. a locally available wall / insulation material) is entered from a background dataset by a comma-separated plain-text CSV file. The output of this module are the values of each design element for possible design solutions, in the form of a CSV file as well. The inputs of this module are listed in Table 7.1, while the tool interface can be seen in Figures 7.1 -7.3. The example input dataset (e.g. the wall infill block) and output CSV file can be seen in Figures 7.4 and 7.5.

Table 7.1: The input for the possible design solutions generating module

<b>Building design elements</b>	<b>Input by tool interface or by CSV file</b>	<b>Data source for input</b>
<b>Geometry design limitations</b>		
Building gross floor area	Input a fixed value in tool interface	Building real requirement / designer`s preference / building regulation / building site limitation
Number of storeys	Input a fixed value / range in tool interface	
Shape-coefficiency		
Building length & width		
Building orientation		
Window-wall ratios for each facade		
Windows and wall material	Glass curtain wall datasets.csv Roof material datasets.csv Wall exterior decoration datasets.csv Wall infill block datasets.csv Wall insulation material datasets.csv Wall interior decoration datasets.csv	All datasets refer to the “China-focused dataset” established for each building component in Chapter 5
Structure type	Select from preset types in tool interface	Related to the number of stories
<b>Building service and renewable energy system</b>		
HVAC type	Select from preset types in tool interface, and HVAC efficiency datasets.csv	Refers to the “China-focused dataset” in Chapter 5
Office hot water availability	Select from YES/NO in tool interface	Designer`s preference
Solar thermal collector area	Input a fixed value / range in tool interface, Renewable energy performance datasets.csv	Refers to the “China-focused dataset” in Chapter 5
PV area		

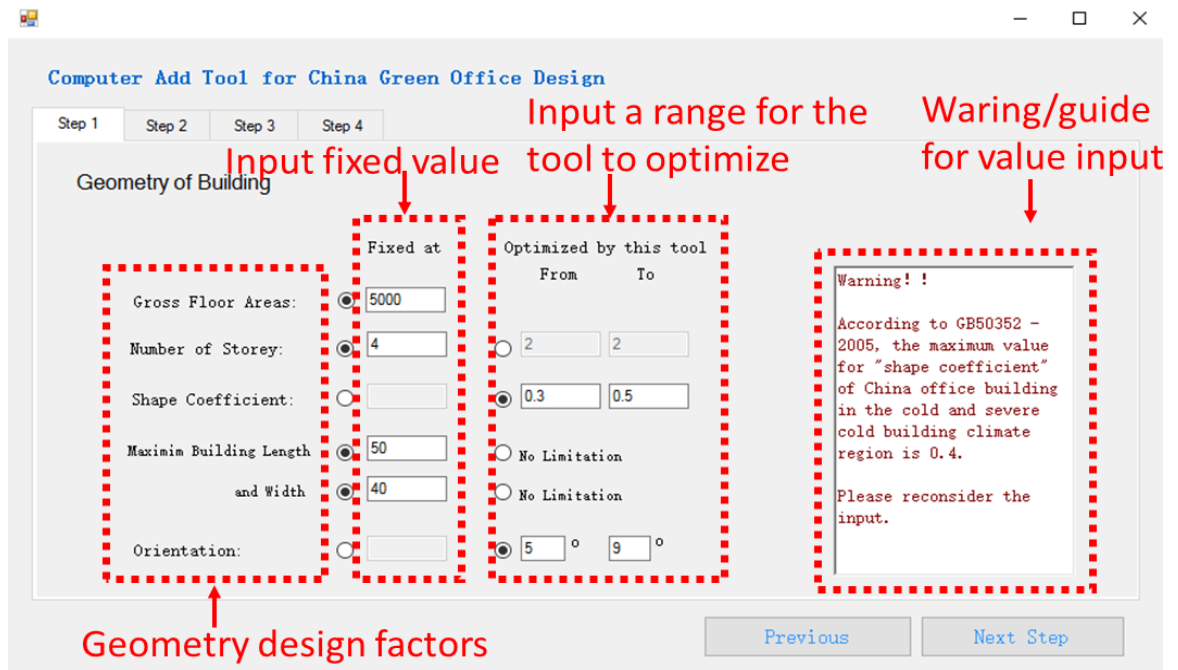


Figure 7.1: The tool interface 1

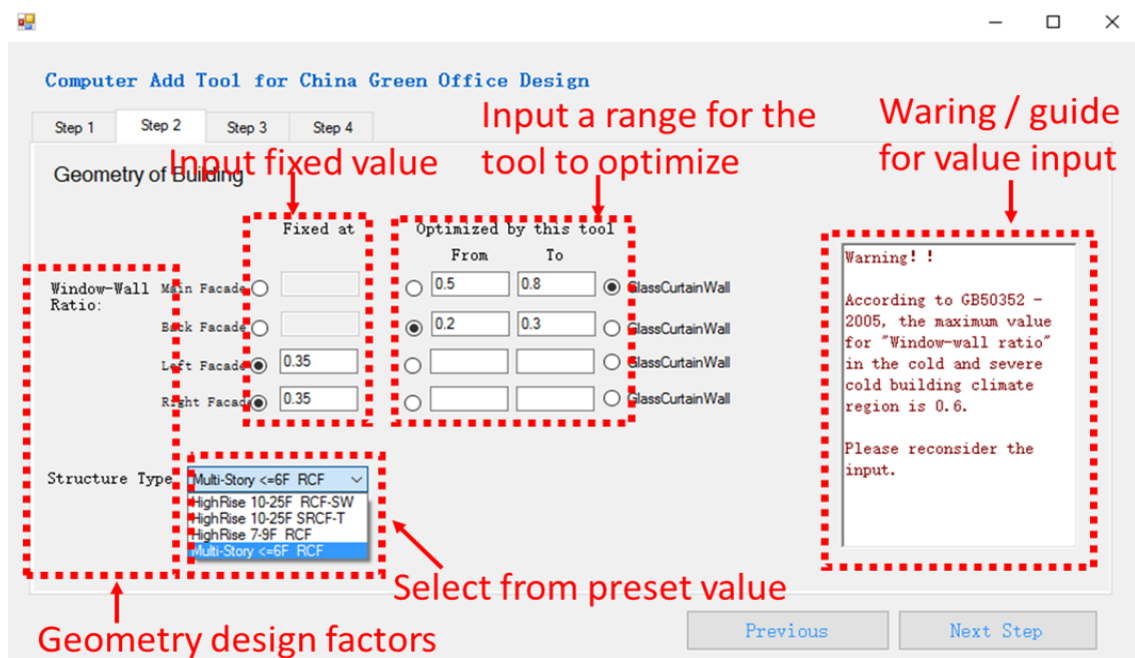


Figure 7.2: The tool interface 2

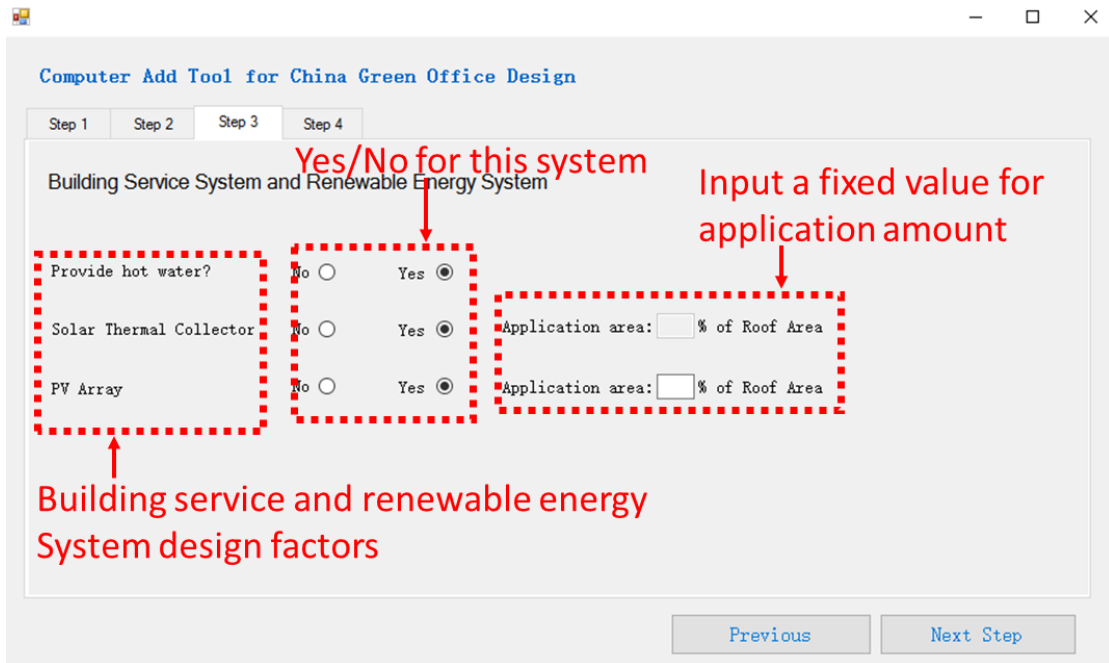


Figure 7.3: The tool interface 3

No.	Material description	Thickness	Conductivity	R	Price(RMB)	Price+Fund	LCE (MJ)	CO2 (Kg)	SO2 (Kg)	NOx (Kg)	PM (Kg)
1	1.1 AAC Al.4 B03	0.1	0.07	1.129	170	193.5	1313.5	176.5	69.16	0.395	0.607
2	1.1 AAC Al.4 B03	0.12	0.07	1.714	204	232.2	1481.0	186.8	73.29	0.416	0.639
3	1.1 AAC Al.4 B03	0.15	0.07	2.143	255	290.3	1697.2	217.3	78.89	0.449	0.688
4	1.1 AAC Al.4 B03	0.18	0.07	2.571	306	348.3	1838.4	217.8	84.49	0.481	0.736
5	1.1 AAC Al.4 B03	0.2	0.07	2.857	340	387	1950.9	226.8	88.03	0.503	0.769
6	1.1 AAC Al.4 B03	0.25	0.07	3.571	425	483.8	2244.6	253.9	97.55	0.557	0.850
7	1.1 AAC Al.4 B03	0.3	0.07	4.286	510	599.4	2538.3	309.4	117.55	0.611	0.931
8	1.2 HB Single hol	0.09	0.76	0.118	21.6	42.7599	957.9	146.0	56.66	0.322	0.494
9	1.2 HB Single hol	0.115	0.76	0.151	27.6	54.6379	1008.4	151.9	58.26	0.331	0.507
10	1.2 HB Single hol	0.14	0.76	0.184	33.6	64.6379	1058.9	157.8	59.85	0.341	0.521
11	1.2 HB Single hol	0.19	0.76	0.250	45.6	90.2709	1159.9	169.5	63.05	0.361	0.548
12	1.2 HB Double hol	0.09	0.56	0.161	22.32	43.4799	957.9	146.0	56.66	0.322	0.494
13	1.2 HB Double hol	0.115	0.56	0.205	28.52	55.55765	1008.4	151.9	58.26	0.331	0.507
14	1.2 HB Double hol	0.14	0.56	0.250	34.72	67.6354	1058.9	157.8	59.85	0.341	0.521
15	1.2 HB Double hol	0.19	0.56	0.339	47.12	91.7909	1159.9	169.5	63.05	0.361	0.548

Figure 7.4: The example dataset CSV file for wall infill block (screenshot in Excel)

pti	No	SC	Length	Width	MF	OMF	AreaMF	VWVWF	WallMF	WinABF	OrBF	AreaBF	VWRBF	WallABF	WinARF	OrARF	AreaARF	VWRARF	WallLRF	WinLRF	OrLRF	AreaLRF	WLF	WallLRF	WinLRF	Roof	ArGround
1	2	0.008	31.6	31.6	0	227.7	0.3	68.3	159.4	180	227.7	0.2	45.5	182.1	-90	227.7	0.2	45.5	182.1	90	227.7	0.2	45.5	182.1	1000.0	1000.0	0
2	2	0.008	31.6	31.6	1	227.7	0.3	68.3	159.4	181	227.7	0.2	45.5	182.1	-89	227.7	0.2	45.5	182.1	91	227.7	0.2	45.5	182.1	1000.0	1000.0	0
3	2	0.005	54.8	18.3	0	394.4	0.3	118.3	276.1	180	394.4	0.2	78.9	315.5	-90	131.5	0.2	26.3	105.2	90	131.5	0.2	26.3	105.2	1000.0	1000.0	0
4	2	0.005	54.8	18.3	1	394.4	0.3	118.3	276.1	181	394.4	0.2	78.9	315.5	-89	131.5	0.2	26.3	105.2	91	131.5	0.2	26.3	105.2	1000.0	1000.0	0
5	2	0.004	70.7	14.1	0	509.1	0.3	152.7	356.4	180	509.1	0.2	101.8	407.3	-90	101.8	0.2	20.4	61.5	90	101.8	0.2	20.4	61.5	1000.0	1000.0	0
6	2	0.004	70.7	14.1	1	509.1	0.3	152.7	356.4	181	509.1	0.2	101.8	407.3	-89	101.8	0.2	20.4	61.5	91	101.8	0.2	20.4	61.5	1000.0	1000.0	0
7	2	0.004	83.7	12.0	0	602.4	0.3	180.7	421.7	180	602.4	0.2	120.5	481.9	-90	86.1	0.2	17.2	68.8	90	86.1	0.2	17.2	68.8	1000.0	1000.0	0
8	2	0.004	83.7	12.0	1	602.4	0.3	180.7	421.7	181	602.4	0.2	120.5	481.9	-89	86.1	0.2	17.2	68.8	91	86.1	0.2	17.2	68.8	1000.0	1000.0	0
9	3	0.010	25.8	25.8	0	78.9	0.3	83.7	195.2	180	278.9	0.2	55.8	223.1	-90	278.9	0.2	55.8	223.1	90	278.9	0.2	55.8	223.1	666.7	666.7	0
10	3	0.010	25.8	25.8	1	78.9	0.3	83.7	195.2	181	278.9	0.2	55.8	223.1	-89	278.9	0.2	55.8	223.1	91	278.9	0.2	55.8	223.1	666.7	666.7	0
11	3	0.006	41.2	11.9	0	183.0	0.3	114.9	337.1	180	483.0	0.2	96.6	388.8	-90	161.0	0.2	38.2	138.8	90	161.0	0.2	38.2	138.8	666.7	666.7	0
12	3	0.006	41.2	11.9	1	183.0	0.3	114.9	337.1	181	483.0	0.2	96.6	388.8	-89	161.0	0.2	38.2	138.8	91	161.0	0.2	38.2	138.8	666.7	666.7	0
13	3	0.005	57.7	11.5	0	122.7	0.3	187.7	439.5	180	423.5	0.2	120.5	481.9	-90	124.7	0.2	24.9	99.8	90	124.7	0.2	24.9	99.8	666.7	666.7	0
14	3	0.005	57.7	11.5	1	122.7	0.3	187.7	439.5	181	423.5	0.2	120.5	481.9	-89	124.7	0.2	24.9	99.8	91	124.7	0.2	24.9	99.8	666.7	666.7	0
15	3	0.005	68.3	9.9	0	237.8	0.2	261.3	511.4	180	237.8	0.2	147.5	690.2	-90	105.1	0.2	21.1	84.3	90	105.1	0.2	21.1	84.3	666.7	666.7	0
16	3	0.005	68.3	9.9	1	237.8	0.2	261.3	511.4	181	237.8	0.2	147.5	690.2	-89	105.1	0.2	21.1	84.3	91	105.1	0.2	21.1	84.3	666.7	666.7	0

Figure 7.5: The example output CSV file (screenshot in Excel)

**(2) The “green performance” estimation module will estimate the energy, environmental impact, and the cost for every possible design solution based on the methods stated in Chapter 3 to Chapter 5 and in Appendix III. The related supporting data including weather data, building operation schedules (relevant to energy consumption and internal gain), and the ventilation and infiltration schedule, are entered**

by a background dataset (the CSV file). The results for the “green performance” of each possible design solution is temporarily stored in the PC`s memory and will be recalled in the design solution selection model.

**(3) The design solution selection module will select the most appropriate office building design solution for this design task based on the GBAS method elaborated in Chapter 6.** As the designer`s preference setup, 12 optimized design solutions and 2 reference solutions will be selected and outputted in the form of a CSV file. Followed by the design option no. (referring to the possible design solutions generating module) in the CSV file, the value for their design elements and “green performance” are also provided for the designer`s convenience.

### **7.3 The Validation of the computer-aided tool by case study**

#### **7.3.1 Introduction of the validation process and the office building design case**

In order to test the applicability of the proposed computer-aided tool as well as the GBAS method (especially the feasibility of weight assignment in each preference scenario), an example office building design case is prepared and the appropriate design solution will be selected by this proposed tool. Based on the situation of the building site and the limitations within real design practice, the basic principle of this office building design case is entered into the tool through the interface and background dataset (CSV file), including the design requirements for a geometric parameter, building service and renewable energy systems.

**The basic principle for the example office building design task is entered into the tool interface and given below:** The building is proposed to be composed of 4 stories with a reinforced concrete frame structure and a GFA of 9600m<sup>2</sup>, the story height is 4.5m and no loft or basement is required. The building site is located in Shanghai China, according to the site limitation and local regulation, the layout will be rectangular with the main façade`s orientation between 0° to 10° south; the aspect ratio is fixed at 2.67, the shape coefficient is about 0.15, and the windows-wall ratio is fixed at 0.4 for all façades. The

site map and proposed building shape can be seen in Figure 7.6, which illustrate the possible orientation and the schematic façade design for the 0.4 windows-wall ratio.



Figure 7.6: Schematic site and example building

The Other building design information is entered by a dataset in the CSV file, including the windows and wall constructions, building service and renewable energy system that is considered in the design task. Meanwhile, the ventilation, infiltration, building operation and internal gain schedule are also defined in the dataset, based on the local design guide.

In summary, in this design task, 5 types of building component designs are variable, the extraction of the dataset for the specification of component design options. Also, other design conditions are entered by the dataset as listed in Table 7.2.

Table 7.2: The specification of possible component design options

Types	No. of Opts	Specification
Orientation	2	<b>Opt 1:</b> 0° to (South); <b>Opt 2:</b> 10° (South-west)
Windows	2	<b>Opt 1:</b> 9mm double glazing window with thermal breaking aluminium frame and 9mm air gap <b>Opt 2:</b> 9mm Low-E double glazing window with thermal breaking aluminium frame and 12mm argon filled gap
External wall block	2	<b>Opt 1:</b> Autoclaved aerated concrete A3.5 B06, 150mm <b>Opt 2:</b> Concrete hollow block, Double hole, 190mm
External Insulation	3	<b>Opt 1:</b> 25mm EPS panel; <b>Opt 2:</b> 40mm EPS panel <b>Opt 3:</b> 120mm EPS panel
HVAC	2	<b>Opt 1:</b> Water cooled air conditioning screw chillers + Gas boiler heating + nature ventilation <b>Opt 2:</b> Water cooled air conditioning screw chillers + nature ventilation

Renewable energy	2	<b>Opt 1:</b> None renewable energy installed <b>Opt 2:</b> 400×SHARP U235F1 PV Panel, 650m <sup>2</sup>
External decoration	1	Marble curtain wall
Roof construction	1	Waterproofing mortar + concrete panel + 100mm EPS panel
Lighting	1	CFL lighting system
Internal gain	1	Based on “Design standard for energy efficiency of public buildings”: GB 50189-2005 and “Design code for office building”: JGJ 67-2006
Indoor comfort temperature zone	1	
Ventilation and infiltration	1	

### 7.3.2 Possible design solutions and their key “green performance” as generated by the computer-aided tool.

According to the input of building design limitations, there are 96 possible design solutions (2×2×2×3×2×2=96) generated by the tool for the proposed example office building design task. Meanwhile, the relevant key “green performances” of each design solution are generated, including the energy consumption (i.e. Life-Cycle - C1, embodied - C1.1, operational - C1.2), environmental impact (i.e. Life-Cycle - C2, embodied - C2.1, operational - C2.2), cost (i.e. Life-Cycle - C3, initial - C3.1, operational - C3.2). The results are presented in Table 7.3.

Table 7.3: The key “green performance” value for 96 design solutions

Design solution No.	C1	C1.1	C1.2	C2	C2.1	C2.2	C3	C3.1	C3.2
	MJ / m <sup>2</sup>			EP / m <sup>2</sup>			£ / m <sup>2</sup>		
1	22054	5897	16157	46.733	27.803	18.931	986.1	331.7	654.4
2	22064	5897	16168	46.728	27.803	18.925	985.9	331.7	654.2
3	23688	6062	17626	47.625	29.320	18.306	970.7	335.6	635.1
4	23735	6062	17672	47.650	29.320	18.331	970.9	335.6	635.3
5	21982	5753	16229	45.196	26.022	19.174	988.5	330.5	658.0
6	21996	5753	16243	45.199	26.022	19.177	988.5	330.5	658.0
7	23065	5918	17147	45.760	27.539	18.222	969.2	334.3	634.9
8	23101	5918	17179	45.780	27.539	18.241	969.4	334.3	635.1
9	22043	5900	16146	46.657	27.805	18.852	984.9	332.0	652.9
10	22054	5900	16157	46.654	27.805	18.849	984.8	332.0	652.8
11	23782	6062	17716	47.614	29.322	18.291	970.2	335.8	634.4
12	23807	6062	17744	47.625	29.322	18.303	970.3	335.8	634.5
13	21935	5753	16178	45.022	26.024	18.998	985.4	330.7	654.7
14	21946	5753	16193	45.022	26.024	18.997	985.2	330.7	654.5
15	23180	5918	17262	45.681	27.541	18.140	967.1	334.5	632.6

16	23227	5918	17309	45.712	27.541	18.171	967.4	334.5	632.9
17	21985	5904	16081	46.469	27.819	18.649	983.3	333.3	650.0
18	21996	5904	16092	46.465	27.819	18.645	983.2	333.3	649.9
19	22147	6066	16078	46.489	29.336	17.153	957.4	337.1	620.3
20	22165	6066	16099	46.506	29.336	17.170	957.8	337.1	620.7
21	21848	5756	16088	44.719	26.038	18.681	981.2	331.9	649.3
22	21856	5756	16099	44.714	26.038	18.676	981.1	331.9	649.2
23	22018	5922	16092	44.745	27.555	17.190	955.5	335.7	619.8
24	22025	5922	16103	44.752	27.555	17.196	955.6	335.7	619.9
25	19778	6073	13705	42.630	28.634	13.996	925.2	348.8	576.4
26	19789	6073	13716	42.624	28.634	13.990	925	348.8	576.2
27	21413	6239	15174	43.544	30.173	13.371	909.8	352.7	557.1
28	21460	6239	15221	43.569	30.173	13.396	910	352.7	557.3
29	19706	5929	13777	41.059	26.820	14.240	927.7	347.6	580.1
30	19717	5929	13788	41.062	26.820	14.242	927.6	347.6	580.0
31	20790	6095	14695	41.646	28.359	13.287	908.3	351.4	556.9
32	20822	6095	14728	41.666	28.359	13.306	908.5	351.4	557.1
33	19768	6077	13691	42.554	28.637	13.917	924	349.1	574.9
34	19778	6077	13702	42.551	28.637	13.914	923.9	349.1	574.8
35	21506	6239	15264	43.532	30.175	13.357	909.3	352.9	556.4
36	21532	6239	15289	43.543	30.175	13.368	909.4	352.9	556.5
37	19656	5929	13727	40.885	26.822	14.063	924.4	347.8	576.6
38	19670	5929	13738	40.885	26.822	14.063	924.3	347.8	576.5
39	20905	6095	14807	41.567	28.362	13.205	906.1	351.6	554.5
40	20952	6095	14857	41.598	28.362	13.236	906.5	351.6	554.9
41	19706	6080	13630	42.365	28.651	13.714	922.3	350.3	572.0
42	19717	6080	13640	42.361	28.651	13.710	922.2	350.3	571.9
43	19868	6242	13626	42.407	30.189	12.218	896.6	354.2	542.4
44	19890	6242	13644	42.424	30.189	12.235	896.9	354.2	542.7
45	19570	5933	13637	40.582	26.836	13.746	920.3	349.0	571.3
46	19580	5933	13644	40.577	26.836	13.741	920.2	349.0	571.2
47	19739	6098	13640	40.631	28.376	12.255	894.5	352.8	541.7
48	19746	6098	13648	40.637	28.376	12.262	894.7	352.8	541.9
49	21640	5897	15739	59.470	27.803	31.667	1273.6	331.7	941.9
50	21632	5897	15736	59.461	27.803	31.658	1273.3	331.7	941.6
51	19836	6062	13774	57.029	29.320	27.710	1205	335.6	869.4
52	21373	6062	15311	60.121	29.320	30.801	1264.7	335.6	929.1
53	21758	5753	16006	58.225	26.022	32.203	1281.3	330.5	950.8
54	21766	5753	16009	58.234	26.022	32.213	1281.5	330.5	951.0
55	21067	5918	15149	58.016	27.539	30.477	1255.7	334.3	921.4
56	21092	5918	15174	58.067	27.539	30.528	1256.7	334.3	922.4
57	21553	5900	15656	59.302	27.805	31.497	1270.8	332.0	938.8
58	21553	5900	15653	59.300	27.805	31.494	1270.7	332.0	938.7
59	21373	6062	15307	60.122	29.322	30.799	1265	335.8	929.2
60	21388	6062	15325	60.154	29.322	30.832	1265.7	335.8	929.9
61	21568	5753	15815	57.840	26.024	31.815	1274.3	330.7	943.6
62	21568	5753	15815	57.843	26.024	31.819	1274.3	330.7	943.6
63	20999	5918	15080	57.880	27.541	30.339	1253.5	334.5	919.0
64	21038	5918	15120	57.960	27.541	30.419	1255.1	334.5	920.6
65	21337	5904	15433	58.870	27.819	31.050	1264.7	333.3	931.4
66	21334	5904	15430	58.864	27.819	31.045	1264.6	333.3	931.3
67	19930	6066	13864	57.229	29.336	27.893	1211.5	337.1	874.4
68	19951	6066	13885	57.272	29.336	27.936	1212.3	337.1	875.2
69	21226	5756	15469	57.158	26.038	31.120	1263.3	331.9	931.4
70	21222	5756	15466	57.150	26.038	31.112	1263.2	331.9	931.3
71	19829	5922	13907	55.532	27.555	27.977	1210.4	335.7	874.7
72	19836	5922	13914	55.547	27.555	27.992	1210.7	335.7	875.0
73	19361	6073	13288	55.367	28.634	26.732	1212.6	348.8	863.8





### 7.3.3 The optimized office building design solution selected by the computer-aided tool

The optimized design solutions (ODS) and reference design solutions (RDS) for each preference scenario are selected by the computer-aided tool based on the GBAS method.

The selection results and the rationality of the selection are discussed as follows:

#### **A. The optimized office building design solution for energy saving oriented preference scenarios:**

The ODSs and RDSs selected by the computer-aided tool for the energy saving oriented scenarios group, as well as their design specification, are presented in Table 7.5.

Table 7.5: ODSs, RDSs and the specification for energy saving oriented preference scenarios group

Preference scenario	optimized solution No.	Design solution specification
1.1 MVEC	ODS1.1: No. 95	0°, EPS120mm, CHB190mm, Low-e TB double glazing window, Water cooled screw chillers AC, BIPV
1.2 MOEC	ODS1.2: No. 75	0°, EPS25mm, AAC150mm, Low-e TB double glazing window, Water cooled screw chillers AC, BIPV
1.3 WECS	ODS1.31: No. 95	0°, EPS120mm, CHB190mm, Low-e TB double glazing window, Water cooled screw chillers AC, BIPV
	ODS1.32: No. 95	0°, EPS120mm, CHB190mm, Low-e TB double glazing window, Water cooled screw chillers AC, BIPV
1.4 OECS	ODS1.41: No.75	0°, EPS25mm, AAC150mm, Low-e TB double glazing window, Water cooled screw chillers AC, BIPV
	ODS1.42: No.75	0°, EPS25mm, AAC150mm, Low-e TB double glazing window, Water cooled screw chillers AC, BIPV
1.5 WEC-OC	ODS1.5: No.31	0°, EPS25mm, CHB190mm, Low-e TB double glazing window, Water cooled screw chillers AC + Gas boiler heating, BIPV
	RDS1.51: No.47	0°, EPS120mm, CHB190mm, Low-e TB double glazing window, Water cooled screw chillers AC + Gas boiler heating, BIPV

In order to analyse the rationality of the ODS selection, the criteria value and rank position, in the form of a closeness degree to best performance (CDBP) and closeness degree to best rank (CDBR), are observed. These indicators represent the closeness of the current solution's performance to the best one. For example, assuming that the lowest operational energy consumption in 96 design solutions is 10 MJ/m<sup>2</sup>yr, one solution that has an annual energy consumption of 20 MJ/m<sup>2</sup>yr is ranked to no.40 in 98 solutions (energy consumption rank from low to high). For the operational energy consumption

criterion, this solution`s CDBP is  $10/20 \times 100\% = 50\%$ , the CDBR is  $(96-40+1)/96 \times 100\% = 59.4\%$ . Thus, the closer for the criteria value / rank to the best value / rank, the higher the score will be given to the CDBP and CDBR, the solution with the best performance (rank no.1) for a criterion will score 100% for both CDBP and CDBR in this criterion.

- The solution no.95 is selected as the ODS1.1, ODS1.31 and ODS1.32, a radar chart for CDBP and CDBR for the best design solution can be seen in Figure 7.7 where criteria are involved in a radar chart, in which the key criteria of preference scenarios are represented by bold open circles, other criteria are used for referencing purposes. The 1.1 MWECS scenario only prefers the best life-cycle energy consumption performance (LC-E), the solution 95 is obviously the correct one as it scores 100% in both CDBP and CDBR for the LC-E. In the 1.3 WECS scenarios (ODS1.31 and ODS1.32), life-cycle energy consumption performance (LC-E) functions dominantly, meanwhile the life-cycle environmental impact (LC-EI) and the life-cycle cost (LC-COST) or initial cost (INI-COST) are considered with less weight. Solution 95 has a strong advantage in these two scenarios as its LC-E scores top in CDBR and LC-EI and the LC-COST remains in the middle-level in CDBR. Although it's INI-COST only score is 39.6% in CDBR, it still archives 93.7% to the best one in terms of criterion value, not much different to the best one. Therefore, solution 95 is considered as the rational solution can match the requirement for ODS1.1, ODS1.31 and ODS1.32.

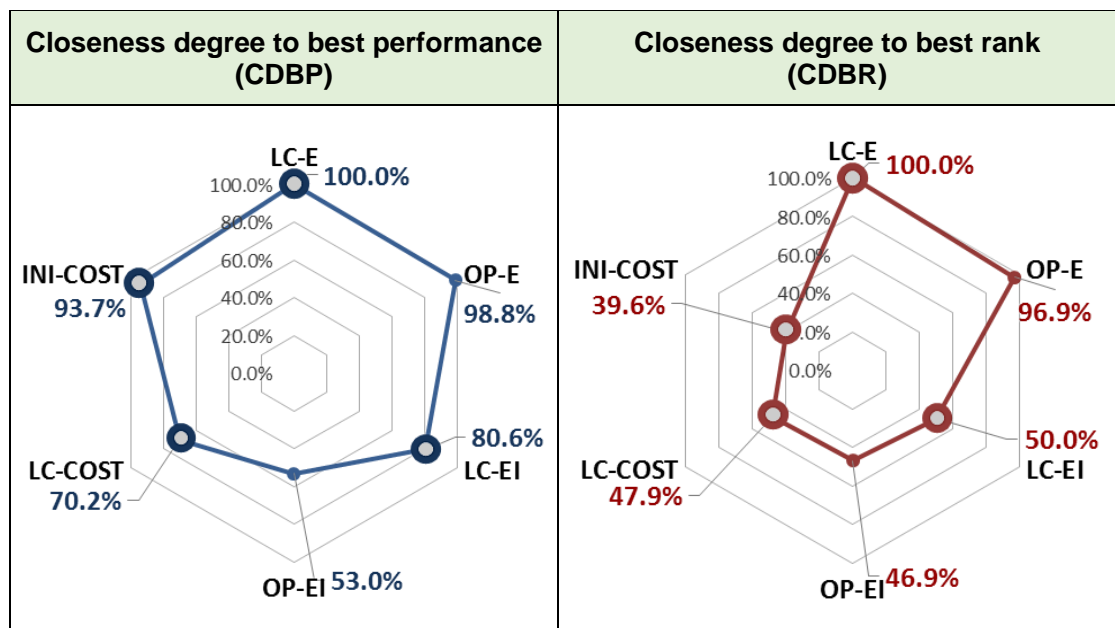


Figure 7.7: Radar chart for CDBP and CDBR of design solution no. 95

- The solution no.75 is selected as the ODS1.2, ODS1.41 and ODS1.42, a radar chart for solution no.75 can be seen in Figure 7.8. The solution no. 75 is obviously the correct one for the 1.2 MOEC scenario as it scores 100% in both CDBP and CDBR for operational energy consumption (OP-E). For 1.4 OECS scenarios (ODS1.41 and ODS1.42), OP-E functions dominantly, meanwhile the LC-EI and LC-COST or INI-COST are considered with less weight. According to Figure 7.8, design solution 75's OP-E scores top in CDBR, meanwhile the LC-EI and LC-COST remain in the middle-level in CDBR. Although it's INI-COST scores 41.7% in CDBR, it is still very close to the best one in terms of criterion value (93.7% of CDBP). Therefore, solution 75 is considered as a rational solution that can match the requirement ODS1.2, ODS1.41 and ODS 1.42.

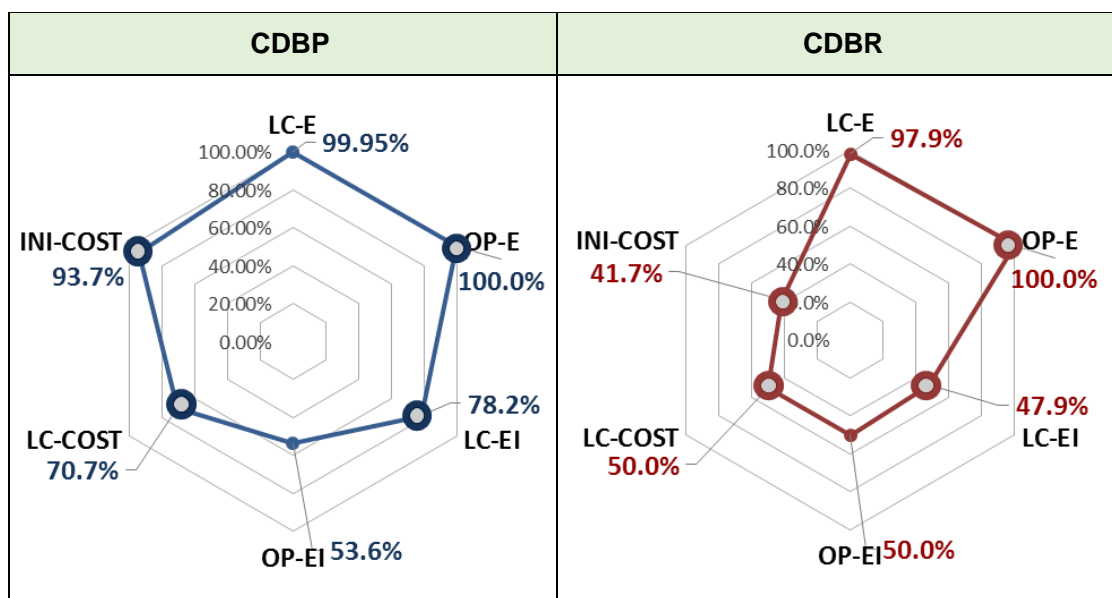


Figure 7.8: Radar chart for CDBP and CDBR of design solution no. 75

- The design solution no. 31 is selected as the ODS1.5, while its radar chart can be seen in Figure 7.9. As the OP-E for this solution lies within the required range of the green building standard, depending on its OP-E value, the weight for LC-E lies in a dedicated position between 100% to 10% and the weights for LC-EI and LC-COST lie in a dedicated position between 0% to 45%. In this situation, the LC-E is not the only important criterion, it scores 66.3% in CDBR, meanwhile LC-EI and LC-COST scores are 89.6% and 91.7% respectively. The same situation can be seen in CDBP as well, once the OP-E satisfy the green building standard's requirement, the importance of the LC-E is reduced and the importance of LC-EI and LC-COST is raised. The results from

the tool closely match the purpose of ODS1.5.

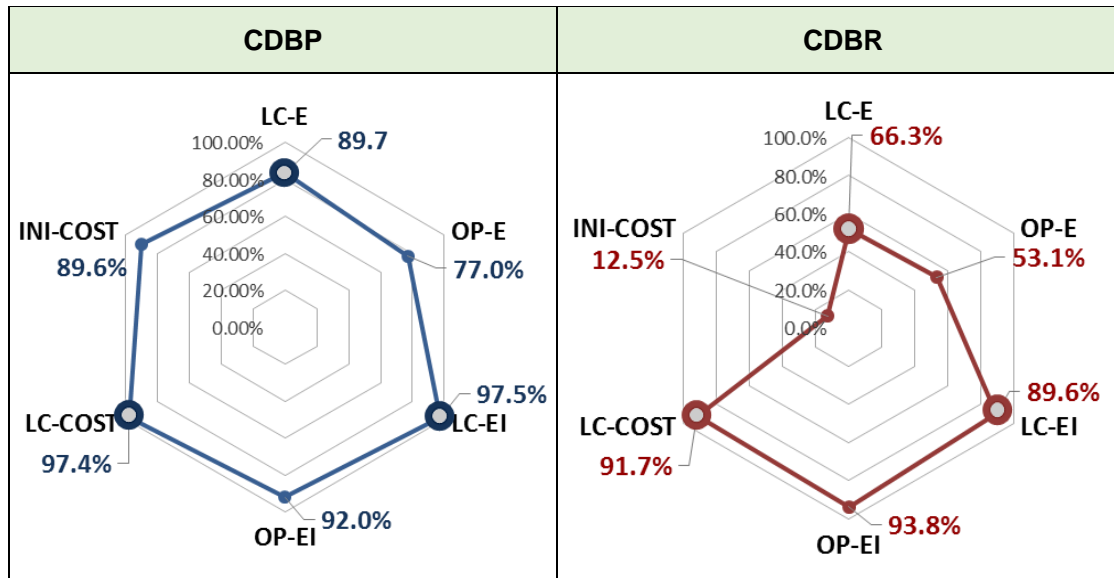


Figure 7.9: The Radar chart for CDBP and CDBR of design solution no. 31

- The design solution 47 is selected as the RDS1.51, and its radar chart is shown in Figure 7.10. RDS1.51 represents the solution with the OP-E as better than the suggested range for green building standard, while the importance of LC-E is low and the importance of the LC-EI and LC-COST is high. According to Figure 7.10, solution 47's CDBR for LC-EI and LC-COST are both at the top level (100% and 97.9%) while LC-E score is 61.5%. The ranks of LC-EI and LC-COST are higher than them in the best solution of the ODS1.5, while the same situation can be seen in the CDBP. This result can be considered to reasonably reflect the purpose of RDS1.51.

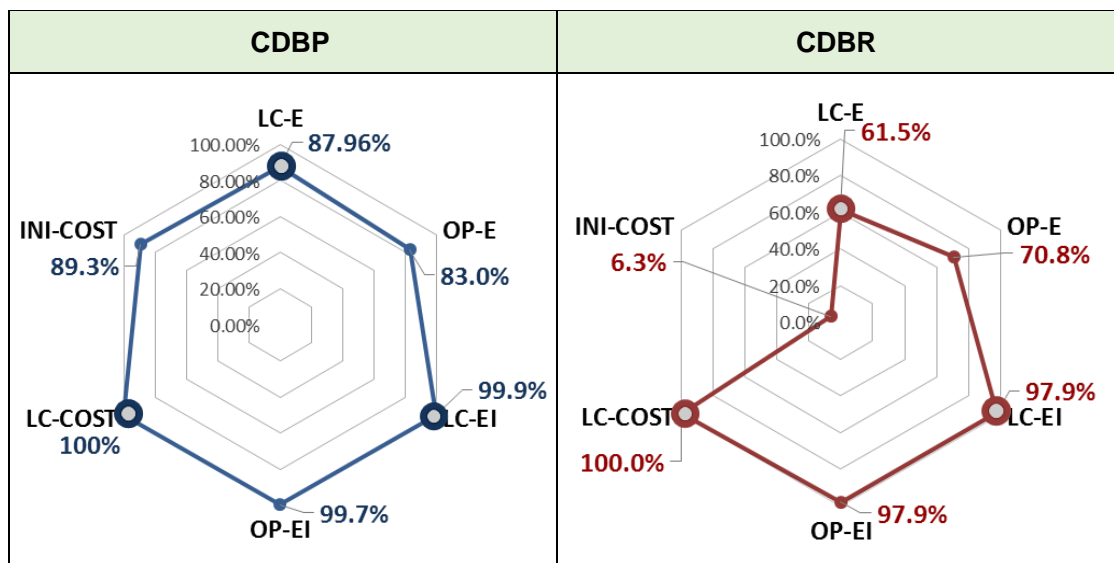


Figure 7.10: Radar chart for CDBP and CDBR of design solution 47

**B. The appropriate office building design solution for environmental impact reducing oriented preference scenarios and balanced considered scenario group:**

The ODSs and RDSs for each preference scenario in these two preference scenario groups are also selected using the computer-aided tool based on the GBAS method, they are shown in the section below.

- The selected ODSs / RDSs for each preference scenario in the environmental impact reducing oriented group are listed in Table 7.6. The radar chart of the CDBP and CDBR for the selected ODSs / RDSs are shown in Figures 7.11-7.12. The detailed description is omitted as the principle of solution selection is similar to the solution selection for the energy consumption saving oriented scenarios group described in the last section.

Table 7.6: ODSs, RDSs and the specification for the environmental impact reducing oriented preference scenarios group

Preference scenario	Optimized solution No.	Design solution specification
2.1 MWEI	ODS2.1: No. 46	10°, EPS120mm, CHB190mm, Double glazing window, Water cooled screw chillers AC + Gas boiler heating, BIPV
2.2 MOEI	ODS2.2: No. 43	0°, EPS120mm, AAC150mm, Low-e TB double glazing window, Water cooled screw chillers AC + Gas boiler heating, BIPV
2.3 WEIR	ODS2.31: No. 47	0°, EPS120mm, CHB190mm, Low-e TB double glazing window, Water cooled screw chillers AC + Gas boiler heating, BIPV
	ODS2.32: No. 46	10°, EPS120mm, CHB190mm, Double glazing window, Water cooled screw chillers AC + Gas boiler heating, BIPV
2.4 OEIR	ODS2.41: No. 47	0°, EPS120mm, CHB190mm, Low-e TB double glazing window, Water cooled screw chillers AC + Gas boiler heating, BIPV
	ODS2.42: No. 47	0°, EPS120mm, CHB190mm, Low-e TB double glazing window, Water cooled screw chillers AC + Gas boiler heating, BIPV
2.5 WEI-OC	ODS2.5: No. 21	0°, EPS120mm, CHB190mm, Double glazing window, Water cooled screw chillers AC + Gas boiler heating
	RDS2.51: No. 47	REF 1: 0°, EPS120mm, CHB190mm, Low-e TB double glazing window, Water cooled screw chillers AC + Gas boiler heating, BIPV
	RDS2.52: No.95	REF 2: 0°, EPS120mm, CHB190mm, Low-e TB double glazing window, Water cooled screw chillers AC, BIPV

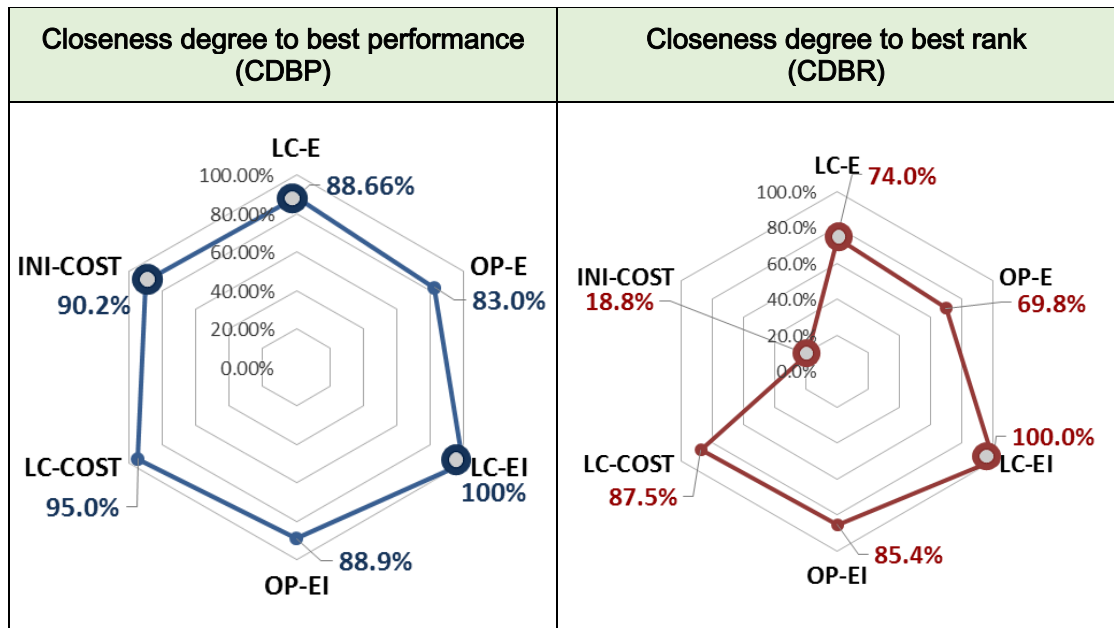


Figure 7.11: Radar chart for CDBP and CDBR of design solution 46

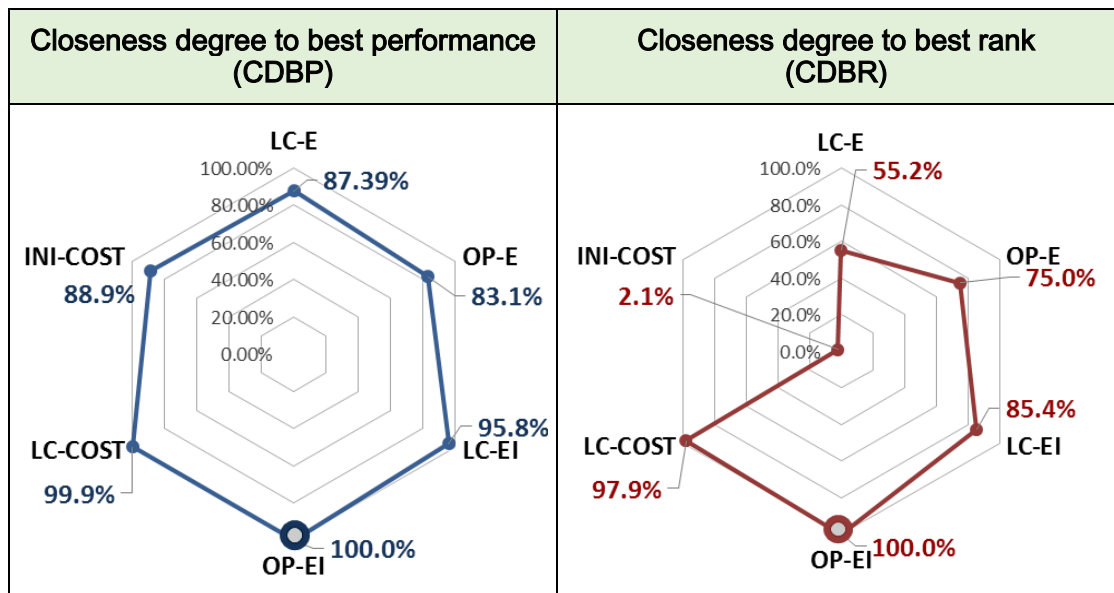


Figure 7.12: Radar chart for CDBP and CDBR of design solution 43

- The selected ODSs / RDSs for each preference scenario in the balance- considered scenario group are listed in Table 7.7. The radar chart for the CDBP and CDBR for the selected ODSs / RDSs are shown in Figure 7.13 According to the CDBP score, both solutions can provide a well-balanced performance in terms of energy, environment and cost. Solution no. 45 has a better score in the INI-COST than solution no. 47. Meanwhile, the LC-COST is better from no.47 than from no.45. To be more specific, while keeping the similar value of energy consumption and environmental impact, no.45 will save 36.5k £ in the initial building cost for the build-to-let building owner, whereas no.47 will save

247.7k £ in life-cycle building cost for the self-using building owner. Therefore, the performance of no.45 and no.47 can satisfy the requirement of ODS3.1 and ODS3.2 respectively.

Table 7.7: ODSs, RDSs and the specification for the comprehensive considered scenario preference group

Preference scenario	Optimized solution No.	Design solution specification
3.1 WB-BTL	ODS2.1: No. 45	0°, EPS120mm, CHB190mm, Double glazing window, Water cooled screw chillers AC + Gas boiler heating, BIPV
3.2 WB-SU	ODS2.2: No. 47	0°, EPS120mm, CHB190mm, Low-e TB double glazing window, Water cooled screw chillers AC + Gas boiler heating, BIPV

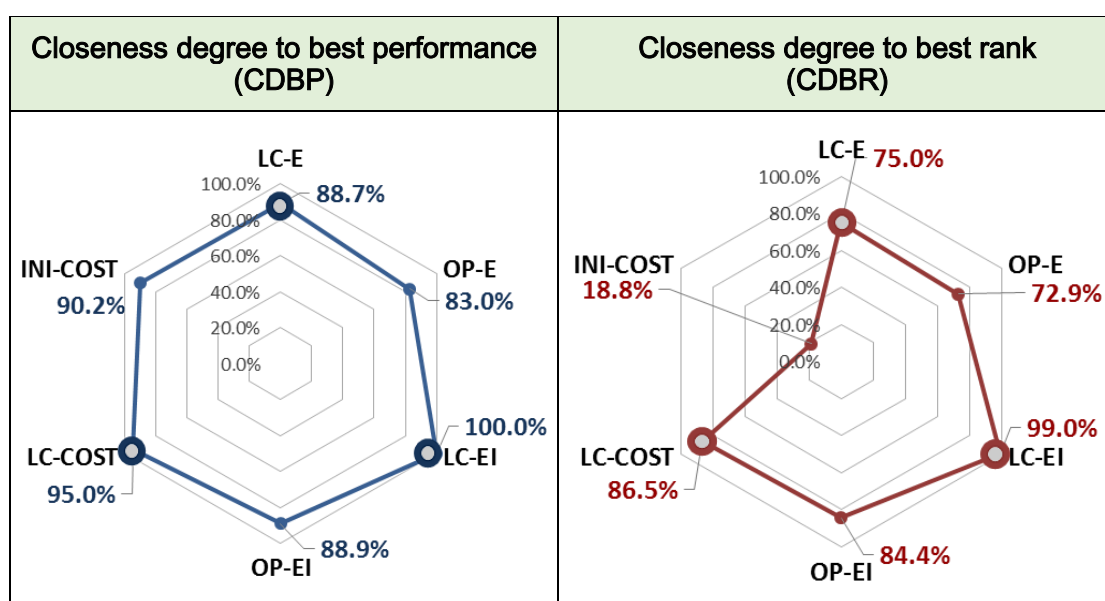


Figure 7.13: Radar chart for CDBP and CDBR of design solution 45

#### 7.4 Conclusion:

In this chapter, a computer-aided tool was developed to generate the possible conceptual design solutions and select the appropriate one for green office building design tasks in China. To achieve this function, the energy, environmental impact and cost estimation methods, as well as the localized dataset developed in the previous chapters are integrated into this tool.

The principle of the computer-aided tool and its basic input/output have been described in this chapter, followed by a case study to validate both the applicability of the tool and the feasibility of the GBAS method which is the foundation for the design solution

selection of this tool. The case study shows that:

- (1) The GBAS method and its weight assignment are rational and feasible. Based on GBAS, the selected design solutions are able to satisfy the requirements of each preference scenario. It is worth noticing that some design solutions have strong advantages in specific areas and that some preferences scenarios share the same best solutions. An example could be solution no. 75 in the studied case, since its great advantage is in the LC-E area, all preference scenarios that mainly focus on LC-E will select it as the best solution, because it provides the reasonable performance for other relevant key criteria as well. All the selected best solutions are able to reflect the original purpose of the designer`s preference scenarios, therefore, the weights are properly assigned for each preference scenario, the GBAS is well established to select the correct design solution for the building designer and decision-maker.
- (2) The computer-aided tool is applicable and practical. It is a useful and efficient tool for green office building designers in the early conceptual design stage. The simplified input by both interface (for simple parameters in building design, e.g. possible orientation range) and the background dataset (for complicated system with more than one options, e.g. wall material), that in the form of a CSV file are very easy to handle for designers. The information needed to be inputted is just the most basic data that can be obtained at this design stage.

In summary, the computer-aided tool and its foundation the GBAS method is a helpful tool for the conceptual early stage design of office buildings in China. It has benefits both from its appropriate design in the tool`s input/output and from its accuracy in the design option generation and selection. Meanwhile, apart from the localized building elements / system dataset that has already been developed in the prior chapters, the open sourced plain-text CSV file has proved to be invaluable because the datasets are easy to update in the future for every specific design task.



## Chapter 8: Conclusion

## 8.1 Thesis conclusion

The optimised green office design solution needs to simultaneously solve the problem of reducing energy demand, decreasing the environmental impact (i.e. from multiple pollutant emissions) and saving building costs during the whole life-cycle of an office building. Various technologies and design strategies have been developed in these fields to overcome these drawbacks at different stages of a building's life. For the early conceptual design stage that largely affects the "green performance" of the whole-life-cycle of the office building, the application of green design methods / tools is the most efficient approach. These include computer simulation tools and manual-calculation methods used to generate the key figures for the whole building (e.g. operational energy consumption, on-site construction CO<sub>2</sub> emission, etc.) and specific building system (e.g. peak power output of PV panel).

**The overall achievement of this thesis** is the development of an innovated design assessment and optimisation method in order to improve the quality of the conceptual design in Chinese office building at the early design stage. Meanwhile, its accuracy and practicality are achieved through the establishment and integration of a full range of "green performance" (i.e. life-cycle energy, environmental impact and cost) estimation methods and China-focused datasets which are the fundamental elements for the assessment and optimisation.

**The major works of the PhD research and conclusions derived from it are given below:**

**The missing points in current research are discussed.** As reviewed in Chapter 2, the current research of the green office building field has been investigated, including the general situation of its energy consumption and pollutant emissions, the appropriate green building technologies and strategies, the simulation and estimation tools, as well as the green building codes and evaluation tools. **4 weak points in the current research, which have been overcome in this research, are indicated as follows:** (1) There is no

adequate method to comprehensively reflect the overall environmental impact from the whole life-cycle of an office building. Although the environmental impact from single factor (e.g. energy or CO<sub>2e</sub>) has been deeply studied, there is still no generalized metric to represents the trade-off between different pollutants and to reflects the overall environmental impacts together; **(2)** The study of the reaction of multi green building technologies, especially between active technologies and passive design strategies, is still incomplete. **(3)** The current energy estimation tool is not appropriate for use in the early conceptual design stage. These are either complicated (i.e. dynamic simulation tools – require design details that are not available at this stage) or are inaccurate (i.e. the manual calculation methods). The lack of proper estimation tool will cause imperfect (e.g. inaccurate and ineffective) green building design and develop negative consequences for further detailed design stages. **(4)** The current green building evaluation systems are all process-oriented, score-based systems, which are not directly related to the final results (e.g. energy, environmental impact). Points are given to environmental protection related aspects accounted in the evaluation system, thus, the result (sum of points) only reflects the application of green measures rather than the final “green performance” of the building design.

**A new building operational energy estimation method, the CN13790 for the early (conceptual) design stage of the office building in China, is developed and validated.** As described in Chapter 3, this overcomes the problem of lacking an appropriate energy estimation tool for early design stage. It is composed of three modules: the HVAC module, the additional energy consumption module (i.e. lighting, office appliance and hot water energy demand) and the renewable energy generation module (i.e. PV and solar thermal). The major one, the HVAC module, is established by the refinement of the EN ISO13790 method which is based on a thermal 5 resistance -1 capacitance model. 6 simplified models for specific building elements and systems are built and localised for the Chinese office building context, and the dataset for the typical input is summarised subject to local building standards and market-available materials. The validation of the CN19790 method used 9 building cases to represent all Chinese

climate zones and 4 common design variations that mostly affect the energy demand of the Chinese office buildings. The results show that in both heating and cooling demand calculations, the results' difference for the CN13790 and the existing dynamic simulation method are reasonable and predictable (around 15%), whereas the calculation speed is 168 times faster. It can replace the traditional manual degree-day method to provide a more reliable result in all the Chinese climate zones, while requiring a similar sample input that is suitable for the conceptual design stage.

**The estimation methods for the life-cycle energy consumption (LCE) and the life-cycle pollutants (LCP) emission are developed.** As seen in Chapter 4, the sources of LCE and LCP (i.e. CO<sub>2</sub>e, SO<sub>2</sub>, NO<sub>x</sub> and PM) are studied in 4 major phases of a building's life separately. The characteristics of LCE and LCP from China office buildings are investigated, including those from 4 structural types, 4 types of window / curtain walls with more than 100 possible changes of materials, as well as 3 types of HVAC and 2 types of lighting systems. A method for a brief prediction of the LCE and LCP for designers in the early conceptual design stage is established, based on the statistical data collection and analysis. The outcome of this research includes the simplified model, regression equations and Chinese-focused datasets for the relationship of building features and LCE/LCP. Through this estimation method, the LCE/LCP, as the criteria in Chapter 5 and Chapter 6, are easy to be generated in the early design stage of China office building.

**The innovated environmental impact metric, namely the pollutant equivalent (PE), is developed.** As described in Chapter 5, PE is a holistic metric that enables the reflection of the overall environmental impact from 4 types of pollutant involved in this research together in a measurable, reportable and verifiable way. 25 sets of the monetization environmental cost data from 3 types of data sources are investigated through an AHP method to derive the comparative importance among pollutant types, based on which the PE is created. The practicality of the PE metric is tested by a case study of a real-world office design comparison. It has proved that: **(1)** PE has great advantage and unique characteristics from other existing metrics. There is an obvious

difference between the PE results and the other single pollution metrics results at any stage of the life-cycle of a building (e.g. the SO<sub>2</sub> emission only contributes 1.9% of emission amounts in terms of weight, however, it takes over 28% of the environmental impact reflected by PE); **(2)** PE has the ability to reflect the comprehensive environmental impact. The overall environmental impact can be represented and assessed by using the PE, without considering the complex relationships and trade-offs between single pollutants.

**The result-oriented multiple criteria based green design assessment and selection (GBAS) system is established.** As seen in Chapter 6, GBAS was developed to deal with the comprehensive “best” design solution finding problem. To achieve this, **(1)** 12 designer preference scenarios which belong to 3 scenario groups (i.e. energy oriented, environmental impact oriented and balanced oriented) are summarized, in order to represent the designer’s preference for most of the building design situations in the China; **(2)** The dedicated criteria’s weights for each preference scenario are generated by an AHP method based on expert surveys; **(3)** The mathematical method (16 sets of mathematical equations) for appropriate design solution selection of each design preference scenarios is generated, based on the TOPSIS method using criteria weights. Through this research, the innovated GBAS system selects the optimised design solution by both “subjective” (e.g. the preference scenario definitions) and “objective” (e.g. mathematical calculation) approaches. This is a very design-oriented quantitative way rather than the inaccurate qualitative analysis in the traditional building design process.

**The computer-aided tool that enables the fast and convenient green design optimisation and selection is programmed.** As described in Chapter 7, a computer-aided tool is developed to generate the possible conceptual design solutions (based on the design requirement input) and the selection of the appropriate one for green office building design tasks in China. The innovated tool that integrated all the estimation and assessment methods in the Chapters above is composed by (1) The possible design solutions generating module; (2) The “green performance” estimation module; and (3) The design solution selection module. The tool is validated by applying it to a design

case, in which 5 types of building component options are variable and thus 96 possible design solutions are generated by the tool. It has been proven that the tool (and its background GBAS method) are rational in terms of accuracy, and applicable at the early design stage of green office building design in China due to its easy and simplified input requirement and output format.

## 8.2 Recommendations for further work

The series of “green performance” estimation methods, the design assessment and optimization method, as well as the computer-aided-tool for China office building in early design stage is developed in this research, and has been proven to have a certain optimum accuracy and applicability, thus improving the quality of the conceptual design for green office building in China.

However, to optimise the present system and accelerate its wide application, further research is required as follows:

- The PE can be further studied and localized to improve its representativeness for a specific region. The PE involved in this research is created as a global figure, based on the analysis of existing research data for the EU, the US and China. Whereas the environmental impact of each pollutant varies by region. Thus, in order to reflect the environmental impact more accurately for a specific region, the weight of each pollutant in PE should be reviewed through the use of local environment research data.
- This application area of this research can be further extended. The series of “green performance” estimation methods established in this research are specialised for China’s green office building. The application area for these can be extended to other regions by remaining using the principles of these methods while updating the energy / pollutant estimation datasets through the study of localised building material / component data. For example, a simple approach to extending the China-focused cost estimation method (addressed in Appendix III) to another region is based on

using the updated international cost factor [185] to convert the building cost of China to that of the other country.

- The interface, input/output of the computer-aided tool can be refined to more user-friendly. Although the computer-aided tool developed in this research has full function, the interface for the input function of this tool can still be improved to enhance its applicability to building designers. Meanwhile, the current output format of this tool is the simple text file (CSV file), which is efficient for information gathering for tasks meant for research purpose. In the further development for output function, the key features of selected design solutions should be represented by simple figures that come with its “green preference” in the form of vivid tables and charts, in order to provide more intuitive and effective information for building designers.

## Appendix I: Datasets for building material

### Dataset 1: Specification for common glass products in China market

Unit: Thickness—m, Conductivity—W/mk,		Thickness	Conductivity	Transmittance
Clear glass	Clear glass 3mm	0.003	0.76	0.87
	Clear glass 5mm	0.005	0.76	0.84
	Clear glass 6mm	0.006	0.76	0.82
	Clear glass 12mm	0.012	0.76	0.74
Heat-absorbing glass	Green heat-absorbing glass	0.005	0.60	0.64
	Blue heat-absorbing glass	0.006	0.60	0.62
	Brown heat-absorbing glass	0.005	0.60	0.62
	Grey heat-absorbing glass	0.005	0.60	0.6
Heat reflective glass	High transmittance reflective glass	0.005	0.76	0.56
	Mid-transmittance reflective glass	0.006	0.76	0.43
	Low transmittance reflective glass	0.005	0.76	0.26
Low-E glass	High transmittance low-e glass	0.006	0.7	0.44
	Mid-transmittance low-e glass	0.006	0.7	0.35

### Dataset 2: The R-value for insulation material and infill wall block in China market

Specification: thickness (m)										
<b>XPS</b>	0.01	0.02	0.025	0.03	0.04	0.05	0.075	0.1	0.12	0.15
<b>R-value</b>	0.33	0.67	0.83	1.00	1.33	1.67	2.50	3.33	4.00	5.00
Specification: thickness (m)										
<b>EPS</b>	0.01	0.02	0.025	0.03	0.04	0.05	0.075	0.1	0.12	0.15
<b>R-value</b>	0.24	0.49	0.61	0.73	0.98	1.22	1.83	2.44	2.93	3.66
Specification: thickness (m)										
<b>Glasswool</b>	0.03		0.05			0.08		0.1		
<b>R-value</b>	0.97		1.61			2.58		3.23		
Specification: thickness (m)										
<b>EPS</b>	0.03		0.05			0.08		0.1		
<b>R-value</b>	0.86		1.43			2.29		2.86		
Specification: thickness (m)										
<b>AAC</b>	0.1	0.12	0.15	0.18	0.2	0.25	0.3			
<b>R-value</b>	0.63	0.75	0.94	1.13	1.25	1.56	1.88			
Specification: thickness (m)										
<b>CHB</b>	0.09		0.115			0.14		0.19		
<b>R-value</b>	0.16		0.21			0.25		0.34		
Specification: thickness (m)										
<b>CSB</b>	0.14					0.19				
<b>R-value</b>	0.11					0.15				
Specification: thickness (m)										
<b>CSSB</b>	0.14					0.19				
<b>R-value</b>	0.52					0.71				



Dataset 3:  $EF_M$  &  $PF_{M,j}$  for key materials of block/brick and insulation options

	Thickness (m)	$EF_M$ (MJ/ m <sup>2</sup> )	$PF_{M,CO_2e}$ (kg/ m <sup>2</sup> )	$PF_{M,SO_2}$ (kg/ m <sup>2</sup> )	$PF_{M,NO_x}$ (kg/ m <sup>2</sup> )	$PF_{M,PM}$ (kg/ m <sup>2</sup> )
AAC	0.1	587.4	51.6	18.66	0.108	0.162
	0.12	704.9	61.9	22.392	0.1296	0.1944
	0.15	881.1	77.4	27.99	0.162	0.243
	0.18	1057.3	92.9	33.588	0.1944	0.2916
	0.2	1174.8	103.2	37.32	0.216	0.324
	0.25	1468.5	129.0	46.65	0.27	0.405
	0.3	1762.2	154.8	55.98	0.324	0.486
CHB single hole	0.09	186.5	21.7	5.904	0.036	0.0504
	0.115	238.3	27.7	7.544	0.046	0.0644
	0.14	290.1	33.7	9.184	0.056	0.0784
	0.19	393.7	45.8	12.464	0.076	0.1064
CHB double hole	0.09	181.8	21.1	5.7564	0.0351	0.04914
	0.115	232.3	27.0	7.3554	0.04485	0.06279
	0.14	282.8	32.9	8.9544	0.0546	0.07644
	0.19	383.8	44.6	12.1524	0.0741	0.10374
CSB	0.14	561.8	59.9	17.7408	0.09856	0.14784
	0.19	762.4	81.3	24.0768	0.13376	0.20064
CCHB	0.14	191.5	20.4	6.048	0.0336	0.0504
	0.19	259.9	27.7	8.208	0.0456	0.0684
XPS	0.01	4.2	0.1	0.0216	0.00012	0.00018
	0.02	8.4	0.1	0.0432	0.00024	0.00036
	0.025	10.5	0.2	0.054	0.0003	0.00045
	0.03	12.6	0.2	0.0648	0.00036	0.00054
	0.04	16.8	0.3	0.0864	0.00048	0.00072
	0.05	21.0	0.4	0.108	0.0006	0.0009
	0.075	31.5	0.5	0.162	0.0009	0.00135
	0.1	42.0	0.7	0.216	0.0012	0.0018
	0.12	50.4	0.9	0.2592	0.00144	0.00216
	0.15	63.0	1.1	0.324	0.0018	0.0027
EPS	0.01	3.5	0.1	0.018	0.0001	0.00015
	0.02	7.0	0.1	0.036	0.0002	0.0003
	0.025	8.7	0.2	0.045	0.00025	0.000375
	0.03	10.5	0.2	0.054	0.0003	0.00045
	0.04	14.0	0.2	0.072	0.0004	0.0006
	0.05	17.5	0.3	0.09	0.0005	0.00075
	0.075	26.2	0.5	0.135	0.00075	0.001125
	0.1	35.0	0.6	0.18	0.001	0.0015
	0.12	42.0	0.7	0.216	0.0012	0.0018
	0.15	52.5	0.9	0.27	0.0015	0.00225
Glasswool	0.03	9.0	0.9	0.000432	0.003888	0.003744
	0.05	15.0	1.5	0.00072	0.00648	0.00624
	0.08	23.9	2.5	0.001152	0.010368	0.009984
	0.1	29.9	3.1	0.00144	0.01296	0.01248
Rockwool	0.03	15.6	2.0	0.0036	0.0324	0.0312
	0.05	26.0	3.3	0.006	0.054	0.052
	0.08	41.6	5.3	0.0096	0.0864	0.0832
	0.1	52.0	6.6	0.012	0.108	0.104

## Appendix II: Questionnaire

**Dear Sir / Madam,**

This questionnaire is used for a research on green building design optimization, carried out by PhD candidate Zishang Zhu in University of Hull. Your expertise and professional opinion is quite precious and valuable. Thank you very much for your time.

### **Part 1: Personal information** (You can ignore the optional questions if concerning privacy)

Name (optional): \_\_\_\_\_ Organization (optional): \_\_\_\_\_

Organization status (tick):

Industrial / Company       Education       Research institute

Other: \_\_\_\_\_

Occupation/position (tick):

Architect

MEP Engineer

Building owner / shareholder / investor       Building occupant / tenant only

Do you have experience or certificate on green building design/operation?

Yes       No

If yes, how many year experience do you have? \_\_\_\_\_

Type of certificate: \_\_\_\_\_

### **Part 2: Subjective judgment for 10 building design scenario**

The following tables (table 1 - table 10) are prepared respectively for different green building design preference scenario, each design preference scenario is set to achieving dedicate design purpose. For each table, could you please select no more than 3 key criterion (from options below) that you believe significantly relevant to the key performance and purpose of this preference scenario? The selection should base on the aim and usage scenario of each preference scenario that described in each table.

After select the key criterion, please judge the importance among each criteria for specific scenario. Please use the fundamental verbal scale 1 to 9 (see table 11) to representing the pairwise importance.

The judgment result should be recorded in the “Pairwise Importance” section in the bottom of each table. For example, key criteria 2 is strongly important than the key criteria 3, then key criteria 2 is 5 times as importance as key criteria 3, the pairwise importance of A23 is 5.

#### **Key criterion options for table 1-10:**

**A**--Life-cycle energy consumption

**B**-- Embodied energy consumption

**C**-- Operational energy consumption

**D**-- Life-cycle environmental impact

**E**-- Embodied environmental impact

**F**--Operational environmental impact

**G**—Life-cycle cost

**H**—Initial building cost

**I**—Operational building cost











Table 11: Fundamental verbal scale

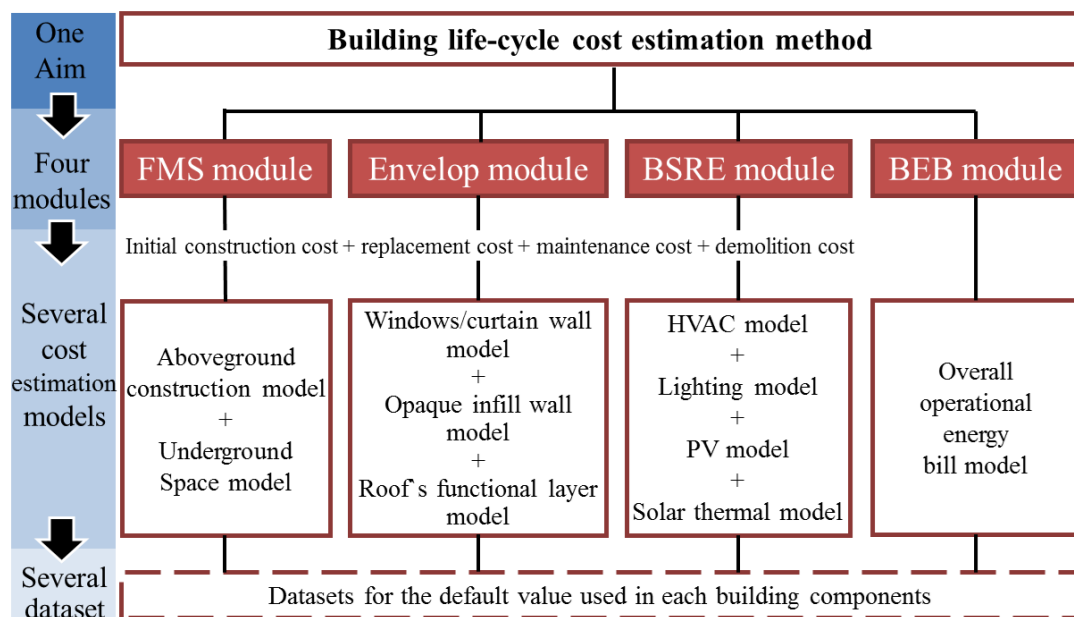
Importance	Definition	Explanation
1	Equally important	Two activities contribute equally to the objective
2	Weakly or slightly important	
3	Moderately more important	Experience and judgment slightly favor one activity over another
4	Moderately plus important	
5	Strongly important	Experience and judgment strongly favor one activity over another
6	Strongly plus important	
7	Very strong or demonstrably important	An activity is favored very strongly over another; its dominance demonstrated in practice
8	Very, very strongly important	
9	Absolutely or extremely important	The evidence favoring one activity over another is of the highest possible order of affirmation



## Appendix III: The simplified life-cycle office building cost estimation method

### 1. Methodology

The cost estimation method for office building falls into 4 modules which are (1) **fix main structure module (FMS module)**, (2) **envelope module**, (3) **building service and renewable energy system module (BSRE module)**, and (4) **building energy bill module (BEB module)**. For the former three module, the building cost come from 4 phases, including (1) initial construction cost, (2) replacement cost caused by the service life of components, (3) maintenance cost and (4) demolition cost, whereas for the latter module, the cost is simply calculated as a whole. The structure of building cost estimation method is described in figure below.



The cost-area ratio (£ / m<sup>2</sup>) method is used in the cost estimation for FMS module, and envelope module. For FMS module, the gross floor area is used in estimation, whereas for envelop module, the applied area each for building components (e.g. windows, wall blocks, insulation layers) is used.

The cost-power ratio (£ / kW) method is used in the cost estimation for BERE module and BIRE module. The heating/cooling capacity and design lighting power is used for

HVAC and lighting system, as well as design output power for PV and solar thermal system.

The fixed electricity price (£/kWh) method is used in BEB module, the multistep electricity price or daytime nighttime price difference is not considered in order to simplify the calculation.

Dataset for typical cost-area ratio and cost-power ratio is summarized for each module by the study of “construction cost statistical data” of typical building case and literature review of renewable energy cost study, the value is only used for convenience of this study. The dataset need to be reviewed and revised base on the local and real-time data before each green building design task.

## **2. Simplified cost estimation method and dataset for fixed main structure (FMS module)**

The FMS module is the fabric of building, contains all load-bearing structure including floor and ceiling, load-bearing pillars, share wall, load-bearing layer of roof, basement and foundation, as well as the embedded pipelines and wiring. The initial construction cost, maintenance cost and demolition cost are considered, whereas the replacement cost is nil as the FMS can serve for all building design life (50year). The FMS cost ( $C_{FMS}$ ) can be estimated by equation below:

$$C_{FMS} = [r_{a,i}(1 + m_{a,i})t_{i,B} + d_{a,i}]GFA_a + [r_u(1 + m_u)t_{i,B} + d_u]GFA_u$$

Where:  $r_{a,i}$  and  $d_{a,i}$  are the cost-area ratio (£ / m<sup>2</sup>) for the above ground area of structure type  $i$  for construction and demolition work respectively;  $m_{a,i}$  and  $m_u$  are the maintenance cost ratio per year for the above ground area and underground area respectively;  $t_{i,B}$  is the service life of building, take 50 in this research;  $r_u$  and  $d_u$  are the cost-area ratio (£ / m<sup>2</sup>) for the underground ground area of structure type  $i$  for construction and demolition work respectively;  $GFA_a$  and  $GFA_u$  are the gross floor area for aboveground part and underground part respectively.

**The dataset for typical area-cost ratio and related variables** are represented by simple steady state values for each structure type, They are summarized from 93 building samples, which has been described in chapter 4, section 4.2.2 b, including 12 MS-RCF office buildings, 23 HR-RCF office buildings, 31 HR-RCF-SW/T office buildings and 27 HR-SF-SW/T office buildings. The dataset of default value can be seen in table below.

Construction type	$r_{a,i}$ (£/m <sup>2</sup> )	$r_u$ (£/m <sup>2</sup> )	$m_{a,i}$ (%)	$m_u$ (%)	$d_{a,i}$ (£/m <sup>2</sup> ) [186]	$d_u$ (£/m <sup>2</sup> ) [186]
MS-RCF	290	280	0.5	0.5	5	5
HR-RCF	465				5	
HR-RCF-SW/T	635				7	
HR-SF-SW/T	680				7	

### 3. Simplified cost estimation model for building envelope

The estimated total cost for building envelop module ( $C_{env}$ ) including the cost from windows/glass curtain wall ( $C_{WIN}$ ), infill wall ( $C_{WALL}$ ), and the functional layer of roof ( $C_{FLR}$ ). The life-cycle cost comes from the initial installation cost, maintenance cost and replacement cost, whereas the demolition cost is nil as it` has already included in FMS module. The cost estimation method is descried below.

**For the windows and glass curtain wall,** the life-cycle cost is derived from the cost-area ratio (£/m<sup>2</sup>) of frame and glass for the window/glass curtain wall applied area, and expressed in equation below.

$$C_{WIN} = (r_{frame,m} + r_{glass,n})A_{win} \left[ \frac{t_B}{t_i} \right] (1 + m_j)t_B$$

Where:  $r_{frame,m}$  and  $r_{glass,n}$  are the cost-area ratio (£/m<sup>2</sup>) for frame and glass respectively;  $A_{win}$  is the windows window/glass curtain wall applied area. The service life for windows/glass curtain wall,  $t_i$ , is 30 year. The annual maintenance cost ratio,  $m_j$ , is 1%.

**For the infill wall,** the life-cycle cost is derived from the cost-volume ratio (£/m<sup>3</sup>) of wall block, insulation layer and decoration layer for the applied wall area, and expressed in equation below.

$$C_{WALL} = (R_{block,m} + R_{block,funda,m})d_{block,m}A_{wall} + (R_{insu,n}d_{insu,n} + r_{insu,funda,n})A_{wall} \left[ \frac{t_B}{t_i} \right] + r_{exter,h}A_{wall} \left[ \frac{t_B}{t_e} \right] + r_{inter,k}A_{wall} \left[ \frac{t_B}{t_r} \right]$$

Where:  $R_{block,m}$  and  $R_{block,funda,m}$  are the cost-volume ratio (£/m<sup>3</sup>) for wall block and the fundamental cost (i.e. mortar, accessory, labor) in wall block construction respectively;  $R_{insu,n}$  is the cost-volume ratio (£/m<sup>3</sup>) of insulation layer;  $r_{insu,funda,n}$  are the cost-area ratio (£/m<sup>2</sup>) of the fundamental cost in insulation layer construction;  $r_{exter,h}$  and  $r_{inter,k}$  are the cost-area ratio (£/m<sup>2</sup>) for external and internal decoration layer respectively;  $d_{block,m}$  and  $d_{insu,n}$  is the thickness (m) of building block and insulation layer respectively;  $A_{wall}$  is the infill wall area. The service life for insulation layer,  $t_i$ , external decoration layer,  $t_e$ , and internal decoration layer,  $t_r$ , is 30 years, 30 years and 10years respectively.

**For the functional layer on roof**, the life-cycle cost is derived from the cost-volume ratio (£/m<sup>3</sup>) of insulation layer and cost-area ratio (£/m<sup>2</sup>) of green roof layer for the applied roof area, and expressed in equation below.

$$C_{FLR} = (R_{insu,m} + r_{insu,funda,m})A_{roof} \left[ \frac{t_B}{t_i} \right] (1 + m_m)t_B + r_{green,n}A_{roof}(1 + m_n)t_B$$

Where:  $R_{insu,m}$  is the cost-volume ratio (£/m<sup>3</sup>) of insulation layer;  $r_{insu,funda,m}$  is the cost-area ratio (£/m<sup>2</sup>) of fundamental cost (i.e. waterproofing, accessory, labor) in roof insulation construction;  $r_{green,n}$  is the cost-area ratio for green roof layer;  $A_{roof}$  is the roof area. The service life for insulation layer,  $t_i$ , is 30 years.

**The dataset for typical variables in building envelope module** are represented by simple steady state values and listed in table below.

Window/Glass curtain wall				
Windows frame	Aluminum frame	Aluminum frame with thermal break	PVC frame	Wood frame
$r_{frame,m}$ (£/ m <sup>2</sup> )	25	40	22	20
Glass curtain	Aluminum frame	Aluminum frame	Aluminum frame	Aluminum frame

<b>wall frame</b>	(<5 storey)	with thermal break (<5 storey)	(6-20 storey)	with thermal break (6-20 storey)
$r_{frame,m}$ (£/ m <sup>2</sup> )	70	95	117	142
<b>Glass</b>	9mm clear	9mm Low-E	9mm Low-e+12A+9mm	9mm Low-e+12A (argon)+9mm
$r_{glass,n}$ (£/ m <sup>2</sup> )	5	9	28	33
<b>Infill wall</b>				
<b>wall block</b>	AAC	CHB	CSB	CCHB
$R_{block,m}$ (£/ m <sup>3</sup> )	76	27	23	40
$R_{block,funda,m}$ (£/ m <sup>3</sup> )	26	26	26	26
<b>Insulation</b>	XPS	EPS	Glasswool	Rockwool
$R_{insu,n}$ (£/ m <sup>3</sup> )	73	55	25	45
$r_{insu,funda,n}$ (£/ m <sup>2</sup> )	5	5	5	5
<b>External decoration</b>	Glazed facing tile		Dry hanging marble curtain wall	
$r_{exter,h}$ (£/ m <sup>2</sup> )	10		68	
<b>Internal decoration</b>	lime mortar plaster			
$r_{inter,k}$ (£/ m <sup>2</sup> )	6			
<b>Functional layer on roof</b>				
<b>Insulation</b>	XPS		EPS	
$R_{insu,m}$ (£/ m <sup>3</sup> )	73		55	
$r_{insu,funda,m}$ (£/ m <sup>2</sup> )	5		5	
$m_m$ (%)	3		3	
<b>Green roof</b>	Simple green roof		Garden style green roof	
$r_{green,n}$ (£/ m <sup>2</sup> )	35		62	
$m_n$ (%)	6		4	

#### 4. Simplified cost estimation method for building service and renewable energy system module (BSRE module)

The estimated total cost for BSRE module ( $C_{BSRE}$ ) including the cost from HVAC ( $C_{HVAC}$ ), lighting ( $C_{light}$ ), BIPV ( $C_{BIPV}$ ) and building integrated solar thermal system ( $C_{BIST}$ ). The life-cycle cost also comes from the initial installation cost, maintenance cost and replacement cost, the demolition cost has already included in FMS module. The cost estimation method is described below.

**For HVAC system**, the life-cycle cost is derived from the designed maximum heating/cooling capacity ( $\Phi_{HC,nd,max}$ , estimated by chapter 3), and expressed in equation below.

$$C_{HVAC} = r_{HVAC,i} \Phi_{HC,nd,max} \left[ \frac{t_B}{t_i} \right] (1 + m_i) t_B$$

Where:  $r_{HVAC,i}$  is the cost-power ratio for HVAC type  $i$ ;  $\Phi_{HC,nd,max}$  is the maximum

heating/cooling need estimated in chapter 3;  $t_i$  is the service life for HVAC system.

**For lighting system**, the life-cycle cost is derived from the cost-power ratio (£/m<sup>2</sup>) and designed lighting power density (kW/m<sup>2</sup>), and expressed in equation below.

$$C_{light} = (r_{light,i}D_{light,a}GFA_a + r_{light,i}D_{light,u}GFA_u) \left[ \frac{t_B}{t_i} \right]$$

Where:  $r_{light,i}$  is the cost-power ratio for lighting type  $i$ ;  $D_{light,a}$  and  $D_{light,u}$  are the designed lighting power density (kW/m<sup>2</sup>) for aboveground space and underground space respectively.

**For BIPV system**, the life-cycle cost is derived from the designed output (kW) of PV array, and expressed in equation below.

$$C_{BIPV} = r_{BIPV} \Phi_{BIPV} \left[ \frac{t_B}{t_i} \right]$$

Where:  $r_{BIPV}$  is the cost-power ratio for lighting type  $i$ ;  $D_{light,a}$  and  $D_{light,u}$  are the designed lighting power density (kW/m<sup>2</sup>) for aboveground space and underground space respectively.

**For building integrated solar thermal system**, the life-cycle cost is derived from the panel area (m<sup>2</sup>) of solar thermal collector, and expressed in equation below.

$$C_{BIST} = r_{BIST} A_{BIST} \left[ \frac{t_B}{t_i} \right] (1 + m_i) t_B$$

**The dataset for typical variables in BSRE module** are represented by simple steady state values and listed in table below.

HVAC [187]	$r_{HVAC,i}$ (£/kW)	$t_B$ (yr)	$t_i$ (yr)	$m_i$ (%)	
VRV/VRF	490	50	20	1	
Air-cooled chilled water system	425			1.2	
Water-cooled chilled water system	450			1.5	
Lighting	$r_{light,i}$ (£/kW)	$t_B$ (yr)	$t_i$ (yr)	$D_{light,a}$ (w/m <sup>2</sup> )	$D_{light,u}$ (w/m <sup>2</sup> )
CFL	2.4	50	3	9	4
LED	3.8		10	7	3

<b>BIPV</b>	$r_{BIPV}$ (£/kW)	$t_B$ (yr)	$t_i$ (yr)		
BIPV array (poly-Si)	550	50	20		
<b>Building integrated solar thermal</b>	$r_{BIST}$ (£/m <sup>2</sup> )	$t_B$ (yr)	$t_i$ (yr)	$m_i$ (%)	
Flat solar panel	56	50	20	1	

### 5. Simplified cost estimation method for building energy bill module (BEB module).

The estimated total cost for BEB module ( $C_{BEB}$ ) is the sum of energy bill for all energy source and expressed in equation below.

$$C_{BEB} = \sum_j^i Q_i r_i t_B$$

Where: the  $Q_i$  is the annul energy cost (kWh) for energy source  $i$ ;  $r_i$  is the unite-price (£/kWh) for energy source  $i$ ;

In this research, the only energy source for office building is electricity (taken from chapter 3), the average price for commercial electricity in Shanghai (£ 0.102) [188] is taken to reflect the price in China.

### Appendix IV: Calculation data for validation of CN13790

The annual heating demands (kWh/m<sup>2</sup>) of 9 building cases by each calculation method

Building cases Tools	Standard	H-W	L-W	H-I	L-I	H-GR	L-GR	H-IG	L-IG
CN13790	43	43	52	29	78	64	32	29	54
EnergyPlus	40	37	45	28	65	53	29	27	47
ESP-r	38	32	43	27	62	50	27	26	45
Degree-Day	51	51	51	39	99	78	40	39	71

The annual cooling demands (kWh/m<sup>2</sup>) of 9 building cases by each calculation method

Building cases Tools	Standard	H-W	L-W	H-I	L-I	H-GR	L-GR	H-IG	L-IG
CN13790	69	69	74	54	90	80	64	75	48
EnergyPlus	55.1	54.15	62.7	44.65	74.1	67.45	53.2	64.6	42.75
ESP-r	59.85	58.9	62.7	48.45	75.05	68.4	56.05	66.5	44.65
Degree-Day	85	85	85	65	108	98	72	88	62

The annual heating demands (kWh/m<sup>2</sup>) of 9 building cases by each calculation method

Building cases Tools	Harbin (H)	Harbin (C)	BeiJing (H)	BeiJing (C)	ShangH (H)	ShangH (C)	GuangZ (C)	KunM (C)
CN13790	83	45	67	54	43	69	96	16
EnergyPlus	76	35	62	42	40	55.1	78	13
ESP-r	73	38	59	47	38	59.85	83	14
Degree-Day	116	62	82	73	56	85	138	25



## References

1. U.S. DEPARTMENT OF ENERGY , D&R INTERNATIONAL, LTD.. **2005 Buildings Energy Data Book**. Silver Spring, Maryland: DOE, 2005.
2. NATURE RESOURCE CANADA. **Energy efficiency trends in Canada 1990-2001**. Ottawa: Natural Resources Canada, 2003,.
3. EUROPEAN UNION. **EU energy in figures, statistical pocket book 2007/2008**. Luxembourg: Publications Office of the European Union, 2008.
4. COMMISSION OF THE EUROPEAN COMMUNITIES. **COMMISSION STAFF WORKING DOCUMENT: PROPOSAL FOR A RECAST OF THE ENERGY PERFORMANCE OF BUILDINGS DIRECTIVE (2002/91/EC) - SUMMARY OF THE IMPACT ASSESSMENT**. Eu. Brussels. 2008.
5. CAI, W. G. . W. Y. . Z. Y. . R. H. China building energy consumption: situation, challenges and corresponding measures.. **Energy Policy**, , n. 37, p. 2054–2059., 2009.
6. ZHAO, J. . Y. W. A. N. Z. Implementing effect of energy efficiency supervision system for government office buildings and large-scale public buildings in China.. **Energy Policy**, v. 37, n. 6, p. 2079-2086., 2009.
7. ENERGY COMMISSION (EC). **Statistics of Electricity Supply in Malaysia**. . Malaysia: Energy Commission. [S.l.]. 2007..
8. HAN, B. . Y. D. Calculation and analysis of energy consumption of energy efficient buildings in heating period.. **Architectural Design Management**, v. 5, p. 56–60., 2006.
9. SU, M. **Research on Economic Incentives and Policy to Promote Construction Energy Saving in China**. Beijing: China Finance and economic publishing house, 2011.
10. DEPARTMENT OF ENERGY. **Building Energy Data Book**. US: [s.n.], 2003.
11. RESERACH CENTER FOR BUILDING ENERGY SAVING, TSINGHUA UNIVERSITY. **Annual report for the progress of China building energy saving**. Beijing: China building industry press, 2015.
12. WANG, W. . R. Z. A. H. R. Applying multi-objective genetic algorithms in green building design optimization. **Building and Environment**, v. 40, n. 11, p. 1512-1525, 2005.
13. SUSTAINABLE BUILDINGS AND CLIMATE INITIATIV. **TOWARDS A COMMON CARBON METRIC: Protocol for Measuring Energy Use and Reporting Greenhouse Gas Emissions from Building Operations**. UNEP. [S.l.], p. 66. 2013.
14. JAN CORFEE-MORLOT, JANE ELLIS, SARA MOARIF. **Measurable, Reportable and Verifiable Mitigation Actions and Support ---A summary of OECD/IEA analyses for COP 15**. OECD, IEA. Bali. 2008.
15. PENG WU, Y. S. W. S. H. C. H.-Y. C. M. S. A comprehensive analysis of the credits obtained by LEED 2009 certified green buildings. **Renewable and Sustainable Energy Reviews**, v. 68, p. 370-379, fev. 2017.
16. U.S. DEPARTMENT OF ENERGY (DOE). **Buildings Energy Data Book**. [S.l.]: DOE, v. 1.1.1, 2008.
17. DEPARTMENT OF ENERGY AND CLIMATE CHANGE, UK. **DECC Annual Report and Accounts**. LONDON: The Stationery Office, 2010–2011.
18. LI, D. et al. **Research on Energy Consumption Standard for Public Buildings**. China Energy

- Foundation, China Ministry of Housing and Urban-Rural Development. Beijing. 2014.
19. PACHAURI, R. K. A. R. A. **IPCC Fourth Assessment Report: Climate Change 2007**. IPCC. Geneva, Switzerland, p. 104. 2007.
  20. OSTRO, B. **Outdoor air pollution: assessing the environmental burden of disease at national and local levels**. WHO. Geneva, Switzerland. 2004. (ISSN1728-1652).
  21. IPCC. **TOWARDS A COMMON CARBON METRIC: Protocol for Measuring Energy Use and Reporting Greenhouse Gas Emissions from Building Operations**. Sustainable Consumption & Production, IPCC, UNEP. [S.l.]. 2013.
  22. EGGLESTON H.S., B. L. . M. K. . N. T. **2006 IPCC Guidelines for National Greenhouse Gas Inventories**. IPCC National Greenhouse Gas Inventories Programme Technical Support Unit. Kamiyamaguchi, Hayama, Kanagawa, Japan. 2006.
  23. EPA. Air Emissions Inventories--Air Emission Sources. **United States Environmental Protection Agency**, 2016. Disponivel em: <[https://www3.epa.gov/cgi-bin/broker?polchoice=NOX&\\_debug=0&\\_service=data&\\_program=dataprog.national\\_1.sas](https://www3.epa.gov/cgi-bin/broker?polchoice=NOX&_debug=0&_service=data&_program=dataprog.national_1.sas)>. Acesso em: 10 nov. 2016.
  24. ICOPAL GROUP. Nitrogen Oxide (NOx) Pollution. **ICOPAL Group**, 2016. Disponivel em: <<http://www.icopal-noxite.co.uk/nox-problem/nox-pollution.aspx>>. Acesso em: 10 dez. 2016.
  25. DEPARTMENT OF THE ENVIRONMENT AND HERITAGE. Environment protection publications and resources: Sulfur dioxide (SO2). **Australian Government, Department of the Environment and Energy**, 2005. Disponivel em: <<https://www.environment.gov.au/protection/publications/factsheet-sulfur-dioxide-so2>>. Acesso em: 10 dez. 2016.
  26. EPA. Air Emissions Inventories: Air Emission Sources- National Summary of Sulfur Dioxide Emissions. **United State Environmental Protection Agency**, 2016. Disponivel em: <[https://www3.epa.gov/cgi-bin/broker?polchoice=SO2&\\_debug=0&\\_service=data&\\_program=dataprog.national\\_1.sas](https://www3.epa.gov/cgi-bin/broker?polchoice=SO2&_debug=0&_service=data&_program=dataprog.national_1.sas)>. Acesso em: 10 dez. 2016.
  27. MORRIS, P. I. **Understanding Biodeterioration of Wood in Structures**. Forintek Canada Corp, and British Columbia Building Envelope. BritishColumbia.
  28. JINCHUN SHEN, X. Z. X. Z. W. H. Active Solar Thermal Facades (ASTF) – from Concept, Fundamental to Application. **Renewable & Sustainable Energy Reviews**, n. 50, p. 32-63, 2015.
  29. RAINER ARINGHOFF, G. B. S. T. **CONCENTRATED SOLAR THERMAL POWER – NOW! Edit by Cecilia Baker. 2005**. [S.l.]: [s.n.].
  30. PENG XU, JINGCHUN SHEN, XINGXING ZHANG, WEI HE, XUDONG ZHAO. Design, Fabrication and Experimental Study of a Novel Loop-heat-pipe Based Solar Thermal Facade Water Heating System. **Energy Procedia**, v. 75, p. 566-571, 2015. ISSN ISSN 1876-6102.
  31. X.Q. ZHAI, R. Z. W. Y. J. D. J. Y. W. Q. M. Experience on integration of solar thermal technologies with green buildings. **Renewable Energy**, n. 33, p. 1904–1910., 2008.
  32. FLORSCHUETZ, L. W. Extension of the Hottel-Whillier model to the analysis of combined photovoltaic/thermal flat plate collectors. **Solar Energy**, v. 22, n. 4, p. 361-366, 1979.
  33. MAYANK PATEL, K. P. A CRITICAL REVIEW OF EVACUATED TUBE COLLECTOR. **International Journal**

of **Advanced Engineering Research and Studies**, v. 2, n. 3, p. 55-56, April-June 2013.

34. C, PERL. Flatplate vs. EHTP. **Wayback Machine**. Disponível em: <<http://www.ateliving.com/pdf/Vacuum-Tube-Collector-andFlat-Plat-Collector-comparation.pdf>>. Acesso em: 25 out. 2015.
35. P. XU, J. S. X. Z. W. H. X. Z. **Design, Fabrication and Experimental Study of a Novel Loopheat-pipe based Solar Thermal Facade Water Heating System**. The 7th International Conference on Applied Energy – ICAE2015. Abu Dhabi: [s.n.]. March 2015.
36. LI ZF, S. K. Experimental studies on a solar powered air conditioning system with partitioned hot water storage tank.. **Sol Energy** **2001**, v. 5, n. 75, p. 285-297, 2001.
37. ZINIAN H, N. Z. E. A. Design and performance of a solar absorption air-conditioning and heat-supply system (in Chinese).. **Acta Energiae Solaris Sinica** , v. 1, n. 22, p. 6-11, 2001.
38. HAYWOOD A, S. J. P. P. V. G. G. S. S. **A sustain-able data center with heat-activated cooling**. Proceedings of IThERM 2010, 12th intersociety conference. ;. Las Vegas (NV, USA): [s.n.]. June 2 - June 5, 2010.
39. HAYWOODA, S. . V. G. Thermo-dynamic feasibility of harvesting datacenter waste heat to drive an absorption chiller. **EnergyConversManage**, n. 58, p. 26–34, 2012.
40. HAGEMANN, I. B. **Gebäudeintegrierte Photovoltaik – Architektonische Integration der Photovoltaik in die Geba "uhu " lle**. [S.l.]: [s.n.], 2002.
41. REIJENGA, T. What do architects need?. **Proceedings of the IEA PVPS Task VII**. , fev. 2000.
42. XINGXING ZHANG, J. S. X. Z. Y. X. B. N. **A Pilot-scale Demonstration of a Novel Solar Photovoltaic/thermal (PV/T) System and its Scenarios for Future Development**. 2nd International Symposium on Energy Challenges and Mechanics (ECM2). Aberdeen, UK: [s.n.]. 08/2014.
43. GIPE, P. Germany To Raise Solar Target for 2010 & Adjust Tariffs,. **Renewable Energy News Article**. Disponível em: <<http://www.renewableenergyworld.com/rea/news/article/2010/06/germany-to-raise-solar-target-for-2010-adjust-tariffs>>. Acesso em: 10 dez. 2015.
44. CHANGE, D. O. E. A. C. **UK Solar PV Strategy Part 2: Delivering a Brighter Future**. Information Policy Team of Department of Energy and Climate Change. London.
45. UNIVERSITY OF CALIFORNIA, SAN DIEGO.. Solar panels keep buildings cool.. **Science Daily**. Disponível em: <<http://www.sciencedaily.com/releases/2011/07/110718151558.htm>>. Acesso em: 19 jul. 2011.
46. S-ENERGY. BIPV Module. **S-Energy official website**. Disponível em: <[http://www.s-energy.com/epage.php?it\\_id=1426727258](http://www.s-energy.com/epage.php?it_id=1426727258)>. Acesso em: 02 dez. 2016.
47. TUĞÇ, E KAZANASMAZ, E. U. G. G. E. A. On the relation between architectural considerations and heating energy performance of Turkish residential buildings in Izmir. **Energy and Buildings**, n. 72, p. 38-50, 2014.
48. XINZHI GONG\*, Y. A. D. S. Optimization of passive design measures for residential buildings in different Chinese areas. **Building and Environment**, n. 58, p. 46-57, 2012.
49. DEVELOPMENT, C. M. O. H. A. U.-R. **Design standard for energy efficiency of residential buildings in hot summer and cold winter zone**. Beijing: China Building Industry Press, 2010.

50. KERRY HAGLUND, E. W. C. Windows for high-performance commercial buildings. **Design: Parameters--Window Area**, 2015. Disponivel em: <[www.commercialwindows.org/wvr.php](http://www.commercialwindows.org/wvr.php)>. Acesso em: 10 dez. 2016.
51. CHINA MINISTRY OF HOUSING AND URBAN-RURAL DEVELOPMENT. **GB 50189 Design standard for energy efficiency of public buildings**. China Ministry of Housing and Urban-Rural Development. Beijing. 2015.
52. MCBRIDE, S. L. Insulation: EPS and XPS. **Buildings Smarter Facility Management**, 2016. Disponivel em: <<http://www.buildings.com/article-details/articleid/8498/title/insulation-eps-and-xps>>. Acesso em: 15 dez. 3.
53. KAI WANG, Y. Y. The advantages and disadvantages of XPS, EPS and their`s part used in building exterior insulation. **New building material and technology**, v. 03, 2009. ISSN TU761.12.
54. EUROPEAN COMMITTEE FOR STANDARDIZATION. **EN 1996-1-1: Eurocode 6 - Design of masonry structures. Part 1-1: General rules for reinforced and unreinforced masonry structures**. 1996 Edition. ed. [S.l.]: European Committee, 2005.
55. INSYSME. **Report on types of structural frames, related enclosure wall systems, and requirements for the construction systems, INSYSME, Innovative Systems for Earthquake Resistant Masonry Enclosures in RC buildings**. INSYSME. [S.l.]. 2015.
56. YANYI SUN, Y. W. **How to achieve comfortable in a glass-box building**. 9th International Energy Forum on Advanced Building Skins. Bressanone, Italy: [s.n.].
57. UNIVERSITY OF MINNESOTA AND LAWRENCE BERKELEY NATIONAL LABORATORY. WINDOW TECHNOLOGIES: Glass, Visible Transmittance (VT or Tvis). **Windows for high-performance commercial buildings**, 2015. Disponivel em: <<http://www.commercialwindows.org/vt.php>>. Acesso em: 6 dez. 2016.
58. DU SILE, L. R. Z. Optimization of Spacing Design for Double Hollow Glass. **Forest Engineering**, Harbin, n. 5, 2012.
59. ZINCO GMBH. **Planning Guide: System Solutions for Extensive Green Park**. ZinCo GmbH. [S.l.]. 2011.
60. THE GREEN ROOF CENTRE, SHEFFIELD UNIVERSITY. **The green roof development guide**. The Green Roof Centre, Sheffield University. Sheffield, UK. 2011.
61. C. FENG, Q. M. Y. Z. Theoretical and experimental analysis of the energy balance of extensive green roofs. **Energy and Buildings**, n. 42, p. 959–965, 2010.
62. CAMBRIDGE UNIVERSITY. **FiBRE—Findings in Built and Rural Environments, Can Greenery Make Commercial Buildings More Green?** Cambridge : Cambridge University PRESS, 2007.
63. GAFFIN. **Energy balance modelling applied to a comparison of white and green roof cooling efficiency, in: Greening Rooftops for Sustainable Communities**. Washington, DC: [s.n.], 2005.
64. WASHINGTON STATE UNIVERSITY. **Energy Efficiency Factsheet - Reflective Roof Coatings**. Washington State University. Washington DC. 1993.
65. A. NIACHOU, E. A. Analysis of the green roof thermal properties and investigation of its energy performance. **Energy and Buildings** , v. 33, n. 7, p. 719–729., 2001.
66. N.H. WONG, E. A. The effects of rooftop garden on energy consumption of acommercial building in Singapore. **Energy and Buildings** , v. 35, n. 4, p. 353–364, 2003.

67. MONCEF KRARTI. **Energy Audit of Building Systems: An Engineering Approach**. 2. ed. Boca Raton, USA: CRC Press Tylor&Francis Group, 8 November 2010. ISBN ISBN: 13:978-1-4398-2872-2.
68. H.C., T. Seasonal degree day statics for the United States. **Monthly Weather Review**, v. 80, n. 2, p. 143-149, 1952.
69. PARKEN, W. H. . A. K. G. E. **Estimating residential seasonal cooling requirements**. Washington, DC: National Bureau of Standards, 1981.
70. KUSUDA, T. **A variable-base degree-day method for simplified residential energy analysis**. Washington, DC: National Bureau of Standards, 1981.
71. WEN, J. **Doctoral thesis: "Basic study of evaluation method of energy consumption in buildings"**. The University of Tokyo. Tokyo. 1989.
72. STEFANO CORGNATI, T. B. Y. J. **Statistical analysis and prediction methods: Separate Document Volume V (Total energy use in buildings, analysis and evaluation methods,Final Report Annex 53)**. International Energy Agency. [S.l.]. 14.11.2013.
73. HARRIMAN, L. G. E. A. New weather data for energy calculation. **ASHRAE Journal**, v. 39, n. 11, 1999.
74. COHEN, B. A. K. D. R. Humidity issues in bin energy analysis. **Heating/Piping/Air Conditioning**, v. 72, n. 1, p. 65-78, 2000.
75. DOE. The home of DOE-2 based building energy use and cost analysis software. **DOE-2**, 2000. Disponivel em: <<http://doe2.com/>>. Acesso em: 18 dez. 2016.
76. INTERNATIONAL ORGANIZATION FOR STANDARDIZATION. **ISO 832**. 2. ed. [S.l.]: ISO, 11.1994.
77. INTERNATIONAL ORGANIZATION FOR STANDARDIZATION. **ISO 13790: 2008 Energy performance of buildings -- Calculation of energy use for space heating and cooling**. 2. ed. [S.l.]: ISO, 3.2008.
78. JOKISALO, J. . A. J. K. J. Performance of EN ISO 13790 utilisation factor heat demand calculation method in a cold climate. **Energy and Buildings**, v. 39, p. 236-247., 2007.
79. CORRADO, V. . A. E. F. E. Assessment of building cooling energy need through a quasi-steady state model: Simplified correlation for gain-loss mismatch. **Energy and Buildings**, v. 39, p. 569-579, 2007.
80. J.A. OROSA, J. A. . A. A. C. O. A. C. Implementation of a method in EN ISO 13790 for calculating the utilisation factor taking into account different permeability levels of internal coverings. **Energy and Buildings**. , v. 42, p. 2282-2288., 2010.
81. M.J.N. OLIVEIRA PANÃO, M. J. N. . S. M. L. C. S. M. L. . A. H. J. P. G. H. J. P. Assessment of the Portuguese building thermal code: Newly revised requirements for cooling energy needs used to prevent the overheating of buildings in the summer. **Energy**, v. 36, p. 3262-3271, 2011.
82. GASPARELLA, A. Extensive comparative analysis of building energy simulation codes: Heating and cooling energy needs and peak loads calculation in TRNSYS and EnergyPlus for southern Europe climates. **HVAR&R Research**, out. 2012.
83. RICHARD B. CURTIS, B. B. W. F. B. E. E. E. C. THE DOE-2 BUILDING ENERGY ANALYSIS PROGRAM. **Conference on Energy Conservation in Buildings in Singapore**, Singapore, maio 1984.
84. BIRDSALL, B. . B. W. F. . E. K. L. . E. A. E. . A. W. F. C. **Overview of the DOE-2 building energy analysis program, Version 2.1D**. Lawrence Berkeley Laboratory. CA, p. 53. 1990.

85. U.S. DEPARTMENT OF ENERGY. **EnergyPlus™ Version 8.6 Documentation: Engineering Reference**. U.S. Department of Energy. [S.I.]. 30.09.2016.
86. D.B. CRAWLEYA, L. K. L. F. C. W. W. F. B. Y. J. H. C. O. P. R. K. S. R. J. L. D. E. F. M. J. W. J. G. EnergyPlus: creating a new-generation building energy simulation program. **Energy and Buildings** , v. 33, p. 319-331, 2001.
87. NATIONAL LABORATORY OF THE U.S. DEPARTMENT OF ENERGY. **Engineering Reference: The Reference to EnergyPlus Calculations**. National Laboratory of the U.S. Department of Energy, Alliance for Sustainable Energy, LLC. [S.I.].
88. THE BOARD OF TRUSTEES OF THE UNIVERSITY OF ILLINOIS AND THE REGENTS OF THE UNIVERSITY OF CALIFORNIA THROUGH THE ERNEST ORLANDO LAWRENCE BERKELEY NATIONAL LABORATORY. **Getting Started with EnergyPlus-Basic Concepts Manual - Essential Information**. [S.I.]. 1996-2010.
89. WILTSHIRE J, W. A. **The evaluation of the simulation models ESP, HTB2 and SERI-RES for the UK Passive Solar Program**. Energy Technology Support Unit. Department of Energy,. London. 1987.
90. HAND, J. W. **Strategies for Deploying Virtual Representations of the Built Environment**. Energy Systems Research Unit, Department of Mechanical and Aerospace Engineering, University of Strathclyde. Glasgow. 22.06.2015.
91. CAKMANUS, I. Renovation of existing office buildings in regard to energy economy: An example from Ankara, Turkey. **Building and environment**, n. 42, p. 1348-1357, 2007.
92. BÖHRINGER, C. **The Kyoto Protocol: A Review and Perspectives**. ZEW, Centre for European Economic Research. [S.I.].
93. EUROPEAN COUNCIL. **Limit Carbon Dioxide Emissions by Improving Energy Efficiency (SAVE)**. Council Directive 93/76/CEE, EC. [S.I.]. 13.09.1993.
94. LUIS PÉREZ-LOMBARDA, J. O. J. F. C. I. R. M. A review of HVAC systems requirements in building energy regulations. **Energy and Buildings Volume 43**, v. 34, n. 2-3, p. 255-268, February-March 2011.
95. EUROPEAN COUNCIL. **Directive 2002/91/EC on the Energy Performance of Buildings**. Directive 2002/91/EC. [S.I.]. 16.12. 2002.
96. SCOTTISH BUILDING STANDARDS AGENCY. **European Union Energy Performance of Building**. Scottish Building Standards Agency. Livingston. 2008.
97. OFFICE OF THE DEPUTY PRIME MINISTER. **The Building Regulations 2000 Part L: Conservation of Fuel and Energy**. [S.I.]: BRE press, 2000.
98. NANNAN WANG, Y.-C. C. V. D. Carbon print studies for the energy conservation regulations of the UK and China. **Energy and Buildings**, v. 42, p. 695–698, 2010.
99. BRIAN ANDERSON. **Energy Performance of Buildings Directive**. BRE. [S.I.]. April 2008.
100. ASHRAE. **ANSI/ASHRAE/IES Standard 90.1-2016 -- Energy Standard for Buildings Except Low-Rise Residential Buildings**. ASHRAE. [S.I.], p. 388. 2016.
101. U.S. DEPARTMENT OF ENERGY. **Saving Energy and Money with Building Energy Codes in the United States**. DOE. [S.I.]. May 2014. (DOE/EE-1087 ).
102. U.S. DEPARTMENT OF HOUSING AND URBAN DEVELOPMENT. **Energy Codes for HUD-Assisted and FHA-Insured Properties**. **U.S. Department of Housing and Urban Development**, 2016.

- Disponível em:  
<[https://portal.hud.gov/hudportal/HUD?src=/program\\_offices/economic\\_resilience/eegb/standards](https://portal.hud.gov/hudportal/HUD?src=/program_offices/economic_resilience/eegb/standards)>. Acesso em: 19 out. 2016.
- 103 MINISTRY OF URBAN AND RURAL CONSTRUCTION AND ENVIRONMENTAL PROTECTION. **Design standard for energy efficiency of civil buildings (JGJ26-86)**. Beijing: [s.n.], 1986.
- 104 MINISTRY OF URBAN AND RURAL CONSTRUCTION AND ENVIRONMENTAL PROTECTION. **Design standard for energy efficiency of civil buildings (JGJ26-95)**. Beijing: [s.n.], 1995.
- 105 MINISTRY OF URBAN AND RURAL CONSTRUCTION AND ENVIRONMENTAL PROTECTION. **Design standard for energy efficiency of residential buildings in hot summer and warm winter zone (JG75-2003)**. Beijing: China Construction Industry Press.
- 106 MINISTRY OF URBAN AND RURAL CONSTRUCTION AND ENVIRONMENTAL PROTECTION. **Design standard for energy efficiency of residential buildings in hot summer and cold winter zone (JGJ134-2010)**. ISBN: 1511217848. ed. Beijing: China Construction Industry Press, 2010.
- 107 MINISTRY OF HOUSING AND URBAN-RURAL DEVELOPMENT. **Design standard for energy efficiency of public buildings (GB50189-2015)**. Beijing: China Construction Industry Press, 2015.
- 108 USGBC. **LEED Illustrated™ Green Associate Study Guide**. 2009 Edition. ed. [S.l.]: Prentice Hall, 2009.
- 109 USGBC . **Green Building By the Numbers**. USGBC. [S.l.]. 22.08.2011.
- 110 MINISTRY OF HOUSING AND URBAN-RURAL DEVELOPMENT OF CHINA. **Assessment standard for green building (GB50378)**. Beijing: China Construction Industry Press, 2006.
- 111 NEW WAYS WIKI. **China's green building evaluation standard and comparison to the LEED rating system**. NEW WAYS WIKI. [S.l.]. 2010.
- 112 SHUI, B. . E. A. . **Country Report on Building Energy Codes in China**. Medium. ed. Beijing: [s.n.], 2009.
- 113 XIANGFEI KONG, S. L. Y. W. A review of building energy efficiency in China during —Eleventh Five-Year Plan|| period. **Energy Policy**, v. 41, p. 624–635, 02.2012.
- 114 GREEN BUILDING MAP. Statistical data of green building projects in China. **Green Building Map**, 2016. Disponível em: <<http://www.gbmap.org/tools/cgbl.php>>. Acesso em: 05 dez. 2016.
- 115 E, H. J. Calculation of monthly mean solar radiation for horizontal and inclined surface. **Solar Energy**, v. 23, n. 4, p. 301-307, 1979.
- 116 CRANK, J.; NICOLSON, P. A practical method for numerical evaluation of solutions of partial differential equations of the heat conduction type. **Mathematical Proceedings of the Cambridge Philosophical Society**, v. 1, n. 43, p. 50–67. ISSN doi:10.1007/BF02127704.
- 117 ENERGY FOUNDATION CHINA. **Research on Energy Consumption Standard for Public Buildings**. Energy Foundation China. [S.l.]. 2014.
- 118 INTERNATIONAL STANDARD ORGANIZATION. **ISO 13786 Thermal performance of building components -- Dynamic thermal characteristics -- Calculation methods**. International Standard Organization. [S.l.]. 2007. (ISO/TC 163/SC 2).
- 119 WONG, N. H. . Y. C. C. L. O. A. A. S. 2. Investigation of thermal benefits of rooftop garden in the

- . tropical environment. **Building and Environment** , 2003, n. 38:, p. 261–270.
- 120 ANDERSON, B. **Conventions for U-value calculations**. BRE Press, BRE Scotland. [S.l.]. 2006.
- . .
- 121 CHINA MINISTRY OF HOUSING AND URBAN-RURAL DEVELOPMENT. **GB 50176 Thermal Design Code for Civil Building**. China Ministry of Housing and Urban-Rural Development. Beijing. 1993.
- 122 CIBSE. **CIBSE Guide A: Environmental Design 2015**. [S.l.]: CIBSE, 2015.
- . .
- 123 U.S. DEPARTMENT OF ENERGY. **Life-Cycle Assessment of Energy and Environmental Impacts of LED Lighting Products, Part I: Review of the Life-Cycle Energy Consumption of Incandescent, Compact Fluorescent, and LED Lamps**. Building Technologies Program, Office of Energy Efficiency and. [S.l.]. 2012.
- 124 SOLARCITY PARTNERSHIP. **Horse Palace Photovoltaic Pilot Project: Update Report**. SolarCity Partnership. Toronto. 2012.
- 125 CHIA QUALITY CERTIFICATION CENTRE. **Technical Specifications for Energy Conservation Certification for Solar Collectors**. Beijing: China construction industry press, 2012.
- 126 C.K. CHAU\*, W. K. H. W. Y. N. G. P. Assessment of CO<sub>2</sub> emissions reduction in high-rise concrete office buildings using different material use options. **Resources, Conservation and Recycling**, n. 61 (2012) 22– 34, January 2012.
- 127 RUI, L. **Master Dissertation: Methodology and Tool to Calculate Building's Equivalent Carbon Dioxide during Design Stage**. University: Southeast University. Nanjing. 2013.
- 128 Y.SONG, H. L. Design on evaluation methods for the environmental pressure of energy consumption in building's life-cycle. In: WEN-PEI SUNG, J. C. M. K. R. C. **Frontiers of Energy and Environmental Engineering**. [S.l.]: CRC Press, 23 Nov 2012. p. 872.
- 129 HAIYONG YU, Q. W. Servicelife Period-Based Carbon Emission Computing Model for Ready-Mix Concrete. **Fly Ash** , n. 6, p. 42-47, 2011.
- 130 LI, B. CO<sub>2</sub> estimation model for building construction. **infotmation technolog of civil engineering**, v. 3, n. 6, p. 5-10, 2011.
- 131 YAN, Y. **Research of Energy Consumption and CO<sub>2</sub> Emission of Buildings in Zhejiang Province Based on Life Cycle Assessment ( master degree desertation)**. Zhejiang University. Hangzhou. 2011.
- 132 CHINA, E. P. D. O. **Iron and steel industry cleaner production evaluation index system**. [S.l.]. 2014.
- 133 CHINA, E. P. D. O. **The specific requirement for main pollutant emission reducing in 12th 5 year plan**. [S.l.]. 2011.
- 134 CHINA, E. P. D. O. **Emission standard of pollutants for petroleum chemistry industry GB 31571-2015**. [S.l.]. 2015.
- 135 JONES, P. G. H. & C. **Inventory of Carbon & Energy (ICE) Version 2.0**. Sustainable Energy Research Team (SERT), Department of Mechanical Engineering, University of Bath, UK. Bath.
- 136 ZHANG, Y. **PhD Thesis: LIFE CYCLE ASSESSMENT ON THE REDUCTION OF CARBON DIOXIDE EMISSION OF BUILDINGS**. Building research institute, National central university. Taipei.
- 137 WIREMOLD. V500/V700/700WH One-Piece Surface Steel Raceway, April 2005. Disponivel em:



- . <<http://www.newark.com/pdfs/datasheets/Wiremold/ED532.pdf>>. Acesso em: 21 dez. 2015.
- 138 INTERNAL and external diameters, areas, weights, volumes and number of threads for schedule  
. 40 steel pipes. **The engineering tool box**. Disponível em:  
. <[http://www.engineeringtoolbox.com/ansi-steel-pipes-d\\_305.html](http://www.engineeringtoolbox.com/ansi-steel-pipes-d_305.html)>. Acesso em: 20 dez. 2015.
- 139 PHYSICAL characteristics of copper tubes. **The engineering tool box**. Disponível em:  
. <[http://www.engineeringtoolbox.com/copper-tubes-dimensions-d\\_357.html](http://www.engineeringtoolbox.com/copper-tubes-dimensions-d_357.html)>. Acesso em: 20  
dez. 2015.
- 140 ALMONAPLAST. PPR Technical Data Sheet, 2010. Disponível em:  
. <[http://www.almonaplast.com/ppr\\_techincal\\_data\\_sheet.pdf](http://www.almonaplast.com/ppr_techincal_data_sheet.pdf)>. Acesso em: 20 dez. 2015.
- 141 CHINA MINISTRY OF ENVIRONMENTAL PROTECTION. **Emission standard of pollutants for  
. mineral wool industry, Appendix 7**. Edit group of Emission standard of pollutants for mineral  
wool industry. Beijing. 2015.
- 142 PROTECTION, C. M. O. E. **Emission standard of pollutants for petroleum chemistry industry (GB  
. 31571-2015)**. Beijing. 2015. (ICS 13.040.40).
- 143 DUAN PENG-XUAN, W. Z.-J. J.-P. C.-X. G.-M. The Studies and Application of the External Self  
. Thermal Insulation System of Autoclaved Fly-ash Aerated Concrete. **Journal of Shanxi University  
(Natural Science Edition)**, Taiyuan, n. 4, 2009.
- 144 HUANG, P. **The life-cycle energy assessment for new material in building wall (master degree  
. desertation)**. Hubei Industry University. Wuhan. 2013.
- 145 CHEN QINGWEN, M. X. LIFE CYCLE ASSESSMENT ON THE BUILDING CERAMIC. **CHINA CERAMICS**,  
. v. 2008,44, n. 7, September 2008. ISSN DOI: 10.3969/j.issn.1001-9642.2008.07.010.
- 146 CHEN WENJUAN ET AL. Life Cycle Inventory and Characterization of Flat Glass in China. **China  
. Building Materials Science & Technology**, Beijing, March 2006.
- 147 CHINA MINISTRY OF ENVIRONMENTAL PROTECTION. **Emission Standard of pollutants for  
. domestic glass industry**. Emission Standard of pollutants for domestic glass industry Edition  
Group. Beijing. 11, 2015.
- 148 GROPU, N. Embodied CO<sub>2</sub> in Float Glass. **NSG GROPU**, 2014. Disponível em:  
. <<http://www.nsg.com/en/sustainability/glassandclimatechange/embodiedc02infloatglass>>.  
Acesso em: 30 Oct 2015.
- 149 CHINA LANGSHI DEVELOPMENT COP. products sheet: windows. **Langshi Development**, 2015.  
. Disponível em: <[www.langshi.com.cn](http://www.langshi.com.cn)>. Acesso em: 05 mar. 2015.
- 150 LIN, Y. The life-cycel assessment for the environment load of aluminum. **Energy saving (Chinese  
. edition)**, n. 5, p. 46-50, 2011.
- 151 CHINA MINISTRY OF HOUSING AND URBAN-RURAL DEVELOPMENT. **Load code for the design of  
. building structures. GB 50009—2001**. China Ministry of Housing and Urban-Rural Development.  
[S.l.]. 2010.
- 152 FRANCIS K DACIS, H. N. The variation of gust factors with mean wind speed and with height.  
. **Journal of Applied Meteorology**, v. 7, p. 372, fev. 1968.
- 153 LIZHAOJIAN, J. Y. Material consumption analsis of room air conditioner manufacturing in China.  
. **HV & AC (China)**, v. 37, n. 3, p. 25, 2007.
- 154 DAIKIN. **VRV catalogue 2015**. Daikin Air conditioning UK Limited. Surrey, p. 92. 2015.

- 155 LI ZHAOJIAN, Z. S. J. Y. Analysis on energy and resource consumption in producing process of compression-type waer chillers. **HV&AC (China)**, v. 38, n. 11, 2008.
- 156 OSRAM. **Material Declaration Sheet and RoHS Compliance Declaration**. OSRAM. [S.l.]. 2008.
- 157 DEPARTMENT OF ENERGY, T. N. B. O. S. **China Energy Statistical Year Book**. Beijing: [s.n.], 2013. ISBN ISBN978-7-5037-6766-1.
- 158 BRINKMAN, N. et al. **Well-to-Wheels Analysis of Advanced Fuel/Vehicle Systems — A North American Study of Energy Use, Greenhouse Gas Emissions, and Criteria Pollutant Emissions**. Argonne National Laboratory. [S.l.], p. ES.1 Background, pp1. May 2005.
- 159 ROBERT EDWARDS, J.-F. L. D. R. **Well-to-Wheels analysis of future automotive fuels and powertrains in the European context WELL-TO-WELL-TO-TANK Report**. JRC, European Commission. [S.l.]. April 2014.
- 160 XIAOFEI HE, J. H. **The Research of Energy Consumption and Energy Conservation in Construction Technology**. Department of Civil Engineering, Chongqing University. Chongqing, China. 2013.
- 161 FABRE, GUILLAUME. **The Low-Carbon Buildings Method 3.0**. First Edition. ed. [S.l.]: Guillaume Fabre, 14 January 2012.
- 162 BIOMASS ENERGY CENTRE. Carbon emissions of different fuels. **Biomass energy centre**, 2015. Disponivel em: <[http://www.biomassenergycentre.org.uk/portal/page?\\_pageid=75,163182&\\_dad=portal&\\_schema=PORTAL](http://www.biomassenergycentre.org.uk/portal/page?_pageid=75,163182&_dad=portal&_schema=PORTAL)>. Acesso em: 20 dez. 2015.
- 163 ZHANG, Y. **RC building life cycle environment impact assessment**. Department of Architecture, Chengong University. [S.l.]. 1997.
- 164 AMELIA CRAIGHILL, J. C. P. **A LIFECYCLE ASSESSMENT AND EVALUATION OF CONSTRUCTION AND DEMOLITION WASTE**. Centre for Social and Economic Research on the Global Environment, University of East Anglia, University College London. London. (ISSN 0967-8875).
- 165 JOHNKE, B. **Good Practice Guidance and Uncertainty Management in National Greenhouse Gas Inventories: EMISSIONS FROM WASTE INCINERATION**. IPCC. Montreal. 2001.
- 166 HARVARD UNIVERSITY. Math 20 Chapter 5 Eigenvalues and Eigenvectors. **Harvard University**, last updated at 2017. Disponivel em: <[http://www.math.harvard.edu/archive/20\\_spring\\_05/handouts/ch05\\_notes.pdf](http://www.math.harvard.edu/archive/20_spring_05/handouts/ch05_notes.pdf)>. Acesso em: 3 maio 2017.
- 167 SAATY, T. L. How to make a decision: The analytic hierarchy process. **European Journal of Operational Research**, n. 48, p. 9-26, 1990.
- 168 SATTY, T. L. **The Analytic Hierarchy Process: Planning, Priority Setting, Resource Allocation**. ISBN 0-07-054371-2. ed. [S.l.]: McGraw-Hill, 1980.
- 169 DEPARTMENT FOR ENVIRONMENT, F. A. R. A. **Air quality economic analysis: Damage costs by location and source**. DEFRA. London. 2015.
- 170 DILOUIE, C. **The lighting management handbook**. Indian, USA: The fairmont press, INC., 1994.

- 171 SEATTLE CITY LIGHT. **Intergrated resource plan, Final environmental impact statement**. Seattle . city light. Seattle, USA. 2012.
- 172 CHINA, M. O. E. P. O. **Annual statistic report on environment**. Beijing: [s.n.], 2012.
- 173 DG ENVIRONMENT. **Damages per tonne emission of PM2.5, NH3, SO2, NOx and VOCs from eachEU25 Member State (excluding Cyprus) and surrounding seas**. AEA Technology Environment. [S.I.]. 2005.
- 174 HOLLAND, M. R. A. W. P. **Benefits Table database: Estimates of the marginal external costs of air pollution in Europe BeTa Version E1.02a**. European Commission DG Environment by netcen. [S.I.].
- 175 HONG LI, L. D. Promoting Green Employment and Enhancing the Eco-Efficiency of the Industry: An Empirical Study Based on Wind Energy Industry. **Journal of Peking University**, v. 1, n. 48, p. 109-118, jan. 2011.
- 176 Acid Rain Program 2007 Progress Report. **Clean Air Markets - Air & Radiation. US EPA**. Disponivel em: <<https://www.epa.gov/airmarkets>>. Acesso em: jun. 2015.
- 177 UNITED STATES ENVIRONMENT PROTECTION AGENC. Cross-State Air Pollution Rule (CSAPR). **US EPA**, 2011-07-09. Disponivel em: <<https://www3.epa.gov/crossstaterule/>>. Acesso em: 10 jun. 2015.
- 178 ADMINISTRATION, U. E. I. Emissions allowance prices for SO2 and NOX remained low in 2011. **US Energy Information Administration**, 2012. Disponivel em: <<http://www.eia.gov/todayinenergy/detail.cfm?id=4830>>. Acesso em: 03 maio 2016.
- 179 HWANG, C. L.; YOON, K. **Multiple Attribute Decision Making: Methods and Applications**. New York: Springer-Verlag, 1981.
- 180 NUNNALLY, J. **Psychometric theory**. New York: McGraw-Hill., 1978.
- 181 PRC, M. O. H. A. U.-R. D. O. T.; GENERAL ADMINISTRATION OF QUALITY SUPERVISION, I. A. Q. O. T. P. **Standard for Energy Consumption of Buildings -- (draft version to public opinions)**. Beijing. 2016.
- 182 LIN BORONG, L. Field investigation of operation performance of green office building in China. **HV&AC (China)**, Beijing, v. 45, n. 3, 2015.
- 183 PANG JUN, W. J. M. Z. L. L.-N. Air pollution abatement effects of replacing coal with natural gas for central heating in cities of China. **China Environmental Science** , Beijing, v. 35, n. 1, p. 55-61, 2015.
- 184 DEFRA. Emission levels. **Biomass energy centre**, 2015. Disponivel em: <[http://www.biomassenergycentre.org.uk/portal/page?\\_pageid=77,109191&\\_dad=portal&\\_sc\\_hema=PORTAL](http://www.biomassenergycentre.org.uk/portal/page?_pageid=77,109191&_dad=portal&_sc_hema=PORTAL)>. Acesso em: 20 maio 2016.
- 185 RAWLINSON, S. **INTERNATIONAL CONSTRUCTION COSTS: A CHANGE OF PACE**. EC HARRIS RESEARCH. [S.I.]. 2013.
- 186 SHANGHAI CONSTRUCTION PRICING AGENCY. **Shanghai building renovation pricing handbook**. ISBN 9787542720603. ed. Shanghai: Shanghai Popular Science Press, 2011.
- 187 DOCUMENT ACHIVE WENKU. The comparison of VRV and other HVAC system. **Document archive**

- . wenku, 23 mar. 2011. Disponível em: <<http://wenku.baidu.com/view/6ce4b37202768e9951e738ee.html>>. Acesso em: 21 out. 2016.
- 188 SHANGHAI MUNICIPAL COMMISSION OF ECONOMY AND INFORMATIZATION. Electricity price for Shanghai. **Shanghai Municipal Commission of Economy and Informatization**, 2012. Disponível em: <<http://www.sheitc.gov.cn/dfjf/637315.htm>>. Acesso em: 16 ago. 2016.
- 189 SAATY, T. L. **Decision Making for Leaders: The Analytical Hierarchy Process for Decisions in a Complex World**. ISBN 0-534-97959-9, ed. [S.l.]: Wadsworth, 1982.